HHS Public Access

Author manuscript

Chem Rev. Author manuscript; available in PMC 2017 October 26.

Published in final edited form as:

Chem Rev. 2017 April 26; 117(8): 5226–5333. doi:10.1021/acs.chemrev.6b00478.

Oxidative Cyclization in Natural Product Biosynthesis

Man-Cheng Tang[1,#], **Yi Zou**[1,#], **Kenji Watanabe**[3], **Christopher T. Walsh**[2,*], and **Yi Tang**[1,*]

[1]Department of Chemical and Biomolecular Engineering, Department of Chemistry and Biochemistry, University of California, Los Angeles, 420 Westwood Plaza, Los Angeles, CA 90095, USA

[2]Stanford University Chemistry, Engineering, and Medicine for Human Health (ChEM-H), Stanford University, 443 Via Ortega, Stanford, CA 94305

[3]Department of Pharmaceutical Sciences, University of Shizuoka, Shizuoka 422-8526, Japan

Abstract

Oxidative cyclizations are important transformations that occur widely during natural product biosynthesis. The transformations from acyclic precursors to cyclized products can afford morphed scaffolds, structural rigidity and biological activities. Some of the most dramatic structural alterations in natural product biosynthesis occur through oxidative cyclization. In this review, we examine the different strategies used by Nature to create new intra-(inter-)-molecular bonds via redox chemistry. The review will cover both oxidation- and reduction-enabled cyclization mechanisms, with an emphasis on the former. Radical cyclizations catalyzed by P450, nonheme iron, α-KG dependent oxygenases and radical SAM enzymes are discussed to illustrate the use of molecular oxygen and *S*-adenosylmethionine to forge new bonds at unactivated sites via one-electron manifolds. Nonradical cyclizations catalyzed by flavin-dependent monooxygenases and NAD(P)H-dependent reductases are covered to show the use of two-electron manifolds in initiating cyclization reactions. The oxidative installation of epoxides and halogens into acyclic scaffolds to drive subsequent cyclizations are separately discussed as examples of “disappearing” reactive handles. Lastly, oxidative rearrangement of rings systems, including contractions and expansions will be covered.

Graphical Abstract

[*]Correspondence: yitang@ucla.edu, cwalsh2@stanford.edu.
[#]These authors contributed equally.

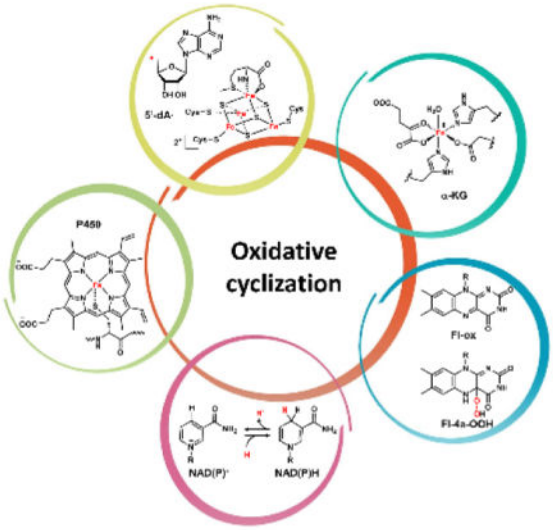

1. INTRODUCTION

The importance of natural products to human health is unquestioned. Many of the natural products and their semisynthetic derivatives have served as front line therapeutics to treat a wide variety of diseases, ranging from microbial infections, cancer, cardiovascular conditions, and as immunosuppressants.[1–3] The vast collection of bioactivities displayed by natural products is a direct result of the immense structural diversity introduced during the biosynthetic assembly.[4] Several major families of natural products have been classified during the decades of isolation and structural characterization since the golden age of antibiotics. Based on biosynthetic origin and fundamental building blocks, the major families of natural products include polyketides (PKs), nonribosomal peptides (NRPs), ribosomally synthesized and post-translationally modified peptides (RiPPs), isoprenoids, alkaloids including phenylpropanoids and indole alkaloids, aminoglycosides, nucleosides, etc.[5]

For the major families of natural products including PKs, NRPs, RiPPs, terpenes, etc., nature builds structural complexity in two major phases. The first phase involves the polymerization of building blocks, such as acetate for PKs, amino acids for NRPs and RiPPs, and isoprene units for terpenes. The polymerization process builds the carbon backbone of the molecules, and in most cases, cyclizes the molecule in a regioselective fashion to yield a basic scaffold of the final natural product. This scaffold, which can be called the aglycone in some cases, is then subjected to a barrage of post-assembly modifications that serve a variety of purposes, such as rigidifying the molecule and fixing the three-dimensional conformation; introducing polar groups to increase the water solubility; reveal structural motifs and reactive sites as warheads for target inhibition; and appending oligosaccharides that bind to specific DNA sequences. It is during the post-assembly steps that the natural products can undergo significant structural morphing to result in the final bioactive compounds. Obtaining a complete understanding of these enzymatic transformations is therefore important to not only allow chemists to appreciate Nature’s

chemical strategy to forge complex small molecules, but also increases the toolbox of biocatalysts that can used to generate structural diversity and biological activities into both biological and synthetic molecules.

The types of enzyme modifications that will be reviewed here are cyclization reactions through redox alteration of acyclic substrates. We define oxidative (or reductive) cyclization as 1) formation of new rings as a result of oxidative modification, such as in the case of P450-catalyzed formation of phenyl ether rings during vancomycin biosynthesis; 2) a tandem redox/cyclization combination, in which a discrete redox modification occurs to set up the subsequent enzyme-catalyzed/spontaneous step that forges a new ring system. This is exemplified in the epoxide-mediated cyclization of terpenes and polyethers, as well as the cryptic oxidative halogenation steps that lead to cyclopropanation; and 3) oxidative morphing of existing ring systems to either contract, expand or rearrange to a new ring system. All cyclization reactions covered in this review must involve a net redox state change in the starting substrates, i.e. addition or removal of electrons to drive the formation of new intramolecular covalent bonds, although in many cases the overall reaction can be redox neutral. Nonredox-mediated cyclization mechanisms are not covered except a brief discussion of [4+2] cycloadditions that are setup by prior redox steps. Nonredox cyclizations include acyltransferase/thioesterase catalyzed macrocyclization of PKs and NRPs,[6] intramolecular Aldol and Claisen condensation reactions in aromatic PK biosynthesis,[7] pyran synthase in many PK pathways,[8] etc.

Oxidative cyclization can introduce some of the most dramatic structural changes in a natural product biosynthetic pathway. The use of high-valent iron-containing enzymes such as P450 and nonheme iron α-ketoglurarate (α-KG, also known as 2-oxoglutarate) dependent oxygenases can result in the formation of radicals through homolysis of different types of bonds in a molecules, including unactivated C-H bonds, phenolic O-H bonds, indole N-H bonds and thiol S-H bonds.[9,10] The resulting radical can then be the starting point to regioselective forging of new bonds that are otherwise difficult to construct. Section 2 will cover this type of oxidative cyclization sorted by both enzymes and the types of bonds that are formed. In addition to the one-electron manifold oxidation of substrates, Nature also uses two-electron redox manifolds facilitated by the flavin and β-nicotinamide adenine dinucleotide (phosphate), reduced form (NAD(P)H) cofactors. While enzymes use these cofactors to catalyze oxidation/reduction of more reactive sites in the molecules, the flexibility of the flavin cofactor, serving either as an electron sink in desaturation reactions or as an electrophilic [OH^+] equivalent, propels this family of enzymes into central importance during oxidative cyclizations.[11] Section 3 will discuss prominent examples of nonradical-mediated oxidative cyclizations, including both flavin and NAD(P)H mediated mechanisms. Several examples of [4+2] cycloaddition will also be discussed, although we use these to highlight the importance of precise redox tuning of the acyclic substrates that set up such dramatic transformations. Section 4 and 5 will discuss the use of reactive handles installed by oxidative enzymes to initiate a cyclization sequence, ultimately forging new ring systems while masking the use of the handles in the final molecules. Section 4 will discuss the use of “disappearing” epoxides in promoting ring closing steps in a variety of natural product pathways. Regioselective epoxidation of a double bond in the substrate can trigger a cascade of cyclization steps that rigidify an otherwise linear precursor, as in the example of

lanosterol biosynthesis. Section 5 will discuss the oxidative halogenation of natural products as a strategy to initiate cyclization. Both the vanadium haloperoxidases (VHPOs) and α-KG dependent families of oxidative halogenases will be discussed. In Section 6, oxidative ring rearrangements catalyze by all major families of oxygenases will be discussed. Finally in Section 7, a unifying discussion of the examples presented here will conclude the review.

Types of Redox Enzyme in Nature

Before we discuss the specific examples of oxidative cyclizations, a general introduction to the types of enzymes that participated in these reaction will be briefly summarized here. The mechanisms of the reactions have been well-worked out and have been reviewed in many excellent articles and books that are cited throughout.

Iron and Heme-Dependent Cytochrome P450 Monooxygenases

P450s are ubiquitous oxidative enzymes that span across all organisms, from bacteria to humans. P450s are heme-binding enzymes and share a highly conserved protein fold.[12] These oxygenases form iron-porphyrin complexes to oxidize a vast multitude of different substrates using molecular oxygen. Despite their substantial range of substrate diversity, P450 oxidations can be highly stereoselective and regioselective. P450 enzymes in natural product biosynthesis use a single-electron manifold to produce radical intermediates via a high-valent oxoiron cationic radical (or Fe^{IV}=O, ferryl) (Scheme 1).[13,14] This Compound I can readily abstract hydrogen from C-H, N-H, O-H and S-H bonds to yield a reactive radical species.[10,12] These reactive radical intermediates can lead to a variety of modifications including hydroxyl rebound, epoxide formation, dehydrogenation, radical addition, diradical combination, etc.[10,12] In typical hydroxylation mechanisms, rebound of the [OH•] from the resulting Fe^{IV}-OH leads to insertion of the oxygen atom which is derived from molecular oxygen. Alternatively, the radical species can perform intramolecular addition (for example, with an olefin) or recombination with another radical to forge new bonds in the product scaffold. In this case, the net reaction is the four-electron reduction of molecular oxygen without insertion of any oxygen atom into the final product. The use of these powerful oxidative enzymes in natural product cyclization will be discussed in Section 2.2.

Nonheme Iron Dependent Oxygenases

In addition to heme-dependent oxygenases, nonheme iron-dependent oxygenases are also widely found in biosynthetic pathways.[15,16] In particular, mononuclear nonheme $Fe^{(II)}$- α-KG-dependent oxygenases comprise a large family of oxidative enzymes that are widely distributed in Nature.[17,18] Enzymes in this family utilizes an Fe^{IV}-oxoiron intermediate to initiate otherwise challenging oxidative transformations at unactivated sites, such as hydroxylation, desaturation and halogenation.[19] Mechanistic and structural studies of this family of enzymes have clarified the catalytic cycle.[9,20] As shown in Scheme 2 using a classical hydroxylation reaction as an example, the resting Fe^{II} is coordinated by two His residues and the carboxylate from an Asp residue to form the 2-His-1-carboxylate facial triad. This can be coordinated to three water molecules until binding of α-KG to the Fe^{II} center displaces two of the three metal-bound water molecules. Binding of substrate (R-H) to the enzyme active site displaces the remaining water molecule and vacates a site for binding to the triplet O_2 molecule to generate the Fe^{III}-superoxo intermediate. The distal

oxygen atom of the Fe^{III}-superoxo species can attack C_2 of α-KG to yield a peroxohemiketal bicyclic intermediate, which collapses via oxidative decarboxylation to release CO_2. This step also sets up a high valence Fe^{IV}=O (ferryl) intermediate and a bound succinate. It is this ferryl species (functionally analogous to compound I in the P450 cycle) that can abstract a hydrogen atom from the substrate (R-H) to reduce the iron to the Fe^{III}-OH state with concomitant formation of the substrate radical (R•). To complete the catalytic cycle, hydroxyl radical rebound onto the substrate radical yields the hydroxylated product (R-OH), returning the iron back to the Fe^{II} state with product and succinate release. Examples of using this family of enzymes in natural product cyclization will be covered in Section 2.3. The use of nonheme, noncofactor-dependent oxygeneases to perform oxidative cyclization involving unactivated C-H bonds will be covered in Section 2.4. One notable example is the Rieske oxygenase discussed in section 2.4.3. Similar to the α-KG-dependent oxygenases, the iron within the Rieske nonheme iron-dependent oxygenases is also coordinated by the 2-His-1-carboxylate facial triad.[21] The key difference is that duing the catalytic process, instead of using α-KG directly as the reductant, the Rieske oxygenases use a [2Fe-2S] cluster to deliver the necessary electrons from an external reductant.[21]

Radical SAM Superfamily

The radical *S*-adenosylmethionine (SAM) enzymes is a relatively new enzyme superfamily discovered to catalyze radical reactions such as H-atom abstraction from an unactivated C–H bond, mostly under anaerobic conditions in the bacterial world.[22] This family is rarely found in eukaryotic organisms such as fungi and plants, but are vastly powerful biocatalysts in both primary and secondary metabolisms of bacteria.[22] As shown in Scheme 3, these enzymes use a [4Fe-4S] cluster to transfer an electron from an external source (such as flavodoxin shown) to SAM, which is homolytically cleaved to methionine and the reactive 5′-deoxyadenosyl radical intermediate (5′dA•).[23,24] This 5′dA• radical is able to abstract a proton and an electron from unactivated substrate (R-H) to form 5′dA and generate a radical (R•) that can participate in downstream oxidation and cyclization reactions. This superfamily of enzymes, which has over one hundred thousand homologs in the database of which mostly of unknown function, greatly expands Nature's ability to use Fe-S clusters in oxidative catalysis beyond the textbook examples of electron transport.[25] Some examples will be covered in Section 2.4.

Copper-Dependent Tyrosinase

Copper is a relatively rarely used metal cofactor in enzymes catalysis. Three notable examples that have relevance to metabolism are cytochrome c oxidase,[26] laccase,[27] and tyrosinase[28]. The most well-studied example of tyrosinase is the hydroxylation of tyrosine to yield L-3,4-dihydroxyphenylalanine (DOPA) as shown in Scheme 4.[29–31] In the active site of tyrosinase, six histidine residues coordinate to a pair of copper ions (Cu^{II}) and one oxygen molecule to give the oxy starting complex. The substrate monophenol (M) binds to one of the copper metals and forms the oxy-M intermediate. This weakens the O-O bond, resulting in cleavage and rearrangement of original trigonal bipyramidal active site and forming the diphenolate (D) intermediate (met-D). The product is then oxidized to the quinone through the transfer of two electrons to the coppers, with the active site in the reduced di-Cu^{I} form (oxy-red) to be reoxidized by molecular oxygen for a second round of catalysis.

Flavin-Dependent Monooxygenase

Flavin-dependent monooxygenases (FMOs) are widespread enzymes that catalyze a large variety of substrate oxidations such as dehydrogenation, hydroxylations, epoxidations, Baeyer-Villiger oxidations, and sulfoxidations.[32,33] FMOs use a flavin cofactor such as flavin adenine dinucleotide (FAD) or flavin mononucleotide (FMN), to generate reactive peroxyl species that serve as nucleophiles (peroxyflavin, Fl-4a-OO^-) or electrophiles (hydroperoxyflavin, Fl-4a-OOH) (Scheme 5A).[11] After each round of catalysis, the flavin cofactor can be reduced in the presence of NAD(P)H to repeat the catalytic cycle.

The oxidized flavin can also serve as electron sink in oxidases that catalyze dehydrogenation reactions such as the berberine bridge enzyme family (Scheme 5B). Here the flavin is often covalently attached to the active site through histidine and cysteine residues.[34,35] During the net two-electron reduction of molecular oxygen, a corresponding oxidation of substrate takes place to generate a degree of unsaturation that result in an electrophilic carbon (C=N, C=O, etc). This carbon is then subject to intramolecular attack by a nucleophile to forge a new bond and a cyclized structure as will be shown in Section 3. The reduced flavin is oxidized back to the Fl-ox form with release of hydrogen peroxide. As this species can be reactive and toxic to the cell, an accompanying catalase is often found in the gene cluster for detoxification.

NAD(P)H Dependent Reductases/Dehydrogenases

NAD(P)H-dependent enzymes catalyze reversible redox reactions including reduction and dehydrogenation as shown in Scheme 6.[36,37] The reduced form of the cofactor NAD(P)H is employed in substrate reduction, while the oxidized form $NAD(P)^+$ are used in oxidative dehydrogenation. During substrate reduction such as ketone/aldehyde to alcohols, NAD(P)H is a hydride-donating cofactor. Delivery of a hydride from the dihydropyridine ring to substrate in a stereospecific manner is coupled with oxidation of NAD(P)H to $NAD(P)^+$. In the reverse reaction of dehydrogenation, such as from alcohols to ketone/aldehydes, two hydrogen atoms are removed from the substrate with one of them transferred as a hydride to reduce $NAD(P)^+$ to NAD(P)H while the other as a proton to captures by the aqueous solution. While NAD(P)H is typically a non-covalent cofactor in these enzymes, Erb and coworkers observed a covalent ene intermediate between NADPH and α,β-unsaturated carbonyl substrate during catalysis of crotonyl-CoA carboxylase/reductase.[38,39] One notable use of NAD(P)H as a reducing cofactor in oxidative cyclization is in the reductive release of PK and NRP products that are bound as thioesters to the thiolation domains.[40] Releasing the products as aldehydes can trigger intramolecular cyclization reactions that are widely found in many natural product biosynthetic pathways (Section 3.2).

2. RADICAL CYCLIZATION MECHANISMS

2.1 Introduction

This section will describe examples of oxidative cyclization in which radical intermediates are formed through one electron oxidation of carbon or heteroatoms. The main enzyme families involved are those use a high-valent ferryl oxoiron reactive species, including P450s and nonheme iron α-KG-dependent oxygenases. Other enzyme families such as copper-

dependent tyrosinases and radical SAM-dependent enzymes are also used for this purpose. Structural morphing catalyzed by these enzymes are typically the most dramatic and chemically challenging. Several recurring cases of radical mechanisms are summarized in Scheme 7. In Scheme 7A, an otherwise unactivated C-H bond is subjected to homolytic cleavage to yield a carbon radical, which can be further oxidized into carbocation or alcohol through [OH•] rebound, and subject to intramolecular nucleophilic attack. This mechanism is observed in the synthesis of nitrogen heterocycles, as in the formation of methlyproline from either L-leucine or L-isoleucine (Scheme 46). In Scheme 7B, an X-H bond is oxidized to the corresponding X•, which can intramolecularly add to an electron-rich double bond to form a cyclized intermediate and form a new *C*-radical. This is followed by an additional one electron transfer to the iron center to yield the doubly oxidized product. There are increasing evidences to support this mechanism in oxidative cyclization, such as during spirocycle formation during griseofulvin biosynthesis (Scheme 25). In Scheme 7C, two successive oxidations at two different sites in the same molecules result in formation of diradicals that can be combined to form the cyclized product. For many reactions listed in this section, both mechanisms B and C can be proposed, such as for the two C-C bond forming steps during rebeccamycin synthesis (Section 2.2.2). Differentiation between the two mechanisms has come from crystal structures, computational analysis or both. The remaining section will be grouped by enzyme families that catalyze these reactions.

2.2. Cyclization Catalyzed by Heme-dependent Enzymes

This section will discuss oxidative cyclization catalyzed by heme-dependent enzymes. In each example, the cyclization process starts with abstraction of one hydrogen and generation of a radical intermediate. In most examples, the oxygenation half of the reaction is not completed as in the P450 catalytic cycle (no water rebound), and instead the radical is combined internally with an electron rich site (Scheme 7B), or with another radical to forge the new cyclizing bond (Scheme 7C). Mechanisms can be proposed using either scheme for many of the cyclizing reactions. We will first discuss the P450 catalyzed cyclization during the biosynthesis of vancomycin and rebeccamycin families, each featuring multiple C-C and C-O coupling steps. This will be followed by examples of cyclization categorized by the different types of atoms coupled to carbon.

2.2.1. P450-Catalyzed Phenyl Crosslinking in Glycopeptide Biosynthesis—The members of glycopeptide family compounds are a class of antibiotics of microbial origin, exemplified by the anti-infective antibiotics vancomycin (**1**) and teicoplanin (**2**) (Scheme 8A).[41,42] Compounds in this family are considered to be the last line of defense against antibiotic resistant bacteria, especially methicillin resistant *Staphylococcus aureus*.[41] The heptapeptide backbones for both are derived from NRPS assembly lines, incorporating a number of unnatural amino acids that have dedicated biosynthetic enzymes in the gene clusters.[41,42] Using **2** as an example, seven nonproteinogenic aromatic amino acids are introduced, including three 4-OH-phenylglycine (rings B, E and G), two 3-chloro-tyrosine (rings A and C), and two 3,5-dihydroxyphenylglycin (rings D and F). Extensive phenyl-coupling reactions take place after completion of linear peptide synthesis to effectively crosslink the side chains and introduce architectural rigidity that is crucial for the biological properties. The five phenol-couplings are catalyzed by five dedicated P450

monooxygenases. In a related compound complestatin (**3**), there is also a C-C coupling between the phenyl ring of 4-OH-phenylglycine and the phenyl ring of the tryptophan.[43,44] In the biosynthesis of arylomycin A_2 (**4**), a lipopeptide anti-infective agent, similar P450 catalyzed coupling reaction was proposed for C-C coupling between two phenyl side chains.[45–47]

Two different types of P450-catalyzed phenol coupling reactions take place between the different phenol rings: *ortho-ortho* C-C coupling and *ortho* C-O coupling. Both coupling regioselectivity will be seen in many other examples in this section of the review and is therefore useful to examine the possible mechanisms (Scheme 9). Based on structural and mechanistic studies of these P450s,[48–55] diradical coupling mechanisms were proposed for these reactions. In a single round of iron reduction from compound I (Fe^{IV}=O) to Fe^{III}-OH_2, two sequential hydrogen abstraction steps from two phenolic hydroxyl groups of **11** yields the diradical **12**. In the C-O coupling case, delocalization of one phenoxyl radical to the *ortho* carbon to give **13** is followed by diradical combination to yield the new C-O bond in **14** which can rearomatize into the diphenyl **15** as seen with three of the four coupled rings. If resonance delocalization of both radicals in **12** takes place to the *ortho* position as in **16a**, diradical combination forges the new C-C bond in **17** and can similarly rearomatize to **18** as in the case of D and E rings. Single-electron transfer and nucleophilic addition via **16b** can also be proposed for the C-C bond forming step. Current state of research favors the diradical mechanism over the radical addition mechanism, although more data are needed to fully distinguish the two. The radical addition mechanism will be presented for other coupling pathways in this section, some of which are favored over diradical coupling.

The order of these P450 reactions during maturation of **2** is shown in Scheme 8B. All the coupling steps take place after the heptapeptide is assembled and while still attached to the thiolation (T) domain as a thioester **5**. The new C-C and C-O bonds are introduced in a stepwise fashion: i) OxyB catalyzed C-O coupling of A/B phenyl rings to yield **6**; OxyE catalyzed C-O of the F/G phenyl rings to yield **7**; iii) OxyA catalyzed C-O coupling of B/C phenyl rings to yield **8**; and iv) OxyC catalyzed C-C coupling of D/E phenyl rings to yield **9**. The rigidified aglycone **10** is then released from the NRPS assembly through hydrolysis by the terminal thioesterase domain, which can be further glycosylated to yield the mature glycopeptide **2**. The crystal structures of all four P450s in the pathway have been solved, giving insights into the mechanistic proposal in Scheme 9 and their differences in substrate specificity.[48–50,55] In addition, the structural basis of the interaction between the P450s and the NRPS enzyme was recently elucidated by Cryle and coworkers.[56] They showed that there is an X domain present in the last module of the teicoplanin NRPSs. While the X domain is structurally similar to the Condensation (C) domains used by NRPS for peptide bond formation, it is catalytically inactive due to mutations in the active site. Extensive protein-protein interactions are present between the X domain and the suite of P450s as shown by crystal structure and biophysical characterization.[56,57] The working model is that together with the adjacent T domain, the X domain is crucial in the recruitment of P450 enzymes to the NRPS for on-assembly line oxidative cyclization.

2.2.2. Oxidative Coupling in Indolocarbazole Biosynthesis—Rebeccamycin (**19**), together with staurosporine (**20**), and K-252a (**21**) (Scheme 10A), are examples of the indolocarbazole superfamily of natural alkaloids produced by actinomycete strains.[58] Members of this family have been found to exhibit a broad spectrum of antitumor activities.[58] For example, **20** and **21** are potent inhibitors of protein kinase C, and **19** is an inhibitor of topoisomerase I.[59–61] Biosynthetic studies revealed that the aglycones of these compounds are derived from two molecules of L-tryptophan via a series of oxidative coupling transformations.[62–68] The pathway to the aglycones follow a unified route. Variations in biosynthetic routes of this family include the chlorination step in the pathway of **19** and the different oxidation state of the pyrrole-derived five-membered ring.

During the biosynthesis of the aglycone, the first oxidative cyclization is the coupling of two L-tryptophan derived indole-3-pyruvate imine (IPAI, **22**) to form the key biosynthetic intermediate chromopyrrolic acid (CPA, **27**), catalyzed by the heme-dependent oxidase RebD and its homologs (Scheme 10B).[62,66] The cytochrome b protein RebD first generates two IPAI radicals **23** and catalyzes the formation of the new C-C bond to yield the adduct **24**. Tautomerization of one of the imines to an enamine forms a free amine group in **25**, which can attack the remaining imine group to form the dihydropyrrole **26**. Finally, the pyrrole ring in **27** is formed by removing the ammonia. Recent mechanistic studies revealed that during the C-C oxidative coupling step, RebD can use both peroxidase and peroxygenase chemistry as shown in Scheme 10C.[69]

Although current studies of RebD provide evidence for the diradical coupling mechanism to form **27**, the radical addition route is still not ruled out. As shown in Scheme 11 the first step in this mechanism is the tautomerization of the first molecule of **22** to yield a free amine **28**. This can serve as the nucleophile to attack the imine group of a second molecule of **22** to form an intermolecular C-N bond and **29**. This intermediate can lose ammonia to form the imine **30**. RebD can then catalyze the hydrogen abstraction at the allylic position to generate the *C*-radical **31**, which can lead to radical addition to the C=C double bond in the left half of the molecule to form the new C-C bond in **32** that can also form pyrrole radical **33**. Abstraction of a second hydrogen following radical migration yields **34** which can followed by tautomerization to yield the pyrrole ring and complete the biosynthesis of **27**.

The next biosynthetic step in the biosynthetic pathway is the oxidative C_2-C_2 coupling of the two indole rings in **27** to form the indolocarbazole aglycone **41**. This reaction is catalyzed by a second P450, StaP in the staurosporine pathway or RebP in the rebeccamycin pathway which works on the 7,7-dichloro-CPA.[68] Recent X-ray crystal structural studies suggested a catalytic mechanism for StaP as shown in Scheme 12.[65] The first step is the one electron oxidation of the one indole NH by StaP to afford **35** or **36**, which can undergo hydrogen abstraction to form the *N*-radical **37**. From here both diradical combination and radical addition mechanisms can be proposed. In the diradical route *a*, a second hydrogen abstraction of the other indole yields the second nitrogen radical **38**. Following migration of both radicals to the C_2 carbons and C-C coupling to give **39**, tautomerization of the adduct forms the indolocarbazole ring and **41**. In the radical addition route *b*, migration of the single radical of **37** to C_2 can lead to addition to the other indole ring and generate a C_3 radical

intermediate **40**, which can be followed by electron transfer to the heme to form the final product **41**. In both mechanisms, a single round of iron reduction from the ferryl state to the Fe^{III} state is sufficient to perform the C_2-C_2 coupling. In the Scheme 15, a P450-catalyzed indole couple with C_3-$C_{3'}$ regioselectivity is discussed.

Shaik and coworkers performed both computational and experimental studies with StaP to propose a new mechanism (Scheme 13).[70] The first step is again hydrogen abstraction from one of the indole NH to yield a *N*-radical **37**. This is followed by radical addition to form the C_2-$C_{2'}$ bond together with a single electron transfer from the NH of the recipient indole **42** to heme-iron to form the iminium **43** and the Fe^{III}-hydroxide species. Abstraction of a proton gives **44** and returns the heme to the Fe^{III}-OH state followed by indole tautomerization of **45** yields the indolocarbazole ring system.

In the structures of **20** and **21**, one additional ring is formed via two C-N bonds between the indolocarbazole aglycone and the deoxysugar 2,3,6-trideoxy-3-aminoaldohexose. Biosynthetic studies revealed that this ring formation is catalyzed by the P450 StaN in the pathway to **20**.[71] The first C-N bond is formed by StaG, an *N*-glycosyltransferase using the TDP-activated form of the deoxysugar and K252c (**46**) as substrates. This yields holyrine A **47** which then undergoes intramolecular oxidative cyclization by StaN to yield staurosporine **20**. A proposed mechanism is shown in Scheme 14. The first step is the hydroxylation on the C_5 through the rebound mechanism shown in Scheme 2.1A to form a hemiketal **48a**, which undergoes dehydration to form the oxonium ion **48b**. The amine from the indole ring can then act as a nucleophile to attack the oxonium ion to form the new C-N bond in **49,** which is further transformed to **20** by both O- and N-methylations. Therefore, in the remarkably complex biosynthetic pathway of **20**, a total of three P450 enzymes are recruited to form two C-C bonds and one C-N bond.

2.2.3. C-C Coupling

2.2.3.1. Fungal P450 Catalyzed Cyclization: Communesins (**65–67**) are fungal indole alkaloids produced by various *Penicillium* species and have been noted to have strong insecticidal properties.[72–76] There are ~ 10 members of this family isolated, each containing a heptacyclic core that is among the most complex observed in fungal alkaloids. The seven interconnected rings consist of two indole containing fragments fused through a vicinal quaternary C-C bond and two aminal bonds. Four contiguous stereocenters run through the junction of two fragments. While numerous total syntheses of communesin have been reported,[77–87] the biosynthetic pathway was only recently uncovered from *P. expansum* and was shown to be highly efficient (Scheme 15).[88,89] The two indole-containing building blocks are tryptamine (**50**) derived from decarboxylation of L-tryptophan, and (−)-aurantioclavine (**53**) derived from the decarboxylative cyclization of 4-dimethylallyltryptophan. A P450 enzyme (CnsC) was found to be solely responsible in combining the two fragments to generate the core structure **63**, which is one *N*-methylation step away from the stable communesin K (**65**).[89] **65** is then further elaborated through epoxidation and *N*-acylation to yield communesin A (**66**) and communesin B (**67**).

Characterization of the P450 using either yeast based-biotransformation and/or in vitro microsomal assay showed formation of the three bonds between **50** and **53** is regioselective as no other products are formed.[89] Formation of the two aminal bonds (N_1-C_2-$N_{1'}$ and N_{10}-$C_{2'}$-$N_{10'}$) in **63** requires ring opening of the pyrroloindole **60** to generate the aniline species **62**. The *N*1 hydrogens on the indole nitrogens of both **50** and **53** were found to be required for coupling, as *N*-methyl substituents were not reactive. The P450 displayed broad substrate promiscuity towards C_3-substituted indoles. When N_{10}-methyl tryptamine (**51**) was used in place of **50**, a coupled "isocommunesin" product **59** with alternative aminal bond regioselectivity was the major product (4:1 ratio between isocommunesin **59** and communesin scaffold **64**). The isocommunesin scaffold of **59** is not naturally observed and is derived from the direct N_1-C_2-$N_{10'}$ and $N_{1'}$-$C_{2'}$-N_{10} aminal bonds formation after C_3-$C_{3'}$ coupling.

Density functional theory (DFT) calculation was performed to assess whether a radical addition mechanism, involving a tryptaminyl radical addition to the indole of **53**, takes place.[89] Computation showed the radical addition has a 10^5 preference for the formation of C_3-$C_{2'}$ adduct, therefore excluding this mechanism and favoring the diradical coupling between **52** and **54** as shown in Scheme 15. Other mechanisms such as radical cation addition, electrophilic aromatic addition were also ruled out based on C-C coupling regioselectivity. Further calculation on the aminal formation steps showed that formation of the isocommunesin scaffold **59** is energetically favorable and is predicted to take place spontaneously from **56** via **57** or **58**, while formation of the communesin scaffold **63** from **55** is energetically uphill in the pyrroloindole ring opening step (**60** or **61** to **62**). Hence, it was proposed that CnsC is responsible for the formation of all three bonds: first catalyzing the C-C coupling to yield **55**, followed by promoting the regioselective aminal bond forming steps (while suppressing isocommunesin formation).

In parallel with the biosynthetic studies, Movassaghi and coworkers developed an efficient total synthesis of **65** using a strategy that mimics the diradical coupling strategy shown in Scheme 16.[87] In their strategy, the two indole fragments were first synthesized as azepine **68** and cyclotryptamine **69**. Coupling of the two fragments can yield the sulfamide **70** on a gram scale. Chemoselective oxidation in the presence of *N*-chloro-*N*-methylbenzamide and 2-tert-butylimino-2-diethylamino-1,3-dimethylperhydro-1,3,2-diazaphosphorine yields the diazene **71**, which can be subjected to photoexcitation and release of N_2 to yield the diradical **72** that can be coupled to forge the quaternary C-C bond in **73**. This reaction yields a single diastereomer, which can be reacted in three more steps to yield **65**. Such later stage coupling strategy can be applied to the synthesis of other homo- and heterodimeric indole alkaloid natural products.

Mycocyclosin (**82**) is a cyclized diketopiperazine (DKP) produced by *Mycobacterium tuberculosis* (Scheme 17).[90] Two genes are responsible for the biosynthesis. The first is Rv2275, which is a cyclodipeptide synthase (CDPS) that synthesizes cyclo-Tyr-Tyr (cYY, **75**) using two molecules of tyrosyl-$tRNA^{Tyr}$ (**74**).[91] The second is a P450 CYP121 that was shown to perform the C-C coupling of **75** to yield **82**.[90] Interestingly, CYP121 is essential for *M. tuberculosis* viability, as knockout of the gene requires plasmid complement of

cyp121 to survive.[92] The activity of CYP121 was confirmed in vitro, and the structure in complex with **75** was solved.[90] It was shown that the DPK ring of **75** is perpendicular to and offset from the center with respect to the heme, with one phenol pointing at the iron and the other pointing away. A diradical combination mechanism was proposed in route *b*, in which the first radical is formed on the phenolic oxygen in the presence of Compound I, followed by delocalization of the radical in the benzene ring. This is followed by rotation around the DKP core and placing the other phenol at the iron center to undergo second hydrogen abstraction by Compound II to yield the diradical **80**.[90] Computation modeling of the reaction steps and energetics led to a later proposal that the second radical formation may be due to proton-coupled electron transfer (PCET) instead of substrate rotation.[93] Diradical combination of the *C*-diradical **81** that yields **79** likely takes place in bulk solution and is followed by aromatization to yield the rigidified **82**. An alternative mechanism involving radical addition can also be proposed in route *a*, in which the first radical **77** directly adds to the *ortho* position of the second phenyl ring to forge the C-C bond and yield **78**. This can be followed by a second step of hydrogen abstraction and formation of the diketone **79** which can aromatize into **82**. CYP121 was shown to be highly specific to **75**, as alternative DKP substrates were not recognized. The physiological role of **75** and **82** in *M. tuberculosis* virulence are not clearly understood, however, the indispensable role of CYP121 in *M. tuberculosis* viability makes it an intriguing therapeutic target.

A similar P450-catalyzed intramolecular coupling of phenols can be seen in herquline A (**93**) and herquline B (**91**), which are platelet aggregation inhibitors produced by *Penicillium* strains.[94–97] **93** has also been shown to inhibit replication of the influenza virus without notable toxicity to humans.[94] In contrast to the DKP core of **82**, **91** contains a reduced piperazine core, likely derived from a multitude of reductions on the L-Tyr-L-Tyr dipeptide. Both radical addition (route *a*) and diradical combination (route *b*) mechanisms can be proposed starting from diphenylpiperazine precursor **83** and the phenoxy radical **84** as shown in Scheme 18. Whereas the C-C coupled product **89** can undergo aromatization in mycocyclosin pathway, here **89** is proposed to be further reduced to yield the fused cyclohexanone structure **90**. While the stereochemistry of the coupling reaction is not known (and is also masked in mycocyclosin), it is expected that the two cyclohexanone rings will be oriented in *anti*-fashion to minimize steric and electronic clashes. Selective methylation of one of the nitrogen yields **91**, which may undergo isomerization to yield the α-β unsaturated **92** that be subjected to intramolecular 1,4-addition to yield **93**. The extensive number of reduction steps involved in herquline biosynthesis thus provide stark contrast to that of mycocyclosin.

Usnic acid (**98**) is a polyketide-derived substance widely found in lichens.[98–100] The biosynthetic proposal is shown in Scheme 19 in which two molecules of methylphloroacetophenone (**94**) are coupled regioselectively via radical intermediates **95** to form the dienone **96**. Again both radical addition and diradical combination (shown) can be proposed for this coupling step. As in the herquline pathway and will be seen repeatedly in following examples, 1,4-addition of the phenoxy oxygen to the dienone establishes the 6-5-6 ring system in hydrated usnic acid **97**, which can readily dehydrate to form **98**.

Viridicatumtoxin (**105**) is a meroterpenoid (polyketide-terpene hybrid) synthesized by the fungus *Penicillium aethiopicum* (Scheme 20).[101,102] The spirocycle-containing compound shows strong antibacterial properties especially towards methicillin resistant *Staphylococcus aureus* (MRSA).[103] The entire biosynthetic pathway of **105** has been mapped from genome sequencing and biochemically studied.[104,105] The anhydrotetracycline-like aglycone is synthesized by a polyketide synthase using malonamyl-CoA as a starter unit. A prenyltransferase VrtC was shown to perform Friedel-Craft like alkylation of the C ring with geranylgeranyl diphosphate as the electrophile to yield **99**.[106] The linear prenyl chain then must undergo two cyclization steps and form two new C-C bonds to yield **105**, a reaction that was surprisingly shown to be catalyzed by a single P450 VrtK.[104] The proposed mechanism, which is supported by DFT calculations, is shown in Scheme 20. The allylic C_{17} position is first proposed to undergo hydrogen abstraction to yield the radical **100**. A second electron transfer to the heme yields the allylic cation **101**. [OH•] rebound at the allylic radical site follow by loss of water may also lead to the cation **101**. From there, it was suggested that a C_{15}-C_{19} cyclization step can yield the C_{20} tertiary carbocation **102**, which can undergo concerted 1,2-alkyl shift and 1,3-hydride shift to yield a new C_{15} tertiary carbocation **103**. The origin of the two hydrogen atoms on C_{19} (shown in blue) is consistent with prior labeling studies using C_3-^{2}H-labeled mevalonate. From **103**, quenching of the carbocation by the aromatic D-ring (C_7) forges the second C-C bond (C_7-C_{15}) in **104** and rearomatization yields **105**. VrtK represents the first example of a P450 capable of catalyzing terpene cyclization, although its exact catalytic role in the C-C bond forming steps are not known.

The last example in P450 catalyzed C-C cyclization in fungi is that of brefeldin A (**111**), a potent inhibitor for blockade of secretory cargo moving from the endoplasmic reticulum to the Golgi organelles.[107–109] **111** is a bicyclic polyketide containing a cyclopentane fused to a 13-membered macrolide. Biosynthetic reasoning suggests the cyclopentane ring is formed via an intramolecular C-C coupling within the 16-membered macrolactone. The likely *bref* biosynthetic cluster was found in *Eupenicillium brefeldianum*.[110] Reconstitution of the *bref*-PKS and an associated hydrolase in yeast led to the formation of the triene acid **106**, which is of the same length (16 carbons) and expected functionalization required for formation of **111**.[110] The gene cluster encodes four P450 enzymes, one of which is proposed to be responsible for a radical mediated cyclization shown in Scheme 21. The activities of the P450s have not been reconstituted, thereby leaving timing of the cyclopentane formation in question. The inability of the reconstituted PKS to form the macrocycle provides some evidence for cyclopentane formation to proceed macrocyclization, with the former possibly rigidifying the hydrocarbon backbone for macrolactone formation. The P450 catalyzed C-C coupling can either take place on the PKS-bound intermediate **107** or the isolated linear acid **106**. Abstraction of the C_9 hydrogen to give **108** followed by radical addition to C_5 yields the allylic radical **109**, which can undergo [OH•] rebound to yield **110**. Further modification including C_7 hydroxylation and macrocyclization would yield **111**. A detailed study of the roles of the P450s is needed to complete the biosynthetic pathway.

2.2.3.2. Plant P450 Catalyzed Cyclization: P450-catalyzed C-C couplings are widespread in the plant kingdom, especially during alkaloid and phenylpropanoid biosynthesis.[111–113]

Recently, comparative transcriptome analysis has enabled the identification of many plant biosynthetic pathways in their entirety and has revealed the key P450 steps that have been elusive for many years.[114–116] A case in point is the biosynthetic pathway of morphine (**117**), which has been referred to as the king of alkaloids. A key step in forging the morphine scaffold is the C-C coupling of *R*-reticuline (**112**) to yield salutaridine (**116**) (Scheme 22A). In the 1950s, Barton and Cohen proposed that such a connection can be formed via phenolic coupling.[117] A P450 activity that catalyzes this reaction was first observed in the microsomal fractions of *Papaver somniferum* capsule.[118,119] Zenk et al observed that both NADPH and O_2 are required for the reaction, indicative of heme chemistry. Kutchan and coworkers identified CYP719B1 is the responsible P450, by first comparing P450 transcriptome profile to non-producing *P. somniferum* strains, followed by expression in insect cells and activity confirmation.[120] The enzyme exhibited very strict substrate specificity towards **112** and has essentially no activity towards all other structurally related isoquinoline alkaloids. Both radical addition via **114** (route *a*) and diradical coupling via **115** (route *b*) have been proposed for this reaction, with either one starting with abstraction of one phenolic hydrogen to generate the phenolate radical **113**. Under either mechanism, a single cycle of iron redox is sufficient to turn over the coupled product **116**. At nearly the same time, Sato and coworkers discovered a comparable P450 CYP80G2 in the biosynthetic pathway of magnoflorine (**120**) in *Coptis japonica*, which can perform phenolic coupling on *S*-reticuline (**118**) to yield *S*-corytuberine (**119**) (Scheme 22B).[121] Both CYP719B1 and CYP80G2 are close sequence homologs to berbamunine synthase (CYP80), which was discovered to catalyze C-O phenolic coupling during biosynthesis of bisbenzylisoquinoline alkaloids in higher plants.[122]

The Amaryllidaceae alkaloids which include galantamine (**125**), marithidine (**128**) and lycorine (**131**) display a variety of biological activities (Scheme 23).[123] **125** inhibits acetylcholine esterase and binds to nicotinic receptor, and has been used in the treatment of Alzheimer's disease.[124] These related alkaloids are all multicyclic compounds derived from L-Phe and L-Tyr, and go through a common intermediate norbelladine.[125] Following *O*-methylation by a specific methyltransferase to give 4-*O*′-methylnorbelladine (**121**)[126], a P450 is suggested to initiate phenolic coupling by hydrogen abstraction from the B ring. Delocalization of the radical on the *ortho* and *para* positions of the ring can lead to different coupling regioselectivity as shown in Scheme 23. Both radical addition and diradical combination mechanisms can be written for the coupling steps. Formation of different dienone intermediates are proposed depending on the coupling regioselectivity, each can undergo spontaneous 1,4-addition by either the phenolic oxygen in ring B or the secondary amine nitrogen to yield tetracyclic products. The $para_A$-$para_B$ connection, which occurs most readily under chemical conditions, leads to dienone **126**. Intramolecular 1,4-addition forms noroxomaritidine (**127**) (C-N bond) which can be reduced and methylated to yield **128**. The P450 enzyme CYP96T1 responsible for the coupling was identified from transcriptome analysis of producing plants.[127] The $para_A$-$ortho_B$ coupling product **123** can undergo 1,4-addition to yield the dibenzofuran **124**, which can be *N*-methylated to yield **125**.[127] The $ortho_A$-$para_B$ coupling product **129** can be converted to noroxopluviine **130**, which is the precursor to **131**.[127] The tandem P450-coupling/1,4-addition steps for Amaryllidaceae alkaloids parallel closely that of herquline A biosynthesis (Scheme 18),

although the former is from the plant world while the latter is found in fungi, demonstrating converging biosynthetic strategy to construct the constrained alkaloids.

The homo-coupling of monolignol (*E*)-coniferyl alcohol (**132**) to yield (+)-pinoresinol (**136**) is an essential step in the biosynthesis of plant lignans (Scheme 24).[128] One electron oxidation of **132** can readily generate the phenoxy radical **133**. Delocalization of the radical in the phenyl ring through resonance can lead to **134** and coupled products with different regioselectivity and stereoselectivity, in a process that at first appears random. Lewis and coworkers discovered a noncatalytic dirigent protein from *Forsythia intermedia* that is responsible for controlling the coupling step between the allylic coniferyl alcohol radical **134** to yield exclusively (+)-C_8-$C_{8'}$ linked product **135**, which can undergo addition by the hydroxyl group to yield the furanofuran **136**.[128] Mechanistic studies showed the dirigent proteins bind to the radical **134** with an apparent K_M of 10 nM, ~40,000-fold lower than that of the weak binding **132**, suggesting the radical species is the substrate and the dirigent protein spatially controls the diradical combination outcome.[129] Schaller and coworkers subsequently purified an enantiocomplementary dirigent protein from *Arabidopsis thaliana* that mediates the exclusive formation of (−)-pinoresinol (**137**).[130] A P450 CYP81Q1 catalyzes methylenedioxy bridge formation in **136** to yield sesamin (**138**),[131] a cyclization mode that will be discussed in Scheme 33 (Section 2.2.4). In addition to serving as a lignan build block, **136** is also the biosynthetic precursor to the antitumor podophyllotoxin as shown in Scheme 39 (Section 2.3.1).

2.2.4. C-O Coupling—In addition to catalyzing C-C bond formation and cyclization, P450s are also widely involved in the formation of C-O bonds. We have already seen an example of this in the formation of aryl ethers during vancomycin biosynthesis (Scheme 9, Section 2.2.1). This section will provide more examples of oxidative cyclization via C-O bonds catalyzed by P450s. As in the previous section, both radical addition or diradical combination mechanisms can be written for many of the reactions described here.

The first example is the formation of the grisan spirocycle in griseofulvin (**146**) biosynthesis (Scheme 25). Griseofulvin in a “classical” fungal polyketide that helped established the polyketide hypothesis. It was originally used as an antifungal drug, but recently has been shown to disrupt mitotic spindles and as a potential antitumor compound.[132–135] **146** is produced by various *Aspergillus* and *Penicillium* species, and the biosynthetic pathway from *P. aethiopicum* was elucidated first.[105,136] The carbon backbone is synthesized from a nonreducing PKS and undergoes one aldol and one Claisen cyclization to yield the benzophenone scaffold seen in griseophenone. Methylation and chlorination of the nascent cyclized product afford griseophenone B (**139**), which is the substrate of P450-catalyzed conversion to the grisan product desmethyl-dehydrogriseofulvin A (**145**). An additional *O*-methylation and enoylreduction yield the final product **146**.

The P450 GsfF catalyzes the oxidative transformation of benzophenone **139** to grisan structure **145** and formation of a oxa-spiro core. The activity was verified using yeast microsomes containing overexpressed enzyme. Two mechanisms (B and C) were initially proposed (Scheme 25). Mechanism B involves the formation and recombination of a diradical intermediate **142** through two successive phenolic hydrogen abstraction steps. In

mechanism C, the enzyme catalyzes epoxidation of A ring to **143** followed by nucleophilic opening of the epoxide by the B ring phenol to yield the hemiacetal **144** that can be aromatized to yields **145**. The C-O coupling step was studied computationally by Grandner et al, in which they concluded a third, mechanism A, is the most likely and energetically favorable.[137] This is the radical addition mechanism in which the enzyme performs the O-H abstraction on B ring to give **140**, but avoids diradical formation. Direct attack of the phenoxy radical on A ring leads to ring closure and intermediate **141**, subsequent phenolic O-H abstraction by the heme affords **145**.

An interesting contrast to the use of GsfF in forming the spirocycle is found in the (+)-geodin (**150**) and trypacidin (**154**) pathways, which contain a similar 6-5-6 spiro grisan structure derived from benzophenone precursors (Scheme 26). **150** is a common fungal metabolite produced by many strains, most notably *A. terreus*. After formation of dihydrogeodin (**147**) by the polyketide synthase and accessory enzymes, a multi-copper protein GedJ was found to be responsible for transformation into geodin.[138,139] The enzyme, dihydrogeodin oxidase (DHGO) shows significant sequence homology to other copper-containing oxidases, including laccase and ascorbate oxidase. Based on the known mechanisms of laccases,[27] formation of a phenoxy radical intermediate **148** and diradical coupling of **149** have been proposed (Scheme 26). The closely related **154** isolated from *A. fumigatus* was found to be a potential virulence factor and has a protective function against phagocytosis during invasion.[140,141] The gene clusters of **150** and **154** are highly homologous and a side by side comparison suggests TynJ is the responsible copper oxidase for C-O bond formation.[141]

Radical recombination is also proposed in the biosynthesis of tubocurarine (**160**), which is a monocationic, dimeric benzylisoquinoline alkaloid isolated from the South American plant *Chondrodendron tormentosum*.[142] The compound is an acetylcholine agonist and has been used as skeletal muscle relaxant in African arrow poison.[143,144] The biosynthesis involves a heterodimeric radical coupling between the enantiomers (*R*)-*N*-methyl-coclaurine (**155**) and (*S*)-*N*-methyl-coclaurine (**157**) (Scheme 27). Both building blocks are derived from dopamine and 4-hydroxyphenylacetaldehyde via Pictet-Spengler reaction (Section 3.2.2). A P450-catalyzed dimerization mechanism has been proposed in which diradical species of both enantiomers are formed. Two *O*-radicals are formed on the (*S*)-isomer in **156**, while two *C*-radicals are generated on the (*R*)-isomer via *O*-radical delocalization in **158**. Two regioselective C-O couplings between the diradical species forge two new C-O bonds in the dimer **159**, which can be methylated at one of the tertiary amine to yield **160**.

Another pathway where the diradical combination mechanism is likely at play is during the synthesis of aureothin (**165**), which is an antitumor, antifungal, and insecticidal compound isolated from *Streptomyces thioluteus* (Scheme 28).[145,146] The notable structural features include a nitroaryl moiety and an *exo*-methylene tetrahydrofuran (THF) ring. Biosynthetic studies revealed that the carbon backbone of aureothin is assembled by a modular PKS using *p*-nitrobenzoic acid as the starter unit.[147] Starting from **161**, formation of the *exo*-methylene THF moiety is catalyzed by a multifunctional P450 AurH, using a stepwise mechanism.[148–150] First, AurH catalyzes the hydroxylation of C_7 position to yield **162** using standard hydrogen abstraction and [OH•] rebound mechanism. Two possible routes are

likely to transform **162** into **165**. Route *a* requires a second P450 catalyzed hydroxylation at the C_{9a} position to yield **163**, followed by cyclization and dehydration to form the THF ring. Route *b* involves abstraction of two hydrogens from C_{9a} and the C_7 hydroxyl group during a single P450 catalytic cycle to generate the allylic *C*-radical and the *O*-radical in **164**, respectively. Diradical combination then furnishes the THF ring and the **165**.

Like the previous example, two mechanisms can also be proposed for cyclic ether bond formation during penitrem D (**171**) biosynthesis. Penitrems are tremorgenic mycotoxins isolated from several *Penicillium* species and are the most complex indole diterpenes isolated to date.[151–154] These compounds contain a paxilline backbone fused with a 6-4-8 tricyclic ring system. Formation of the six-membered ring involves a ring-expansion step that will be discussed in Scheme 135 (Section 6.2.6). Reconstitution of the biosynthetic pathway of penitrem A in *A. oryzae* revealed that the P450 PtmU is responsible for the construction of the eight-membered cyclized ether ring in **171** using secopenitrem D (**166**) as a substrate (Scheme 29).[155] The mechanism of the cyclization step is unresolved but is expected to be analogous to that of the THF ring in **165**. Two routes are proposed in which route *a* is diradical **168** formation and recombination; while route *b* is via hydroxylation of the cyclopentane ring in the paxilline core to give **169**, followed by dehydration to **170** and nucleophilic addition to arrive at **171.**

Pyrrocidine B (**173**)[156] and related compounds, such as hirsutellone B (**172**)[157], GKK1032A_2 (**174**)[158] and embellicine A (**175**)[159] (Scheme 30A), are multicyclic hybrid PK-NRP compounds isolated from different fungal species with various biological activities.[160] These compounds share several common structural features: a fused 6-5-6 decahydrofluorene core, a 13-membered and strained paracyclophane, and a 5-hydroxypyrrolidinone moiety derived from reductive cyclization catalyzed by PKS-NRPS (see section 3.2).[160] Early isotopic labeling studies of **174** carried out by the Oikawa group established the biosynthetic origin of the carbon backbone of the molecule.[161] Recently, Nay and coworkers performed feeding studies of **173** by using doubly labeled ^{18}O,^{13}C-L-tyrosine **176**.[162] The feeding studies confirmed that both of the labeled atoms were incorporated into **173**, suggesting that oxygen atom of cyclophane ether is derived from the nucleophilic phenolic oxygen of tyrosine. Several P450-catalyzed cyclization mechanisms can be proposed for morphing the acyclic PK-NRP product **177** into the paracyclophane as shown in Scheme 30B. In route *a*, cyclization is initiated through the allylic hydroxylation of the terminal C_{16} methyl to give **178**, which can trigger olefin rearrangement to yield a C_4 carbocation that can be quenched by the phenolate oxygen to form paracyclophane **182**. This common intermediate for all three mechanisms can undergo intramolecular Diels-Alder cyclization to yield the 6-5-6 ring system and **183**. In route *b*, epoxidation of the acyclic precursor to **179** can set up a general base/general acid catalyzed epoxide opening to form the cyclohexane ring **181**. Attack by the phenolate oxygen at C_4 is followed by dehydration to afford the Diels-Alderase substrate **182**. Finally in route *c*, P450-catalyzed hydrogen abstraction by the high-valent oxoiron yields a phenoxy radical **180** that can add to the triene system with the Fe^{IV}-OH as the second electron recipient to directly setup the diene and dienophile system in **182**. Following Diels-Alder cyclization, several tailoring steps complete the biosynthetic pathway to **173**. Regardless of which exact mechanism is used, it

is worth noting the rapid construction of all the rings systems of this family of compounds from a PK-NRP product via oxidation.

Salinamides are members of a family of unusual bicyclic depsipeptides with antibacterial and anti-inflammatory bioactivities isolated from the marine actinomycete *Streptomyces* sp. CNB-091 (Scheme 31A).[163–165] The backbone of salinamides is assembled by a NRPS and PKS hybrid biosynthetic pathway. A type I thioesterase performs an intermolecular transesterification of the salinamide aglycone with a (4-methylhexa-2,4-dienoyl)glycine handle to yield the monocyclic desmethylsalinamide C (**184**).[166] Forging an intramolecular C-O bond between the phenyl ring of the depsipeptide and the olefin of newly added handle is followed by epoxidation to yield salinamide A (**185**). This reaction was shown to be catalyzed by the P450 Sln10, but the exact mechanism is not known. A phenoxy radical addition mechanism can be proposed as shown in Scheme 31B. Following one hydrogen abstraction to yield the phenoxy radical **188**, addition of the radical to the terminal double bond in the ester handle yields a new radical species **189** that is stabilized by the conjugated α-β double bond. Abstraction of a second hydrogen by the Fe^{IV}=O heme center affords the *exo*-methylene intermediate **190**. Epoxidation of this compound by the same P450 installs the epoxide in **185**. This epoxide can be subjected S_N2 ring opening by either Cl^- or OH^- to yield salinamide B (**186**) or salinamide F (**187**), respectively.

Allene oxides (**193** and **196**) are unstable vinyl epoxides and are key biosynthetic intermediates to a series of plant signaling molecules.[167] The epoxides are formed by the enzymatic dehydration and cyclization of lipoxygenase-catalyzed peroxidation of polyunsaturated fatty acids, such as linolenic acid (**191**) and arachidonic acid (**194**) (Scheme 32). The responsible enzyme for this transformation is the P450 allene oxide synthase (CYP74A). A proposed mechanism is shown in Scheme 32 in which the first step is the homolytic cleavage of the O-O bond of the peroxide (either **192** or **196**) to generate an *O*-radical **197**. This is proposed to be catalyzed by the Fe^{III} state of the heme center. The *O*-radical can add to the adjacent C=C double bond to form the epoxide ring and an allylic *C*-radical **198**. One electron oxidation of this intermediate by the Fe^{IV}=O heme center yields the allylic carbocation **199**, which can form the vinyl epoxide by proton abstraction. Recently another type of allene oxide synthase was identified from corals, which is a catalase-like hemoprotein.[168] The allene epoxide sets up significant morphing of the linear fatty acid into jasmonic acid and clavulone I as described in Scheme 112 (Section 4.5).

The cyclized 1,3-benzodioxole functional group is a common structural unit found in many plant and microbial natural products. A list of representative compounds (**200**–**210**) is shown in Scheme 33A, in addition to the compounds already discussed in this review such as lycorine (**131**)[169] and sesamin (**138**)[170]. This ring system is formed via a methylenedioxy O-C-O bridge between phenylic oxygen and an *ortho* methoxy carbon, catalyzed by P450 enzymes as shown in Scheme 33B.[171–174] P450 catalyzes hydroxylation of the methoxy group **211** via a hydrogen abstraction and [OH•] rebound to form the hemiacetal **212**. After dehydration to **213**, the *ortho* hydroxyl group serve as nucleophile to attack the oxonium cation to form the new C-O bond in **214**.

2.2.5. C-N Coupling—Two examples of P450-catalyzed C-N coupling and intramolecular cyclization will be included here. The first is during biosynthesis of fumitremorgin C (**219**), which is a L-Trp-L-Pro diketopiperazine mycotoxin produced by *A. fumigatus* that has been well-characterized as a breast cancer resistance protein inhibitor (Scheme 34).[175–177] **219** contains a fused 6-5-6-6-5 rigid ring system that is formed after oxidative coupling between the amide nitrogen in the DKP ring and a C_5 prenyl chain grafted onto the indole ring. The biosynthetic gene cluster of **219** was recently identified by Osada and coworkers and studies showed the transformation from tryprostatin A (**215**) to **219** is catalyzed by the P450 FtmE.[178] Two oxidative mechanisms can be proposed for this reaction. The first step is hydrogen abstraction in the dimethylallyl unit to generate **216** of which the radical is stabilized by both the indole ring and the Δ^2-olefin. Subsequently in route *a,* a second hydrogen abstraction from the amide nitrogen generates a diradical intermediate **217** that can undergo recombination to yield **219**. Alternatively in route *b*, a second electron transfer from the allylic radical to the heme center yields the carbocation **218**, which can be quenched by the amide nitrogen to afford the rigidified ring system. It is interesting to note in many indole alkaloid pathways, the amide nitrogen originally derived from tryptophan acts as a nucleophile to attack the C_2 position of the indole ring to form a 6-5-*5*-6 ring system. In these cases, the C-N bond formation is triggered by either epoxidation of the indole ring as in the notoamide example (Scheme 106, Section 4.4.2), or alkylation of the C_3 position (such as prenylation[179] or methylation[180]). In the case of **219**, the oxidative cyclization occurs *exo* of the indole ring. **219** can still undergo indole epoxidation and further structural morphing to yield the spirocyclic spirotryprostatin as shown in Scheme 107 (Section 4.4.2).

The indole alkaloids teleocidin B (**220**) and lyngbyatoxin A (**221**) are bacterial natural products that share the same cyclic indole backbone (the indolactam V core, **222**) (Scheme 35). These compounds are potent activator of various protein kinase C isozymes,[181] making them potentially valuable reagents in pharmaceutical research. Biosynthetic studies of these compounds showed that **222** is cyclized from *N*-methyl-L-valyl-tryptophanol (**223**), which is synthesized by a bimodular NRPS that releases product as a free alcohol.[182–184] Cyclization of **223** into the 9-membered ring indolactam V structure is catalyzed by a P450, such as LtxB from the biosynthetic pathway of lyngbyatoxin A, via C-N coupling. Three different routes have been proposed for the mechanism of ring construction. Route *a* is via epoxidation on the phenyl ring of the indole moiety to give **224**, followed nucleophilic ring opening upon attack by the amine group to yield **225**. Rearomatizing the phenyl ring completes the cyclization to **222**. Route *b* is via a diradical coupling between the *C*-radical on the phenyl ring and the *N*-radical from the amine group in **227**, presumably catalyzed by two consecutive hydrogen abstraction (via **226**) by the heme center. Route *c* is via formation of the *N*-radical **226**, followed by radical addition to the phenyl ring and hydrogen abstraction that affords **228** and rearomatization to **222**. Alkylation of **222** by geranylgeranyl diphosphate leads to **221**.

2.2.6. C-S Coupling—Griseoviridin (**229**), belonging to the streptogramin family, is a cyclic polyunsaturated macrolactam produced by *S. griseoviridis* and exhibits broad-spectrum antibacterial activity (Scheme 36).[185] **229** contains a unique 9-membered lactone

with a thioene connection (S-C_2 linkage). The macrolactam backbone of **229** is biosynthesized by a hybrid PKS-NRPS assemble line featuring one oxazole derived from cyclization and dehydration of serine (Scheme 68, Section 3.3.3).[186] Gene inactivation experiments identified that a P450 monooxygenase, SgvP, is responsible for forging the thio-ene linkage starting with **232**.[187] Both epoxidation and radical mechanisms can be proposed for the C-S coupling catalyzed by SgvP, analogous to those outlined for **220**. Route *a* initiates with epoxidation of the α-β C_2-C_3 double bond to **233**, followed by nucleophilic attack of the thiol to open the epoxide ring and forms the C-S bond in **234**, and subsequent dehydration leads to **229**. Route *b* is the radical addition mechanism in which extraction of the thiol hydrogen leads to a *S*-radical in **235** that can add to the C_2-C_3 double bond in **236**. Abstraction the C_2 hydrogen results in the thio-ene moiety. Two other examples of cyclic natural products containing the thioether linkage, α-amanitin (**230**) and phallacidin (**231**) have been isolated from the mushroom *Amanita bisporigera*.[188] The biosynthetic origin and the enzymatic basis for these examples of C-S coupling remains unexplored.

2.3. Cyclization Catalyzed by Nonheme Iron α-KG-Dependent Oxygenases

In section 2.2, we have reviewed P450-catalyzed oxidative cyclization during natural product biosynthesis. The use of a high-valent oxoiron heme center to abstract hydrogen atoms from different scaffolds and heteroatoms is also catalyzed by nonheme iron α-KG-dependent oxygenases (Scheme 2). As in the previous section, different mechanisms of the transformations can also be proposed, including diradical recombination, radical addition, and cyclization mediated through [OH•] rebound. The examples in this section will also be grouped by the type of atom that is coupled to the carbon atom to forge the new cyclic structures.

2.3.1. C-C Coupling—Cycloclavine (**245**) is an ergot indole alkaloid produced by the fungus *A. japonicas* (Scheme 37).[189] The most notable structural feature of **245** is a cyclopropyl moiety fused to the ergot core. O'Connor and coworkers recently identified and heterologously reconstituted the pathway in *S. cerevisiae*.[190] The biosynthetic pathway, as with other ergot alkaloids, is derived from the oxidative cyclization of 4-dimethylallyl-L-tryptophan (**237**) through oxidation of the prenyl chain. Chanoclavine-I aldehyde (**238**) was shown to be a precursor of **245**, and is first proposed to undergo ene-reduction by the Old Yellow Enzyme (OYE) EasA to **239** and cyclize to yield the imine **240** (Scheme 37A). Tautomerization of the imine to enamine **241** then sets up the oxidative transformation by the nonheme iron α-KG-dependent enzyme EasH as shown in Scheme 37B. Two likely mechanisms of intramolecular cyclopropanation are shown. Route *a* involves the hydroxylation of the enamine **241** to **242**, followed by water elimination to **244**. Although chlorination of the same carbon is also possible using the mechanism discussed in Section 5.1, EasH lacks the active site motif that is signature of an oxidative chlorinase. Alternatively, route *b* involves hydrogen abstraction at the same position and radical migration to yield the intermediate **243**, which can undergo a second hydrogen abstraction by EasH to afford the iminium **244**, which can be reduced by EasG to yield **245**. In section 3.5.2, we discuss an alternative fate of **238** to yield lysergic acid.

Nogalamycin (**250**) is an anthracycline antibiotic produced by the soil-dwelling *S. nogalater* (Scheme 38).[191] Unlike other anthracyclines, **250** is derived from a diglycosylated anthracycline scaffold **246**. The C_7 position is glycosylated with D-olivose, while the unusual bicyclic ring systems attached to C_1 and C_2 are derived from rhodosamine. The O_1-rhodosamine deoxysugar is further coupled to the C_2 position via a new C-C bond, but is also epimerized at the $C_{4'}$ position to give nogalamine in the final product. Prior genetic studies showed that the glycosyltransferase SnoD and SnoE are glycosyltransferases that establish the classic *O*-glycosidic bonds at C_1 and C_7 respectively in **246**.[192] Recently, two α-KG dependent iron enzymes from the gene cluster were characterized.[193] SnoK was shown to catalyze the C-C bond formation of **248**. The radical mechanism is shown in Scheme 38, in which abstraction of $C_{5'}$ hydrogen to **247** and subsequently the C_2-hydrogen by the iron center can lead to radical coupling for formation of the new C-C bond in **248**. The other α-KG dependent iron enzyme SnoN was found to be the C4′ epimerase that affords nogalamycin R (**249**) via a diradical mechanism. It is interesting that SnoK and SnoN share 38% sequence identity and have very similar active sites as determined by X-ray crystallography, yet catalyze very different reactions in the late stage of this pathway.

In Scheme 24, we showed (+)-pinoresinol (**136**) is derived from the regioselective and stereoselective coupling of coniferyl alcohol radical in the presence of a dirigent protein. In mayapple, **136** is further modified into the antitumor natural product podophyllotoxin **262** as shown in Scheme 39.[114] The biosynthetic pathway of **262** is of considerable interest since the semisynthetic etoposide (**261**) is a front-line anticancer drug.[194,195] The transformation of **136** to (−)-pluviatolide (**253**) was known for some time, while the remaining pathway was recently mapped by Satterly and coworkers using tobacco plant as a heterologous host.[114] Successive introduction of candidate genes identified from transcriptome analysis enabled the heterologous production of (−)-4-desmethylepipodophyllotoxin (**260**), which is the precursor of the desired stereochemistry for **261** semisynthesis.[196] Of note in the pathway are several cyclization reactions, including dehydrogenation of (−)-secoisolariciresinol (**251**) to (−)-matairesinol (**252**); P450-catalyzed formation of methylenedioxy bridge in **253**, and the key C-C coupling in (−)-yatein (**254**) to forge the nonaromatic, 6-membered central ring of the 5-6-6-5 tetracyclic framework in (−)-deoxypodophyllotoxin (**258**). The responsible enzyme 2-ODD is a nonheme iron α-KG-dependent enzyme of which the activity was confirmed using purified enzyme. The proposed mechanism of 2-ODD is first the radical mediated benzylic hydroxylation to yield **255**, which can lose water to form the intermediate **256**. Aromatic addition to the enenone furnishes the C-C bond in **257** and rearomatization gives **258**. Identification and reconstitution of the entire set of enzymes required to transform pinoresinol to **260** sets the stage for a more scalable and cost-effective pathway to **261**.

2.3.2. C-O Coupling—Returning to ergot alkaloids briefly, the ergopeptine are well-documented toxins that can cause intoxications in mammals.[197] Dihydroergotamine (**266**) is a known precursor to some of the ergopeptine natural products. Biosynthesis of the diketopiperazine-derived core in **266** starts with two NRPSs, LPS1 and LPS2, that use D-lysergic acid as a starter unit and adds L-alanine, L-phenylalanine and L-proline to yield a tetrapeptide.[198] Intramolecular cyclization releases L,L-dihydroergotamam (**263**) as the product of the NRPS enzymes (Scheme 40). Cloning and characterization of *cp*EasH from

the ergot fungus *Claviceps purpurae* demonstrated this nonheme iron α-KG-dependent enzyme is responsible for the formation of the oxazolidinone ring found in **266**.[198] The reaction mechanism is proposed to be first hydrogen abstraction at the α-carbon of the alanine unit in the DKP substrate to give **264**, followed by [OH•] rebound to yield the transient hydroxylated intermediate **265.** Spontaneous attack of the newly introduced hydroxyl group on the prolyl amide carbonyl forms the oxazolidinone ring in **266**. Structural characterization of *cp*EasH was performed and showed this enzyme is highly similar to phytanoyl-CoA hydroxylase PhyH from humans.

Orthosomycins are oligosaccharide antibiotics that contain at least one interglycosidic spirocyclic *ortho*-δ-lactone linkages between a pair of carbohydrates.[199] This family of natural products are exemplified by avilamycin A (**267**), everninomicin D (**268**), and hygromycin B (**269**) (Scheme 41A), which are broad spectrum antibiotics.[199] The orthoether linkages are essential for the biological activities of these natural products. In both **267** and **268**, methylenedioxy bridges are also present. The biosynthetic gene clusters of **267** and **268** are large and encode up to fifty enzymes, many of them with unknown biosynthetic function.[200,201] Recently, Bachmann and Iverson and coworkers identified a group of conserved nonheme iron α-KG-dependent enzymes from the biosynthetic gene clusters and solved their X-ray crystal structures.[202] Although direct biochemical evidence is still lacking, the presence of long substrate channels in these structures, and co-crystal structure of HygX with **269** provide initial evidence that the orthoether linkages are forged by these enzymes. Genetic inactivation abolished the biosynthesis, further demonstrating their essential roles. The proposed mechanism for the orthoether linkage formation is shown in Scheme 41B. After formation of the high-valent Fe^{IV}=O ferryl oxo species, abstraction of hydrogen from the α-carbon of one sugar unit **270** forms the *C*-radical **271** and Fe^{III}-OH. A second hydrogen abstraction from the hydroxyl group forms the *O*-radical that can be combined with the *C*-radical to form the spirocyclic structure **272** and return the iron to the resting state. Although no direct evidence is available, the same enzyme may also catalyze the methylenedioxy bridge **275** starting with **273** with the same mechanism as proposed for P450 enzymes in Scheme 33 (Section 2.2.4), using a different prosthetic iron center.

Clavulanic acid (**286**) is a commercially important β-lactam that is produced by *S. clavuligerus* (Scheme 42).[203] It has a bicyclic ring system, consists of one 4-membered β-lactam and one 5-membered oxazolidine ring. Like penicillin and cephalosporinβ-lactams, the multicyclic ring system is derived from oxidative cyclization of a linear tripeptide **276** (Scheme 42A).[204] Following β-lactam formation to yield deoxyguanidinoproclavaminic acid (**277**), a nonheme iron α-KG-dependent enzyme clavaminate synthase (CAS) plays key roles in the remaining pathway.[205–212] CAS first catalyzes the stereoselective C_3 hydroxylation to yield guanidinoclavaminic acid (**278**), which can be hydrolyzed to proclavaminic acid (**279**). CAS then performs oxidative cyclization between the C_3 hydroxyl group and the $C_{4'}$ position in the β-lactam to yield dihydroclavaminic acid (**281**). CAS next performs a third oxidation reaction to dehydrogenatively form clavaminic acid (**285**), which can be eventually converted to **286**. Scheme 42B shows two of the proposed mechanisms for CAS in the cyclization step. Route *a* is similar to the mechanism discussed in the formation of the orthoether linkage in Scheme 41. The hydrogen on $C_{4'}$ can be first abstracted by the

Fe^{IV}=O ferryl species to form the *C*-radical **280**. A second hydrogen abstraction on the C_3 hydroxyl group and accompanying C-O coupling forms the oxazolidine ring and **281**. In route *b*, the first hydrogen abstraction is on the hydroxyl group to form *O*-radical **282**, followed by a retro-aldol-like decomposition to form an aminoaldehyde and a C_2 radical **283**. After another hydrogen abstraction from $C_{4'}$ to yield the azomethine ylide **284**, a 1,3-dipolar cycloaddition between the ylide and the aldehyde forms the **281**. Regardless of the mechanism, CAS is a remarkable enzyme that catalyzes three different oxidation reactions in one biosynthetic pathway: hydroxylation, C-O oxidative cyclization and dehydrogenation. The crystal structure of CAS showed an unusual jellyroll fold uncharacteristic of this family of enzymes.[213,214]

Another iterative nonheme iron α-KG-dependent oxygenase is hyoscyamine 6β-hydroxylase (H6H) found in the biosynthetic pathway of the classic plant alkaloid scopolamine (**290,** also known as *S*-hyoscine) (Scheme 43A).[215–217] **290** is a tropane alkaloid that is used in the treatment of motion sickness and postoperative nausea. The tropane portion is derived from putrescine (**287**), which originated from L-ornithine. The phenyl portion is derived from L-phenylalanine via oxidative rearrangements catalyzed by P450. Conversion hyoscyamine (**288**) to **290** is catalyzed by H6H via two successive oxidation steps (Scheme 43B). In the first step, H6H catalyzes the hydroxylation at the C_6 position via hydrogen abstraction and [OH•] rebound to yield 6β-hydroxyl-hyoscyamine **289**. The second step catalyzed by H6H is the oxidative cyclization to form the epoxide. The likely mechanism is first abstraction of hydrogen from C_7 to generate a *C*-radical (**291**), followed by abstraction of hydrogen from the freshly introduced C_6-OH to facilitate radical C-O coupling.

Verruculogen (**292**) is a tremorgenic mycotoxin produced by various *Aspergillus* and *Penicillium* strains (Scheme 44A).[218] The most unusual feature of **292** and its prenylated derivative fumitremorgin A (**293**) is the eight membered endoperoxide ring bridging the two middle rings of the 6-5-6-6-6 system. We have previously discussed the P450 catalyzed C-N bond formation that gives rise to the unusual 6-5-6-6-6 system in fumitremorgin C (**219**) (Scheme 34, section 2.2.5). Further modification in *A. fumigatus* converts **219** to fumitremorgin B (**294**), which is *N*-prenylated in the indole ring and hydroxylated in the middle ring (at C_{13}). FtmOx1 is a nonheme iron α-KG-dependent oxygenase that connects the two linear prenyl chains in **294** with molecular oxygen to yield the endoperoxide-containing ring of **292**.[219] The crystal structure of FtmOx1 was solved and detailed mechanistic studies were carried out by Zhang and coworkers.[220] The results from the assays with different ratios of α-KG/FtmOx1/substrate suggested one equivalent of α-KG and two equivalents of O_2 were consumed during each turnover. The C_{13} ketone version of **292**, **295**, is the dominant product under the assay conditions. One important finding is that a tyrosine residue (Y224) was confirmed to participate in the catalytic cycle of FtmOx1 during endoperoxide formation.

A radical mechanism was proposed for the endoperoxide formation as shown in Scheme 44B. The first molecule of oxygen is activated to form the active species Fe^{IV}=O. Then a tyrosine (Y224) *O*-radical was formed through a hydrogen abstraction step. This phenoxy radical then abstracts a hydrogen from the *N*-linked prenyl group to yield **296** which is a *C*-radical that can be resonance stabilized. The *C*-radical then adds to a second molecule of

oxygen to yield a peroxyl radical **297**, which can undergo radical addition to the olefin present in the prenyl chain of the neighboring ring to forge the endoperoxide ring and the *C*-radical **298**. Y224 is then re-oxidized to a tyrosine *O*-radical and affords **292**. Starting from here, two pathways are possible: in the first pathway, this tyrosine *O*-radical can restart the catalytic cycle to turnover additional endoperoxide **292** from **294**. In the second and more dominant pathway observed under assay conditions, a two electron oxidation of the C_{13} hydroxyl group in **292** to **295** reduces the iron in FtmOx1 back to the resting state.

2.3.3. C-N Coupling—The examples in this section are not direct radical coupling between carbon and nitrogen atoms. Instead, these example illustrate a sequence in which a nonheme iron α-KG-dependent enzyme catalyzes oxidation of unactivated C-H bond leading to an electrophilic carbon that can be subjected to nucleophilic attack by a nitrogen to form a new C-N bond and a cyclic structure. We previously illustrated this example in the P450-catalyzed conversion of holyrine (**47**) to staurosporine (**20**) (Scheme 14, Section 2.2.2). In both examples here, formation of unnatural, cyclized amino acids that are incorporated into NRP assembly lines are illustrated.

The tuberactinomycin family natural products, such as viomycin (**299**) and capreomycin IIA (**300**) (Scheme 45) are pentacyclic NRPs produced by different actinomycetes and display anti-tuberculosis activity.[221] The common pharmacophore of this family has a number of nitrogen-containing unnatural amino acids, including the cyclic guanidine *2S,3R*-capreomycidine (**301**), β-lysine and β-ureidodehydroalanine. The cyclic guanidine is essential for the activity of the tuberactinomycin compounds and has been found to be derived from L-arginine (**302**). Two enzymes are required for the cyclic C-N bond formation.[222,223] The first enzyme (VioC) is a nonheme iron α-KG-dependent oxygenase that hydroxylates the β-position of **302** to yield *3S*-OH-L-arginine **303**. The second enzyme (VioD) is a pyridoxal phosphate (PLP) dependent aminotransferase that reacts with *3S*-OH-L-arginine to form an PLP-imine **304**. Elimination across α-β carbons affords (*E*)-2,3-dehydroarginine/PLP adduct **305**, which can undergo cyclization by nucleophilic attack of the guanidine amine to give **306** and subsequent product release to afford **301**.

Methylproline residues are found as building blocks in numerous NRP natural products, such as echinocandin B (**307**)[224], nostopeptolide A1 (**308**)[225], polyoxypeptin B (**309**)[226], griselimycin (**310**)[227], perthamide C (**311**)[228], and monamycin D (**312**)[229] (Scheme 46A). Different combinations of methyl substitution regioselectivity and stereochemistry on the prolyl ring have been observed, including 2*S,4R*-4-methylproline (**317**), *2S,4S*-4-methylproline (**321**), and 2*S*,3*S*-3-methylproline (**326**). The dedicated biosynthetic machinery for synthesizing **317** and **321** have been found, all originating from the acyclic aliphatic amino acid L-leucine (**313**) (Scheme 46B). In the echinocandin pathway, formation of **317** requires EcdK, a nonheme iron α-KG-dependent oxygenase.[230] Enzyme assays support the mechanism of consecutive hydroxylation of the terminal methyl to yield 4*R*-5-OH-leucine first then the *gem* diol product **314**, which can dehydrate to form the γ-methyl-glutamic acid-γ-semialdehyde (**315**) that can exist in equilibrium with the cyclic imine 3*R*-methyl-Δ^1-pyrroline-5-carboxylic acid (**316**). Subsequent reduction in an NAD(P)H-dependent fashion can afford **317**. Although no such reductase was found in the *ecd*

pathway, it was proposed that the pyrroline-5-carboxylate reductase from the proline biosynthetic pathway could be shared. In the biosynthesis of **321** for nostopeptolide assembly in *Nostoc sp.* GSV224.6, Moore and coworkers showed following the first hydroxylation to yield 4*S*-5-OH-leucine (**318**), an NAD^+ dependent alcohol dehydrogenase NosE catalyzes the dehydrogenation of the hydroxyl group to form the aldehyde **319**.[231,232] The cyclized imine **320** can be reduced by NosF, a dedicated reductase to yield the building block **321**. Ogawa subsequently found an α-KG dependent leucine 5-hydroxylase in *Nostoc punctiforme* that can hydroxylate **313** to **318**, suggesting this enzyme is widely present in other *Nostoc* species, including the nostopeptolide producer.[233] Hence the two examples above provide contrasts in biosynthetic strategy to generate the 4-methylproline piece. In fungi, a radical mechanism via α-KG oxygenase is employed all the way to the aldehyde product, while in bacteria the first hydroxylation is radical dependent but the second oxidation is NAD^+ dependent, a route that will be discussed more in section 3.5. Although the exact enzymes in biosynthesis of **326** have not been identified, it is expected that similar transient oxidation of the C_5 position in L-isoleucine (**322**) followed by cyclization and reduction are involved (Scheme 46B).

2.4. Other Fe-Dependent Oxygenases and Oxygen-Independent Radical Cyclases

Besides P450 and nonheme iron α-KG-dependent oxygenases, nature also uses an arsenal of other iron-dependent oxygenases in oxidative cyclization. These include i) mononuclear, nonheme dependent oxygenase, such as HppE involved in epoxide formation in fosfomycin biosynthesis, and isopenicillin N synthase (IPNS) in penicillin biosynthesis; and ii) Rieske-type oxygenases that are non-heme iron-dependent oxygenases using a [2Fe-2S] cluster as one electron mediators.

In addition there is an extensive set of molecular oxygen–independent cyclases that work by radical mechanisms. These are the radical SAM enzymes that use bound 4Fe-4S clusters to cleave SAM into methionine and 5′dA•, the latter serving as the radical initiator. This section will cover notable examples of cyclization catalyzed by enzymes in each of these subfamilies.

2.4.1. Noncofactor Fe-Dependent Peroxidase: Fosfomycin Biosynthesis—

Fosfomycin (**332**) is a representative member of the phosphonate family of natural products, all of which contain a C-P bond that is rarely observed among primary metabolites (Scheme 47A).[234,235] **332** is a clinically useful antibiotic produced by various *Streptomyces* and *Pseudomonas* species.[236] The warhead of **332** is the epoxide ring and its biological target is uridine diphosphate (UDP)-*N*-acetylglucosamine enolpyruvyl transferase (MurA), which catalyzes the first committed step in bacterial cell wall peptidoglycan assembly.[237] Biosynthetic studies had shown that the biosynthesis of all phosphonates start with the action of PEP mutase, which isomerizes phosphoenolpyruvate (**327,** PEP) into phosphonopyruvate (**328**). Following decarboxylation to **329**, aldehyde reduction to HEP (**330**), and *C*-methylation by a radical SAM-and cobalt-dependent enzyme (Fom3), the immediate precursor to **332,** (*S*)-2-hydroxypropylphosphonate (**331**, *S*-2-HPP) is formed.[238] The last step is the oxidative cyclization of **331** to form the epoxide ring and **332**, which is catalyzed by a mononuclear non-heme iron dependent enzyme HppE.[239,240] HppE has a

cupin fold that is associated with other noncofactor dependent oxygenases.[241] The mechanism of HppE remained elusive, especially with regard to the nature of the oxidant. Recent studies by Liu and coworkers confirmed that HppE is actually a non-heme iron peroxidase.[242]

The mechanism for the H_2O_2-driven epoxide ring formation is shown in Scheme 47B: the substrate **331** is first coordinated to the active site Fe^{II} through the C_2 oxygen and one of the phosphate oxygen atoms (in addition to two His and one Asp residue from HppE) to give **333**. Reduction of H_2O_2 to H_2O leads to the formation of the high-valent Fe^{IV}=O reactive species **334**, which abstract a hydrogen from the C_1 methylene to form **335** and is followed by an additional one electron oxidation to form a C_1 carbocation **336** that can be stabilized by the adjacent phosphonate. Quenching of the carbocation **336** by the C_2 oxygen forms a new C-O bond and completes the biosynthesis of the epoxide ring in **332**. The notable feature of the overall reaction catalyzed by HppE is that the oxygen atom in the epoxide ring originates from the C_2-hydroxyl group of **331**, not from H_2O_2 or O_2. During the mechanistic studies of HppE, this enzyme was shown to catalyze two interesting reactions when alternative substrates are used (Scheme 47C): *R*-2-HPP (**337**) is converted to the ketone **338**, while *S*-1-HPP (**339**) is converted to the aldehyde **340** via oxidative 1,2-phosphono migration reaction.[243,244]

2.4.2. Noncofactor Fe-Dependent Oxidase: Penicillin and Cephalosporin Biosynthesis—Penicillins and cephalosporins are well known β-lactam antibiotics for the treatment of bacterial infections. The β-lactam antibiotics irreversibly inhibit the function of transpeptidase that are essential to the biosynthesis of the bacterial cell wall peptidoglycan.[245] The shared precursor to penicillins and cephalosporins is isopenicillin N (**345**), which is synthesized in two steps (Scheme 48A).[246,247] In the first step, a trimodular NRPS ACV synthetase assembles the tripeptide precursor δ-(L-α-aminoadipoyl)-L-cysteinyl-D-valine (ACV) (**344**). The linear tripeptide **344** is then oxidatively cyclized into the fused 4,5-ring system in **345** by the non-heme iron dependent oxidase, isopenicillin N synthase (IPNS). In the biosynthetic pathway to cephalosporins, **345** will be epimerized to penicillin N, followed by ring expansion of the 4,5-fused ring system into the 4,6-fused ring system by deacetoxycephalosporin C synthetase, another non-heme iron dependent enzyme, which will be discussed in Scheme 131 (Section 6.2.2).

Mechanistic studies of the IPNS have been performed for decades and we will only briefly summarize here as other reviews can provide more detailed analysis. As shown in Scheme 48B, the reaction proceeds in two stages, each resulting in a two electron oxidative cyclization via C-H bond cleavage. The net result in terms of oxygen consumption is that one O_2 is reduced by four electrons into two water molecules, therefore the cofactor α-KG is not needed. In the first stage, the substrate **344** and molecule oxygen bind to the active site iron center, forming the peroxide radical **347**, which can abstract a hydrogen from the β-carbon of the cysteine residue to form the *C*-radical **348** (first C-H cleavage). After this, a C=S double bond and **349** is formed with one electron reduction of the Fe^{III} to Fe^{II}. Nucleophilic attack of the valinyl amide nitrogen on the thioaldehyde forms the β-lactam ring in **350**, this is accompanied by cleavage of the peroxo bond to generate Fe^{IV}=O and loss

of water. In the second stage, a valinyl radical **351** is generated via hydrogen abstraction by the ferryl-oxoiron (second C-H cleavage). Attack of the valinyl radical on the sulfur yields the new C-S bond and thereby the thiazolidine ring in **352** and completes the penicillin core structure that is released as **345**. Recent transient-state kinetics and spectroscopic methods with labeled substrates led to the identification of both C-H cleavage intermediates (**348** and **351**), thus validating the proposed mechanism.[248] We also note the comparison to the 4,5-lactam-oxazolidine ring system formed during clavulanic acid (**286**) biosynthesis in Scheme 42 (Section 2.3.2). There the β-lactam ring is formed nonoxidatively and α-KG is used as cofactor by CAS to generate the high valent ferryl oxoiron required for the oxazolidine ring formation.

2.4.3. Rieske Oxygenase: Prodiginine Biosynthesis—Prodiginines, including metacycloprodigiosin (**353**)[249], streptorubin B (**354**)[250], and marineosin A (**355**)[251], are a family of red-pigmented compounds containing the tri-pyrrole moiety (Scheme 49A). These 10- and 12-membered carbocycles have different bioactivities, such as immunosuppressive and anticancer activities, and are produced by both Gram-positive and Gram-negative bacteria.[252,253] The most interesting connectivities in the structures of members in this family is the C-C bond between the pyrrole ring and the unreactive alkyl side chain. Oxidative cyclizations of the carbocycle from the acyclic precursors in **353** and **354** are catalyzed by the Rieske non-heme iron-dependent oxygenases McpG and RedG, respectively.[254] The substrate of these enzymes is the linear undecylprodigiosin (**356**), which is derived from the condensation of 4-methoxy-2,2′-bipyrrole-5-carbaldehyde and 2-undecylpyrrole.[255] The differences in regioselectivity and stereoselectivity of the C-C bond forming step lead to different products as seen in Scheme 49A.

Rieske oxygenases are non-heme iron-dependent oxygenases with a *N*-terminal [2Fe-2S] cluster and a *C*-terminal nonheme iron center. Electron transfer from the [2Fe-2S] cluster to the iron center is facilitated by a hydrogen bond network between them. The proposed catalytic cycle of RedG is shown in Scheme 49B: after the substrate **356** and oxygen sequentially bind to the nonheme iron center, and with the assistant of one electron transfer from the [2Fe-2S] cluster, the Fe^{III}-OOH complex abstracts the *pro-R* hydrogen from the alkyl chain of **356** and generates the Fe^{IV}=O species.[256] The *C*-radical in the **357** then adds to the pyrrole ring stereoselectively to form the new C-C bond and the (*S*)-configured carbocycle **358**. Another hydrogen abstraction from the hydropyrrole ring by the ferryl oxoiron, followed by rearomatization forms the pyrrole ring and the product **354**. Reduction of the active iron center to the resting state releases the product.

In the biosynthetic pathway of **355**, the enzyme responsible for the oxidative cyclization is MarG, which is a homolog to RedG and McpG.[257] The C-H cleavage and C-C bond forming steps of MarG are similar to RedG starting from the acyclic **359** and the radical intermediates **360** and **361**. A subsequent nucleophile attack of the terminal hydroxyl group on the double bond of **362** forms an additional 6-membered ring fused to the carbocycle (Scheme 49C).

2.4.4. Radical SAM Enzyme: C-C Coupling—The mechanism of radical SAM enzymes is shown in Scheme 3. Although radical SAM-mediated oxidative cyclization is not

as widespread as the other iron-dependent enzymes shown above, several notable examples warrant discussion here. Because of the autoxidizable 4Fe/4S cluster that is the donor of one electron to the bound SAM substrate, the radical SAM enzyme family not only does not use O_2 as cosubstrate, this enzyme family is inactivated by O_2 so these reactions run in anaerobic microenvironments.

Streptide (**363**) is a ribosomally biosynthesized peptide (RiPP) that produced by *Streptococcus thermophiles*, a non-pathogenic streptococcal model strain used in the fermentation of dairy products.[258] Previous studies by Monnet and co-workers demonstrated that **363** is a nonapeptide processed from a 30-mer ribosomally translated precursor **364**.[259–261] Recently, Seyedsayamdost and coworkers solved the structure of this compound and elucidated the biosynthetic pathway (Scheme 50).[258] A macrocycle is generated by forming a C-C bond between the C_β of the terminal lysine residue and C_7 of the phenyl ring of a tryptophan residue. This key oxidative cyclization step is catalyzed by a radical SAM enzyme StrB acting on the 30-mer precursor peptide **364**. A mechanistic model for the oxidative coupling of the otherwise unreactive carbons is shown in Scheme 50. The first step is to form the radical reagent, 5′-dA•, from SAM and iron-sulfur clusters in the active site of StrB. The 5′-dA• initiates the radical mediated cyclization by first abstracting a hydrogen from the C_β of the Lys residue to form a new *C*-radical **365**. This is followed by radical addition to the phenyl ring of the Trp residue, creating the Lys-to-Trp crosslink and an indolyl radical **366**. Reduction of the auxiliary iron–sulfur cluster together with deprotonation and rearomatization complete the biosynthesis of the cross-linked peptide **367**, which can be further processed by a protease to give **363**.

Menaquinone (**374**), also known as vitamin K2, is a membrane-soluble molecule that delivers electrons to protein complexes in the respiratory chain. The classic biosynthetic pathway of **374** involves eight steps starting from chorismate.[262] Dairi and coworkers discovered an alternative chorismate-derived pathway to menaquinone biosynthesis, named the futalosine pathway (Scheme 51).[263] Futalosine (**368**) is converted to dehypoxanthine futalosine (DHFL, **369**) by the hydrolase MqnB, followed by a C-C coupling step that affords cyclic-DHFL (CDHFL, **372**) by the radical SAM enzyme MqnC. The spirocyclic **372** is further converted to 1,4-dihydroxy-6-naphthoic acid (**373**), the precursor to **374**. The proposed mechanism of the oxidative cyclization catalyzed by MqnC[264] is a radical addition mechanism that parallels that proposed for the cyclization step of streptide shown above. After 5′-dA• mediated generation of the *C*-radical **370**, radical addition to the phenyl ring forges the new C-C bond in **371**. Deprotonation and one electron oxidation yields **372**.

Jawsamycin (FR900848, **378**) is a potent antifungal natural product produced by *Streptoverticillium fervens* HP-891 (Scheme 52A).[265] It is one of only two natural products isolated to date that contain the highly unusual polycyclopropanated fatty acyl chain, which has resemblance to the jaws of sharks that accounts for the compound name. In **378**, the polycyclopropanyl chain is amidated with 5′-amino-5′-deoxy-5,6-dihydrouridine. Feeding studies suggested the fatty acyl chain is derived from a polyketide pathway, while the methylene groups of the cyclopropane units are derived from L-methionine.[266,267] Recently, Oikawa and coworkers identified and heterologously reconstituted the biosynthetic pathway of **378**.[268] A notable finding is that a set of three enzymes are responsible for forming the

polycyclopropanated polyketide, they are the iterative PKS Jaw4 (KS-AT-DH-ACP), the associated ketoreductase Jaw6 and the radical SAM enzyme Jaw5. Based on the lack of polyketide production in the absence of Jaw5, and the incorporation of the cyclopropanated acyl fragments into the final product, it is proposed that Jaw5 functions on the α–β unsaturated polyketide acyl chain after each iteration of chain extension, ketoreduction and dehydration.

Two possible mechanisms are proposed for the Jaw5-catalyzed cyclopropanation, using the first polyketide intermediate crotonyl-ACP **375** as an example (Scheme 52B). The two mechanisms use reactive species of SAM generated by 5′-dA•, hence two SAM per catalytic cycle are consumed as in other radical SAM methyltransferases.[269] The first hydrogen abstraction facilitated by 5′-dA• yields the SAM methyl radical **383**, which may receive an electron from the [4Fe-4S] cluster to become the SAM ylide **384** (Scheme 52C). In route *a*, SAM ylide **384** performs a 1,4-addition on **375** to generate the adduct **379**, which can eliminate SAH to yield the methylcyclopropyl thioester **376**. In route *b,* direct attack of the SAM radical **383** on the double bond in **375** yields the adduct **380** that can afford **376** through the elimination of the SAM radical carbocation, which can be further reduced to SAH by receiving one electron from the [4Fe-4S] cluster. The cyclopropanated polyketide intermediate **376** is then proposed to undergo additional chain extension to assemble the full length polyketide product that will be ligated to 5′-amino-5′-deoxy-5,6-dihydrouridine. Effectively, Jaw5 becomes part of the PKS programming cycle to stereoselectively convert the α–β unsaturation into the *R*-cyclopropane. Interestingly, the timing of Jaw5 is stringently controlled as three of the unsaturations are retained in the final structure, suggestive of close coordination of the three enzymes during construction of the remarkable compound.

2.4.5. Radical SAM Enzyme: C-S Coupling—Biotin (**389**) is used as an enzyme cofactor in many enzyme-catalyzed reactions involving CO_2, such as carboxylation, decarboxylation, and trans-carboxylation (Scheme 53). The structure of **389** contains a ureido (tetrahydroimidizalone) ring fused to a thiophane ring (5,5-ring system). The last step in biotin biosynthesis is the insertion of sulfur into dethiobiotin (**385**) to form the thiophane ring, and is catalyzed by a radical SAM enzyme named biotin synthase. Mechanistic studies confirmed that the [4Fe-4S] cluster is responsible for the 5′-dA• formation, while a separate [2Fe-2S] cluster is responsible for sulfur insertion and cyclization.[270–274] A brief mechanism is shown in Scheme 53: following homolytic cleavage of the C-H bond in the methyl group by 5′-dA•, attack of the resulting *C*-radical **386** on the μ-sulfide within the [2Fe-2S] cluster forms the first C-S bond and 9-mercaptodethiobiotin **387**. Subsequently, a new 5′-dA• radical cleaves a second C-H bond in the methylene group. The new *C*-radical **388** attacks the same sulfur atom completes thiophane ring formation and releases **389** from biotin synthase.

The 35-residue head-to-tail cyclized subtilosin A (**390**) is a ribosomally synthesized antibiotic produced by soil bacterium *Bacillus subtilis* (Scheme 54A).[275,276] It belongs to the sactipeptide family that features unusual sulfur to C_α thioether bridges that rigidify the macrocycle at multiple positions. In **390**, there are three thioether bridges of which two are between cysteine thiol and C_α-Phe and one is between cysteine thiol and C_α-Thr. Recent

biosynthetic studies showed that the formation of all three thioether bridges are catalyzed by a radical SAM enzyme AlbA that acts on the linear 43-mer precursor peptide.[276,277] Similar to streptide biosynthesis (Scheme 50), completion of oxidative cyclization is followed by leader peptide cleavage and macrocyclization to yield **390**, which is exported to the extracellular space by an ABC transporter.

A C-S radical coupling mechanism was first proposed to account for the reaction catalyzed by AlbA.[276] As shown in Scheme 54B, the reaction is initialed by the removal of a proton from the thiol group to form the iron-sulfur coordinate bond in **391**, with the iron coming from the [4Fe-4S] cluster. Then cleavage of SAM generates a 5′-dA• radical that can cleave the C_α-H bond in either the Phe or Thr residue. The resultant *C*-radical **392** is then coupled to the cysteine thiol to release from the [4Fe-4S] cluster and form one thioether bridge. More recently, Berteau and coworkers performed mutagenesis studies on AlbA and proposed a different nucleophilic addition mechanism (Scheme 54C).[277] The first step is proton abstraction from the cysteine thiol but no Fe coordination. The second step remains the 5′-dA• mediated cleavage of C_α-H bond to form the C_α radical **393**. However, instead of radical coupling as in Scheme 54B, the C_α radical migrates to become an *O*-radical **394** through resonance, and is further transformed to an imine **395** by one electron oxidation. Finally, the C-S thioether bond is formed through the nucleophile addition of deprotonated thiol to imine.

3. NONRADICAL CYCLIZATION MECHANISMS

3.1. Introduction

The previous section dealt with a set of cyclizations initiated by oxidative reactions proceeding through carbon radical intermediates, many of them driven by enzymatic reductive activation of molecular oxygen. Analogously, the next section in this review deals with oxygenases in the form of epoxide-mediated cyclizations.

In this section we consider ring formations attendant with or subsequent to **two electron redox pathways.** These can, in a few cases involve enzymatic reductions that set up cyclizations, as in nostocyclopeptide, saframycin and ikarugamycin assembly, but are largely cyclizations enabled by oxidation of substrates. The oxidations can involve hydride transfers from substrates as in the berberine bridge and related flavoenzymes, or can yield carbonyl groups that undergo intramolecular capture, as in spirocycle formation in reveromycin. Internal capture of transient imines occurs in scaffolds as simple as the pipecolic acid building blocks and as complex as in fumiquinazolines C and D and saframycin.

We also take up a set of biosynthetic transformations that are formal [4+2] cyclizations, including solanapyrone, lovastatin, spinosyn, abyssomycin and pyrroindomycins. In some of these enzyme cases evidence for Diels-Alder concerted mechanisms is gradually accruing. The cyclizations themselves, whether stepwise or concerted, are nonoxidative and will be covered in a review by Liu et al in this issue. However, the prior enzymatic steps, setting up the diene and dienophile combinations are oxidative. Viewed in this context we look at the two step enzymatic logic for such biosynthetic cyclopentyl and cyclohexyl ring constructions.

Scheme 55 depicts four general possibilities for the reactions in this section. Scheme 55A involves reduction of a carboxylic acid derivative (typically a thioester) to the aldehyde, followed by internal capture by an amine nucleophile. Scheme 55B schematizes intramolecular attack by a nucleophile concomitant with, or after, hydride transfer out of a substrate. Scheme 55C reflects oxidation of a substrate alcohol or amine group to the carbonyl or imine followed by internal capture by a nucleophile. Often subsequent reduction occurs as in pipecolate formation. Scheme 55D suggests assembly-line redox transformation to set up the diene or dienophile for subsequent [4+2] (or perhaps [6+4]) ring-forming reaction.

3.2. Reduction-Enabled Cyclization

In the biosynthesis of polyketide and nonribosomal peptide frameworks by PKS and NRPS assembly lines, the polyketide or peptidyl chains grow as a series of elongated thioesters, tethered to carrier protein domains.[278] The canonical mechanism of product release is through the redox-neutral mechanisms of hydrolysis, esterification and amide formation.[40,279] This is the basis for forming most macrocycle natural products. There are also increasing examples of NAD(P)H-dependent reduction as a release mechanism. The mechanism involves first the reduction of the thioester **396** to the thiohemiacetal **397** by hydride transfer, and this tetrahedral adduct decomposes spontaneously to release the aldehyde product **398** (Scheme 56A). Sometimes the aldehyde can persist, but in many cases the aldehyde is captured by intramolecular nucleophilic attack to form a cyclized product. Attack by alcohol can yield hemiacetal, while attack by amine can lead to imino formation. Alternatively, in PKS-NRPS assembly lines, the aldehyde can be attacked by the C_α carbon of the 1,3-diketo group of the polyketide fragment to yield tetramate or pyrrolidone structures. These examples are abundant, here only a few will be highlighted.

3.2.1. Nostocyclopeptide: Reductive Release from NRPS—Nostocyclopeptides, such as nostocyclopeptide A2 (**401**), are cyclic peptides produced by terrestrial cyanobacterium *Nostoc* sp. ATCC53789 (Scheme 56B).[280] Several features of **401** are worth noting, including the incorporation of the unnatural amino acid such as 4-methylproline of which the formation was discussed in Scheme 46 (Section 2.3.3). The imino linkage between the α-amino group of Tyr1 and the carbonyl of Phe7 suggests reductive release of the nascent linear heptapeptide **399**. This was reflected in the last module of the NPRS in which a Reductive domain (R) was found.[281] The formation of an aldehyde intermediate **400** in an NADH fashion and the subsequent capture by amino of Tyr1 was confirmed in vitro.[282] The carbinolamine adduct loses water and the cyclic imine is stable as found in the accumulating product.

3.2.2. Saframycin: Iterative Pictet-Spengler Condensations—Saframycins including saframycin A (**413**) are NRP-fatty acid hybrid compounds produced by *Streptomyces* and *Pseudomonas* species, and are members of the tetrahydroisoquinoline natural product.[283] This family displays strong antitumor properties and is best represented by the saframycin analog ecteinascidin 743 (ET-743) which is approved for treating soft-tissue sarcoma.[284,285] The central pentacyclic core of **413** from *S. lavendulae* and ET-743 are the same, thereby attracting interests to understand saframycin biosynthesis towards

rational engineering the pathway to afford ET743, of which a likely biosynthetic gene cluster was identified through metagenomic approach.[286,287]

Oikawa and coworkers showed a reductive NRPS assembly line release mechanism is in play (Scheme 57).[288] Three peptidyl aldehydes (**405**, **409** and **411**) are formed transiently via hydride-mediated release from the carrier protein thiol arm of the NRPS assembly line. The first is the *N*-acyl-Ala-Gly dipeptidyl aldehyde **405** derived from thioester **404**. It is condensed with the amine of the tyrosyl-derived methyl DOPA-*S*-carrier protein intermediate **403**. The initial imine **406** is then captured intramolecularly (Scheme 57A) by C_2 of the catecholic ring, acting as an accessible carbanion by virtue of the adjacent phenol oxygen. This adduct **408** then undergoes a second cycle of NADPH mediated reductive release to yield **409**. It then is captured by the identical aminoacyl-S-carrier protein **403** for a second Pictet Spengler reaction, creating the second bicyclic scaffold **410**. This peptidyl thioester is now subjected to a third NADPH-mediated reductive release cycle to give **411**. When **411** is captured internally by the indicated secondary amine to yield **412**, a stable cyclic carbinolamine ring is formed and accumulates (Scheme 57B). The iterative strategy of three reductive release steps on increasingly complex peptidyl thioesters builds the three core six member rings in the saframycin pentacyclic scaffold.

3.2.3. Leporin: Inverse Electron-Demand Diels-Alder—The 2-pyridone leporin B (**419**) is synthesized by a PKS-NRPS hybrid enzyme from *A. flavus* (Scheme 58A).[289] The biosynthetic gene cluster was identified from overexpression of a transcription factor in the cluster which led to the overproduction of the metabolite.[289] **419** was shown to form a trimeric complex with iron, which was attributed to its antiinsectan and antifeedant properties.[289] The biosynthesis of **419** involves a number of initially unobvious biosynthetic transformations.[289] The initial expansion of the five member tetramate product **414** from PKS-NRPS to the 6-membered 2-pyridone **415** was shown for aspyridone[290] was described in Scheme 134 (Section 6.2.5). It is proposed that the subsequent steps begin with enzymatic reduction of the exocyclic ketone **415** to the alcohol **416**. Its subsequent elimination as H_2O creates the exocyclic double bond in **417**. Although mechanistic details are not yet available, one formulation of the next step is an inverse electron-demand Diels-Alder reaction creating two rings in **418** simultaneously, involving the pyridone carbonyl as the surrogate diene. *N*-hydroxylation completes the assembly of tetracyclic **419**.

The hetero Diels-Alder reaction was investigated using synthetic strategies as shown Scheme 58B.[291] Knoevenagel condensation of 4-hydroxy-5-phenyl-2-pyridone (**420**) with 2-methyl-6*E*,8*E*-decadienal (**421**) forms the unstable *O*-quinone methide intermediate **417** that is also proposed for the biosynthetic transformation. A one pot experiment with **420** and **421** in ethanol and trimethylamine at 160°C for 20 hours afforded the desired inverse electron-demand Diels-Alder product **418** with 35% yield. A majority of products were the adduct **422** that displayed alternative stereochemistry as well as the normal Diels-Alder cyclization spiro-adduct **423**. The latter also be formed from the Claisen rearrangement of **422** (but not **418**). Therefore, the synthetic studies suggest enzymatic control is required during leporin biosynthesis to ensure formation of the required leporin intermediate. In the unrelated

marine compounds dibenzo-*p*-dioxins, Moore and coworkers proposed a P450-catalyzed quinone formation leads to a hetero Diels Alder cycloaddition.[292]

3.2.4. Ikarugamycin Cyclization: Hydride-Mediated Coupling—Ikarugamycin (**428**) is isolated from *Streptomyces* sp. and displays a variety of potent biological activities.[293] It is a member of the polycyclic tetramate macrolactams (PTMs) family that also includes clifednaminde (**429**)[294], dihydromaltophilin (HSAF, **430**)[295] and frontalamide A (**431**)[296]. The PTMs are PK-NRP hybrid metabolites with a tetramic acid moiety and most notably 5,6,5 or 5,5,6 fused tricyclic element itself embedded in a 16-membered macrolactam.[297] Later in this section of the review we will note the spinosyn system where a [4+2] enzymatic reaction has been shown for the comparable 5,6,5 tricyclic system (Scheme 83, Section 3.10.4). The logic of assembly of this structural element in ikarugamycin (and presumably its congeners) is completely distinct (Scheme 59).

Zhang and coworkers elucidated the enzymatic basis for forming **428**, which involves only three enzymes.[298] The PKS-NRPS IkaA synthesizes the acyclic tetramic acid **424** that consists of two polyenyl fragments (pentaene and tetraene). IkaB has sequence homology to phytoene desaturase family enzymes, and has been proposed to be responsible for forming the first two rings (5,6 system), although the mechanism is not understood. Formation of the third ring is catalyzed by IkaC, an enzyme with sequence homology to alcohol dehydrogenase.[298] The strategy to form this five-membered ring was shown to be reductive, driven by a hydride donation from NADPH on the terminus of the conjugated 1,6-dienone moiety in **425** (Scheme 59). The incipient carbanion (can be written with charge density all the way out on the oxygen) can mount a transannular attack on the terminus of the conjugated dienyl amide building the indicated cyclopentane ring in **426**. Following IkaC-assisted isomerization (to yield **427**) and ketonization, the natural product **428** is formed. The IkaABC cassette therefore represents an exceptionally concise enzymatic pathway; unsurprisingly, these three genes are well-conserved in the gene clusters of all PTMs family of products.[296,298–300]

3.2.5. Iridoid and Related Plant Metabolites—The 5,6-fused oxazepine system is found in iridoid plant metabolites as noted in Scheme 60, including nepetalactone (**432**)[301], aucubin (**433**)[302] and catapol (**434**)[302.303] The iridoid intermediate nepetalactol (**439**) is an on-pathway metabolite to secologanin and strictosidine, the latter of which is the branch point for medicinally important monoindole alkaloids such as camptothecin and vinblastine.[304] The bicyclic framework of iridoid arises ultimately from the common monoterpene building block geraniol (**435**). The C_1-OH undergoes oxidation to the aldehyde while one of the terminal methyl groups is oxygenated twice in succession to yield the acyclic C_1-C_8 dialdehyde 8-oxogeranial (**436**). The enzyme iridoid synthase (ISY) responsible for the cyclization was identified using comparative transcriptome analysis from *Catharanthus roseus*.[305] ISY has sequence homology to progesterone 5β-reductase (P5βR)[306], a short-chain NADPH-dependent dehydrogenase. ISY mediates transfer of a hydride equivalent from NADPH to the C_4 olefinic terminus of the enone **436** and generates an enolate anion **437**. This sets up intramolecular cyclization to create the fused 5,6-bicyclic ring system in **439**. This could happen in a stepwise fashion, by a Michael addition to form

the cyclopentane **438a** and then the oxazepine **439**. Alternatively, a hetero Diels-Alder reaction, vide supra, as shown with **438b** would construct both rings simultaneously as shown in the scheme. The product *cis-trans* **439** are in equilibrium with the ring opened iridodial (**440**).

The O'Connor group subsequently obtained the crystal structure of ISY to demonstrate the most likely pathway is the stepwise enolization and 1,4-addition.[307] The backbone amide of Ile145 and the phenol of Tyr178 form an oxyanion anchor that stabilizes the enolate anion **437**. The orientation of the active site and cocrystalized $NADP^+$ is also consistent with the stereochemistry of the product. The enzyme is also proposed to undergo conformation change after enolate formation accommodate folding of the substrate and subsequent cyclization.

3.3. Oxidation Enabled Cyclization

The subsequent examples of ring formations during natural product assembly in this section proceed by oxidative not reductive mechanisms as depicted in Scheme 55B. The first set (Section 3.3) involves O-C, N-C, or C-C bond formation at the site where a hydride is ejected from the substrate and passed to FAD in the active site of the relevant enzyme. The second set (Section 3.5) involve oxidation of alcohol or amine groups to the corresponding carbonyl which are then captured by internal nucleophiles. A somewhat distinct mechanistic category that epitomizes oxidative ring construction are disulfide bond formations between two sulfhydryl groups in a metabolite.

3.3.1. Berberine Bridge Enzyme: Nucleophilic Attack with Hydride Transfer to FAD—The best characterized enzyme in this mechanistic class is the berberine bridge enzyme (BBE), involved in plant alkaloid biosynthesis.[34,35,308–315] The enzyme converts (*S*)-reticuline (**118**) derived from L-tyrosine, to (*S*)-scoulerine (**443**) which is on the way to more complex benzophenanthridine alkaloids including berberine (**205**). BBE constructs a new C-C bond between the *N*-methyl and the catechol ring in **443** as shown in Scheme 61. The puzzling element in the reaction had been how the unactivated *N*-methyl group in **118** is converted to the bridging CH_2 in **443** in a low energy path. Interestingly, there is no known synthetic counterpart to this reaction.

As shown in Scheme 61A, the BBE enzyme continues the theme of hydride transfer to or from substrates during biosynthetic ring constructions elaborated in Section 3.2. In this case it is FAD that is the hydride acceptor from substrate rather than NADPH the donor to substrate that sets off the reaction flux. The X-ray crystal structure of *Eschscholzia californica* BBE in complex with **118** showed a glutamic acid E417 is the catalytic base in deprotonating the phenol, and site-directed mutagenesis of this residue had significant effect on catalysis.[311] This mechanistic investigation suggested hydride transfer and S_N2 carbanion attack to form the C-C bond in **441** occur in a concerted fashion, facilitated by the deprotonation of the phenol (resonance contributor to the phenolate anion in a single transition state). More recently, a series of deuterium kinetic isotope effect studies were conducted with both the wild type BBE and the E417Q mutant, suggesting that deprotonation does not occur before or during C–H bond cleavage.[310] Therefore, a step-wise

mechanism for BBE enzyme was proposed (Scheme 61B), in which hydride transfer from the *N*-methyl to the bivalently attached flavin cofactor leads to formation of the iminium cation **442**, followed by attack of the *ortho* phenolate anion to forge the C-C bond to generate **441**, which can aromatize to yield **443**.

3.3.2. Mechanistic Analogies to the Berberine Bridge Enzyme Transformation

—A mechanistically comparable pathway to the plant BBE transformation was found through genome mining from *A. fumigatus.* Transcriptional factor overexpression accompanied with comparative metabolomics found the *fsq* cluster is able to synthesize the tricyclic isoquinoline fumoisoquins A (**449**) and B (**450**) and the related benzoquinone fumisoquins C (**451**).[316] Formation of the berberine-like C-C bond is proposed to arise from a modified dipeptidyl-S-enzyme intermediate **444** on a two module NRPS assembly line (Scheme 62). On-assembly line *N*-methylation and catechol formation by dissociated enzyme partners generate the identical arrangement **445** for a BBE-like oxidative cyclization catalyzed by the flavin-containing enzyme FsqB to give **448**. The reaction was diagrammed as a two-step process, hydride transfer to **446** followed by cyclization to **447** in the original publication (Scheme 62A), but has not been investigated for timing and could happen in one transition state as proposed above for the BBE, with hydride extrusion and C-C bond formation occurring synchronously to give **447** before rearomatization (Scheme 62B).

The last steps in tetrahydrocannabinol (**455**) assembly involves cyclization of the geranyl side chain in **452** onto the electron rich aromatic polyketide moiety to form the tricyclic framework of the cannabinols.[317] Scheme 63 illustrates a comparable chemical logic as BBE for ring construction catalyzed by THCA synthase. X-ray structure of THCA synthases showed a bivalently attached flavin cofactor, identical to that in the BBE enzyme.[317] Phenol-assisted ejection of a hydride ion from the benzylic position in **452** to enzyme-FAD generates (perhaps in a single transition state) the conjugated dienone **453** that acts as electrophile for the π electrons of the terminal double bond. The pyran ring in **454** may be formed in the same transition state as suggested in Scheme 63. The immediate result is formation of the fused tricyclic platform of tetrahydrocannibinol is C-C and C-O bond formation. Tetrahydrocannabinolic acid (**454**) is readily decarboxylated to for **455**, the active ingredient of marijuana.

Lankacidins, including Lankacidin C (**459**) produced from *S. rochei* are macrocyclic antibiotics that display significant antibiotic activities towards many bacteria, and are used in agriculture to treat porcine infections.[318–323] The acyclic substrate LC-KA05 (**456**) is formed by a hybrid NRPS-PKS assembly line with γ-lactone formation as the termination and product release step.[324] Concerted desaturation of the secondary amine to the product iminium (**457**) and capture by the enol carbon to create the new C-N bond that forms the 17 atom macrocycle lankacidinol A (**458**) is catalyzed by the enzyme LkcE (Scheme 64). Subsequent oxidation of α-OH and deacetylation affords **459**. It is of note here that the macrocyclic framework of **458** has an embedded lactone but its formation is not the route to the macrocycle.

An additional example of hydride removal to create an electrophilic center captured in ring formation is provided during biosynthesis of the mycotoxin cyclopiazonic acid (**464**)

(Scheme 65). The pentacyclic metabolite, fashioned from polyketide, amino acid, and isoprenoid building blocks in a short, three enzyme pathway[325,326] and is a nanomolar inhibitor of Ca^{2+}-ATPase[327] (Scheme 65). CpaS is a two module PKS/NRPS hybrid assembly line, notable for a Dieckmann type cyclization as release mechanism to generate the tetramic acid cycloacetoacetyl-tryptophan (**461**).[328] CpaD is a prenyltransferase specifically installing the prenyl group at C_4 of the indole ring to give **462**.[329] The third enzyme is the redox catalyst. CpaO contains covalently bound FAD and is proposed to utilize the indole NH as neighboring group to expel a hydride ion from the indicated methylene center to FAD.[330–332] The conjugated indole iminium **463** is an electrophile capturable by the **π** electrons of the Δ^3-olefin of the prenyl group. Simultaneous participation of the amide nitrogen from the tetramic acid moiety (analogous to the –OH participation in tetrahydrocannabinol construction just above) would again create two rings at once and give the angular pentacyclic framework of the potent mycotoxin **464**.

Chlorizidine A (**467**) provides the sixth and final example in this subsection of a hydride expulsion/ring forming logic, in this case to make a new N-C bond rather than the O-C and C-C bonds noted thus far (Scheme 66).[333] **467** is a tetrachlorinated metabolite isolated from a marine *Streptomyces*, and contains an unprecedented pyrrolo-isoindolone ring system.[334] The precursor molecule **465** shown in the scheme is derived a polyketide assembly line in which two molecules of dichloropyrrole are used as building blocks. Following pyrrole nitrogen mediated chain release and cyclization, phenolate-assisted expulsion of a CH_2-derived hydride ion to FAD yields the conjugated enone **466** that is capturable by the dichloroimidazole nitrogen atom to produce the 5,5 bicyclic system.

These examples provided in this section highlight the ability of the two most abundant cellular redox coenzymes, NAD(P)H and FAD, to engage in hydride transfers, as donor and acceptor respectively, in the biosynthetic directions. This hydride transfer capability undergirds the central enabling chemical logic for this structurally and functionally diverse array of biosynthetic reductive and oxidative cyclizations in plants, bacteria and fungi. These are two electron pathways that lead to a variety of fused ring systems, in contrast to the manifold one electron pathways in the prior Section 2 which also enable great diversification of natural product frameworks.

3.3.3. Peptidyl Oxazoles and Thiazoles—A number of microbially generated nascent proteins can be morphed into small molecule stable frameworks containing five membered oxazole and thiazole rings.[335–337] These include members of the cyanobactin family such as patellamides A (**468**) and C (**469**)[338], telomestatin (**470**)[339], and the thiocillin class of antibiotics (**471)** with a trithiazolylpyridine tetracyclic core[340] (Scheme 67).

The oxazole (**477**) and methyloxazole (**478**) rings arise from cyclization of Ser (**472**) and Thr (**473**) residues to the corresponding oxazolines, respectively.[341] The thiazole ring (**479**) arises from Cys residues (**474**) via comparable thiazolidine intermediates.[341] The cyclization reaction manifolds begin by attack of the Ser/Thr/Cys oxygen or thiolate side chain in the upstream carbonyl (Scheme 68). The resultant tetrahedral adducts **475** are enzymatically phosphorylated on oxygen by a cyclodehydratase that uses ATP as cosubstrate.[342,343] Breakdown of the phosphorylated adduct in the front direction involves elimination of the

elements of phosphoric acid to create the oxazoline and thiazoline rings (**476**).[342,343] These are hydrolytically labile.

The redox step happens next. An FMN-containing dehydrogenase enzyme catalyzes proton abstraction from C_4 and hydride transfer from C_5 of the dihydroheterocycles **476** to create the 2,3-olefin that completes heteroaromatization to the oxazole and thiazole rings.[341] These are stable and represent a dramatic morphing of the peptide backbone of the protein precursors into these protease-resistant heterocycles. The patellamides and telomestatin have heterocycles embedded within the macrocycle where some of the oxazolines have not undergone desaturative aromatization.[338,339] The thiocillin biosynthetic pathway creates the three central thiazoles first with pyridine ring construction simultaneous with 26 atom macrocycle formation as the last biosynthetic step.[344,345]

3.4. S-S Bond Formation from Dithiols

The formation of disulfides from dithiols is featured as a common posttranslational modification in proteins excreted from cells into oxidizing environments. The dithiol-disulfide redox equilibrium is also central to primary metabolism to keep intracellular protein thiols essentially fully reduced.[346] The agent for this function is typically the tripeptide glutathione, or its relatives in a variety of prokaryotes and single cell eukaryotes. Reduced glutathione is accumulated in a 10/1 ration over the glutathione disulfide by the enzyme glutathione reductase which uses hydride equivalents from NADPH, run through the bound FAD in the enzyme (Scheme 69A).[347]

There are a relatively small number of natural products which utilize disulfide bridges as conformationally rigidifying and activity-conferring structural elements. Among them are the histone deacetylase (HDAC) inhibitor spiruchostatins of which FK228 (Romidepsin, **481**) has been approved as a therapeutic agent,[348,349] holomycins (**485**)[350], and the epidithio/disulfide forms of the fungal DKP toxins, of which gliotoxin (**483**)[351] is the best known (Scheme 69B). All of these metabolite sets are made by the producing microbes as the dithiol forms (**480**, **482** and **484**) and in the last or penultimate biosynthetic steps, then oxidized to the disulfides by flavoenzymes in the glutathione reductase superfamily.[352–356] The disulfide forms impart specific conformations to the pathway end products and may confer the toxigenic properties since they can react with thiols of cellular constituents (e.g. proteins) to form covalent mixed disulfide adducts.[357]

Two disulfide variants in natural products are worth mention. One is the disulfide monoxide link found in the DNA damaging macrocyclic leinamycin (**488**) produced from *S. atroolivaceus* (Scheme 70A).[358,359] Enzymatic oxygenation of the disulfide **487** fromed from dithiol **486** is the likely origin of the disulfide monoxide group. The higher oxidation state of the sulfoxide destabilizes the S-S linkage and makes the sulfoxide more likely to depart in the presence of a nucleophile. Thus, one can consider this to be an activated form of a typical disulfide electrophile.

The second intriguing variant is found in the dimeric echinomycins (**492**) (Scheme 70B). These are formed from the *N*-acylated-Ser-Ala-N-MeCys-N-MeVal tetrapeptidyl-*S*-enzyme species by head to tail dimerization as the release mechanism from the biosynthetic NRPS

assembly line.[360] The bislactones **489** have the two Cys-SH side chains in proximity across the macrocyclic ring and are subject to oxidation to the disulfide **490** as shown. This could be nonenzymatic via a sulfenic acid, now electrophilic for capture by the transannular -SH partner. Of special note is that the bridging disulfide can undergo a catalyzed rearrangement to the thiomethyl thioether in **492** in the presence of *S*-adenosylmethionine and via intermediate **491**.[361] Unlike the disulfide which is labile to reduction, the thioether bridge formation should be irreversible and may provide a locked in conformation that is relevant to its bioactivity.

3.5. Capture of Transient Carbonyls

Perhaps the most straightforward two electron route to oxidatively enabled ring formations during natural product biosynthesis is the use of NAD (or less often FAD) as hydride acceptor during transient oxidation of a substrate alcohol or amine to the corresponding ketone or imine. Capture by an intramolecular nucleophile could generate a stable ring system on its own (Scheme 55C, Section 3.1). If not, coupled re-reduction by the just generated NAD(P)H would yield the stable cyclic product.

3.5.1. Pipecolic Acid: Hidden Redox Mechanism—The enzymatic conversion of the proteinogenic amino acid L-lysine (**497**) to the six-member heterocyclic pipecolic acid (**501**) is a simple example of this ring-forming logic (Scheme 71).[362,363] Enzymatic oxidation at the C_2 amine yields the acyclic imine **498** and NADH. Capture by the C_6 amine gives **499**, and loss of NH_3 from the tetrahedral adduct yields the Δ^1 -cyclic imine **500**. Now transfer of the hydride back from NADH to C_2 yields the cyclic **501**. The redox process is cryptic, does not show up in the reaction stoichiometry. **501** is the next higher homolog of the amino acid proline. It is incorporated into several PK-NRP hybrid natural products, among them rapamycin (**493**)[364], FK506 (**494**)[365], meridamycin (**495**)[366] and antascomicin B (**496**)[367] (Scheme 71). **493** and **494** are macrocycles that have been approved as therapeutic immunosuppressive agents. In these pathways, **501** is activated by the terminal NRPS-module and appended to the growing chain as an amide thioester, which is macrocyclized through an internal hydroxyl group to yield the macrolactone/lactam. [368–372]

3.5.2. Lysergic Acid: Formation of the Fourth Ring—Lysergic acid (**505**) and its biosynthetic offsprings are members of the ergot alkaloids from the spores of the fungus *Claviceps purpurea*.[373] These alkaloids can elicit a number of digestive, circulatory and neurological responses in humans. **505** is derived from the tricyclic intermediate chanoclavine-I (**502**), which is derived from the oxidative cyclization of 4-dimethylallyltryptophan (**237**). A comparable cyclization strategy to **501** is in play in the conversion of **502** to **505** (Scheme 72).[373] NAD-linked dehydrogenation of the primary alcohol in **505** yields chanoclavine-I aldehyde(**238**) and NADH. The aldehyde can be attacked by the exocyclic *N*-methyl amine to give the carbinolamine, then the iminium ion **503** as shown. Addition of hydride back from NADH yields the stable cyclic amine in agroclavine (**504**). This metabolite is three oxygenations away from **505**, all involving successive oxygen transfers to the methyl group. The last olefin isomerization to be in conjugation with the indole is thought to be spontaneous. The reversible oxidation of alcohol **502** to aldehyde **238** and back reduction of iminium **503** to secondary cyclic amine **504**

hides the redox process from cursory inspection of reaction stoichiometry. **505** can then serve as a highly unusual starter unit for the LPS NRPS, which can ultimately lead to the formation of ergotamine peptide **266** that is discussed in Scheme 40 (Section 2.3.2).

3.5.3. Reveromycin: 6,6-Spirocycle—The spiroacetal reveromycin A (**515**) from *Streptomyces* sp. SN-593 is a 35-carbon branched polyketide metabolite that can inhibit bone resorption by induction of apoptosis in osteoclast.[374,375] The nascent polyketide RM-A2a (**506**) released from the polyketide synthase machinery undergoes a truncation and spiroacetalization tailoring by RevG and RevJ (Scheme 73A).[376] A P450 mediated hydroxylation at C_{18} in **513** then introduces an OH group in **514** that is the site of subsequent hemisuccinylation in **515**.

The distinguishing 6,6-spiroacetal feature of reveromycin A is installed by action of the short-chain dehydrogenase RevG for NAD-dependent dehydrogenation of the C_{15}-OH in **506** to the ketone in the acyclic precursor **507**. Intramolecular hemiacetal formation creates the first six membered ring **508**. Elimination of water by action of RevJ and transient formation of the oxonium ion **510** sets up stereospecific attack by the C_{11}-OH to complete formation of the stable 15*S* acetal RM-A3a (**512**) while creating the spiro arrangement. In the absence of RevJ, the cyclization cascade can also occur, but affords a 3:2 ratio of the 15*S* to 15*R* isomers. Comparable 6,6-spiroacetal moieties are found in tautomycin (**516**)[377], avermectin B1a (**517**),[378] and spirangien A (**518**)[379] which may utilize the same dihydroxyketone functional group array for spiroacetalization (Scheme 73B). The spiroketal formation in avermectin biosynthesis was characterized by Liu and coworkers in vitro[378]. On the other hand, the 5,6-spiroacetal linkage in monensin rises via epoxyketone cyclization as described in Section 4.2.1.

3.5.4. Fumiquinazoline C and D: Hemiacetal and Hemiaminal—*A. fumigatus* strains make fumiquinazoline peptidyl alkaloids constitutively.[380] We note the formation of fumiquinazoline A and related tryptoquialanine in the Section 4 on epoxidative cyclizations at the 2,3-position of indole rings. In Scheme 74 the further enzymatic processing of fumiquinazoline A (**519**) to fumiquinazoline C (**521**) and D (**522**) by the FAD-dependent enzyme Af12070 is depicted.[381] The enzyme oxidizes the secondary amine in the C ring of the quinazolinedione tricyclic moiety to the imine **520**. This can be captured intramolecularly by the C_3-OH of the imidazoindolone moiety to give **521** as the kinetic product. This spiroheptacyclic structure has a hemiacetal linkage. It can revert back to and equilibrate with the imine **520**. The thermodynamic product that accumulates, nonenzymatically, at later time is the corresponding hemiaminal in **522**, resulting from imine capture instead by the -NH of the imidazoindolone group, yielding an altered heptacyclic connectivity scaffold.

During tryptoquialanine biosynthesis, oxidation of 15-methyl-2-*epi*-fumiquinazoline A (**523**) by TqaG yields the analogous imine product **524** (Scheme 74B).[382] The imine is then hydrolyzed by water to yield the acid **525**, which can be captured by the C_3-OH to form the five-membered lactone deoxytryptoquialanone (**526**), which is three steps (ketone reduction and acetylation, imidazo-nitrogen hydroxylation) from tryptoquialanine.

3.6. Transient Oxidation of Catechols to Set up Cyclization

Two examples of oxidative cyclization of catechols are shown in Scheme 75. The first is the conversion of L-DOPA (**528**) to cyclo- L-DOPA (**531**), revealing the logic of oxidative conversion of catechol **528** to orthoquinone **529** to function as electrophile in intramolecular 1,4-addition by the amine group (Scheme 75A).[383] The tyrosinase is a copper-containing oxidase functioning with a binuclear copper mechanism as described in Scheme 4. A related biosynthetic logic applies in the conversion of the indicated chalcone **532** to aurone (**536**) by aureosidine synthase.[384–386] Aurones are responsible for the yellow color in flowers such as yellow snapdragon flower, from which the first aureosidine synthase was cloned from. Enzymatic oxygenation of the phenol **532** to the catechol **533** and then to the orthoquinone **534** creates the electrophile that determines the regiospecificity of attack of the phenol oxygen on the neighboring double bond which gives **535**. Aromatization creates the conjugated aurone system in **536** and the yellow color (Scheme 75B).

A third example of catechol oxidation is found in the maturation of the phenalenone tricyclic framework, fused tricyclic hydroxyperinaphthenones.[387] Dozens of these aromatic tricyclic metabolites are known in plant and microbial metabolism. The fungal product phenalenone (**540**) and related compounds are synthesized by the strain *P. herquei*.[387] Earlier labeling studies suggested the molecules are synthesized from polyketide pathways, which was confirmed with studies using an identified *phn* biosynthetic pathway.[388–390] Yeast reconstitution studies showed that only PhnA and PhnB are required to synthesize **540**. A nonreducing PKS PhnA was shown to synthesize the angular, hemiketal-containing naphtho-γ-pyrone prephenalenone (**537**) (Scheme 76). A FMO PhnB then catalyzes the hydroxylation of **537** to the trihydroxyphenol product **538** through abstraction of the γ-pyrone hydroxyl proton. The hydroxylated product **538** was then proposed to be more prone to C_3-proton abstraction by general base, which can drive the formation of the C-C bond from C_8 of the catechol onto the C_{13} ketone to afford **539**. Subsequent loss of water gives the stable, aromatic perinaphtheneone framework in **540**. This core structure can then be subjective to a variety of modifications, including prenylation, methylation, and dimerization yield a large assortment of more complex products.

3.7. Enterocin: Favorskii Rearrangement

S. maritimus produces the polyketide enterocin (**547**) with an unusual tricyclic core that has undergone a skeletal rearrangement from the linear nascent product **541** released from aromatic polyketide synthase using benzoic acid as a starting unit.[391,392] In particular, the C_2-C_3 bond has been cleaved while a new C_2-C_4 connectivity has been established along with a new lactone (C_7-oxygen to C_3 ketone) (Scheme 77A). The connectivity alterations are mediated by an FAD dependent enzyme EncM that functions as a C_4 oxygenase, yielding the transient C_3, C_4, C_5 triketone **543** (via the C_4-OH **542**).[393,394] It is proposed that this undergoes a Favorskii type rearrangement, through a cyclopropanone **544** formation and subsequent opening to **545** that is the connectivity altering step. The direction of cyclopropanone opening is controlled by the participation of the C_7-OH in lactone formation. The remaining two rings of the tricyclic core are then proposed to be established by intramolecular aldol condensations (C_5-C_{10}, C_2-C_9) from **545**: a short path to the unique and compact tricyclic core of **547**. Mechanistic and structural examination of the key EncM

catalyst revealed the first example of an N_5-oxide of FAD (**548**) as an on pathway oxygen transfer agent (Scheme 77B).[395,396]

3.8. Piperazic Acid: N-N Bond Formation

We noted the enzymatic cyclization of lysine to pipecolic-acid (**501**) in Scheme 71 (Section 3.5.1) above, creating the proline homolog that gets inserted into rapamycin (**493**), FK506 (**494**) and related NRP-PK cyclic scaffolds. A related building block homolog to pipecolic acid is piperazic acid (**549**), with an unusual N-N (hydrazo) bond. Piperazate residues are found in several nonribosomal peptide frameworks including sanglifehrin A (**550**)[397], kutzneride 1 (**551**)[398], polyoxypeptins (**309**)[399], dentigerumycin (**552**)[400] and azinothricin (**553**)[401] (Scheme 78A). The mechanisms of N-N bond formation is not fully understood but the first step is enzymatic N_5-hydroxylation of L-ornithine (**554**) by a flavin-dependent oxygenase (KtzI from kutzneride pathway).[402] Whether the -OH group in N_5-OH-Orn (**555**) is further functionalized (top pathway in Scheme 78B) to a leaving group **556** for N-N bond formation or some other oxidative cyclization route to the hydrazo linkage in **557** occurs is yet to be determined.

3.9. Aurafuron

Aurafuron (**562**) is a 5-alkenyl-3 3(2H) furanone metabolite from myxobacterium *Stigmatella aurantiaca* DW4/3-1.[403] It is included in this review because of an oxygenative cleavage of the nascent polyketide chain **558** that simultaneously creates the five ring furanone scaffold (Scheme 79).[404] The cleavage is also proposed to be the release step of the truncated chain **561** from its thioester tether **558** on the polyketide synthase AufG. As shown, “on assembly line” oxygenation at C_2 by a cytochrome P450 to yield **559** is followed by action of a flavoenzyme Baeyer-Villigerase AufJ to create the tetrahedral adduct/oxoester **560** which can decompose to the released triketone. Cyclization of the 6-OH of the enol **561** onto the C_2 ketone yields the product **562**.

3.10. [4+2] Cyclizations Enabled by Prior Oxidations

As noted in the introduction of this section, there are a set of biosynthetic transformations creating 5 and 6 membered carbocycles that can be written as formal [4+2] cyclizations of diene and dienophile.[405,406] Those ring-forming reactions do not involve formal redox chemistry. However, many of them occur in pathways immediately after an oxidative step, often one creating the third olefin in the substrate that then undergoes the ring-forming reaction in the next step. We examine those pairs of steps in six examples below.

3.10.1. Sordarin—Sordarin (**569**) is a glycoside antibiotic with a tetracyclic diterpene aglycone produced by the mold *Sordaria araneosa* Cain (Scheme 80).[407] It is an antifungal agent that targets elongation factor 2.[408,409] Labeling studies indicated that the diterpene cycloaraneosene (**563**) is a biosynthetic precursor of **569**.[410] Recently, the sordarin biosynthetic gene cluster was identified and the diterpene cyclase responsible for the biosynthesis of **563** was biochemically characterized.[411] It was proposed the flavin-dependent monooxygenase SdnN is a multifunctional enzyme that converts the diol **564** to **569** by catalyzing dehydrogenation of **564** to the α-hydroxyl ketone **565**, Baeyer-Villiger

oxygenation to generate the ester **566**, and hydrolysis and dehydration to yield the aldehyde **567** that can undergo [4+2] cycloaddition to furnish the ring system in sordaricin (**568**). The exact mechanism of SdnN and the oxidative cascades are not known. Further glycosylation and methylation complete the biosynthetic pathway to **569**.

3.10.2. Solanapyrone—Solanapyrones are a phytotoxin isolated from the plant pathogen *Alternaria solani.*[412] The solanapyrone case is somewhat distinct from the next four example that follow in that the three olefinic components are present in the precursor alcohol metabolite **570**, which does not engage in the putative Diels-Alder type cyclization. Instead the next enzyme, an FAD dependent dehydrogenase converts the exocyclic alcohol to the aldehyde **571** (Scheme 81).[413,414] At this point the *exo*-and *endo*- derived product solanapyrones A (**572**) and D (**574**) are generated, putatively from the indicated transition state geometries. The argument has been made that the conjugated aldehyde in **571** affects the orbitals of the olefin adjacent to and in conjugation with the pyrone to lower the energy barrier for the *cis*-decalin formation. Interestingly, the biosynthetic pathways continue through reduction of the aldehyde back to the alcohol to yield solanapyrone B (**573**) and E (**575**), masking the introduction of the aldehyde during the cycloaddition step.

3.10.3. Lovastatin—Lovastatin (**581**), the prototypic statin that spawned the synthesis of a range of approved statin drugs, has been extensively examined for biosynthesis over the past two decades (Scheme 82).[415] The compound is biosynthesized from a polyketide pathway in which the nonaketide synthase LovB has been intensively studied.[416–419] LovB together with the enoylreductase LovC catalyze eight chain elongation cycles and reductive tailoring to yield the decalin containing intermediate dihydromonacolin L (**580**).[417] Formation of the *endo* decalin core is proposed to take place during the elongation step at the hexaketide stage using the acyclic intermediate **578**. The electron deficient diene (α-β unsaturated carbonyl) and the dienophile are set up by the precise reductive tailoring of the iterative LovB together with LovC. LovC selectively skips three enoylreduction steps at the diketide **576**, triketide **577** and hexaketide **578** stages to yield the enzyme-tethered **579** (Scheme 82). The exact domain responsible for the cycloaddition has not been uncovered, but the activity must reside in the multidomain LovB as in vitro reconstitution with LovB and LovC alone were sufficient to generate dihydromonacolin L.[417] While the synchronicity or lack thereof of decalin construction is still debated in the *lov* system, the presence of the decalin ring system in natural products has become a default suggestion of [4+2] enzymatic cyclization chemistry.[417]

3.10.4. Spinosyn—The polyketide spinosyn A (**588**) produced from *Saccharopolyspora spinose* is the active ingredient of highly effective insecticides use today.[420] **588** is a structurally complex polyketide natural product containing a perhydro-*as*-indacene moiety fused to a 12-membered macrolactone. Formation of the 5,6,5 tricyclic system embedded within the polyketide macrolactone framework has been intensively studied for the timing and mechanism of cyclization.[421] The SpnF enzyme has been purified to homogeneity, characterized for enzyme activity and X-ray structure determination.[422] It accelerates a nonenzymatic reaction from the macrocyclic precursor **584** to the 5,6-bicyclic system **585** (Scheme 83) by 50-fold. This modest but real acceleration indicates that many of the diene/

dienophile substructures are poised to react nonenzymatically and the enzymes may be lowering energy barriers but not changing the intrinsic reactivity profiles of their substrates. While a transannular [4+2] mechanism can be written to produce the 6,5 fused bicyclic **585** in the SpnF reaction, calculations of the energy barriers[423] have also suggested that a [6+4] electrocyclization could proceed to first form **586**, followed by a rapid Cope rearrangement to get to the observed product **586**. Glycosylation of **585** by the glycosyltransferase SpnG affords **587.**

The steps immediately antecedent to SpnF action are catalyzed by SpnJ and SpnM to create a ketone from an alcohol **582** and then dehydration to the γ-hydroxy α,β-enone **583** from which dehydration unveils the diene **584** required for SpnF action. Thus the three enzymes SpnJ, SpnM and SpnF can be viewed as an oxidative generation of the diene that can then undergo the cyclization reaction.

Completion of the tricyclic core in **588** from **587** is achieved by the next enzyme SpnL, a homolog of SAM-dependent methyltransferases, to form five-membered cyclopentene C ring (Scheme 83). A Rauhut-Currier reaction mechanism[421], has been proposed but not validated. The Rauhut-Currier reaction "involves the coupling of one active alkene/latent enolate to a second Michael acceptor, creating a new C–C bond between the α-position of one activated alkene and the β-position of a second alkene under the influence of a nucleophilic catalyst".[424] This reaction was also proposed for nepetalactol (**439**) formation from 8-oxogeranial (**436**) (Scheme 60, Section 3.2.5), but was ruled out after structural studies of ISY.[307]

It is worth comparing the chemical logic and enzymatic machinery to create the 5,6,5 tricyclic core in **588** with the related 5,6,5 core in ikarugamycin (**428**) in Scheme 59 (Section 3.2.4). In the ikarugamycin case the last cyclization was initiated by a hydride transfer from NADH rather than the proposed Rauhut-Currier route, while formation of the first two 5,6 ring system is not completely understood.

3.10.5. Abyssomicin—The abyssomicins, including abyssomicin C (**593**) are polyketide metabolites isolated from marine *Streptomycete* collected from the abyss in the Sea of Japan.[425] They act as irreversible inhibitors of *para*-aminobenzoate synthase in bacterial metabolism.[425] Recent studies on the enzymes AbyA4, AbyA5 and AbyU have provided evidence for a [4+2] cyclization catalyzed by AbyU[426] (Scheme 84) on the acyclic **591** to create the indicated two ring 5,6-spirocycle **592** at the core of the **593** framework. The Aby4 and Aby5 enzymes act on the precursor tetronate ring **589** to acetylate (to give **590**) and then eliminate the -OH group to produce the *exo* methylene double bond in **591**. This oxidation process creates the dienophile that then participates in the AbyU cyclization reaction.

3.10.6. Pyrroindomycins—The pyrroindomycin B (**597**) biosynthetic pathway is noted here not so much for how the substrates are manipulated by biosynthetic enzymes to create the diene and dienophile partners but rather because two enzymatic [4+2] transformations occur in consecutive steps in the maturation pathway (Scheme 85). PyrE3 is known to produce the characteristic monounsaturated *cis*-decalin moiety **595** from **594**.[427] It is argued to arise from a [4+2] process as shown. Then the next enzyme PyrI4 reprises the AbyU

logic, this time on an *exo* methylene tetramate rather than an *exo* methylene tetronate to produce the spiro 6,5-bicyclic moiety **596**. In two enzymatic steps remarkable complexity has been built into the aglycon of the pyrroindomycin framework. An enzyme catalyzing the analogous cycloaddition as PyrI4 to yield the spirocycle in versipelostatin.[428]

4. CYCLIZATION VIA EPOXIDATION

4.1. Introduction

Olefin epoxidation is a widely employed functional group transformation in both synthetic organic chemistry, and in natural product biosynthesis across the major structural classes of secondary metabolites.[429–435] Conversion of the olefin via reaction of its π electrons to the three membered oxygen ring (epoxide = oxirane), creates a potential electrophile. The epoxide group can and does persist in many natural product scaffolds. These can subsequently react with nucleophilic groups (Nu) on cellular targets and lead to covalent adducts that can be sources of problematic toxicity.[436]

The susceptibility of epoxides to ring opening reactions by covalent capture by nucleophiles is a key strategic element of the biosynthetic logic in a wide range of natural product scaffold maturations, as detailed in this section. Scheme 86 shows five schematic contexts in which epoxides are generated and then used as key functional groups for ring-forming reactions. The two steps of epoxide formation and then nucleophilic opening to larger ring systems constitute a general strategy for oxidative cyclizations. When the two steps are taken together, the epoxide is a “disappearing” functional group, not persisting in the maturing scaffold, but essential for ring creations.

In Scheme 86A, intramolecular attack on either the proximal or distal carbon of an epoxide by a nucleophile (Nu) represents as a common pattern will be exemplified in lasalocid and aurovertin production, among others. Scheme 86B represents intramolecular capture of the epoxide by the oxygen atom of a tetrahedral adduct arising from (prior/simultaneous) nucleophilic attack in a carbonyl group. This is a common route to polycyclic ethers in monensin and nanchangmycin assembly. Scheme 86C shows a prototypic bis-epoxidation of a pair of olefins with water attack as the external nucleophile, leading to cyclic ether formation, as found in glabrescol and solamin assembly. Scheme 86D involves regiospecific epoxidation of one among multiple olefins that sets off a cascade of carbocycle formation as the other olefins react as nucleophiles via their π electrons. This is the classic oxidosqualene cyclase cascade, among others, that turns a linear substrate into a rigidified polycyclic product. Scheme 86E is a variant of D in which a terminal intramolecular nucleophile initiates the olefin cascade on the epoxide and is seen in meroterpenoid assembly.

Routes to Epoxide Formation—Before taking up the specific examples of epoxide-mediated cyclizations in this section we note in Scheme 87 that the two major classes of monooxygenases, flavin-based and iron-based- can each deliver one oxygen atom from O_2 to olefinic cosubstrates. The schematic mechanism for the hemeprotein P450 oxygenases can be formulated as a one electron pathway with donation of one electron from the olefin to the high-valent oxoiron species and then collapse of the Fe^{IV}-O-carbon radical to the coordinated epoxide by an effective [OH•] transfer (Scheme 87A). As shown in Scheme

87B, the proposed oxygen transfer route in the flavin-based epoxygenases (such as squalene-2,3-epoxidase) is from the flavin-4a-OOH and delivery of an [OH^+] equivalent to the π electrons of the olefin as nucleophile, result in olefin epoxidation and oxidized flavin. A NAD(P)H-dependent two-electron-reduction of the flavin completes the catalytic cycle of epoxygenases. In all the pathways noted in the subsequent subsections the first step of the two step epoxide formation/epoxide opening with attendant ring formation is always catalyzed by one of the above forms of epoxygenases. Epoxidation can also be catalyzed by nonheme iron α-KG dependent oxygenase and is shown in an example of ring contraction in Section 6.1.1.

4.2. Formation of Cyclic Polyethers via Epoxide Intermediates

4.2.1. Polyether Formation—The formation of the large class of polyethers has been intensively investigated for decades and has borne out seminal hypotheses that the placement and stereochemistry of cyclic ether rings in the isoprene and polyketide-derived class can be explained by conversion of nascent polyolefinic frameworks to epoxides which could then be opened in intramolecular cascade reactions.[437] Scheme 88A shows such a transformation of the acyclic hexaene **598** into glabrescol (**600**) with five furan rings via hexa-epoxide intermediate **599**.[438] Six of the seven oxygens in **600** derive from molecular oxygen, the seventh from the water molecule that initiates the epoxide opening furan-forming cascade. Analogously, the paired furan and pyran rings in the ionophore lasalocid A (**604**) arise by action of Lsd19 on bisepoxyprelasalocid (**602**) as shown in Scheme 88B. The flavin-dependent epoxidase Lsd18 first oxidizes the two *E*-olefins in prelasalocid A (**601**) into epoxides to give **602**. Water initiated cyclization into **604** occurs in two tandem epoxide opening steps, catalyzed by a didomain epoxide hydrolase Lsd19.[439–442] The *N*-terminal domain Lsd19A catalyzes the 5-*exo*-tet cyclization of **602** to form the tetrahydrofuran ring in **603**, while the *C*-terminal domain Lsd19B catalyzes an *anti*-Baldwin 6-*endo*-tet cyclization to form the pyran ring and give **604**.[443] The X-ray crystal structure of Lsd19 showed that Lsd19A and Lsd19B are arranged in a head-to-tail manner. The substrate binding pocket of Lsd19A is unoccupied while Lsd19B contains the product **604**.[444] Comparison of lasalocid A-Lsd19B and product analogue-Lsd19B complexes shows that the change of conformation of Lsd19B active site residues as well as precise three-dimensional arrangement of the substrate are needed to overcome the thermodynamically disfavored *6*-endo cyclization (while suppressing 5-*exo*-tet cyclization) under enzymatic catalysis.[444] Computation modeling of the crystal structure of Lsd19B supports the mechanistic proposal for favoring 6-*endo*-tet under enzymatic catalysis conditions.[443,444]

Scheme 89 and 90 depict analogous strategies of epoxidation during monensin A (**611**) and nanchangmycin (**615**) assembly, respectively. The formation of the initial hydroxypyran **606** from the linear substrate **605** in monensin is an example of Scheme 86B, where a tetrahedral adduct oxygen is the initiating nucleophile in the epoxide opening cascade. Interestingly, although the MonBI/MonBII pair are functional parallels of Lsd19A/Lsd19B, MonBI/MonBII have been shown to catalyze three ring opening reactions (via **607**, **608** and **609**) to afford the pentacyclic structure **610**.[445,446] The X-ray crystal structure of MonBI dimers suggested that a KSD motif is important in MonBI/MonBII interactions.[447] Likewise, in formation of the cyclized intermediate **614** of nanchangmycin (**615**), following formation of

the bisepoxide **613** from the PKS-bound **612,** one of the spiro pyran/furan pair arises by Scheme 86B while the second pair exemplifies the mechanism Scheme 86C.[448]

The family of heronapyrroles A-D (**620–623**), which contains an unusual nitropyrrole moiety attached with an oxidized farnesyl chain, represents alternative fates of epoxide ring opening from two bis-epoxide regioisomers (**617** and **618**) vs the tris-epoxide metabolite (**619**) (Scheme 91).[449] In heronapyrroles A (**621**) and B (**620**), the two isolated epoxides of **617** are opened hydrolytically without neighboring group participation in ring formations; whereas in heronapyrroles D (**622**), neighboring group participation in **618** generates the tetrahydrofuran ring. By comparison, the tris-epoxide (**619**) can be opened with intramolecular formation of the indicated bis furan grouping in heronapyrrole C (**623**).[450]

4.2.2. Formation of Other Cyclic Ethers—The conversion of muricadienin (**624**) into solamin (**626**) is another example of the "disappearing" epoxide biosynthetic logic as shown in Scheme 92A.[451] Double epoxidation of two *Z*-olefins in **624** yields the bis-epoxide **625** that is the progenitor to the indicated dihydroxy furan functionality in **626**. The stereochemistry of the epoxidation step dictates the outcome of the two hydroxyl groups to be either *trans* (shown) or *cis*.[452] Aurovertins are polyketide metabolites from fungal strains that have potent cytotoxic activities and are noncompetitive inhibitors of ATP synthases.[453,454] Biosynthesis of the simplest member, aurovertin E (**632**) was studied in the endophytic fungus *Calcarisporum arbuscula.*[455] Formation of **632** from its hexaene-pyrone polyketide precursor **627** reflects three epoxidative steps by the only one FMO AurC (Scheme 92B).[455] The first two epoxidations of the (*E, Z*) terminal diene **628** yield the indicated bis-epoxide **629** which gets converted in a water-addition/epoxide opening cascade to the now anticipated dihydroxyfuran **630** by the hydrolase AurD. A subsequent epoxidation of the exocyclic double bond (the third overall from AurC action) to **631** sets up an intramolecular anti-Baldwin 6-*endo*-tet cyclization under the catalytic aegis of AurD again to generate 2,6-dioxabicyclo [3.2.1]-octane ring scaffold of **632**. Overall only four enzymes are required to assemble aurovertin E, representing a remarkably efficient biosynthetic pathway.

4.3. Cyclizations via Epoxides on Terpene Scaffolds

4.3.1. 2,3-Oxidosqualene Cyclase and Triterpenes—The most famous of the terpene cyclizations that proceed via an epoxy substrate are those carried out by oxidosqualene cyclases.[456–458] In this tandem epoxidation-cyclization reaction, the head-to-head coupled C_{30} hexaenoic hydrocarbon squalene (**598**) is morphed into polycyclic six- and five ring fused triterpenes that account for all of the steroids in plants (cycloartenol, **642**),[459] animal and fungi (lanosterol, **647**) (Scheme 93).[460] While **598** itself can be cyclized by the squalene-hopene cyclase (SHC) into hopene (**652**) and hopanol (**653**) (Scheme 94),[461,462] for the context of this review, the majority of discussion will be devoted to the epoxidative route.

The relevant substrate arises by the action of the FAD-containing squalene epoxidase which selects one of the terminal double bonds in **598** to form 3S-2,3-oxidosqualene (**633**) via the general mechanism of Scheme 93.[457] The effect of this action is to polarize the squalene

scaffold and results in epoxide at the end serving as an electrophilic functional group. Oxidosqualene cyclases then catalyze the cascade of cyclization steps, starting from a pre-chair-boat-chair configuration, to form the proposed protosterol cation intermediate (**640**). The epoxide opening step is facilitated through the concerted protonation of an active site Brønsted acid. The implications of which will be discussed in subsequent section. Following a series of 1,2-hydride and methyl shifts, abstraction of a proton leads to the internal double bond and yield **647**, as catalyzed by lanosterol synthase. Under different cyclases from different organisms, the cation **640** can also undergo rearrangement to form the C_{11} cation **641**, which can be quenched by either *a*) new C-C bond formation catalyzed by cycloartenol synthase in biosynthesis of **642** that results in cyclopropane ring formation.[463] This is the starting point of all steroids in plants;[464] *b*) migration of the cation from C_{11} to C_6 in **648** followed by quenching via proton removal yields the internal olefin placement in cucurbitadienol (**650**) by cucurbitadienol synthase;[465] c) C_{12} proton elimination to yield parkeol (**649**).[466] This is just gliding over the surface of the many variants that can leak out of squalene oxidocyclase active sites. Baruol synthase from *Arabidopsis thaliana* can leak up to 22 minor products, reflecting cations quenched at eleven carbon sites in the tetracyclic sterol framework.[458]

A different cyclization of **633** by a cascade of four internal olefins yields the classic tetracyclic scaffold of the sterol natural product family, as the dammarenyl cation (**643**).[467] This is the path directed by the Lup1 variant of the oxidocyclase plant family. Rearrangement of the **643** via the remaining olefin yields the lupenyl cation (**644**), which can be quenched by loss of a proton to afford the pentacyclic lupeol (**645**), which has a variety of biological activities.[468] Further rearrangement of the **644** yields the ring expanded oleanyl cation, which can be quenched by proton abstraction to yield β-amyrin (**646**),[469] the most abundant cyclic triterpenes in most higher plants.

In some triterpene cyclization pathways, the squalene epoxidase can further epoxidize the other terminal olefin in **633** to yield bis-epoxide intermediate **634**. This can be cyclized into 24,25-oxido-lanosterol (**636**) by lanosterol synthase, the derailed product preonocerin (**635**) or the epoxydammarenyl cation (**637**) in the presence of Lup1.[467] The latter cation **637** can be captured as pentacyclic scaffolds with a pyran or furan to yield the epoxydammerane products **638** and **639**. This pathway shows that the epoxidase can actually act also on the other terminal olefin to form **634** which can be carried through all the way to **636** by the lanosterol synthase member of the squalene oxidocyclase family.

The reaction catalyzed by oxidosqualene cyclase exemplifies the role of the epoxide in facilitating the electrophilic cyclizations observed in many other families of natural products, including indole diterpenes and meroterpenoids. The concerted protonation and anchimeric addition of the C_6-C_7 double bond is facilitated by the presence of a Brønsted acid residue in the terminal end of the active site. Crystal structure of the human lanosterol synthase showed a conserved Asp residue donates an *syn* proton that is hydrogen-bonded to two Cys residues.[456] In SHC (Scheme 94), protonation of the terminal double bond of **598** is more challenging and requires the presence of a stronger Brønsted acid.[461] In turn, crystal structure showed the SHC performs protonation with the *anti*-oriented Asp acid proton.[461] The acidity of the proton is further increased through a specialized amino acid network that

includes a protonated histidine side chain that polarizes the Asp acid carbonyl, and hydrogen bonded water molecule that bridges the carboxylated oxygen and a tyrosine side chain. In turn to take advantage of this strong active site Brønsted acid, the SHC was rationally engineered into a protonation based biocatalyst (protonase).[470] Structural based mutagenesis to enable better binding of smaller substrates led to the isolation of the Y420W or Y420W/G600F mutant that can stereoselectively cyclize *S*-(6,7)-epoxygeraniol (**654**) to hydroxylcyclogeraniol (**656**) via **655**.[470]

A very different cyclization pattern is observed in yardenone (**659**) and abudinol (**662** and **663**), which are triterpenes isolated from marine sponges *Ptilocaulis spiculifer*.[471] Multiple epoxidations on different olefins of squalene **598** are proposed to initiate the cyclization cascades (Scheme 95). The formation of the pentacyclic framework of **659** requires formation of the tris-epoxide **657**. An epoxide-opening cascade on the right half of the precursor substrate is accompanied by an analogous capture of a proton as stand-in electrophile, on the left hand side of substrate. These cyclizations build the 7/5 and 7/6 bicyclic rings in **658** respectively, on the route to the final **659** (with an additional furan moiety).[472] The formation of abudinol A (**662**) and B (**663**) is proposed to start from the tetra-epoxidized substrate **660**.[473–475] Once the epoxide-opening cascade on the left half of **661** is completed, abstraction of H_{14} could induce the tandem cyclization on the right half of the molecule to generate **662** and **663** through different epoxide opening regioselectivity.

4.3.2. Indole Terpenes—Three examples of cascade reactions on the terpene side chains in three indole terpene biosynthetic pathways illustrate the applicability of the "disappearing" epoxide logic in this hybrid class of natural products. One is the conversion of 3-farnesyl indole (**664**) into xiamycin (**667**) (Scheme 96). XiaO catalyze the epoxidation on the terminal olefin of the C_{15} **664** to form the 3-(epoxyfarnesyl)-indole (**665**). Like a terpene cyclase, XiaH sets up the enzyme-mediated cyclization cascade to form the 6,6 bicyclic system in preindosespene (**666**).[476] Further, epoxidation of the indole ring sets the fifth ring, bridging six membered ring and a ring expansion to the seven membered cyclic ether in ring D of **667** (see section 4.4.2).

The second case is the related processing of fungal indole diterpene family compounds, such as paxilline (**675**) and emindoles (**679** and **680**) (Scheme 97). This is a large family of natural product frequently found in fungal sclerotia and exhibit potent insecticidal properties.[477,478] Construction of these molecules starts with the C_3-alkylation of indole-3-glycerol phosphate to yield geranylgeranyl-indole **668**. In biosynthesis of **675**, regiospecific epoxidation is effected at the third of the four olefins in the C_{20} side chain by PaxM to **669**, as preamble to the intramolecular epoxide ring opening by PaxB through cations **670** and **671**, yielding a pentacyclic framework of **672** with one remaining olefin.[479] A second epoxidation by PaxM on the residual olefin yield **673** and capture by the indicated -OH group creates the pyran ring in **674** as the sixth ring in the paxilline scaffold. The final enzymes in the pathway are the P450s PaxP and PaxQ which are involved in creation of the enone functionality and hydroxylation in the end product **675**. The emindole framework represents an alternative capture and diversion of the indicated cationic intermediate **671** by Ats5B1 to create another tetracyclic framework **676** with one remaining olefin. Subsequent

epoxidation of the residual olefin by AtmM to yield **677** and pyran formation in **678** create the connectivity and architecture found in the prenylated emindole PA (**679**) and emindole PB (**680**).[480]

Scheme 98 is an expansion of the enzymatic processing of one of the cation intermediates (**670**) in the pathway of the previous Scheme 97. Unlike PaxB, AtS2B or AfB cyclases can catalyze three additional rearrangements of cation **670** with i) quenching by proton removal of **682** yields the anominine (**686**) scaffold, which is a proposed precursor of tubingensin A/B (**690** and **691**) catalyzed by an unidentified FMO or P450, following an indole 2,3-oxidation induced cyclization (for **690**) and a further series of cation shifts induced rearrangement (for **691**, like xiamycin biosynthesis, Scheme 108) ; ii) instead of quenching **682**, two additional intervening cation rearrangements via cations including **683** and **684** yield the olefins in the context of the highly rearranged congeners of aflavinine (**687**) with endocyclic (**689**) and exocyclic (**685**) olefin regioisomers. Interestingly, the anominine and aflavinine cyclases (AtS2B and AfB) were found to be separated from the enzymes that produce **686**, suggesting the likelihood of siphoning this substrate from other indole diterpene pathways.[480] The unclustered cyclases was found using a genome-guided, heterologous reconstitution approach in yeast. The activities of these compounds as strong insecticidal natural products found in the sclerotia of fungi hints likely differential regulation of these unclustered genes. Overall, the ability of cationic intermediates to drive skeletal rearrangements in these reactions and the promiscuity of epoxidases allows evolution of new skeletal frameworks in natural products.

4.3.3. Fungal Meroterpenoids—Meroterpenoids constitute a large family of molecules of mixed terpene-polyketide origin, exhibit diverse chemical structures and a wide range of biological activities (Scheme 99).[481] Compounds in this family share a modular assembly pathway and can diverge in structure during the oxidative cyclization and rearrangement steps (Scheme 100).[482] The typical sequence of biosynthetic steps is i) synthesis of an aromatic polyketide unit such as methyl-orsellinic acid; ii) Friedel-Craft alkylation of the polyketide with either farnesyl-PP or geranylgeranyl-PP; iii) epoxidation of the terminal olefin in the prenyl chain to set up the cascade of cyclization steps; iv) protonation-assisted cyclization of the prenyl portion; and v) oxidative rearrangement of the scaffolds. The tandem epoxidation/cyclization steps therefore serve as the key steps in defining the cyclized skeleton of the final products.

The first completely elucidated pathway for compounds in this family is that of the pyridine-containing pyripyropene A (**695**), followed by related compounds oxalicine (**696** and **697**) and decaturins (**698–703**) (Scheme 99).[483–487] **695** produced from *A. fumigatus* is one of the strongest acyl-coenzyme A: cholesterol acyltransferase (ACAT) inhibitor, and is a potential antihypercholesterolemia drug.[484] The polyketide building block, 4-hydroxy-6-(3-pyridinyl)-2H-pyran-2-one (HPPO) is synthesized by a nonreducing polyketide synthase, using nicotinyl-CoA as the start unit.[488] Attachment of farnesyl group to the C_3 position of the pyrone yields the linear precursor farnesyl-HPPO (**692**). The flavin-dependent enzyme Pyr5 installs the epoxide at the terminal olefin to yield **693**. Pyr4 was discovered as the first membrane-bound cyclase that can perform the proton-initiated cyclization of **693** to yield

the cyclized deacetyl-pyripyropene E (**694**).[488] The cyclization cascade can be written as in Scheme 99 to initiate from the pyrone 4-hydroxyl group, an example of the mechanism shown in Scheme 86E. The result of the cyclization step is a pentacyclic product **694**, which contains a fused pyrone-pyran-two carbocyclc core. Further hydroxylations and acetylations yield the natural product **695**. In the oxalicine and decaturin pathways, more oxidative rearrangements are responsible for the spirocycle formation.[487]

Additional complexity/versatility in meroterpenoid biosynthesis continues in Scheme 100, which represents alternative fates of one common polyketide precursor 3,5-dimethylorsellinic acid (**704**) to different complex meroterpenoid scaffolds through regio- and stereo-selective prenylation and epoxidation.[482] For example, tropolactone D (**708**) arises from the *S*-farnesyl adduct **705** in an epoxide opening cascade (via **706**) to provide tetracyclic intermediate (**707**) exemplifying Scheme 86B. This is followed by oxidation of the cyclohexanol of **707** to the ketone, hydroxylation and a Baeyer-Villiger enzymatic conversion to the lactone that gives tropolactone D.[489]

Alternatively, action of the *R*-specific C15 prenylation (AdrG/AusN/Trt2) to **709** leads ultimately to more complex andrastin (**713**)/austinol (**715**)/terretonin (**717**) and novofumigatonin (**721**) scaffolds.[490–493] Unlike biosynthesis of **708**, the *S*-configuration epoxidation opening cascade starting from **718** leads to the formation of a cationic intermediate **719** instead of tetracyclic intermediate **707** in **708** biosynthesis.[494–496] Quenching via H-shift results in the formation of spirocyclic intermediate **720**, which is proposed to be the precursor of **721**.[493] Another set of epoxidases (AdrH/AusM/Trt8) with different product selectivity yield *R*-configuration epoxidation intermediate **710**. When the initiating nucleophile in the epoxide-opening cascade is not the pyrone-OH or the tetrahedral adduct oxygen, but instead the olefin to form the cation intermediate **711**, the frameworks of **713**, **715** and **717** are generated through loss of different protons in **711**. One lesson is that the pyrone moiety can employ three distinct nucleophiles in the intramolecular cascade of epoxide opening to enter into three distinct kinds of scaffold connectivity and complexity.

One more pathway for anditomin (**726**) biosynthesis requires conversion of **704** to phthalide (**722**), a transformation catalyzed by a chimeric protein (AndK) consists of P450 monooxygenase and hydrolase domains.[497,498] Although *R*-specific C15 prenylation is installed on **722** by AndD to yield **723**, the epoxide opening cascade follows that of the *S*-configured **724** via **723**, and afford a tetracyclic intermediate preandiloid A (**725**) that can be further morphed into **726** with extensive oxygenation and rearrangement.[498]

4.3.4. Quinolone and Quinoline Alkaloids—Two insecticidal quinolone alkaloids, penigequinolone A/B (**737** and **738**) (from *P. thymicola)* and aspoquinolone A/B (**742** and **743**) (from *A. nidulans*) feature the same quinolone alkaloid core (as in quinolinone B, **729**) attached with differently cyclized C10 terpenoid pieces (Scheme 101).[499–501] **729** is derived from 4′-methoxyviridicatin (**728**), which is rearranged from the cyclic dipeptide 4′-methoxycyclopeptide (**727**) by the PhyH-like dioxygenase AsqJ through an epoxidation reaction (see Section 6.1.1).[502] Following formation of **729**, two prenyltransferases PenI and PenG sequentially transfer two DMAPP molecules, together with the action of a FAD-dependent dehydrogenase PenH, to form the hydroxylated, acyclic precursor **730**. The most

striking result of using three enzymes to install the ten-carbon chain in **730**, instead of a direct geranylation, is the installment of a C_3 hydroxyl group that is critical for the subsequent epoxide rearrangement reactions.[503]

In both pathways, a flavin-dependent monooxygenase (PenE and AsqG) is responsible for epoxidizing the terminal olefin in **730** to yield the epoxide **731**, which can readily undergo the canonical 5-*exo*-tet cyclization to yield the tetrahydrofuran containing yaequinolone C (**732**).[504,505] **732** was initially thought of as an intermediate towards the formation of penigequinolone and aspoquinolone. Subsequent feeding and biochemical studies, however, demonstrated this is a shunt and co-metabolite.[506] A dedicated epoxide hydrolase is encoded in each pathway to further accelerate the formation of **732** as a cometabolite. In the penigequinolone pathway, a carotenoid hydratase-like enzyme, PenF, catalyzes a novel cationic epoxide rearrangement to yield the aldehyde **734**, which can spontaneously cyclize to form the hemiacetal yaequinolone D (**735**).[506] This compound can be dehydrated and reduced to form the pyran-containing **737** and **738**. PenF is proposed to not only suppress the favorable 5-*exo*-tet cyclization, but more impressively, to promote a discrete epoxide cleavage step to yield the carbocation **733**, which can undergo a Meinwald-like rearrangement to afford **734** and the quaternary C_8. Such reaction requires strong acid in organic synthesis, but occurs under physiological condition in the active site of PenF which was proposed to have a strong Brønsted acid as found in SHC (Scheme 94). In the aspoquinolone pathway, a dehydratase (AsqC) catalyzes the loss of water from epoxide **731** to form the dienyl epoxide **739**. The ability of PenF to catalyze cationic epoxide rearrangement was further demonstrated through converting **739** to the aldehyde **740**. A related Brønsted acid enzyme AsqO was found in the aspoquinolone pathway to catalyze the 3-*exo*-tet cyclization of **739** followed by intramolecular quenching of the carbocation **741** to yield the cyclopropyl furan containing **742** and **743**. Hence, the dienyl epoxide **739** can be directed towards two distinct epoxide opening pathways dependent on exposure to either PenF or AsqO.[506]

Aurachins are secondary metabolites produced by the myxobacterium *Stigmatella aurantiaca* Sg a15 (Scheme 102).[507] The gene cluster was found by Müller and coworkers to be localized on two separate regions in the genome.[508] The bicyclic quinolone aurachin D (**744**) is converted to the tricyclic ring system of aurachin A (**751**) under the auspices of two oxygenases. AurG is proposed to transiently epoxidize the quinolone double bond of aurachin C (**745**), the *N*-hydroxylation product of **744** to **746**, which is then opened intramolecularly with assistance by the *N*-OH functionality of **745.** 1,2-Migration of the farnesyl side chain of epoxide-opened **747** through a proposed semi-pinacol rearrangement that gives **748** is followed by reduction of ketone to hydroxyl group by AurH to give aurachin B (**749**). Yet another epoxidation of the proximal olefin of the farnesyl side chain in **749** to **750** is followed by capture by the adjacent -OH group via a 5-*exo*-tet cyclization. This forms the fused pyran ether and the side chain -OH in **751**.

4.3.5. Oxetane Formation During Taxol Maturation—During the late stages of taxol (**756**) biosynthesis, the tricyclic C_{20} hydrocarbon taxadiene core is oxygenated at multiple sites around the periphery and acylated with acyl groups of differing complexity.[509] The

most striking oxygen functionality in mature taxol is the four membered oxetane ring with an acetoxy side chain. The formation of the oxetane is postulated to arise as shown in Scheme 103. Epoxidation of the exocyclic olefin **752** to **753** would lead to subsequent internal opening by the oxy anion of a tetrahedral adduct of the acetoxy side chain to yield the adduct **754**. The oxy anion from the opened epoxide could attack **754**, becoming the four membered Oxetane **755** as the acetoxy group is reconstituted, now with a net 1,2 shift.

4.4. Arene Oxides as Biosynthetic Intermediates

4.4.1. Phenyl Ring Epoxidations—Among the most notable proposed arene oxides in biosynthesis of natural products are those in the pathways to epidithiodioxopiperazines, such as acetylaranotin (**760**) and the notorious fungal metabolite gliotoxin (**483**).[510,511] As depicted in Scheme 104, **760** assembly from the epidisulfide adduct of the Phe-Phe diketopiperazine **757** is proposed to occur via action of a cytochrome P450 oxygenase (AtaF) that acts on both phenyl rings to form a proposed bis-epoxide intermediate **758**. While the arene oxides could rearrange to the phenols, a typical outcome, they are instead captured intramolecularly by the amide nitrogens of the diketopiperazine ring. This action forms the two C-N bonds and generates the cyclohexadienol forms of the pentacyclic precursor **759** that can be converted to **760**.[510] Action of a cognate arene epoxide enzyme (GliC or GliF) on **761** during **483** assembly yields the dithiol form **482** of gliotoxin, thought to oxidize to the disulfide **483** as shown in Section 3.4 as the producing *A. fumigatus* cells export the metabolite[512]. Ring expansion oxygen insertion (discussed in Section 6.2.4) occurs in the cyclohexadienol rings of **760** but not in **483**.

4.4.2. Indole 2,3-Epoxidations—The heterocyclic pyrrole ring in the bicyclic indole system has recently been found to undergo epoxidation by a class of flavin-dependent oxygenases involved in fungal natural product biogenesis, exampled as fungal alkaloids fumiquinazoline A (**519**), tryptoquialanine A (**767**), notoamide D (**778**) and spirotryprostatin A (**781**).[513] Scheme 105 shows the conversion of the indole moiety of fumiquinazoline F (**763**)[514] in the presence of O_2, a single module NRPS (used for activation of L-alanine), and an epoxidase (AF12060 or TqaH) into the annulated imidazoneindole tricyclic ring structure of **519**.[382,515] The proposed 2,3-epoxyindole **764** can be in equilibrium with the indicated hydroxyiminium form that can be captured by the amine group of the NRPS-bound alanine or aminoisobutyrate cosubstrate **765** to yield **766**; and then the indoline NH can complete the annulation by capture of the aminoacyl thioester carbonyl and yield **519**. Further elaboration of the fumiquinazoline scaffold gives both fumiquinazoline D (**522**) (see Scheme 74) or **767**. Scheme 105 also depicts additional fungal peptidyl alkaloids **768–772** that arise via comparable indole ring epoxidation.[516–520]

Another example in the indole epoxidation manifold is provided for the biosyntheses of notoamide C (**776**) and D (**778**) from notoamide E (**773**) (Scheme 106). When the proposed 2,3-epoxyindole **774** catalyzed by NotB is formed, two pathway of the epoxidation intermediate could be occurred. Like fumiquinazoline scaffold biosynthesis, **778** is pictured as arising by internal capture of the hydroxyiminium tautomer **777** by the diketopiperazine amide nitrogen, giving rise to the complex 6,6,5,5,6,5 hexacyclic framework of **778**.[521] Alternatively, a comparable participation of the *para*-oxygen lone pair on the substituted

phenol **774** yields **775**, followed by ketonization of the carbinolamine and a migration of a C-C single bond yields the isomerized framework of **776**, which result in shift of the reverse prenyl group from C_2 to C_3 in indole ring.

The spirotryprostatins produced by *A. fumigatus* are fungal peptidyl alkaloids with antimitotic properties.[522] The key feature is the quaternary carbon at the nexus of a 5,5-spiro center. Scheme 107 shows the third example for indole epoxidative rearrangement of fumitremorgin C (**219**) into spirotryprostatin A (**781**). In this case the lone pair of electrons on the methoxyphenol moiety of **779** is suggested as the internal initiating nucleophile. The tetrahedral carbinolamine adduct **780** rearranges with C-C bond migration leading to produce the spiro system in **781**.[523] A different oxidative rearrangement mechanism that affords spirotryprostatin G is shown in Section 6.1.5.

The indole epoxidation mechanism is proposed to be involved in bacterial alkaloid xiamycin (**667**) biosynthesis.[524] The indole epoxidation “disappears” (shown in Scheme 108) as an early step in creation of the carbazole framework in **667**.[524] The proposed 2,3-epoxyindole **783** can be in equilibrium with the indicated hydroxyiminium form **784** that can be captured by the adjacent double bond to form a new C-C bond and generate a cation intermediate **785**. The product after cation quenching and water elimination is the pentacyclic cyclohexene intermediate **786,** which can be ring-expanded to form **667.**

Except FMOs, the indole 2,3-epoxidation can also be catalyzed by P450 enzymes. Two distinct plant cytochrome P450s convert the plant secondary metabolite brassinin (**787**) into spriobrassinol (**789**) or cyclobrassinin (**790**) as depicted in Scheme 109.[115] Internal opening of the putative indole epoxide **788** at either carbon center by the thioimidate yields the 5 or 6-membered nitrogen and sulfur heterocycles.

4.5. Additional Epoxide-Mediated Cyclizations

The hybrid polyketide/peptide amides, known as heronamides, from Heron Island in Australia feature two kinds of cyclizations in proceeding from heronamides C (**791**) and F (**792**) to heronamide A (**797**) and B (**798**), respectively. (Scheme 110). The completed natural products contain a 5,5 ring system embedded within the larger polyene macrocycle.[525] The first cyclization follows the O_2-mediated regioselective epoxidation of one of the seven double bonds in substrate to yield **795**. The exact trigger of this epoxidation is unclear and was proposed to be possible without enzyme catalysis. Spontaneous internal capture by the amide nitrogen builds the first five membered ring in **796**.[526] The subsequent conversion to the 5,5- bicyclic **797** and **798** is thought to be either a [4+2] or a direct [6+4] (followed by a facile Cope rearrangement) cyclization route.[527] The starting macrocyclic compounds **791** and **792** can also be cyclized into heronamide B (**793**) and heronamide E (**794**) when exposed to UV light.

Pseurotin A (**804**) produced by *A. fumigatus* arises from a short, hybrid nonribosomal peptide/polyketide assembly line (Scheme 111).[528] Chain release from the tethered thioester enzyme intermediate **799** is mediated by reduction to the thiohemiacetal and dissociation of the free aldehyde **800** as shown in Scheme 56A. Tetramate ring formation in **801** is proposed to occur by attack of the acetoacetyl enolate on the aldehyde **800**. An extensive list of

oxidative tailoring steps ensues to afford the oxo-spirocyclic framework in **804**. An interesting enzyme encoded in the gene cluster is an unusual didomain PsoF, which contains a *N*-terminal methyltransferase domain and a *C*-terminal FMO domain.[529,530] The MT domain was shown to be essential for introducing the α-methyl group in the polyketide portion of the **799**.[531] The FMO domain was shown to be required for the formation of the oxo-spiro structure of **803**.[531] The proposed mechanism of PsoF is the epoxidation of the endocyclic olefin in the pyrrolidone portion of **801** to yield **802**, which sets up an internal opening/capture by the enol to produce **803**. Recent studies by Watanabe and coworkers show that *trans* to *cis* isomerization of the diene portion requires a glutathione S-transferase PsoE.[532] PsoF was shown to be responsible for an additional epoxidation step to introduce an epoxide which can be hydrolyzed to yield the *trans* diol found in **804**.[530]

Jasmonic acid (**808**), the important regulator in plant responses to biotic and abiotic stresses as well as in development, is a long chain fatty acid-derived plant hormone biosynthesized from linolenic acid (**191**).[530] As shown in Scheme 112A, *S*-hydroperoxide **192**, installed by lipoxygenase, is the internal source of the resultant epoxide oxygen in the allene oxide **193** (see Scheme 32). One electron opening by allene oxide cyclase yields a delocalized radical pair (**805** and **806**) that can cyclize and unravel to the cyclopentenone core intermediate **807**.[533] Further chain shortening through β-oxidation as well as reduction leads to the **808**. On the other hand as shown in Scheme 112B, the *R*-hydroperoxide **195** from arachidonic acid (**194**) is the precursor of clavulone I (**809**), which possibly carries a similar pathway of **808**.[534] Additionally, instead of β-oxidation and reduction, the post-modification steps including hydroxylation, acetylation and O-methylation are required for biosynthesis of **809** following opening of the allene oxide **196**.

5. CYCLIZATION VIA HALOGENATION

5.1. Introduction: Haloperoxidases and Oxygen-Consuming Halogenases

In synthetic organic transformations, the displacement of halogen substituents by nucleophiles can constitute efficient substitution reactions. In natural product biosyntheses two of the four major classes of biosynthetic halogenases can participate in oxidative cyclization processes. The two halogenase classes that can carry out the generalized transformations noted in Scheme 113 are hydrogen peroxide-dependent vanadium halogenases, known as vanadium haloperoxidases (VHPOs), and mononuclear nonheme iron oxygen-dependent halogenases. The VHPOs can engage directly in concomitant halogenation and cyclization as exemplified in Scheme 113A and 113B. The iron-dependent halogenases are part of a two-step process (Scheme 113C), where a second enzyme carries out intramolecular displacement of the halide.

Scheme 114A shows the catalytic cycle for VHPOs in which H_2O_2 is the exogenous source of oxidizing equivalent for the halide ions. HOOH replaces a coordinated water molecule as a vanadium ligand. Binding of a halide, typically chloride or bromide ion (in seawater microenvironments) leads to generation of a hypochlorite or hypobromite equivalent ligated to the vanadium. The -OX species acts as an $[X^+]$ equivalent: the polarity of chloride and bromide ions has been reversed from X^- to X^+ and can be captured with nucleophiles.

Scheme 114B depicts the ligand sphere around the nonheme Fe^{II} with chloride as a first sphere ligand. Reaction of O_2 with the iron halogenases yields a high-valent Fe^{IV}=O. In a typical oxygenase mode it would cleave a bound C-H to yield a carbon centered radical and transfer an [OH•] equivalent in a rebound step to effect substrate hydroxylation. In halogenase mode, instead a [Cl•] equivalent is transferred to a carbon radical to produce the halogenated product.

5.2. Vanadium Haloperoxidases as Cyclization Catalysts

The biosynthetic capability of VHPOs as a cyclization catalyst is demonstrated in the merochlorin biosynthetic pathways (Scheme 115). Tetrahyrdoxynaphthalene (THN, **810**) is a prototypic aromatic polyketide arising from utilization of five molecules of malonyl-CoA.[535,536] Installation of a rearranged farnesyl moiety by Mcl23 creates the substrate **811** for haloperoxidase-mediated chlorinations.[537,538] Mlc24, the vanadium-dependent chloroperoxidase, catalyzes a site-selective naphthol chlorination to **812a** and initiates oxidative dearomatization to afford cation intermediate **812b**. This triggers terpene cyclization to create the possible cation **813**. Two possible cyclization routes complete the stereochemically complex carbon framework of merochlorin A (**814**) and merochlorin A (**815**) in one more step.

A third variation in route leads to merochlorin C (**820**). As in the other two cases above, chlorination can occur on a nucleophilic carbon *ortho* to a phenol in **817** to yield merochlorin D (**818**). Then generation of the cyclic chloronium ion at the terminal olefin in **819** can be followed by attack of the indicated OH to install a second chlorine substituent as the macrocyclic ether **820** forms.[539]

Scheme 116 shows a route from the same starting substrate **810**, with *ortho* chlorination and also double prenylation, with a C_5 and a C_{10} unit to yield SF2415B1 (**821**). Again, attack of the terminal olefin on V-OCl in the haloperoxidase active site by NpaH1 leads to a species shown as a cyclic chloronium ion intermediate **822**, which is captured by the indicated OH to create the pyran ring fused to the original naphthalene core to form SF2415B3 (**824**).[540,541] In the case of bromine activation, formation of the bromonium **823** lead to the bromo-SF2415B3 (**825**) as shown. In some organisms, **824** can be elaborated to a further chlorinated product A80915C (**826**) by a comparable olefin attack on a vanadium-coordinated [Cl^+] equivalent.

Two examples of brominated isoprenoids induced cyclization are displayed in Scheme 117. In Scheme 117A the laurencin (**828**) and prelaureatin (**830**) are generated by attack on the V-OBr by the olefins in laurediols (**827** and **829**), respectively. The source of the [Br^+] is from KBr shown in the scheme.[542] Cyclic brominated eight-membered ethers are the core frameworks in the products. In Scheme 117B, the origin of the three α-,β-and γ-snyderols (**834**–**836**) is the isoprene nerolidol (**831**). The nascent cation **833** from attack of the olefin on the bromonium ion **832** can be quenched by loss of a proton from the endocyclic (α-snyderol, **834** and γ-snyderol, **836**), or exocyclic (β-snyderol, **835**) position.[543]

5.3. Iron Halogenases and Partner Cyclases

Three examples of two step enzymatic processes to convert an unactivated carbon center into a cyclopropyl group are shown in this subsection. In all three cases the halogenases act on a precursor metabolite tethered in thioester linkage to an acyl carrier protein domain/subunit that is part of either a PKS (curacin, **841**) or a NRPS (coronatine, **847** and kutzneride, **851**) assembly line. The nonheme iron halogenases as noted in Scheme 114B reductively activate and cleave O_2 while generating a high-valent Fe^{IV}=O active site reagent that can cleave an unactivated C-H bond in a bound substrate. The resultant carbon radical is thought to capture the [Cl•] in a rebound step.

As shown in Scheme 118 the CurA halogenase has effected a radical chlorination of the unactivated terminal methyl group of the Δ^3-prenyl-acyl carrier protein **837**.[544–546] Subsequent conjugate addition of a hydride equivalent from NADH by the enolyl reductase (ER) domain component of the PKS assembly machinery yields the C_2 thioester enolate anion **839**. This carbanion equivalent can now carry out an intramolecular S_N2 displacement on the chlorine substituent. In this ring-forming reaction the cyclopropane **840** has been created on its thioester, ready to be incorporated as a building block in the assembly line to **841**.

Coronatine **847** is a hybrid PK/NRP produced by phytopathic bacteria as a mimic of the jasmonic acid hormone noted in Scheme 112. It causes opening of the stomata in plant leaves allowing the pathogenic *Pseudomonas syringae* producers to gain access to the internal nutrients of the leaf.[547,548] The aminocarboxycyclopropane building block is generated from L-*allo*-isoleucine (**842**) by a comparable strategy to the curacin case (Scheme 119).[549] **842** is selected, activated and tethered on its peptidyl carrier protein CmaD by the CmaA enzyme to yield **843**. CmaB is an O_2-requiring, nonheme mononuclear iron halogenase that regiospecifically chlorinates the unactivated C_γ methyl group to afford **844**. CmaC can remove the activated C_α-H as a proton, generating the thioester enolate **845**. That has carbanion character at C_α and can react in an intramolecular S_N2 displacement of the chlorine under the catalytic agency of the enzyme CmaC. The result is the cyclopropane-containing aminocarboxy building block known as coronamic acid (**846**) that gets incorporated into the hormone agonist **847**.

The third example is embedded in the antifungal hexapeptidolactone kutzneride (**851**) (Scheme 120). All six amino acid constituents are nonproteinogenic, signaling its nonribosomal peptide synthetase assembly line origin.[550] The 2-(1-methylcyclopropyl)-D-glycine is the most unusual residue. The details of mechanism in this case are not clearly worked out but KtzD is again an oxygen-reducing mononuclear iron halogenase so a cryptic chlorination mechanism for cyclopropane **850** formation starting with the KtzC-tethered isoleucine **848** is anticipated.[551] Despite the fact that a corresponding C_α carbanion equivalent derived from the chlorinated **849** will not suffice for formation of the methylcyclopropyl glycine scaffold (but can form **850**).

6. OXIDATIVE RING REARRANGEMENT

Ring sizes in natural product scaffolds can expand or, less often, contract during enzyme-mediated transformations, many of these occur during iron-dependent oxygenase catalysis.[552] As noted in Section 2 the hallmark of iron-based oxygenases are the involvement of carbon-centered radicals at different stages in the catalytic cycles and those can drive scaffold rearrangements, both to larger and smaller rings systems.

6.1. Ring Contractions

6.1.1. Viridicatin: Diazepinone Contraction—4′-methoxyviridicatin (**728**), the precursor of penigequinolone and aspoquinolone discussed in Section 4.3.4, contains a 6,6 quinolone scaffold. This core structure is derived from cyclic dipeptide **852** built from cyclization of anthranilate and O-methyl-tyrosine by a two module NRPS assembly line.[502] The biosynthesis of **728** from cyclic dipeptide substrate **852** was confirmed through *in vitro* biochemical analysis of a dioxygenase enzyme AsqJ.[502,553,554] The experiments revealed two key roles of AsqJ in driving scaffold rearrangement and expulsion of methylisocyanate (**857**). As noted in Scheme 121, the first transformation effected by AsqJ is a net desaturation to generate an exocyclic olefin **854** on the diazepinedione moiety. It is shown as a radical process in which the carbon centered radical **853** arising from the initial C-H homolysis step transfers a second electron to the Fe^{III}-OH rather than experiencing an [OH•] rebound. This exocyclic olefin **854** is then substrate for a second catalytic cycle by the AsqJ enzyme, this time resulting in a more typical epoxide product **855**. This epoxide is spontaneously opened by neighboring group participation of the π electrons of the anthranilyl aromatic ring, creating a tetracyclic framework **856**. This can break down with expulsion of **857** and yield the phenyl substituted dioxoquinolone **858** framework in viridicatin.

The net result is a ring contraction of the seven member diazepinedione of the starting cyclic dipeptide **852** to the six member dioxopyridine ring in the quinolone product **858**. The one carbon bridge between the phenyldiazepinedione and the methoxyphenol ring in starting substrate is the carbon atom that gets extruded as **857**, along with one of the two nitrogens in the diazepine ring.

6.1.2. Gibberellic Acid 12: Cyclohexanol Contraction—The gibberellins are cyclic diterpenes that have a variety of hormonal and developmental effects in plants.[555] Gibberellic acid 12 (GA_{12}, **864**) is generated from *ent*-7α-hydroxykaurenoic acid (**859**) by the steps catalyzed by P450 CYP88A, involving two oxygen transfer events (Scheme 122).[556,557] The first step is an exceptional one. Homolytic cleavage of the indicated C-H bond by the high-valent oxoiron in the CYP88A active site yields a radical **860** that rearranges rather than undergoing immediate hydroxylation. The net result is conversion of the B ring of the initial substrate radical from a hydroxycyclohexane to a cyclopentane with an exocyclic •CHOH functional group as in **861**. At this juncture the [OH•] rebound occurs to give the product as an aldehyde hydrate **862**, which is in equilibrium with the aldehyde **863**. A second CYP88A mediated oxygenation of the aldehyde **863** to carboxylic acid

functionality creates **864**. The net result of CYP88A action is to trap out the ring-contracted gibberellic acid framework in the form of the aldehyde intermediate **863**.

6.1.3. Saliniketal: Macrocycle Opening and Dioxabicyclo[3.2.1]octane Formation—Saliniketals (**872** and **873**) from *Salinospora arenicola* block transcription of the gene encoding ornithine decarboxylase, the gatekeeper enzyme in polyamine biosynthesis.[558] The ansa bridge is reminiscent of rifamycin framework. Moore and colleagues have shown that rifamycins and saliniketal share common biosynthetic intermediates and then diverge at the stage of 34a-deoxyrifamycin W (**865**) (Scheme 123).[559] The cytochrome P450 CYPSare1259 is proposed to oxidize the C_{34} methyl group up to the carboxylate (**866**) (via three successive oxygen transfer events). At this juncture loss of the carboxylate as CO_2 is enabled by the vinylogous keto group to stabilize the product enol **867**. Dioxygenative cleavage of that 11, 12-double bond would generate the acyclic keto acid **868**, breaking up the macrocycle. Subsequent reductive saturation of the 28, 29-double bond gives a conformationally mobile chain **869** for hemiketal **870** formation. The oxyanion of the hemiketal is postulated to act as trans-annular nucleophile for displacement of the original 27-OH group. This generates the dioxabicyclo-[3.2.1]octane ring system **871**, the precursor of **872** and **873** prior to C-N bond cleavage. In a formal sense the large macrocyclic bridge of the rifamycin precursor has been replaced by the much more compact bicyclooctane in **871**.

6.1.4. Griseorhodin A: Ring Contraction in a 6,6- to a 6,5- Spiroketal System—Griseorhodin A (**881**) is a member of the rubromycin family of spiroketal-containing polyketides, assembled by oxidative cleavage and rearrangement of the angular tridecaketide collinone (**874**) (Scheme 124).[560,561] From gene deletion and heterologous expression studies, Piel and colleagues showed that the 6,6-spiroketal **875** is further along the biosynthetic pathway and need to lose one more carbon atom to form **881**. An FAD-dependent oxygenase (GrhO6) was identified as the catalyst likely to contract the 6,6-spiroketal framework into the 6,5-spiroketal framework in the rubromycin family.[562] One of two possible routes proposed was the Baeyer-Villiger pathway (route *a*) to the carbonate ester **876** followed by water attack to the hydroxy acid (**877**). Decarboxylation attendant to ring closure would generate the contracted 5,6-spiroketal **880**. In route *b,* the transformation would start with hydroxylation at the B/C ring juncture to yield **878**. Loss of CO_2 would be driven by rearomatization that generates a transient cyclic oxonium ion **879** that gets captured in 6,5 spiroketal **880** formation.

6.1.5. Spirotryprostatin: Ring Contraction in a 6,5- to a 5,5- Spiroketal System—We noted the formation of spirotryprostatin A (**781**) in Scheme 107 *via* a proposed 2,3-indole epoxidation route. Spirotryprostatin G (**887**) differs from **781** by an additional desaturation in the C ring. Scheme 125 shows the proposed route from fumitremorgin C (**219**), involving both spirocycle formation and ring contraction of the C ring of the substrate. FqzG is the responsible P450 oxygenase.[523] First it inserts an -OH group at the C/D ring juncture via the *C*-radical **882** to yield **883**. In its second catalytic cycle FqzG starts the reaction by homolysis of a specific C-H bond in the substrate to give a new *C*-radical **884**. In this instance it is in resonance with radical density at the lower B/C ring juncture and

gives the indolyl radical **885**. That is the site of delivery of [OH•] in the rebound step to give the diol **886**. The diol is proposed to be the transient species which rearranges, with ring contraction, to the spirocycle framework of **887** as the initial –OH group is expelled from the C/D bridgehead position and the second -OH group becomes the indolone carbonyl.

6.1.6. Xenovulene A: Cyclopentenone Formation via a Ring Expansion-Contraction Mechanism—Active against human GABA receptor, xenovulene A (**899**) is a meroterpenoid consist of a sesquiterpene fused with 2,4-dihydroxyl-3,6-dimethyl-benzoic acid (**888**).[563] The sesquiterpene portion in **899** is reminiscent of the humulene scaffolding. Its biosynthesis is remarkable for a net contraction of a fused methyl phenol in substrate to a fused cyclopentenone ring in **899**.[564] Most remarkably, the starting phenol **889** first undergoes catalyzed ring expansion to a tropolone **891** (Scheme 126) before two successive ring contractions by extrusion of formyl groups and their subsequent hydrolytic elimination as formic acid. The rearrangements are set off by three oxygenation steps that produce the 5,6-hydroxy formyl intermediate **890** which rearranges to the 5,7-trisubstituted tropolone **891**. In turn that can ring contract to an alternate aldehyde **893** from which loss of formic acid regenerates a fused 5,6-ring system in **894** with the six-membered ring now a catechol. One more oxygen transfer yields the trihydroxybenzene metabolite **895** which can undergo a second round of ring contraction and formyl group extrusion to give **897**. Repeat of the hydrolytic loss of formate yields the tautomer **898** of the final 5,5-hydroxycyclopentenone ring of **899**.

6.2. Ring Expansion Processes

6.2.1. Baeyer-Villigerases: Cyclic Ketones to Lactones—A predominant route to ring expansions in cyclic ketones is the oxygen insertion adjacent to the carbonyl group carried out by oxygenases that act as Baeyer-Villigerases.[565–568] Most of those enzymes are flavoproteins, using the flavin-4a-OO^- as the initiating nucleophile on the substrate carbonyl group to generate a covalent Criegee intermediate (Scheme 5A). We note below one example in the hemeprotein cytochrome P450 family during maturation of the brassinosteroid plant hormones.

Pentalenolactone (**906**) is a *Streptomyces* sesquiterpenoid antibiotic with good activity against both Gram-positive and Gram-negative bacteria as well as a variety of fungi and protozoa.[569,570] It features a unique 5-5-6-3 fused cyclic structure within the lactone ring proposed to be synthesized from the expansion of intermediate **901**, the oxidative product of pentalenene (**900**). Scheme 127 shows the expansion of the methylcyclopentanone ring in **901** to the ring-expanded isomeric lactones to yield pentalenolactone D (**904**) or neopentenolactone D (**903**) that can arise from the migration of either neighboring carbon after formation of the Criegee intermediate **902**.[571–573] It is notable that **904**, the precursor of **906** is not the favored product based on migratory aptitude (2° vs. 3°) by Baeyer-Villiger reactions. Further dehydrogenation by an nonheme α-KG iron dependent oxygenase yields an *exo* olefin that can be epoxidized by the same enzyme to yield pentalenolactone F (**905**), which is one additional oxidation step away from the final product **906**.[573]

Baeyer-Villigerases catalyzed ring expansion is also widely found during fungal meroterpene biosynthesis, such as the transformation of preaustinoid A (**907**) to preaustinoid A1 (**909**) (Scheme 128). The FMO AusC inserts one oxygen atom between C_2 and C_3 to yield **909** forms the 7-membere lactone.[574] The Criegee intermediate **908** is shown and in this case the preferred migratory aptitude is followed in the ester formation.

A novel Baeyer-Villigerase that can catalyze transformation of a ketone to a carbonate functionality was confirmed in the biosynthetic pathway of cytochalasin E, a PK/NRP hybrid angiogenesis inhibitor produced by *A. clavatus*.[575,576] Through *in vitro* biochemical characterization, the FMO CcsB was confirmed to catalyze the transformation of cytochalasin Z16 (**918**) from ketochalasin (**910**) via two successive oxygen insertion reactions (Scheme 129).[577] The first step converts the 11-membered macrocyclic bis-ketone **910** to the 12-membered ketolactone **912** via the Criegee intermediate **911**, notable for the size of the cyclic ketone expanded. The second oxygen insertion creates a cyclic carbonate **918** with a 13-membered macrocyclic ring. While a similar Criegee intermediate can be written for the second oxygen insertion, Scheme 129 depicts a route via epoxy intermediate that might be in play for generation of the unique cyclic carbonate functional group.[577] The mechanism starts with the 1,4-addition of the flavin-peroxo anion onto **912** to yield the adduct **913**. This leads to formation of the epoxide **914** that can ring open to give the α-alkoxide **915.** Subsequent attack of the alkoxide yields the tetrahedral intermediate **916** that can collapse to yield the conjugated carbonate **917.** Ketonization of **917** then affords **918** that is two more oxidation steps away from cytochalasin E. This mechanism depends on the 1,5-vinylogous diketone functionality located on the southern portion of the starting **910**, with the distal ketone serving as an electron sink during the transformation. The discovery of CcsB expands the repertoire of activities of Baeyer-Villigerase and provides a possible synthetic strategy for transformation of ketones into carbonates.

The biosynthesis of the brassinosteroid plant hormones (**924**) involves a cytochrome P450-mediated Baeyer-Villiger expansion of the B-ring ketone in castasterone (**922**) as shown in Scheme 130.[578] CYP85A3 in tomato plants can convert 6-deoxycastasterone (**919**) to **922**, by double hydroxylation at C_6 (first to the alcohol **920**, then to the ketone hydrate **921**, in equilibrium with the ketone **922**).[579] **922** is then the substrate for a third oxygen transfer via CYP85A3, this time as a Baeyer-Villigerase ketone to lactone expandase to yield **924**. The Fe^{III}-OOH is the presumed species attacking the 6-keto group of **922** to yield a Criegee intermediate **923**.

6.2.2. Penicillin N to Desacetoxycephalosporin C: β-Lactam Expandase—

Perhaps the most famous of the enzymes with expandase activity in natural product biosynthesis is the desacetoxycephalosporin synthase (DAOCS), catalyzing the conversion of the penicillin class of β-lactam antibiotics into the cephalosporin class.[580] The penam to cephem conversion involves expansion of the 4,5- bicyclic scaffold penicillin N (**925**) to the 4,6-scaffold in desacetoxy-cephalosporin C (**929**) with an endocyclic double bond in the six-membered ring. As schematized in Scheme 131, DAOCS is a Fe(II)/α-KG-dependent dioxygenase, reducing O_2 with no oxygen insertion into product, while generating substrate radicals **926** and **928** via C-H bond homolytic cleavages.[581,582] The rearrangement of the

initial methyl radical species **926** to the episulfide radical **927** and its opening to the 4,6 bicyclic system is depicted. Quenching of the product radical **928** by H• transfer to iron, creates the endocyclic cephem double bond in **929** and returns the active site iron to its starting Fe^{II} oxidation state. Semisynthetic versions of the cephem antibiotics, in which the 4,6 bicyclic warhead is conserved and synthetic changes to the aminoadipate and 3-methyl substituent implemented, are among the bestselling antibiotics globally.

6.2.3. Stipitatic Acid: Tropolone Ring Formation—A variety of natural products contain the 7-membered hydroxy cycloheptatrienone ring system known trivially as tropolone.[583] A short fungal pathway converts 3-methylorcinaldehyde (**930**) (from action of polyketide synthase TropA) to the 5,7-scaffold of stipitatic acid (**935**) by way of the tropolone intermediate stipitaldehyde (**934**) (Scheme 132).[584] TropB is a flavoenzyme oxygenase that hydroxylates *ortho* to the phenolic oxygen, producing a dearomatized cyclohexenone scaffold **931**. Nonheme iron α-KG-dependent oxygenase TropC is proposed to oxygenate the adjacent methyl group in **931** to the primary alcohol **933** via a rebound mechanism, which sets off the ring expansion to the **934** as shown.[585] We noted an analogous ring expansion to a tropolone in xenovulene biosynthesis in Scheme 126 before an iterated set of ring contractions that takes troplone down to a cyclopentenone. A different mechanism for tropolone ring formation via an epoxide intermediate was confirmed in the degradation of phenylacetyl-CoA,[586] and was proposed in the biosynthesis of omega-cycloheptyl fatty acids. [587]

6.2.4. Acetylaranotin: 4,5–Dihydrooxepine Ring Formation—We have noted an aspect of acetylaranotin (**760**) biosynthesis in Scheme 104 (Section 4.4), where the focus was on enzymatic formation of the aromatic epoxide and its internal capture by the amide nitrogen of the diketopiperazine neighboring group to construct the C-N bonds from each of the DKP nitrogens as the pentacyclic scaffold is created. We also noted the likely route to epidisulfide formation in Scheme 69 (Section 3.4).[510] A brief return to acetylaranotin maturation here is on the conversion of each of the cyclohexadienol esters in **936** to the ring expanded 4,5-dihydrooxepines in **760**, catalyzed by the cytochrome P450 monooxygenase AtaY (Scheme 133). The likely route is via a transient epoxide with ring opening to the seven-membered oxepine **937** followed by a second round of ring expansion to **760**, but the exact mechanism of this transformation remains unresolved.

6.2.5. Aspyridone: Tetramic Acid to Pyridone—Aspyridone (**945**) was first isolated from *A. nidulans* following targeted overexpression of the transcription factor that controls the transcription of the *apd* biosynthetic pathway.[588] Subsequent expression of the hybrid PKS-NRPS ApdA bimodular enzyme in the heterologous host *S. cerevisiae* results in release of the tetramic acid preaspyridone (**939**) shown in Scheme 134. This is the starting compound for expansion of the five member tetramic acid ring to the 2-pyridone ring found in **945**, tenellin, and related metabolites.[589] The P450 enzyme ApdE (and related ones in other pathways) is proposed to carry out homolytic C-H cleavage as the initiation step at the benzylic CH_2 group to yield **940**.[290] While direct [OH•] rebound can yield the off-pathway hydroxy metabolite **941**, a competing internal rearrangement to the cyclopropanol radical **942** can lead to the ring expansion as shown in Scheme 134. Capture of that ring-expanded

carbon radical **943** by [OH•] rebound yields the hydroxy precursor **944** to aspyridones. The delivery of an OH radical equivalent after the substrate radical has rearranged is reminiscent of the spirotryprostatin G biosynthetic sequence in Scheme 125.

6.2.6. Ring Expansion During Penitrem E Biosynthesis—Penitrem A (**950**) and the deschloro-version penitrem E (**949**) are the most complex indole diterpenes isolated from filamentous fungal species to date.[153] The fully tailored natural product features a contiguous decacyclic ring system including a 4,6-bicycle fused to the indole phenyl ring. Formation of the nine-membered macrocyclic ether ring in penitrem D (**171**) from secopenitrem D (**166**) was covered in Scheme 29 (Section 2.2). Formation of **166** itself involves an unusual oxidative ring expansion step with unresolved mechanism. The prenyltransferase PtmE was shown to catalyze the prenylation-initiated cationic cyclization between DMAPP and the prenylated paxilline derivative **946** to yield PC-M4 (**947**). The reaction starting from **947** catalyzed by the P450 PtmK has been reconstituted in the heterologous host *A. oryzae* (Scheme 135).[590] A possible mechanism is shown where consecutive C-H bond homolytic cleavage of the two methyl group, first in **947** followed by **948**, leads to expansion of the cyclopentane to a cyclohexane ring and *exo* methylene formation in **166**.[591]

6.2.7. Ring Expansion During Anditomin Biosynthesis—A dazzling arrays of oxidative modifications catalyzed by two nonheme iron α-KG-dependent oxygenases AndA and AndF are proposed for the transformation of preandiloid C (**951**) to anditomin (**726**).[574] The epoxide-mediated formation of the meroterpenoid scaffold was discussed previously in Scheme 100 (Section 4.3). Starting with **951**, generation of the bicyclo[2.2.2]octane ring system in andiconin (**956**) is catalyzed by AndA (Scheme 136). Methyl C-H bond homolytic cleavage in **951** yields the substrate radical **952**, which can initiate the C-O bond cleavage to form fused 1,3-cyclohexanedione-furanone radical intermediate **953**. The radical then adds to the newly exposed *exo* methylene to form a new seven-membered ring radical intermediate **954**. This radical adds to the furanone double bond to yield a new C-C bond and eventual quenching of the newly formed intermediate **955** arrives at **956**. After an identical Baeyer-Villiger ring expansion as depicted for preaustinoid A1 (**909**) in Scheme 128 to afford andilesin C (**957**), AndF receives the oxidative relay baton and cleaves the C-H bond in the middle cyclopentane ring to form **958**. Following an [OH•] rebound that gives **959,** a ring expansion step takes place to expel water and form **726**. The sequence of [OH•] rebound followed by elimination to drive rearrangement is observed once more in this example (See Scheme 134 and others). In total the dramatic morphing from **951** to **726** forges three new carbon-carbon bonds and represents one of the most complicated sequence of rearrangements characterized to date.

6.3. Additional Oxidative Ring Rearrangements

6.3.1. Fumagillin: Multifunctional P450-Catalyzed Morphing—The *A. fumigatus* metabolite fumagillin (**970**) has a meroterpenoid structure, reflecting convergence of an isoprenoid and polyketide biosynthetic pathways.[592] **970** displays anti-angiogenic activities and has been considered as an antitumor lead.[593] The key structural feature is the heavily oxidized cyclohexanone ring, including the bis-epoxide moiety. The epoxide groups are

sufficiently reactive as electrophiles to target the methionine aminopeptidase in protein biosynthesis.[594–596] Identification and reconstitution of the fumagillin biosynthetic pathway revealed several interesting enzymes. First the sesquiterpene cyclase (Af520) that synthesizes β-*trans*-bergamotene (**960**) from farnesyl-diphosphate was the first membrane-bound Class I-type terpene cyclase discovered.[592] Af520 converts farnesyl-PP to the corresponding nerolidyl-PP and then cyclization via a bisabolyl cation to the indicated 4,6-bicyclic hydrocarbon product.

Second, the P450 Af510 was shown to be a powerful, multifunctional oxidase/oxygenase that converts **960** into the bis-epoxide ketone intermediate **968** (Scheme 137).[51] This remarkable transformation by Af510 corresponds to a net eight-electron oxidation of the substrate. The first oxygen-transfer to the bridgehead alcohol to yield the monohydroxylated **961**. From there several mechanistic proposals have been presented, two of which are shown here.[597] In route *a,* C-H bond cleavage in the prenyl portion that affords **962** is followed by a second one electron oxidation to yield the carbocation intermediate **963**. This species is then attacked by the Iron-peroxo anion to form the heme-bound peroxide **964**, which can collapse to the epoxy-ketone **967** in a concerted series of electron transfer from the bridgehead hydroxyl to the iron center. An alternative mechanism is shown in route *b* that excludes formation of the secondary carbocation **963**. Here Af510 installs another alcohol group in the prenyl side chain to yield a doubly hydroxylated bergamotene product **965**. The third catalytic cycle of Af510 results in fragmentation of the bicyclic framework to yield the indicated cyclohexanone radical **966**. A fourth P450 cycle converts the side chain alcohol to the epoxide **967** before the *exo* methylene is itself epoxidized (five Af510 catalytic cycles) to create the bisepoxide framework **968**. To finish the fumagillin pathway, **968** is further oxidized at the *ortho* position, methylated and finally reduced at the ketone to yield fumagillol (**969**). **969** is then acylated with a pentaene polyketide product to yield prefumagillin, of which the terminal olefin can be oxidative cleaved to yield **970**.

6.3.2. Roquefortine to Meleagrin: Reconfiguring Connectivity in a Tetracyclic Framework—Roquefortines, natural products produced by fungi that are named for their cheese associations, are simple C_3-prenylated diketopiperazine metabolites.[598,599] Roquefortine D (**971**) arises from a tryptophanyl-histidine NRPS bimodular assembly line by internal cyclizing release as the DKP forms.[600,601] Subsequent prenylation at C_3 of the indole is attended by amide nitrogen attack on the incipient indoline at C_2 to create the tetracyclic core of **971** (Scheme 138).[602] RoqR in analogy to AsqJ in viridicatin biosynthesis (Section 6.1) effects a homolytic desaturation of the bridge between the DKP core and the pendant imidazole to produce roquefortine C (**972**).[602] Gene-knock out results indicate that two oxidative enzymes (P450 RoqM and FMO RoqO) are responsible for transformation of **972** to glandicoline B (**976**). First, *N*-hydroxylation by RoqM generates an electrophilic imino N-oxide roquefortine L (**973**). The second hydroxylation catalyzed by RoqO is proposed to occur at the C/D ring juncture to yield a carbinolamine **974,** which reverts to the carbonyl, mediating a transannular disconnection and produce a nine-member ring intermediate **975**. Now another amide nitrogen from the L-histidine portion of DKP core can attack at C_2 of the indole-*N*-oxide, which creates the crowded tetracyclic scaffold of **976** and then meleagrin (**977**) after *O*-methylation. The connectivity of the tetracyclic framework

between **971** and **977** has been distinctly altered, from a 6,5,5,6 starting array to a 6,5,6,5 order in the product.

6.3.3. Xantholipin: Quinone to Xanthone Ring Conversion—The angular heptacyclic antitumor antibiotic xantholipin (**986**) produced by *S. flavogriseus* is assembled by a type II polyketide synthase.[524,603] The conversion of the quinone D ring of the pentatcyclic polyketide intermediate **978** to the xanthone D ring in **985** on the way to **986** is initiated by a FMO XanO4 (Scheme 139).[604] Two successive oxygenations are proposed for the C and D rings of the substrate **978**. The first oxygenation via the adduct **979** yields **980**, which is an arene oxide in the C ring. The second adduct **981** leads to transient ring expansion to the oxazepine **982** that undergoes hydrolysis to liberate the OH group in **983** that attacks the adjacent C ring epoxide and afford **984**. The system is now set up for decarboxylation (and expulsion of methanol), effectively carving out the carbon atom that had been at the top of the D ring. Simultaneously, the oxygen atom from the second Baeyer-Villiger oxygenation reaction has been inserted as the xanthone forms in ring D to arrive at **985**. Subsequent P450-mediated formation of the methylenedioxy bridge and pyridone ring completes the complex heptacyclic scaffold of **986**.

6.3.4. Chartarin: Linear to Angular Polyaromatic Framework—The DNA-binding antitumor agent chartreusin (**993**) produced by *S. chartreusis* is a disaccharide of a pentacyclic aromatic polyketide aglycone chartarin (**992**).[605] As shown in Scheme 140, **992** is derived from a linear tetracyclic anthracycline framework **987**. The conversion to the rearranged connectivity in **992** is initiated by the oxygenase ChaZ which cleaves the B ring quinone as indicated, yielding the acyclic hydroxy ketone **988**.[606] Rotation around the C-C single bond precedes reclosure with C-C bond formation as indicated to yield the angular framework **989**. The quinone is restored but the connectivity between the B and C rings has been flipped. This twist places the carbomethoxy substituent close to the indicated -OH group in **990** which engages in lactone formation to yield **991**. A cupin-like dioxygenase ChaP is proposed to mediate the last step: an oxygenative removal of one of the carbonyl carbons in the cyclohexadienone **991** to **992** by successive possible reactions including hydroxylation, ring opening and lactonization as CO_2 is released. The oxidative carving out of the one carbon unit as CO_2 has analogies to the xantholipin logic above.

6.3.5. Jadomycin: Quinone to Oxazolidinone—Jadomycin A (**1001**) is a type-II angucycline polyketide produced by *Streptomyces* sp. with antitumor activity.[607,608] As shown in Scheme 141, the benzo[d]naphthopyrone framework of **1001** derives from benz[a]anthracene precursors such as dehydrorabelomycin (**994**), the starting substrate, via a series of substantial rearrangements in ring construction, especially ring C cleavage.[609–611] An FMO JadG and its reductase JadY partner work together to hydroxylate the C ring of **994**, as well as to carry out a Baeyer-Villiger type oxygen insertion to create the seven-membered hydroxylactone intermediate **996.** Hydrolytic opening of **996** yields the aldehyde acid **997**. Next, incorporation of L-isoleucine can lead to formation of **1001**. Two possible mechanisms are proposed for this step. In route *a*, a Schiff base intermediate **998** is formed via the reaction of isoleucine amine group with aldehyde in **997**, this is followed by attack on the quinone ring to form the oxazolidinone ring in **1001**. Alternatively in route *b,* attack

of cosubstrate isoleucine amine group in a 1,4-Michael addition to the B ring quinone takes place first to yield **999**. The acid group initially present in the B-ring quinone can now decarboxylate in a low energy pathway since it is a β-ketoacid, and forms **1000**. Attack of the α-NH on the aldehyde in **1000** creates a tetrahedral adduct whose oxyanion can react at the isoleucine carboxylate to create the oxazolidinone ring in the end product **1001**. Combined with the examples of xantholipin and chartarin, this is the third example of an oxidative strategy to carve out one carbon unit from a polycyclic framework during biosynthetic morphing.

6.3.6. PD116198: Anthracycline to Angucycline—The benz[a]anthraquinone antibiotic PD116198 (**1011**) has also undergone skeletal rearrangement from the anticipated octaketonyl-S-PKS enzyme intermediate.[612,613] As suggested in Scheme 142, the initial oxidative tetracyclic metabolite **1003** derived from the released product **1002** from the PKS enzyme undergoes oxygenative Baeyer-Villiger type expansion of the D-ring ketone to the lactone **1004**, catalyzed by BexE.[614] Hydrolysis to the hydroxy acid **1005** allows rotation and reformation of an angular ketone **1008**, thereby altering the connectivity from the linear tetracyclic starting substrate. A second Baeyer-Villiger insertion by the BexM enzyme to afford **1009** is proposed to be followed by a ring contraction back to the indicated hydroxy cyclohexanone **1010**. One more hydroxylation by BexK yields the end metabolite **1011**.[614]

6.3.7. Aflatoxin Structural Rearrangement from Anthraquinone—The most famous fungal toxin aflatoxin B1 (**1034**) is produced by many filamentous fungi. The biosynthesis of **1034** involves significant structural morphing from an aromatic polyketide product to the final product that is hardly recognizable to be derived from polyketide origin.[615] Many of the oxidative rearrangement cascades observed in the previous examples, including Baeyer-Villiger ring expansion, lactone cleavage and CO_2 expulsion will again be in play in this pathway.[616,617] As shown in Scheme 143, the biosynthetic pathway of **1034** involves at least 21 steps starting from the polyketide product norsolorinate anthrone (**1012**), which can undergo oxidation into the anthraquinone **1013**, and reduction of the benzylic ketone to yield norsolorinic acid (**1014**).[506,618–620] From there the structural morphing can be artificially divided into four stages.

The first stage results in formation of the hydroxyl-tetrahydrofuran ring in 1′-hydroxyversicolorone (**1018**). C_5′-hydroxylation of **1014** by the P450 AvnA to (1′*S*, 5′*S*)-5′-hydroxyaverantin (**1015**) is followed by dehydrogenation of the newly introduced hydroxyl group yields the 5′-ketone intermediate (5′-oxoaverantin, OVAN, **1016**).[621] This can be converted to (1′*S*, 5′*S*)-averufin (**1017**) by the OAVN cyclase via intramolecular acetal formation.[622] Subsequently, based on *in vivo* knockout results in the sterigmatocystin pathway, the P450 StcB and FMO StcW are responsible for converting **1017** to **1018**.[623] Based on the isotope labeling together with feeding of synthetically prepared analogs, either a cation- or radical-dependent mechanism can be proposed for this unusual oxidative rearrangement.[624–626]

The second stage includes four reactions to construct the pentacyclic intermediate versicolorin A (**1022**) which contains the bisfuran moiety. **1018** is first converted to

versiconal hemiacetal acetate (**1019**) via a Baeyer-Villiger reaction, during which the aliphatic ketone is converted to an ester.[623,627,628] Hydrolysis of the acetate reveals the terminal hydroxyl group as in versiconal (**1020**), which can be cyclized into versicolorin B (**1021**) by versiconal cyclase.[629,630] The terminal tetrahydrofuran ring can be dehydrogenated to form **1022**.

The third stage converts **1022** to demethylsterigmatocystin (**1030**), which converts the linearly fused anthraquinone to the angular xanthone, both pentacyclic compounds. Two enzymes, a P450 AflN and a probable NADPH-dependent oxidoreductase AflM are involved in this transformation.[631] First, P450-mediated aryl epoxidation by AflN affords the arene oxide **1023**. Oxirane opening converts ring A in **1023** into the hydroxylated dienone in **1024**. AflM mediated reduction of the dienone followed by dehydration yield the triketone intermediate **1026**. Next, as observed in the xantholipin biosynthesis in Scheme 139, the quinone ring is converted to xanthone through Baeyer-Villiger oxygen insertion to **1027**, hydrolytic cleavage to **1028**, xanthone formation to **1029,** and expulsion of carbon dioxide and water to yield demethylsterigmatocystin (**1030**).

The fourth stage starts with methylation of **1030** to yield *O*-methylsterigmatocystin (**1031**), which is morphed into **1034** in a net ring contraction sequence.[632,633] The exact order of reactions and the corresponding enzymes have not been elucidated. It is proposed that a P450-catalyzed hydroxylation to give **1032,** an additional Baeyer-Villiger oxidation to give **1033** are required for the ring expansion, rearrangement and contraction steps.[634–636]

6.3.8. Betalamic Acid: Catechol to Tetrahydropyridine Dicarboxylate—Betalamic acid(**1036**) (Scheme 144) is the chromophore in a variety of plant pigments, including betacyanins (**1037** and **1038**) and betaxanthins (**1039**), which are red and yellow pigments respectively.[637,638] It forms spontaneously from 4,5-*seco* DOPA (**1035**), which arises from action of regiospecific plant dioxygenases on the abundant metabolite L-DOPA (**528**).[639] The enzyme is a member of the extradiol dioxygenase family, cleaving adjacent to one of the catechol-OH groups.[640] The classic product pattern is conversion of the phenol carbon to the carboxylate and the adjacent carbon to the aldehyde, and that is the structure of **1035**. The enol isomerizes to the C_5 ketone that is then captured by the amine. Loss of water generates the **1036** with its dicarboxy tetrahydropyridine framework. The resulting aldehyde can engage in imine formation with several amines in plant cells to form the chromophoric betalins.

7. CONCLUDING THOUGHTS

Ubiquity of cyclic structures in natural products

The preponderance of the >500,000 natural products contain one or more carbocyclic or heterocyclic rings and most of those have multiple fused rings in their scaffolds. Five and Six membered rings predominate although we have delved in depth into the great biosynthetic versatility of the three atom epoxide rings. Seven member diazepinediones and tropolone, and eight member cyclooctanes are also found. In the polyketide family of macrolides, macrolactones from 12–22 atoms are generated by producer microorganisms.

The structural and functional group diversity of cyclic natural product frameworks is nothing short of awesome and have inspired generations of synthetic and medicinal chemists. Many of these scaffolds have still not yielded to total synthesis and the complex ones that have been prepared are typically not suitable for industrial scale production compared to the biological sources. Complexity generation in the conversion of simple, primary metabolic building blocks to polycyclic product architectures can occur by short efficient enzymatic pathways, as noted several times in the several sections of this review.

Several hypotheses have been advanced to comment on the utility of cyclic frameworks to producer organisms. The enzymatic conversion of acyclic precursors into cyclic natural products pays the energy costs upfront for building in entropic constraints. The resulting end products have order of magnitude higher affinities for particular biologic targets (DNA, RNA, Proteins, bacterial lipid II, peptidoglycan) than the linear precursors. This argument for cyclic architectures has the built-in assumption that these natural products are generated by producers for such specific recognition/ligation. The putative functions of the small molecule secondary metabolites span a spectrum of signaling, antibiotic activity, plant defense against predators (phytoalexins, phytoanticipins), development, and pheromone functions.[641]

Many of the natural products that have been active in human pharmacology assays are unlikely to have been the intended targets by the microbial or plant producers. They may reflect shapes, polarities and functional group arrays that have universal chemical properties for interaction with proteins (e.g the immunosuppressive fungal molecules FK506 and rapamycin) or DNA (bleomycin), just to pick two types of human targets.

Nonoxidative cyclizations: outside the scope of this review

In this review we have considered the chemical logic and enzymatic machinery for only a subset of cyclizations of natural products, those that are enabled by or directly involve one or more redox steps. Three examples of large families of nonoxidative cyclizations include macrolactonizing release of polyketides of the erythromycin, fidaxomycin class[40] and the aromatization of polyketonic intermediates into tri-and tetracyclic aromatic ring frameworks (e.g. tetracenomycin)[7,642,643]. (By contrast, prior reduction of the C_9 ketone to the alcohol reflects a redox-controlled cyclization to pretetramid, the precursor to tetracycline). The third major non-redox cyclization route is exemplified by the plethora of cation-driven rearrangements of mono-, sesqui-, di-, and triterpenes into many thousands of mono, bi-, tri-, and tetracyclic product scaffolds.[644–648] The bacterial squalene-hopene cyclases run in parallel to the oxidosqualene cyclases (Section 4.3), reflecting the alternate (and probably earlier evolutionary route) of initiating tetracyclic triterpene formations by either H^+ (non-oxidative) or epoxide (oxidative from the previous enzymatic step) as initiating electrophiles.[649–651]

Redox-Driven Cyclizations in Natural Product Assembly

The biosynthetic cyclizations that are covered in this review encompass C-C, C-O, C-N, C-S, N-N, and S-S bond forming steps in ring formations and occur in all the major classes of

natural products. We have noted two distinct logics in play for the multitude of C-C and C-O bond formations: one electron and two electron reaction manifolds.

One Electron Routes

While radical chemistry is relatively rare in primary metabolism, it is a signature route for the hundreds to thousands of iron-based oxygenases that are sprinkled liberally through so many biosynthetic maturation pathways. The iron-based oxygenases generate high-valent oxoiron species as powerful active site-contained oxidants that can cleave unactivated C-H bonds homolytically in bound substrates. That sets off two possible downstream reaction manifolds. One is [OH•] rebound leading to oxygen transfer. The second is a competing intramolecular reaction/rearrangement of the carbon centered radical (often with electron transfer from internal olefins) that results in ring formations without any net transfer of oxygen atoms to product. The broad reach of these alternate product-determining routes are the subject of Section 2. In many of the examples evidence has not yet accrued to distinguish between formation of a radical pair that combine vs pathways that involve migration of the initial radical with bond formations before transfer of a second electron to the oxoiron cofactor in the enzyme active sites.

The enzymatic generation of the penicillin and cephalosporin classes of β-lactam antibiotics,[246,247] historically the most widely used antibiotics globally over the past forty years, illustrates the separation of O_2-reductive activation, carbon-centered substrate radicals, and the formation of carbacylic and heterocyclic fused ring systems (Section 2.4). The separation of O_2-induced substrate carbon radicals from [OH•] rebound is also emphasized in the O_2-dependent halogenases noted in Section 5. In those cases chlorination, like epoxidation, can be a transient fate on the way in those cases to intramolecular S_N2 eliminations to cyclopropane rings.

Among the various examples of radical-mediated coupling and ring formations the biosynthesis of the glycosylated indolocarbazole staurosporine stands out for having three radical steps during assembly (Section 2.2.2).[64,65,68,71] The first is in construction of the C-C bond in chromopyrrolic acid, the second in the C-C coupling of the two pyrrole rings of the indole moieties to create the hexacyclic indolocarbazole platform. The third is the second N-C bond-creating step in bicyclic attachment of the sugar to create the final octacyclic staurosporine metabolite.

Other prominent examples of biosynthetic generation of radical species on electron rich aromatic rings of pathway intermediates include the oxidative coupling of five side chains in vancomycin and all seven in the heptapeptide framework of the teicoplanin family of antibiotics (Section 2.2.1).[41,42] These one electron manifolds for C-C bond formation also occur in a key step in morphine biosynthesis, (*S*)-reticuline to salutaridine (Section 2.2.3).[120]

At the other end of the oxygen availability spectrum are a set of S-adenosylmethionine (SAM)-dependent radical reactions that require anaerobicity because of attendant auto-oxidizable iron/sulfur clusters as electron donors. More than a hundred thousand predicted radical SAM open reading frames are in protein data bases, suggesting that an enormous range of anaerobic radical chemistry, most of it in secondary metabolism, awaits

discovery.[22,23,25] SAM is progenitor to the 5′-deoxyradical as initiator of C-H bond homolytic cleavages to set one electron reaction manifolds in motion (Section 2.4).[23] It is likely that the radical SAM logic and enzymatic machinery evolved early on in anaerobic/microaerophilic organisms before O_2 rose to current levels of 20% in the atmosphere and aerobic enzymatic machinery came into widespread distribution in secondary metabolic pathways.

The biosynthetically most useful feature of oxygenase chemistry is olefin epoxidation (Section 4). As in synthetic organic chemistry, the epoxides are a useful staging point for further complexity generation.[430,652,653] The three member oxirane ring provides either of two carbon atoms for attack by nucleophiles, intramolecular in all the cases discussed in Section 4. Further, the epoxide oxygen as it is opened by nucleophilic attack at the adjacent carbon center can function as nucleophile, most clearly illustrated in the two step biosynthetic conversion of olefins into furan- and pyran-containing cyclic polyether metabolites.

The most celebrated pathway for two step creation then ring-opening of an epoxy intermediate is in the conversion of squalene to thousands of cyclic triterpene sterol-like frameworks, via 2,3-oxidosqualene. Epoxide-induced cyclizations are also prevalent in indole terpene biosynthesis[648] and in the tri-epoxide skeletal morphing in aurovertin E biosynthesis.[455] In addition to aliphatic epoxide creation and opening are several examples of arene and heteroarene epoxidative intermediates, exemplified in gliotoxin biosynthesis[512] as well as spirotryprostatin spirocycle formations.[523]

Two Electron Routes

A second major route to biosynthetic ring formations during the assembly of natural products involves two electron pathways. These involve heterolytic mechanisms for C-C bond formations, with carbanion equivalents capturing electrophilic partners. Not surprisingly the enzymes that set up these cyclization routes use the two most readily available redox coenzymes of cellular metabolism, NAD(P)H and FAD.

NAD(P)H is the prototypic diffusible reduction currency in cells. In its reduced form it is a hydride donor; in its oxidized form, NAD(P)+ is a hydride acceptor. FAD by contrast is almost always tightly bound to its partner redox enzymes because in its dihydro form it is rapidly autoxidized by O_2. This is a crucially useful feature for FAD-enzymes to function as oxygenases, as noted through examples in Sections 3.6–3.10. But for the reactions in Section 3.3 it is the ability of FAD to accept hydride ions from substrates undergoing oxidation that is determinative.

Hydride Transfers to Drive Ring Formations

Both reductive and oxidative two electron pathways can be utilized to drive ring formations. The ikarugamycin case emphasizes how a hydride ion transfer from NADPH to an olefin sets off a transannular 1,6 carbonyl addition that builds a cyclopentane ring (Section 3.2.4).[298] In a different context NADH-mediated reductive cleavage of peptidyl thioesters from an NRPS assembly line yields the nascent peptidyl aldehyde that can be cyclized to the

imine and then captured in an intramolecular Pictet-Spengler reaction, twice, on the way to the antitumor scaffold of saframycins (Section 3.2.2).[288]

The oxidative transformations that feature hydride transfer to enzyme-bound FAD during cyclization are illustrated by the berberine bridge enzyme in alkaloid assembly (Section 3.3).[654] Comparable hydride transfer logic to Enzyme-bound FMN converts peptidyl thiazoline and oxazoline rings to the stable heteroaromatic thiazole and oxazoles in such metabolites as patellamides and telomestatin (Scheme 67 and 68).[337] Likewise, hydride transfer to flavoenzymes sets the cyclization cascade in tetrahydrocannabinol (Scheme 63) and in cyclopiazonate (Scheme 65) framework maturations.[317,330–332]

Transient Formation of Carbonyls as Cyclization Electrophiles

An alternative logic for two electron reaction manifolds to generate electrophiles employs enzymatic oxidation of alcohols to aldehydes or ketones and of amines to the corresponding imines. Capture of such transient carbonyls is at work in pipecolic acid formation for FK506 and rapamycin (Scheme 71)[363], chanoclavine-I to lysergic acid (Scheme 72)[373], and flavones to the yellow pigment aurones (Scheme 75)[384,386]. Notably this hydroxy ketone route is the path to assembly of the 6,6-spirocycle in reveromycin (Scheme 73).[376] (In passing we note this oxygen-independent route to spirocycles differs from the O_2-dependent routes, e.g. to griseofulvin (Scheme 25)[136,137], reflecting independent routes to this geometry-imposing bicyclic unit.).

Oxidations that Set up [4+2] Cyclizations

We have dealt briefly in this review with examples of [4+2] cyclizations that have differential accrued evidence for concerted (Diels-Alder) vs stepwise mechanisms (Section 3.10). Although the five and six-member ring-forming steps themselves do not involve oxidation or reduction, the enzymes catalyzing the prior step(s) do carry out oxidative transformations to set up the diene/dienophile reactive array. This can be manifested differently in solanapyrone (Scheme 81) where a conjugated aldehyde lowers energy barriers[413,414], versus the lovastatin (Scheme 82)[417], spinosyn (Scheme 83)[421], and abyssomicin (Scheme 84)[426] systems where the prior enzymes create either the dienophilic olefin or the diene array. The pyrroindomycin (Scheme 85)[427] case illustrates the two observed types of [4+2] cyclizations in two successive steps of one biosynthetic pathway.

The hirsutellone maturation logic is worth note at this juncture (Scheme 30). There are three distinct routes for C-C bond formation: (1) epoxidation, (2) radical coupling with phenolate, (3) an apparent Diels-Alder to create the 6-5-6 tricyclic scaffold element.[162]

Redox Dependent Morphing of Existing Ring Structures

Sections 2–5 deal with transformations that create new ring systems in the maturing natural products. Section 6 examines a distinct biosynthetic logic: the redox-dependent interconversion of one ring type to another. In a formal sense the conversion of epoxides to furans and pyrans in the polyethers by the epoxide hydrolases, considered on their own, would also fall into this category. The conversion of the 4,5-fused β-lactam in penicillin N to

the fused 4,6-β-lactam in desacetoxycephalosporin is a notable additional example (Scheme 131), by one electron, O_2-dependent enzyme chemistry.[580–582]

The rearrangements can be divided into ring contractions and ring expansions. Notable among the oxidative ring contractions are the 7-member diazepinedione to 2,3-dioxoquinolone system in viridicatin assembly (Scheme 121)[502] and also the cyclohexanol ring contraction in 7-hydroxy-*ent*-kaurenic acid to gibberellic acid-12 (Scheme 122)[557]. As a third route to a spirocyclic system the pathway from collinone to griseorhodin carves out one carbon from a fused 6,6-bicyclic element to the 5,6-spirocycle in the end product metabolite (Scheme 124)[562]. Perhaps the most convoluted molecular traverse is in xenovulene assembly (Scheme 126)[564]: a formyl catechol is first expanded to a tropolone then successively contracted to a formyl cyclohexanedione and, via loss of formate, generates ultimately a formyl cyclopentenone. Loss of a second formate results in oxidative carving out of two one carbon units to create the final hydroxycyclopentanone ring.

Ring expansion as a route to interconvert an existing ring into a larger lactone is a common strategy employed by Baeyer-Villigerases. Notable among the cadre of flavoenzyme Baeyer-Villigerases is the double insertion of oxygen to convert a ketone macrocycle to a cyclic carbonate ester in cytochalasin scaffold diversification (Scheme 129)[577]. One identified hemeprotein cytochrome P450 with Baeyer-Villiger lactonizing activity occurs at a late stage in maturation of the brassinosteroid plant hormones (Scheme 130).[579]

Enzymatic ring expansion of a tetramate five ring into the six ring pyridone in aspyridone assembly is proposed to proceed via an oxycyclopropyl radical intermediate (Scheme 134).[290,589] Reconfiguring connectivity and/or ring identity within fused polycyclic scaffolds also occurs in a number of biosynthetic pathways. One such is the conversion of the linear tetracyclic connectivity in roquefortine D to the angular framework of meleagrin, driven by a transient hydroxylation step (Scheme 138).[601,602] Another example is in the formation of the benz[a]anthraquinone polyketide antibiotic PD116198 (Scheme 142).[614]

The interchange of an internal benzoquinone to a xanthone in xantholipin (Scheme 139)[604] and aflatoxin (Scheme 143)[631] formation, and of a comparable internal quinone to an oxazolidinone in jadomycin maturation (Scheme 141)[609,610] are three examples of remarkable interchanges of oxidized carbacycles to heterocycles with dramatic changes in functional group properties in the products. An additional remarkable rearrangement is the formation of the pyridazine ring in the phthalazinone meroterpenoid azamerone.[655]

In sum, natural product biosynthesis pathways construct compact polycyclic metabolites whose functional group arrays, connectivities, shapes, and polarities depend both on the initial building blocks and the associated tailoring enzymes. Creation of the active, mature scaffolds employs the two most available two electron redox coenzymes, NAD(P)H and FAD and the one electron radical generators O_2 and SAM to drive an enormous range of carbacycle and heterocycle architectures.

Acknowledgments

Research activities in related areas in YT lab are supported by the by NIH 1R35GM118056 and 1U01GM110706, and the David and Lucile Packard Fellowship in Science and Engineering. K.W. thanks Japan Society for the Promotion of Science (JSPS) Program for Advancing Strategic International Networks to Accelerate the Circulation of Talented Researchers (No. G2604).

ABBREVIATIONS

ACAT	acyl-coenzyme A:cholesterol acyltransferase
ACP	acyl carrier protein
ACV	δ-(L-α-aminoadipoyl)-L-cysteinyl-D-valine
AT	acyltransferase
ATP	adenosine 5′-triphosphate
BBE	berberine bridge enzyme
C domain	condensation domain
CAS	clavaminate synthase
CDHFL	cyclic- dehypoxanthine futalosine
CDPS	cyclodipeptide synthase
CPA	chromopyrrolic acid
cYY	cyclo-Tyr-Tyr
5′dA•	5′-deoxyadenosyl radical
DAOCS	desacetoxycephalosporin synthase
DFT	density functional theory
DH	dehydratase
DHFL	dehypoxanthine futalosine
DHGO	dihydrogeodin oxidase
DKP	diketopiperazine
DMAPP	dimethylallyl pyrophosphate
DOPA	L-3,4-dihydroxyphenylalanine
ER	enolylreductase
FAD	flavin adenine dinucleotide
Fl-OO$^-$	peroxyflavin

Fl-OOH	hydroperoxyflavin
FMO	flavin dependent monooxygenase
FMN	flavin mononucleotide
GABA	γ-aminobutyric acid
GA_{12}	gibberellic acid 12
H6H	hyoscyamine 6β-hydroxylase
HDAC	histone deacetylase
2-HPP	2-hydroxypropylphosphonate
HPPO	4-hydroxy-6-(3-pyridinyl)-2H-pyran-2-one
IPAI	indole-3-pyruvate imine
IPNS	isopenicillin N synthase
ISY	iridoid synthase
α-KG	α-KG
KR	ketoreductase
KS	ketosynthase
MRSA	methicillin resistant *Staphylococcus aureus*
MT	methyltransferase
$NAD(P)^+$	β-nicotinamide adenine dinucleotide (phosphate)
NAD(P)H	β-nicotinamide adenine dinucleotide (phosphate), reduced form
nM	nanomolar
NRP	nonribosomal peptide
NRPS	nonribosomal peptide synthetase
Nu	nucleophile
OYE	old yellow enzyme
OVAN	5′-oxoaverantin
P5βR	progesterone 5β-reductase
PCET	proton-coupled electron transfer
PEP	phosphoenolpyruvate
PK	polyketide

PKS	polyketide synthase
PLP	pyridoxal phosphate
PTM	polycyclic tetramate macrolactam
R domain	reductase domain
RiPP	ribosomally synthesized and post-translationally modified peptide
SAH	*S*-adenosyl-L-homocysteine
SAM	*S*-adenosyl-L-methionine
SHC	squalene-hopene cyclase
T domain	thiolation domain
TDP	thymidine diphosphate
THF	tetrahydrofuran
THN	tetrahyrdoxynaphthalene
UDP	uridine diphosphate
VHPO	vanadium haloperoxidase

References

1. Newman DJ, Cragg GM. Natural Products as Sources of New Drugs from 1981 to 2014. J Nat Prod. 2016; 79(3):629–661. [PubMed: 26852623]
2. Cragg GM, Newman DJ. Natural Products: A Continuing Source of Novel Drug Leads. Biochim Biophys Acta. 2013; 1830(6):3670–3695. [PubMed: 23428572]
3. Mishra BB, Tiwari VK. Natural Products: An Evolving Role in Future Drug Discovery. Eur J Med Chem. 2011; 46(10):4769–4807. [PubMed: 21889825]
4. Walsh CT. A Chemocentric View of the Natural Product Inventory. Nat Chem Biol. 2015; 11(9): 620–624. [PubMed: 26284660]
5. Walsh CT, Fischbach MA. Natural Products Version 2.0: Connecting Genes to Molecules. J Am Chem Soc. 2010; 132(8):2469–2493. [PubMed: 20121095]
6. Kopp F, Marahiel MA. Macrocyclization Strategies in Polyketide and Nonribosomal Peptide Biosynthesis. Nat Prod Rep. 2007; 24(4):735–749. [PubMed: 17653357]
7. Zhou H, Li Y, Tang Y. Cyclization of Aromatic Polyketides from Bacteria and Fungi. Nat Prod Rep. 2010; 27(6):839–868. [PubMed: 20358042]
8. Helfrich EJ, Piel J. Biosynthesis of Polyketides by *trans*-AT Polyketide Synthases. Nat Prod Rep. 2016; 33(2):231–316. [PubMed: 26689670]
9. Martinez S, Hausinger RP. Catalytic Mechanisms of Fe(II)- and 2-Oxoglutarate-dependent Oxygenases. J Biol Chem. 2015; 290(34):20702–20711. [PubMed: 26152721]
10. Meunier B, de Visser SP, Shaik S. Mechanism of Oxidation Reactions Catalyzed by Cytochrome P450 Enzymes. Chem Rev. 2004; 104(9):3947–3980. [PubMed: 15352783]
11. Walsh CT, Wencewicz TA. Flavoenzymes: Versatile Catalysts in Biosynthetic Pathways. Nat Prod Rep. 2013; 30(1):175–200. [PubMed: 23051833]
12. Denisov IG, Makris TM, Sligar SG, Schlichting I. Structure and Chemistry of Cytochrome P450. Chem Rev. 2005; 105(6):2253–2277. [PubMed: 15941214]

13. Jung C. The Mystery of Cytochrome P450 Compound I: A Mini-Review Dedicated to Klaus Ruckpaul. Biochim Biophys Acta. 2011; 1814(1):46–57. [PubMed: 20558327]
14. Jung C, de Vries S, Schunemann V. Spectroscopic Characterization of Cytochrome P450 Compound I. Arch Biochem Biophys. 2011; 507(1):44–55. [PubMed: 21195047]
15. Costas M, Mehn MP, Jensen MP, Que L. Dioxygen Activation at Mononuclear Nonheme Iron Active Sites: Enzymes, Models, and Intermediates. Chem Rev. 2004; 104(2):939–986. [PubMed: 14871146]
16. Abu-Omar MM, Loaiza A, Hontzeas N. Reaction Mechanisms of Mononuclear Non-Heme Iron Oxygenases. Chem Rev. 2005; 105(6):2227–2252. [PubMed: 15941213]
17. Kovaleva EG, Lipscomb JD. Versatility of Biological Non-Heme Fe(II) Centers in Oxygen Activation Reactions. Nat Chem Biol. 2008; 4(3):186–193. [PubMed: 18277980]
18. Wu LF, Meng S, Tang GL. Ferrous Iron and Alpha-Ketoglutarate-Dependent Dioxygenases in the Biosynthesis of Microbial Natural Products. Biochim Biophys Acta. 2016; 1864(5):453–470. [PubMed: 26845569]
19. Krebs C, Galonic Fujimori D, Walsh CT, Bollinger JM Jr. Non-Heme Fe(IV)-Oxo Intermediates. Acc Chem Res. 2007; 40(7):484–492. [PubMed: 17542550]
20. Schofield CJ, Zhang Z. Structural and Mechanistic Studies on 2-Oxoglutarate-Dependent Oxygenases and Related Enzymes. Curr Opin Struct Biol. 1999; 9(6):722–731. [PubMed: 10607676]
21. Barry SM, Challis GL. Mechanism and Catalytic Diversity of Rieske Non-Heme Iron-Dependent Oxygenases. ACS Catal. 2013; 3(10):2362–2370.
22. Broderick JB, Duffus BR, Duschene KS, Shepard EM. Radical *S*-Adenosylmethionine Enzymes. Chem Rev. 2014; 114(8):4229–4317. [PubMed: 24476342]
23. Challand MR, Driesener RC, Roach PL. Radical *S*-Adenosylmethionine Enzymes: Mechanism, Control and Function. Nat Prod Rep. 2011; 28(10):1696–1721. [PubMed: 21779595]
24. Frey PA, Booker SJ. Radical Mechanisms of *S*-Adenosylmethionine-Dependent Enzymes. Adv Protein Chem. 2001; 58:1–45. [PubMed: 11665486]
25. Frey PA, Hegeman AD, Ruzicka FJ. The Radical SAM Superfamily. Crit Rev Biochem Mol Biol. 2008; 43(1):63–88. [PubMed: 18307109]
26. Richter OM, Ludwig B. Cytochrome c Oxidase--Structure, Function, and Physiology of a Redox-Driven Molecular Machine. Rev Physiol Biochem Pharmacol. 2003; 147:47–74. [PubMed: 12783267]
27. Rodriguez Couto S, Toca Herrera JL. Industrial and Biotechnological Applications of Laccases: A Review. Biotechnol Adv. 2006; 24(5):500–513. [PubMed: 16716556]
28. Ramsden CA, Riley PA. Tyrosinase: the Four Oxidation States of the Active Site and Their Relevance to Enzymatic Activation, Oxidation and Inactivation. Bioorg Med Chem. 2014; 22(8): 2388–2395. [PubMed: 24656803]
29. Decker H, Tuczek F. Tyrosinase/Catecholoxidase Activity of Hemocyanins: Structural Basis and Molecular Mechanism. Trends Biochem Sci. 2000; 25(8):392–397. [PubMed: 10916160]
30. Sanchez-Ferrer A, Rodriguez-Lopez JN, Garcia-Canovas F, Garcia-Carmona F. Tyrosinase: A Comprehensive Review of Its Mechanism. Biochim Biophys Acta. 1995; 1247(1):1–11. [PubMed: 7873577]
31. Rolff M, Schottenheim J, Decker H, Tuczek F. Copper-O_2 Reactivity of Tyrosinase Models Towards External Monophenolic Substrates: Molecular Mechanism and Comparison with the Enzyme. Chem Soc Rev. 2011; 40(7):4077–4098. [PubMed: 21416076]
32. Huijbers MM, Montersino S, Westphal AH, Tischler D, van Berkel WJ. Flavin Dependent Monooxygenases. Arch Biochem Biophys. 2014; 544:2–17. [PubMed: 24361254]
33. van Berkel WJ, Kamerbeek NM, Fraaije MW. Flavoprotein Monooxygenases, a Diverse Class of Oxidative Biocatalysts. J Biotechnol. 2006; 124(4):670–689. [PubMed: 16712999]
34. Winkler A, Motz K, Riedl S, Puhl M, Macheroux P, Gruber K. Structural and Mechanistic Studies Reveal the Functional Role of Bicovalent Flavinylation in Berberine Bridge Enzyme. J Biol Chem. 2009; 284(30):19993–20001. [PubMed: 19457868]

35. Winkler A, Hartner F, Kutchan TM, Glieder A, Macheroux P. Biochemical Evidence that Berberine Bridge Enzyme Belongs to a Novel Family of Flavoproteins Containing a Bi-Covalently Attached FAD Cofactor. J Biol Chem. 2006; 281(30):21276–21285. [PubMed: 16728404]
36. Kavanagh KL, Jörnvall H, Persson B, Oppermann U. Medium- and Short-Chain Dehydrogenase/Reductase Gene and Protein Families. Cell Mol Life Sci. 2008; 65(24):3895–3906. [PubMed: 19011750]
37. Oppermann U, Filling C, Hult M, Shafqat N, Wu XQ, Lindh M, Shafqat J, Nordling E, Kallberg Y, Persson B, et al. Short-Chain Dehydrogenases/Reductases (SDR): the 2002 Update. Chem Biol Interact. 2003; 143–144:247–253.
38. Rosenthal RG, Ebert MO, Kiefer P, Peter DM, Vorholt JA, Erb TJ. Direct Evidence for a Covalent Ene Adduct Intermediate in NAD(P)H-Dependent Enzymes. Nat Chem Biol. 2014; 10(1):50–55. [PubMed: 24240506]
39. Rosenthal RG, Vogeli B, Quade N, Capitani G, Kiefer P, Vorholt JA, Ebert M-O, Erb TJ. The Use of Ene Adducts to Study and Engineer Enoyl-Thioester Reductases. Nat Chem Biol. 2015; 11(6): 398–400. [PubMed: 25867044]
40. Du L, Lou L. PKS and NRPS Release Mechanisms. Nat Prod Rep. 2010; 27(2):255–278. [PubMed: 20111804]
41. Kahne D, Leimkuhler C, Lu W, Walsh C. Glycopeptide and Lipoglycopeptide Antibiotics. Chem Rev. 2005; 105(2):425–448. [PubMed: 15700951]
42. Yim G, Thaker MN, Koteva K, Wright G. Glycopeptide Antibiotic Biosynthesis. J Antibiot (Tokyo). 2014; 67(1):31–41. [PubMed: 24220108]
43. Park OK, Choi HY, Kim GW, Kim WG. Generation of New Complestatin Analogs by Heterologous Expression of the Complestatin Biosynthetic Gene Cluster from *Streptomyces Chartreusis* AN1542. Chembiochem. 2016; 17(18):1725–1731. [PubMed: 27383040]
44. Chiu HT, Hubbard BK, Shah AN, Eide J, Fredenburg RA, Walsh CT, Khosla C. Molecular Cloning and Sequence Analysis of the Complestatin Biosynthetic Gene Cluster. Proc Natl Acad Sci U S A. 2001; 98(15):8548–8553. [PubMed: 11447274]
45. Holtzel A, Schmid DG, Nicholson GJ, Stevanovic S, Schimana J, Gebhardt K, Fiedler HP, Jung G. Arylomycins A and B, New Biaryl-Bridged Lipopeptide Antibiotics Produced by *Streptomyces* sp. Tü 6075. II. Structure Elucidation. J Antibiot (Tokyo). 2002; 55(6):571–577. [PubMed: 12195963]
46. Liu WT, Kersten RD, Yang YL, Moore BS, Dorrestein PC. Imaging Mass Spectrometry and Genome Mining Via Short Sequence Tagging Identified the Anti-Infective Agent Arylomycin in *Streptomyces Roseosporus*. J Am Chem Soc. 2011; 133(45):18010–18013. [PubMed: 21999343]
47. Schimana J, Gebhardt K, Höltzel A, Schmid DG, Süssmuth R, Müller J, Pukall R, Fiedler HP. Arylomycins A and B, New Biaryl-Bridged Lipopeptide Antibiotics Produced by *Streptomyces* sp. Tü 6075. I. Taxonomy, Fermentation, Isolation and Biological Activities. J Antibiot (Tokyo). 2002; 55(6):565–570. [PubMed: 12195962]
48. Zerbe K, Pylypenko O, Vitali F, Zhang W, Rouset S, Heck M, Vrijbloed JW, Bischoff D, Bister B, Süssmuth RD, et al. Crystal Structure of OxyB, a Cytochrome P450 Implicated in an Oxidative Phenol Coupling Reaction During Vancomycin Biosynthesis. J Biol Chem. 2002; 277(49):47476–47485. [PubMed: 12207020]
49. Li Z, Rupasinghe SG, Schuler MA, Nair SK. Crystal Structure of a Phenol-Coupling P450 Monooxygenase Involved in Teicoplanin Biosynthesis. Proteins. 2011; 79(6):1728–1738. [PubMed: 21445994]
50. Pylypenko O, Vitali F, Zerbe K, Robinson JA, Schlichting I. Crystal Structure of OxyC, a Cytochrome P450 Implicated in an Oxidative C-C Coupling Reaction during Vancomycin Biosynthesis. J Biol Chem. 2003; 278(47):46727–46733. [PubMed: 12888556]
51. Haslinger K, Maximowitsch E, Brieke C, Koch A, Cryle MJ. Cytochrome P450 $OxyB_{tei}$ Catalyzes the First Phenolic Coupling Step in Teicoplanin Biosynthesis. ChemBioChem. 2014; 15(18):2719–2728. [PubMed: 25358800]
52. Geib N, Woithe K, Zerbe K, Li DB, Robinson JA. New Insights into the First Oxidative Phenol Coupling Reaction During Vancomycin Biosynthesis. Bioorg Med Chem Lett. 2008; 18(10):3081–3084. [PubMed: 18068978]

53. Zerbe K, Woithe K, Li DB, Vitali F, Bigler L, Robinson JA. An Oxidative Phenol Coupling Reaction Catalyzed by OxyB, a Cytochrome P450 from the Vancomycin-Producing Microorganism. Angew Chem Int Ed Engl. 2004; 43(48):6709–6713. [PubMed: 15593150]
54. Woithe K, Geib N, Zerbe K, Li DB, Heck M, Fournier-Rousset S, Meyer O, Vitali F, Matoba N, Abou-Hadeed K, et al. Oxidative Phenol Coupling Reactions Catalyzed by OxyB: A Cytochrome P450 from the Vancomycin Producing Organism. Implications for Vancomycin Biosynthesis. J Am Chem Soc. 2007; 129(21):6887–6895. [PubMed: 17477533]
55. Haslinger K, Cryle MJ. Structure of $OxyA_{tei}$: Completing Our Picture of the Glycopeptide Antibiotic Producing Cytochrome P450 Cascade. FEBS Lett. 2016; 590(4):571–581. [PubMed: 26820384]
56. Haslinger K, Peschke M, Brieke C, Maximowitsch E, Cryle MJ. X-Domain of Peptide Synthetases Recruits Oxygenases Crucial for Glycopeptide Biosynthesis. Nature. 2015; 521(7550):105–109. [PubMed: 25686610]
57. Brieke C, Peschke M, Haslinger K, Cryle MJ. Sequential in Vitro Cyclization by Cytochrome P450 Enzymes of Glycopeptide Antibiotic Precursors Bearing the X-Domain from Nonribosomal Peptide Biosynthesis. Angew Chem Int Ed Engl. 2015; 54(52):15715–15719. [PubMed: 26549530]
58. Sanchez C, Mendez C, Salas JA. Indolocarbazole Natural Products: Occurrence, Biosynthesis, and Biological Activity. Nat Prod Rep. 2006; 23(6):1007–1045. [PubMed: 17119643]
59. Bailly C, Riou JF, Colson P, Houssier C, Rodrigues-Pereira E, Prudhomme M. DNA Cleavage by Topoisomerase I in the Presence of Indolocarbazole Derivatives of Rebeccamycin. Biochemistry. 1997; 36(13):3917–3929. [PubMed: 9092822]
60. Kase H, Iwahashi K, Nakanishi S, Matsuda Y, Yamada K, Takahashi M, Murakata C, Sato A, Kaneko M. K-252 Compounds, Novel and Potent Inhibitors of Protein Kinase C and Cyclic Nucleotide-Dependent Protein Kinases. Biochem Biophys Res Commun. 1987; 142(2):436–440. [PubMed: 3028414]
61. Ward NE, O'Brian CA. Kinetic Analysis of Protein Kinase C Inhibition by Staurosporine: Evidence that Inhibition Entails Inhibitor Binding at a Conserved Region of the Catalytic Domain but Not Competition with Substrates. Mol Pharmacol. 1992; 41(2):387–392. [PubMed: 1538715]
62. Howard-Jones AR, Walsh CT. Enzymatic Generation of the Chromopyrrolic Acid Scaffold of Rebeccamycin by the Tandem Action of RebO and RebD. Biochemistry. 2005; 44(48):15652–15663. [PubMed: 16313168]
63. Sanchez C, Butovich IA, Brana AF, Rohr J, Mendez C, Salas JA. The Biosynthetic Gene Cluster for the Antitumor Rebeccamycin: Characterization and Generation of Indolocarbazole Derivatives. Chem Biol. 2002; 9(4):519–531. [PubMed: 11983340]
64. Onaka H, Taniguchi S, Igarashi Y, Furumai T. Cloning of the Staurosporine Biosynthetic Gene Cluster from *Streptomyces* sp. TP-A0274 and Its Heterologous Expression in *Streptomyces Lividans*. J Antibiot (Tokyo). 2002; 55(12):1063–1071. [PubMed: 12617516]
65. Makino M, Sugimoto H, Shiro Y, Asamizu S, Onaka H, Nagano S. Crystal Structures and Catalytic Mechanism of Cytochrome P450 StaP that Produces the Indolocarbazole Skeleton. Proc Natl Acad Sci U S A. 2007; 104(28):11591–11596. [PubMed: 17606921]
66. Nishizawa T, Gruschow S, Jayamaha DH, Nishizawa-Harada C, Sherman DH. Enzymatic Assembly of the Bis-Indole Core of Rebeccamycin. J Am Chem Soc. 2006; 128(3):724–725. [PubMed: 16417354]
67. Chiu H-T, Chen Y-L, Chen C-Y, Jin C, Lee M-N, Lin Y-C. Molecular Cloning, Sequence Analysis and Functional Characterization of the Gene Cluster for Biosynthesis of K-252a and Its Analogs. Mol Biosyst. 2009; 5(10):1180–1191. [PubMed: 19756308]
68. Howard-Jones AR, Walsh CT. Staurosporine and Rebeccamycin Aglycones Are Assembled by the Oxidative Action of StaP, StaC, and RebC on Chromopyrrolic Acid. J Am Chem Soc. 2006; 128(37):12289–12298. [PubMed: 16967980]
69. Spolitak T, Ballou DP. Evidence for Catalytic Intermediates Involved in Generating the Chromopyrrolic Acid Scaffold of Rebeccamycin by RebO and RebD. Arch Biochem Biophys. 2015; 573:111–119. [PubMed: 25837855]

70. Wang Y, Chen H, Makino M, Shiro Y, Nagano S, Asamizu S, Onaka H, Shaik S. Theoretical and Experimental Studies of the Conversion of Chromopyrrolic Acid to an Antitumor Derivative by Cytochrome P450 StaP: The Catalytic Role of Water Molecules. J Am Chem Soc. 2009; 131(19): 6748–6762. [PubMed: 19385626]
71. Onaka H, Asamizu S, Igarashi Y, Yoshida R, Furumai T. Cytochrome P450 Homolog Is Responsible for C-N Bond Formation Between Aglycone and Deoxysugar in the Staurosporine Biosynthesis of *Streptomyces* sp. TP-A0274. Biosci Biotechnol Biochem. 2005; 69(9):1753–1759. [PubMed: 16195595]
72. Dalsgaard PW, Blunt JW, Munro MH, Frisvad JC, Christophersen C. Communesins G and H, New Alkaloids from the Psychrotolerant Fungus *Penicillium Rivulum*. J Nat Prod. 2005; 68(2):258–261. [PubMed: 15730257]
73. Numata A, Takahashi C, Ito Y, Takada T, Kawai K, Usami Y, Matsumura E, Imachi M, Ito T, Hasegawa T. Communesins, Cytotoxic Metabolites of a Fungus Isolated from a Marine Alga. Tetrahedron Lett. 1993; 34(14):2355–2358.
74. Jadulco R, Edrada RA, Ebel R, Berg A, Schaumann K, Wray V, Steube K, Proksch P. New Communesin Derivatives from the Fungus *Penicillium* sp. Derived from the Mediterranean Sponge *Axinella Verrucosa*. J Nat Prod. 2004; 67(1):78–81. [PubMed: 14738391]
75. Hayashi H, Matsumoto H, Akiyama K. New Insecticidal Compounds, Communesins C, D and E, from *Penicillium Expansum* Link MK-57. Biosci Biotechnol Biochem. 2004; 68(3):753–756. [PubMed: 15056914]
76. Andersen B, Smedsgaard J, Frisvad JC. *Penicillium Expansum*: Consistent Production of Patulin, Chaetoglobosins, and Other Secondary Metabolites in Culture and Their Natural Occurrence in Fruit Products. J Agric Food Chem. 2004; 52(8):2421–2428. [PubMed: 15080656]
77. May JA, Zeidan RK, Stoltz BM. Biomimetic Approach to Communesin B (a.k.a. Nomofungin). Tetrahedron Lett. 2003; 44(6):1203–1205.
78. Han SJ, Vogt F, Krishnan S, May JA, Gatti M, Virgil SC, Stoltz BM. A Diastereodivergent Synthetic Strategy for the Syntheses of Communesin F and Perophoramidine. Org Lett. 2014; 16(12):3316–3319. [PubMed: 24909760]
79. Zuo ZW, Ma DW. Enantioselective Total Syntheses of Communesins A and B. Angew Chem Int Ed Engl. 2011; 50(50):12008–12011. [PubMed: 22006672]
80. Seo JH, Liu P, Weinreb SM. Evolution of a Strategy for Total Synthesis of the Marine Fungal Alkaloid (+/−)-Communesin F. J Org Chem. 2010; 75(8):2667–2680. [PubMed: 20334369]
81. Han SJ, Vogt F, May JA, Krishnan S, Gatti M, Virgil SC, Stoltz BM. Evolution of a Unified, Stereodivergent Approach to the Synthesis of Communesin F and Perophoramidine. J Org Chem. 2015; 80(1):528–547. [PubMed: 25402459]
82. Crawley SL, Funk RL. A Synthetic Approach to Nomofungin/Communesin B. Org Lett. 2003; 5(18):3169–3171. [PubMed: 12943379]
83. Zuo ZW, Xie WQ, Ma DW. Total Synthesis and Absolute Stereochemical Assignment of (-)-Communesin F. J Am Chem Soc. 2010; 132(38):13226–13228. [PubMed: 20812683]
84. Yang J, Wu HX, Shen LQ, Qin Y. Total Synthesis of (+/−)-Communesin F. J Am Chem Soc. 2007; 129(45):13794–13795. [PubMed: 17956099]
85. Belmar J, Funk RL. Total Synthesis of (+/−)-Communesin F via a Cycloaddition with Indol-2-One. J Am Chem Soc. 2012; 134(41):16941–16943. [PubMed: 22978807]
86. Liu P, Seo JH, Weinreb SM. Total Synthesis of the Polycyclic Fungal Metabolite (+/−)-Communesin F. Angew Chem Int Ed Engl. 2010; 49(11):2000–2003. [PubMed: 20175174]
87. Lathrop SP, Pompeo M, Chang WT, Movassaghi M. Convergent and Biomimetic Enantioselective Total Synthesis of (-)-Communesin F. J Am Chem Soc. 2016; 138(24):7763–7769. [PubMed: 27244250]
88. Lin H-C, Chiou G, Chooi Y-H, McMahon TC, Xu W, Garg NK, Tang Y. Elucidation of the Concise Biosynthetic Pathway of the Communesin Indole Alkaloids. Angew Chem Int Ed Engl. 2015; 54(10):3004–3007. [PubMed: 25571861]
89. Lin H-C, McMahon TC, Patel A, Corsello M, Simon A, Xu W, Zhao M, Houk KN, Garg NK, Tang Y. P450-Mediated Coupling of Indole Fragments to Forge Communesin and Unnatural Isomers. J Am Chem Soc. 2016; 138(12):4002–4005. [PubMed: 26963294]

90. Belin P, Le Du MH, Fielding A, Lequin O, Jacquet M, Charbonnier JB, Lecoq A, Thai R, Courçon M, Masson C, et al. Identification and Structural Basis of the Reaction Catalyzed by CYP121, an Essential Cytochrome P450 in *Mycobacterium Tuberculosis*. Proc Natl Acad Sci U S A. 2009; 106(18):7426–7431. [PubMed: 19416919]
91. Gondry M, Sauguet L, Belin P, Thai R, Amouroux R, Tellier C, Tuphile K, Jacquet M, Braud S, Courcon M, et al. Cyclodipeptide Synthases Are a Family of tRNA-Dependent Peptide Bond-Forming Enzymes. Nat Chem Biol. 2009; 5(6):414–420. [PubMed: 19430487]
92. McLean KJ, Carroll P, Lewis DG, Dunford AJ, Seward HE, Neeli R, Cheesman MR, Marsollier L, Douglas P, Smith WE, et al. Characterization of Active Site Structure in CYP121. A Cytochrome P450 Essential for Viability of *Mycobacterium Tuberculosis* H37Rv. J Biol Chem. 2008; 283(48): 33406–33416. [PubMed: 18818197]
93. Dumas VG, Defelipe LA, Petruk AA, Turjanski AG, Marti MA. QM/MM Study of the C-C Coupling Reaction Mechanism of CYP121, an Essential Cytochrome P450 of *Mycobacterium Tuberculosis*. Proteins. 2014; 82(6):1004–1021. [PubMed: 24356896]
94. Chiba T, Asami Y, Suga T, Watanabe Y, Nagai T, Momose F, Nonaka K, Iwatsuki M, Yamada H, Omura S, et al. Herquline A, Produced by *Penicillium Herquei* FKI-7215, Exhibits Anti-Influenza Virus Properties. Biosci Biotechnol Biochem. 2016; :1–4. DOI: 10.1080/09168451.09162016.01162084
95. Enomoto Y, Shiomi K, Hayashi M, Masuma R, Kawakubo T, Tomosawa K, Iwai Y, Omura S. Herquline B, a New Platelet Aggregation Inhibitor Produced by *Penicillium Herquei* Fg-372. J Antibiot (Tokyo). 1996; 49(1):50–53. [PubMed: 8609085]
96. Omura S, Hirano A, Iwai Y, Masuma R. Herquline, a New Alkaloid Produced by *Penicillium Herquei*. Fermentation, Isolation and Properties. J Antibiot (Tokyo). 1979; 32(8):786–790. [PubMed: 500499]
97. Yu X, Liu F, Zou Y, Tang M-C, Hang L, Houk KN, Tang Y. Biosynthesis of Strained Piperazine Alkaloids - Uncovering the Concise Pathway of Herquline A. J Am Chem Soc. 2016; 138(41): 13529–13532.
98. Taguchi H, Sankawa U, Shibata S. Biosynthesis of Natural ProductsVI. Biosynthesis of Usnic Acid in Lichens. A General Scheme of Biosynthesis of Usnic Acid. Chem Pharm Bull (Tokyo). 1969; 17(10):2054–2060. [PubMed: 5353559]
99. Taguchi H, Sankawa U, Shibata S. Biosynthesis of Natural Products. VII. Biosynthesis of Usnic Acid in Lichens. Seasonal Variation Observed in Usnic Acid Biosynthesis. Chem Pharm Bull (Tokyo). 1969; 17(10):2061–2064. [PubMed: 5353560]
100. Taguchi H, Sankawa U, Shibata S. Biosynthesis of Usnic Acid in Lichens. Tetrahedron Lett. 1966; (42):5211–5214.
101. Hutchison RD, Steyn PS, Van Rensburg SJ. Viridicatumtoxin, a New Mycotoxin from *Penicillium Viridicatum* Westling. Toxicol Appl Pharmacol. 1973; 24(3):507–509. [PubMed: 4122267]
102. Kabuto C, Silverton JV, Akiyama T, Sankawa U, Hutchison RD, Steyn PS, Vleggaar R. X-Ray Structure of Viridicatumtoxin: A New Class of Mycotoxin from *Penicillium Viridicatum* Westling. J Chem Soc, Chem Commun. 1976; (18):728–729.
103. Zheng CJ, Yu HE, Kim EH, Kim WG. Viridicatumtoxin B, a New Anti-MRSA Agent from *Penicillium* sp. FR11. J Antibiot (Tokyo). 2008; 61(10):633–637. [PubMed: 19168978]
104. Chooi Y-H, Hong YJ, Cacho RA, Tantillo DJ, Tang Y. A Cytochrome P450 Serves as an Unexpected Terpene Cyclase During Fungal Meroterpenoid Biosynthesis. J Am Chem Soc. 2013; 135(45):16805–16808. [PubMed: 24161266]
105. Chooi Y-H, Cacho R, Tang Y. Identification of the Viridicatumtoxin and Griseofulvin Gene Clusters from *Penicillium Aethiopicum*. Chem Biol. 2010; 17(5):483–494. [PubMed: 20534346]
106. Chooi Y-H, Wang P, Fang J, Li Y, Wu K, Wang P, Tang Y. Discovery and Characterization of a Group of Fungal Polycyclic Polyketide Prenyltransferases. J Am Chem Soc. 2012; 134(22): 9428–9437. [PubMed: 22590971]
107. Oda K, Hirose S, Takami N, Misumi Y, Takatsuki A, Ikehara Y. Brefeldin A Arrests the Intracellular Transport of a Precursor of Complement C3 Before its Conversion Site in Rat Hepatocytes. FEBS Lett. 1987; 214(1):135–138. [PubMed: 3569512]

108. Kato S, Ito S, Noguchi T, Naito H. Effects of Brefeldin A on the Synthesis and Secretion of Egg White Proteins in Primary Cultured Oviduct Cells of Laying Japanese Quail (*Coturnix Coturnix Japonica*). Biochim Biophys Acta. 1989; 991(1):36–43. [PubMed: 2713420]
109. Misumi Y, Misumi Y, Miki K, Takatsuki A, Tamura G, Ikehara Y. Novel Blockade by Brefeldin A of Intracellular Transport of Secretory Proteins in Cultured Rat Hepatocytes. J Biol Chem. 1986; 261(24):11398–11403. [PubMed: 2426273]
110. Zabala AO, Chooi Y-H, Choi MS, Lin H-C, Tang Y. Fungal Polyketide Synthase Product Chain-Length Control by Partnering Thiohydrolase. ACS Chem Biol. 2014; 9(7):1576–1586. [PubMed: 24845309]
111. Mizutani M, Ohta D. Diversification of P450 Genes During Land Plant Evolution. Annu Rev Plant Biol. 2010; 61:291–315. [PubMed: 20192745]
112. Mizutani M. Impacts of Diversification of Cytochrome P450 on Plant Metabolism. Biol Pharm Bull. 2012; 35(6):824–832. [PubMed: 22687470]
113. Nelson D, Werck-Reichhart D. A P450-Centric View of Plant Evolution. Plant J. 2011; 66(1): 194–211. [PubMed: 21443632]
114. Lau W, Sattely ES. Six Enzymes from Mayapple that Complete the Biosynthetic Pathway to the Etoposide Aglycone. Science. 2015; 349(6253):1224–1228. [PubMed: 26359402]
115. Klein AP, Sattely ES. Two Cytochromes P450 Catalyze *S*-Heterocyclizations in Cabbage Phytoalexin Biosynthesis. Nat Chem Biol. 2015; 11(11):837–839. [PubMed: 26389737]
116. Hagel JM, Facchini PJ. Dioxygenases Catalyze the *O*-Demethylation Steps of Morphine Biosynthesis in. Opium Poppy Nat Chem Biol. 2010; 6(4):273–275. [PubMed: 20228795]
117. Barton, DHR., Cohen, T. Festschrift Arthur Stall. Birkhauser; Basel: 1957. p. 117-144.
118. Zenk MH, Gerardy R, Stadler R. Phenol Oxidative Coupling of Benzylisoquinoline Alkaloids is Catalysed by Regio- and Stereo-Selective Cytochrome P-450 Linked Plant Enzymes: Salutaridine and Berbamunine. J Chem Soc, Chem Commun. 1989; (22):1725–1727.
119. Gerardy R, Zenk MH. Formation of Salutaridine from (R)-Reticuline by a Membrane-Bound Cytochrome P-450 Enzyme from *Papaver Somniferum*. Phytochemistry. 1993; 32(1):79–86.
120. Gesell A, Rolf M, Ziegler J, Díaz Chávez ML, Huang FC, Kutchan TM. CYP719B1 Is Salutaridine Synthase, the C-C Phenol-coupling Enzyme of Morphine Biosynthesis in *Opium Poppy*. J Biol Chem. 2009; 284(36):24432–24442. [PubMed: 19567876]
121. Ikezawa N, Iwasa K, Sato F. Molecular Cloning and Characterization of CYP80G2, a Cytochrome P450 that Catalyzes an Intramolecular C-C Phenol Coupling of (*S*)-Reticuline in Magnoflorine Biosynthesis, from Cultured *Coptis Japonica* Cells. J Biol Chem. 2008; 283(14): 8810–8821. [PubMed: 18230623]
122. Kraus PF, Kutchan TM. Molecular Cloning and Heterologous Expression of a cDNA Encoding Berbamunine Synthase, a C-O Phenol-Coupling Cytochrome P450 from the Higher Plant *Berberis Stolonifera*. Proc Natl Acad Sci U S A. 1995; 92(6):2071–2075. [PubMed: 7892226]
123. Jin Z. Amaryllidaceae and Sceletium Alkaloids. Nat Prod Rep. 2013; 30(6):849–868. [PubMed: 23644557]
124. Marco L, do Carmo Carreiras M. Galanthamine, a Natural Product for the Treatment of Alzheimer's Disease. Recent Pat CNS Drug Discov. 2006; 1(1):105–111. [PubMed: 18221196]
125. Kilgore MB, Kutchan TM. The Amaryllidaceae Alkaloids: Biosynthesis and Methods for Enzyme Discovery. Phytochem Rev. 2016; 15(3):317–337. [PubMed: 27340382]
126. Kilgore MB, Augustin MM, Starks CM, O'Neil-Johnson M, May GD, Crow JA, Kutchan TM. Cloning and Characterization of a Norbelladine 4′-*O*-Methyltransferase Involved in the Biosynthesis of the Alzheimer's Drug Galanthamine in *Narcissus* sp. aff. Pseudonarcissus. PLoS ONE. 2014; 9(7):e103223. [PubMed: 25061748]
127. Kilgore MB, Augustin MM, May GD, Crow JA, Kutchan TM. CYP96T1 of *Narcissus* sp. *aff. Pseudonarcissus* Catalyzes Formation of the *Para-Para'* C-C Phenol Couple in the Amaryllidaceae Alkaloids. Front Plant Sci. 2016; 7:225. [PubMed: 26941773]
128. Davin LB, Wang HB, Crowell AL, Bedgar DL, Martin DM, Sarkanen S, Lewis NG. Stereoselective Bimolecular Phenoxy Radical Coupling by an Auxiliary (Dirigent) Protein without an Active Center. Science. 1997; 275(5298):362–366. [PubMed: 8994027]

129. Halls SC, Davin LB, Kramer DM, Lewis NG. Kinetic Study of Coniferyl Alcohol Radical Binding to the (+)-Pinoresinol Forming Dirigent Protein. Biochemistry. 2004; 43(9):2587–2595. [PubMed: 14992596]
130. Pickel B, Constantin MA, Pfannstiel J, Conrad J, Beifuss U, Schaller A. An Enantiocomplementary Dirigent Protein for the Enantioselective Lacease-Catalyzed Oxidative Coupling of Phenols. Angew Chem Int Ed Engl. 2010; 49(1):202–204. [PubMed: 19946920]
131. Ono E, Nakai M, Fukui Y, Tomimori N, Fukuchi-Mizutani M, Saito M, Satake H, Tanaka T, Katsuta M, Umezawa T, et al. Formation of Two Methylenedioxy Bridges by a *Sesamum* CYP81Q Protein Yielding a Furofuran Lignan, (+)-Sesamin. Proc Natl Acad Sci U S A. 2006; 103(26):10116–10121. [PubMed: 16785429]
132. Gentles JC. Experimental Ringworm in Guinea Pigs: Oral Treatment with Griseofulvin. Nature. 1958; 182(4633):476–477. [PubMed: 13577889]
133. Gull K, Trinci AP. Griseofulvin Inhibits Fungal Mitosis. Nature. 1973; 244(5414):292–294. [PubMed: 4583105]
134. Rebacz B, Larsen TO, Clausen MH, Ronnest MH, Loffler H, Ho AD, Kramer A. Identification of Griseofulvin as an Inhibitor of Centrosomal Clustering in a Phenotype-Based Screen. Cancer Res. 2007; 67(13):6342–6350. [PubMed: 17616693]
135. Panda D, Rathinasamy K, Santra MK, Wilson L. Kinetic Suppression of Microtubule Dynamic Instability by Griseofulvin: Implications for Its Possible Use in the Treatment of Cancer. Proc Natl Acad Sci U S A. 2005; 102(28):9878–9883. [PubMed: 15985553]
136. Cacho RA, Chooi Y-H, Zhou H, Tang Y. Complexity Generation in Fungal Polyketide Biosynthesis: A Spirocycle-Forming P450 in the Concise Pathway to the Antifungal Drug Griseofulvin. ACS Chem Biol. 2013; 8(10):2322–2330. [PubMed: 23978092]
137. Grandner JM, Cacho RA, Tang Y, Houk KN. Mechanism of the P450-Catalyzed Oxidative Cyclization in the Biosynthesis of Griseofulvin. ACS Catal. 2016; 6(7):4506–4511.
138. Nielsen MT, Nielsen JB, Anyaogu DC, Holm DK, Nielsen KF, Larsen TO, Mortensen UH. Heterologous Reconstitution of the Intact Geodin Gene Cluster in *Aspergillus Nidulans* through a Simple and Versatile PCR Based Approach. PLoS ONE. 2013; 8:e72871. [PubMed: 24009710]
139. Huang KX, Fujii I, Ebizuka Y, Gomi K, Sankawa U. Molecular Cloning and Heterologous Expression of the Gene Encoding Dihydrogeodin Oxidase, a Multicopper Blue Enzyme from *Aspergillus Terreus*. J Biol Chem. 1995; 270(37):21495–21502. [PubMed: 7665560]
140. Gauthier T, Wang X, Sifuentes Dos Santos J, Fysikopoulos A, Tadrist S, Canlet C, Artigot MP, Loiseau N, Oswald IP, Puel O. Trypacidin, a Spore-Borne Toxin from *Aspergillus Fumigatus*, Is Cytotoxic to Lung Cells. PLoS ONE. 2012; 7(2):e29906. [PubMed: 22319557]
141. Mattern DJ, Schoeler H, Weber J, Novohradská S, Kraibooj K, Dahse HM, Hillmann F, Valiante V, Figge MT, Brakhage AA. Identification of the Antiphagocytic Trypacidin Gene Cluster in the Human-Pathogenic Fungus *Aspergillus Fumigatus*. Appl Microbiol Biotechnol. 2015; 99(23): 10151–10161. [PubMed: 26278536]
142. Wintersteiner O, Dutcher JD. Curare Alkaloids from *Chondodendron Tomentosum*. Science. 1943; 97(2525):467–470. [PubMed: 17789877]
143. Steinbach JH, Chen Q. Antagonist and Partial Agonist Actions of d-Tubocurarine at Mammalian Muscle Acetylcholine Receptors. J Neurosci. 1995; 15(1 Pt 1):230–240. [PubMed: 7529826]
144. Nasiripourdori A, Taly V, Grutter T, Taly A. From Toxins Targeting Ligand Gated Ion Channels to Therapeutic Molecules. Toxins (Basel). 2011; 3(3):260–293. [PubMed: 22069709]
145. Washizu F, Umezawa H, Sugiyama N. Chemical Studies on a Toxic Product of *Streptomyces Thioluteus*, Aureothin. J Antibiot (Tokyo). 1954; 7(2):60. [PubMed: 13174453]
146. Schwartz JL, Tishler M, Arison BH, Shafer HM, Omura S. Identification of Mycolutein and Pulvomycin as Aureothin and Labilomycin Respectively. J Antibiot (Tokyo). 1976; 29(3):236–241. [PubMed: 770405]
147. He J, Hertweck C. Iteration as Programmed Event During Polyketide Assembly: Molecular Analysis of the Aureothin Biosynthesis Gene Cluster. Chem Biol. 2003; 10(12):1225–1232. [PubMed: 14700630]

148. He J, Müller M, Hertweck C. Formation of the Aureothin Tetrahydrofuran Ring by a Bifunctional Cytochrome P450 Monooxygenase. J Am Chem Soc. 2004; 126(51):16742–16743. [PubMed: 15612710]

149. Richter ME, Traitcheva N, Knüpfer U, Hertweck C. Sequential Asymmetric Polyketide Heterocyclization Catalyzed by a Single Cytochrome P450 Monooxygenase (AurH). Angew Chem Int Ed Engl. 2008; 47(46):8872–8875. [PubMed: 18855960]

150. Zocher G, Richter ME, Mueller U, Hertweck C. Structural Fine-Tuning of a Multifunctional Cytochrome P450 Monooxygenase. J Am Chem Soc. 2011; 133(7):2292–2302. [PubMed: 21280577]

151. Kyriakidis N, Waight ES, Day JB, Mantle PG. Novel Metabolites from *Penicillium Crustosum*, Including Penitrem E, a Tremorgenic Mycotoxin. Appl Environ Microbiol. 1981; 42(1):61–62. [PubMed: 7259165]

152. Wagener RE, Davis ND, Diener UL. Penitrem A and Roquefortine Production by *Penicillium Commune*. Appl Environ Microbiol. 1980; 39(4):882–887. [PubMed: 16345552]

153. de Jesus AE, Steyn PS, van Heerden FR, Vleggaar R, Wessels PL, Hull WE. Tremorgenic Mycotoxins from *Penicillium Crustosum*: Isolation of Penitrems A-F and the Structure Elucidation and Absolute Configuration of Penitrem A. J Chem Soc, Perkin Trans 1. 1983:1847–1856.

154. Wilson BJ, Wilson CH, Hayes AW. Tremorgenic Toxin from *Penicillium Cyclopium* Grown on Food Materials. Nature. 1968; 220(5162):77–78.

155. Liu C, Tagami K, Minami A, Matsumoto T, Frisvad JC, Suzuki H, Ishikawa J, Gomi K, Oikawa H. Reconstitution of Biosynthetic Machinery for the Synthesis of the Highly Elaborated Indole Diterpene Penitrem. Angew Chem Int Ed Engl. 2015; 54(19):5748–5752. [PubMed: 25831977]

156. He HY, Yang HY, Bigelis R, Solum EH, Greenstein M, Carter GT. Pyrrocidines A and B, New Antibiotics Produced by a Filamentous Fungus. Tetrahedron Lett. 2002; 43(9):1633–1636.

157. Isaka M, Rugseree N, Maithip P, Kongsaeree P, Prabpai S, Thebtaranonth Y. Hirsutellones A-E, Antimycobacterial Alkaloids from the Insect Pathogenic Fungus *Hirsutella Nivea* BCC 2594. Tetrahedron. 2005; 61(23):5577–5583.

158. Koizumi, F., Hasegawa, K., Ando, K., Ogawa, T., Hara, A. Jpn Kokai Tokkyo Koho. JP 2001147574 A2001147572 2001200109. 2001.

159. Ebrahim W, Aly AH, Wray V, Mandi A, Teiten MH, Gaascht F, Orlikova B, Kassack MU, Lin W, Diederich M, et al. Embellicines A and B: Absolute Configuration and NF-kappaB Transcriptional Inhibitory Activity. J Med Chem. 2013; 56(7):2991–2999. [PubMed: 23484593]

160. Li XW, Ear A, Nay B. Hirsutellones and Beyond: Figuring Out the Biological and Synthetic Logics Toward Chemical Complexity in Fungal PKS-NRPS Compounds. Nat Prod Rep. 2013; 30(6):765–782. [PubMed: 23640165]

161. Oikawa H. Biosynthesis of Structurally Unique Fungal Metabolite GKK1032A_2: Indication of Novel Carbocyclic Formation Mechanism in Polyketide Biosynthesis. J Org Chem. 2003; 68(9): 3552–3557. [PubMed: 12713359]

162. Ear A, Amand S, Blanchard F, Blond A, Dubost L, Buisson D, Nay B. Direct Biosynthetic Cyclization of a Distorted Paracyclophane Highlighted by Double Isotopic Labelling of L-Tyrosine. Org Biomol Chem. 2015; 13(12):3662–3666. [PubMed: 25675395]

163. Miao SC, Anstee MR, LaMarco K, Matthew J, Huang LHT, Brasseur MM. Inhibition of Bacterial RNA Polymerases. Peptide Metabolites from the Cultures of *Streptomyces* sp. J Nat Prod. 1997; 60(8):858–861.

164. Trischman JA, Tapiolas DM, Jensen PR, Dwight R, Fenical W, Mckee TC, Ireland CM, Stout TJ, Clardy J. Salinamides A and B: Anti-inflammatory Depsipeptides from a Marine *Streptomycete*. J Am Chem Soc. 1994; 116(2):757–758.

165. Degen D, Feng Y, Zhang Y, Ebright KY, Ebright YW, Gigliotti M, Vahedian-Movahed H, Mandal S, Talaue M, Connell N, et al. Transcription Inhibition by the Depsipeptide Antibiotic Salinamide A. Elife. 2014; 3:e02451. [PubMed: 24843001]

166. Ray L, Yamanaka K, Moore BS. A Peptidyl-Transesterifying Type I Thioesterase in Salinamide Biosynthesis. Angew Chem Int Ed Engl. 2016; 55(1):364–367. [PubMed: 26553755]

167. Tijet N, Brash AR. Allene Oxide Synthases and Allene Oxides. Prostaglandins Other Lipid Mediat. 2002; 68–69:423–431.
168. Teder T, Lohelaid H, Boeglin WE, Calcutt WM, Brash AR, Samel N. A Catalase-Related Hemoprotein in Coral Is Specialized for Synthesis of Short-chain Aldehydes: DISCOVERY OF P450-TYPE HYDROPEROXIDE LYASE ACTIVITY IN A CATALASE. J Biol Chem. 2015; 290(32):19823–19832. [PubMed: 26100625]
169. Wildman WC, Kaufman CJ. Isolation of Tazettine and Lycorine from Certain *Hymenocallis* Species. J Am Chem Soc. 1954; 76(22):5815–5816.
170. Doskotch RW, El-Feraly FS. Isolation and Characterization of (+)-Sesamin and Beta-Cyclopyrethrosin from Pyrethrum Flowers. Can J Chem. 1969; 47(7):1139–1142.
171. Ikezawa N, Iwasa K, Sato F. CYP719A Subfamily of Cytochrome P450 Oxygenases and Isoquinoline Alkaloid Biosynthesis in *Eschscholzia Californica*. Plant Cell Rep. 2009; 28(1): 123–133. [PubMed: 18854999]
172. Ikezawa N, Tanaka M, Nagayoshi M, Shinkyo R, Sakaki T, Inouye K, Sato F. Molecular Cloning and Characterization of CYP719, a Methylenedioxy Bridge-Forming Enzyme that Belongs to a Novel P450 Family, from Cultured *Coptis Japonica* Cells. J Biol Chem. 2003; 278(40):38557–38565. [PubMed: 12732624]
173. Ikezawa N, Iwasa K, Sato F. Molecular Cloning and Characterization of Methylenedioxy Bridge-Forming Enzymes Involved in Stylopine Biosynthesis in *Eschscholzia Californica*. FEBS J. 2007; 274(4):1019–1035. [PubMed: 17250743]
174. Diaz Chavez ML, Rolf M, Gesell A, Kutchan TM. Characterization of Two Methylenedioxy Bridge-Forming Cytochrome P450-Dependent Enzymes of Alkaloid Formation in the Mexican Prickly Poppy *Argemone Mexicana*. Arch Biochem Biophys. 2011; 507(1):186–193. [PubMed: 21094631]
175. Rabindran SK, Ross DD, Doyle LA, Yang W, Greenberger LM. Fumitremorgin C Reverses Multidrug Resistance in Cells Transfected with the Breast Cancer Resistance Protein. Cancer Res. 2000; 60(1):47–50. [PubMed: 10646850]
176. Cui CB, Kakeya H, Okada G, Onose R, Osada H. Novel Mammalian Cell Cycle Inhibitors, Tryprostatins A, B and Other Diketopiperazines Produced by *Aspergillus Fumigatus*. I. Taxonomy, Fermentation, Isolation and Biological Properties. J Antibiot (Tokyo). 1996; 49(6): 527–533. [PubMed: 8698634]
177. Cui CB, Kakeya H, Osada H. Novel Mammalian Cell Cycle Inhibitors, Tryprostatins A, B and Other Diketopiperazines Produced by *Aspergillus Fumigatus*. II. Physico-Chemical Properties and Structures. J Antibiot (Tokyo). 1996; 49(6):534–540. [PubMed: 8698635]
178. Kato N, Suzuki H, Takagi H, Asami Y, Kakeya H, Uramoto M, Usui T, Takahashi S, Sugimoto Y, Osada H. Identification of Cytochrome P450s Required for Fumitremorgin Biosynthesis in *Aspergillus Fumigatus*. ChemBioChem. 2009; 10(5):920–928. [PubMed: 19226505]
179. Yin W-B, Grundmann A, Cheng J, Li S-M. Acetylaszonalenin Biosynthesis in *Neosartorya Fischeri*. Identification of the Biosynthetic Gene Cluster by Genomic Mining and Functional Proof of the Genes by Biochemical Investigation. J Biol Chem. 2009; 284(1):100–109. [PubMed: 19001367]
180. Liu J, Ng T, Rui Z, Ad O, Zhang W. Unusual Acetylation-Dependent Reaction Cascade in the Biosynthesis of the Pyrroloindole Drug Physostigmine. Angew Chem Int Ed Engl. 2014; 53(1): 136–139. [PubMed: 24227628]
181. Ma D. Recent Advances in the Discovery of Protein Kinase C Modulators Based on the Structures of Natural Protein Kinase C Activators. Curr Med Chem. 2001; 8(2):191–202. [PubMed: 11172674]
182. Huynh MU, Elston MC, Hernandez NM, Ball DB, Kajiyama S, Irie K, Gerwick WH, Edwards DJ. Enzymatic Production of (-)-Indolactam V by LtxB, a Cytochrome P450 Monooxygenase. J Nat Prod. 2010; 73(1):71–74. [PubMed: 20000453]
183. Edwards DJ, Gerwick WH. Lyngbyatoxin Biosynthesis: Sequence of Biosynthetic Gene Cluster and Identification of a Novel Aromatic Prenyltransferase. J Am Chem Soc. 2004; 126(37): 11432–11433. [PubMed: 15366877]

184. Awakawa T, Zhang L, Wakimoto T, Hoshino S, Mori T, Ito T, Ishikawa J, Tanner ME, Abe I. A Methyltransferase Initiates Terpene Cyclization in Teleocidin B Biosynthesis. J Am Chem Soc. 2014; 136:9910–9913. [PubMed: 24992358]

185. Bartz, QR., John, E., Penner, KM., Smith, RM. US Pat. 3023204. 1962.

186. Xie Y, Wang B, Liu J, Zhou J, Ma J, Huang H, Ju J. Identification of the Biosynthetic Gene Cluster and Regulatory Cascade for the Synergistic Antibacterial Antibiotics Griseoviridin and Viridogrisein in *Streptomyces Griseoviridis*. Chembiochem. 2012; 13(18):2745–2757. [PubMed: 23161816]

187. Xie Y, Li Q, Song Y, Ma J, Ju J. Involvement of SgvP in Carbon-Sulfur Bond Formation During Griseoviridin Biosynthesis. ChemBioChem. 2014; 15(8):1183–1189. [PubMed: 24782066]

188. Hallen HE, Luo H, Scott-Craig JS, Walton JD. Gene Family Encoding the Major Toxins of Lethal *Amanita* Mushrooms. Proc Natl Acad Sci U S A. 2007; 104(48):19097–19101. [PubMed: 18025465]

189. Furuta T, Koike M, Abe M. Isolation of Cycloclavine from the Culture Broth of *Aspergillus Japonicus* SAITO. Agric Biol Chem. 1982; 46(7):1921–1922.

190. Jakubczyk D, Caputi L, Hatsch A, Nielsen CA, Diefenbacher M, Klein J, Molt A, Schröder H, Cheng JZ, Naesby M, et al. Discovery and Reconstitution of the Cycloclavine Biosynthetic Pathway-Enzymatic Formation of a Cyclopropyl Group. Angew Chem Int Ed Engl. 2015; 54(17): 5117–5121. [PubMed: 25712404]

191. Klanova K, Blumauerova M, Vanek Z. Spontaneous and Induced Variability in *Streptomyces Nogalater* Producing Nogalamycin. Folia Microbiol (Praha). 1977; 22(4):286–294. [PubMed: 330365]

192. Siitonen V, Claesson M, Patrikainen P, Aromaa M, Mantsala P, Schneider G, Metsa-Ketela M. Identification of Late-Stage Glycosylation Steps in the Biosynthetic Pathway of the Anthracycline Nogalamycin. Chembiochem. 2012; 13(1):120–128. [PubMed: 22120896]

193. Siitonen V, Selvaraj B, Niiranen L, Lindqvist Y, Schneider G, Metsä-Ketelä M. Divergent Non-Heme Iron Enzymes in the Nogalamycin Biosynthetic Pathway. Proc Natl Acad Sci U S A. 2016; 113(19):5251–5256. [PubMed: 27114534]

194. Hande KR. Etoposide: Four Decades of Development of a Topoisomerase II Inhibitor. Eur J Cancer. 1998; 34(10):1514–1521. [PubMed: 9893622]

195. Nitiss JL. Targeting DNA Topoisomerase II in Cancer Chemotherapy. Nat Rev Cancer. 2009; 9(5):338–350. [PubMed: 19377506]

196. Sinkule JA. Etoposide: A Semisynthetic Epipodophyllotoxin. Chemistry, Pharmacology, Pharmacokinetics, Adverse Effects and Use as an Antineoplastic Agent. Pharmacotherapy. 1984; 4(2):61–73. [PubMed: 6326063]

197. Guerre P. Ergot Alkaloids Produced by Endophytic Fungi of the Genus *Epichloë*. Toxins (Basel). 2015; 7(3):773–790. [PubMed: 25756954]

198. Havemann J, Vogel D, Loll B, Keller U. Cyclolization of D-Lysergic Acid Alkaloid Peptides. Chem Biol. 2014; 21(1):146–155. [PubMed: 24361048]

199. McCranie EK, Bachmann BO. Bioactive Oligosaccharide Natural Products. Nat Prod Rep. 2014; 31(8):1026–1042. [PubMed: 24883430]

200. Hosted TJ, Wang TX, Alexander DC, Horan AC. Characterization of the Biosynthetic Gene Cluster for the Oligosaccharide Antibiotic, Evernimicin, in *Micromonospora Carbonacea var. Africana* ATCC39149. J Ind Microbiol Biotechnol. 2001; 27(6):386–392. [PubMed: 11774004]

201. Gaisser S, Trefzer A, Stockert S, Kirschning A, Bechthold A. Cloning of an Avilamycin Biosynthetic Gene Cluster from *Streptomyces Viridochromogenes* Tü57. J Bacteriol. 1997; 179(20):6271–6278. [PubMed: 9335272]

202. McCulloch KM, McCranie EK, Smith JA, Sarwar M, Mathieu JL, Gitschlag BL, Du Y, Bachmann BO, Iverson TM. Oxidative Cyclizations in Orthosomycin Biosynthesis Expand the Known Chemistry of an Oxygenase Superfamily. Proc Natl Acad Sci U S A. 2015; 112(37): 11547–11552. [PubMed: 26240321]

203. Reading C, Cole M. Clavulanic Acid: A Beta-Lactamase-Inhiting Beta-Lactam from *Streptomyces Clavuligerus*. Antimicrob Agents Chemother. 1977; 11(5):852–857. [PubMed: 879738]

204. Song JY, Jensen SE, Lee KJ. Clavulanic Acid Biosynthesis and Genetic Manipulation for Its Overproduction. Appl Microbiol Biotechnol. 2010; 88(3):659–669. [PubMed: 20711575]
205. Salowe SP, Krol WJ, Iwata-Reuyl D, Townsend CA. Elucidation of the Order of Oxidations and Identification of an Intermediate in the Multistep Clavaminate Synthase Reaction. Biochemistry. 1991; 30:2281–2292. [PubMed: 1998687]
206. Borowski T, De Marothy S, Broclawik E, Schofield CJ, Siegbahn PE. Mechanism for Cyclization Reaction by Clavaminic Acid Synthase. Insights from Modeling Studies. Biochemistry. 2007; 46(12):3682–3691. [PubMed: 17323933]
207. Salowe SP, Marsh EN, Townsend CA. Purification and Characterization of Clavaminate Synthase from *Streptomyces Clavuligerus*: An Unusual Oxidative Enzyme in Natural Product Biosynthesis. Biochemistry. 1990; 29:6499–6508. [PubMed: 2207091]
208. Janc JW, Egan LA, Townsend CA. Purification and Characterization of Clavaminate Synthase from *Streptomyces* Antibioticus. A Multifunctional Enzyme of Clavam Biosynthesis. J Biol Chem. 1995; 270(10):5399–5404. [PubMed: 7890654]
209. Busby RW, Townsend CA. A Single Monomeric Iron Center in Clavaminate Synthase Catalyzes Three Nonsuccessive Oxidative Transformations. Bioorg Med Chem. 1996; 4(7):1059–1064. [PubMed: 8831977]
210. Townsend CA. The Stereochemical Fate of Chiral-Methyl Valines in Cephalosporin C Biosynthesis. J Nat Prod. 1985; 48(5):708–724. [PubMed: 4078571]
211. Marsh EN, Chang MD, Townsend CA. Two Isozymes of Clavaminate Synthase Central to Clavulanic Acid Formation: Cloning and Sequencing of Both Genes from *Streptomyces Clavuligerus*. Biochemistry. 1992; 31(50):12648–12657. [PubMed: 1472501]
212. Khaleeli N, Li RF, Townsend CA. Origin of the Beta-Lactam Carbons in Clavulanic Acid from an Unusual Thiamine Pyrophosphate-Mediated Reaction. J Am Chem Soc. 1999; 121(39):9223–9224.
213. Zhang Z, Ren J-S, Harlos K, Mckinnon CH, Clifton IJ, Scho CJ. Crystal Structure of a Clavaminate Synthase-Fe(II)-2-Oxoglutarate-Substrate-NO Complex: Evidence for Metal Centered Rearrangements. FEBS Lett. 2002; 517(1–3):7–12. [PubMed: 12062399]
214. Zhang Z, Ren J, Stammers DK, Baldwin JE, Harlos K, Schofield CJ. Structural Origins of the Selectivity of the Trifunctional Oxygenase Clavaminic Acid Synthase. Nat Struct Biol. 2000; 7(2):127–133. [PubMed: 10655615]
215. Hashimoto T, Yamada Y. Hyoscyamine 6Beta-Hydroxylase, a 2-Oxoglutarate-Dependent Dioxygenase, in Alkaloid-Producing Root Cultures. Plant Physiol. 1986; 81(2):619–625. [PubMed: 16664866]
216. Matsuda J, Okabe S, Hashimoto T, Yamada Y. Molecular Cloning of Hyoscyamine 6 Beta-Hydroxylase, a 2-Oxoglutarate-Dependent Dioxygenase, from Cultured Roots of *Hyoscyamus Niger*. J Biol Chem. 1991; 266(15):9460–9464. [PubMed: 2033047]
217. Zhang L, Ding R, Chai Y, Bonfill M, Moyano E, Oksman-Caldentey KM, Xu T, Pi Y, Wang Z, Zhang H, et al. Engineering Tropane Biosynthetic Pathway in *Hyoscyamus Niger* Hairy Root Cultures. Proc Natl Acad Sci U S A. 2004; 101(17):6786–6791. [PubMed: 15084741]
218. Patterson DS, Shreeve BJ, Roberts BA, MacDonald SM. Verruculogen Produced by Soil Fungi in England and Wales. Appl Environ Microbiol. 1981; 42(5):916–917. [PubMed: 7316507]
219. Steffan N, Grundmann A, Afiyatullov S, Ruan H, Li S-M. FtmOx1, a Non-Heme Fe(II) and Alpha-Ketoglutarate-Dependent Dioxygenase, Catalyses the Endoperoxide Formation of Verruculogen in *Aspergillus Fumigatus*. Org Biomol Chem. 2009; 7(19):4082–4087. [PubMed: 19763315]
220. Yan W, Song H, Song F, Guo Y, Wu C-H, Sae Her A, Pu Y, Wang S, Naowarojna N, Weitz A, et al. Endoperoxide Formation by an α-Ketoglutarate-Dependent Mononuclear Non-Haem Iron Enzyme. Nature. 2015; 527(7579):539–543. [PubMed: 26524521]
221. Wank H, Rogers J, Davies J, Schroeder R. Peptide Antibiotics of the Tuberactinomycin Family as Inhibitors of Group I Intron RNA Splicing. J Mol Biol. 1994; 236(4):1001–1010. [PubMed: 7509881]

222. Ju J, Ozanick SG, Shen B, Thomas MG. Conversion of (2*S*)-Arginine to (2*S*,3*R*)-Capreomycidine by VioC and VioD from the Viomycin Biosynthetic Pathway of *Streptomyces* sp. Strain ATCC11861. ChemBioChem. 2004; 5(9):1281–1285. [PubMed: 15368582]

223. Yin X, McPhail KL, Kim KJ, Zabriskie TM. Formation of the Nonproteinogenic Amino Acid 2*S*, 3*R*-Capreomycidine by VioD from the Viomycin Biosynthesis Pathway. ChemBioChem. 2004; 5(9):1278–1281. [PubMed: 15368581]

224. Nyfeler R, Keller-Schierlein W. Metabolites of Microorganisms. 143. Echinocandin B, a Novel Polypeptide-Antibiotic from *Aspergillus Nidulans var. Echinulatus*: Isolation and Structural Components. Helv Chim Acta. 1974; 57(8):2459–2477. [PubMed: 4613708]

225. Golakoti T, Yoshida WY, Chaganty S, Moore RE. Isolation and Structures of Nostopeptolides A1, A2 and A3 from the Cyanobacterium *Nostoc* sp. GSV224. Tetrahedron. 2000; 56(46):9093–9102.

226. Umezawa K, Nakazawa K, Ikeda Y, Naganawa H, Kondo S. Polyoxypeptins A and B Produced by *Streptomyces*: Apoptosis-Inducing Cyclic Depsipeptides Containing the Novel Amino Acid (2S,3R)-3-Hydroxy-3-Methylproline. J Org Chem. 1999; 64(9):3034–3038. [PubMed: 11674399]

227. Terlain B, Thomas JP. Structure of Griselimycin, Polypeptide Antibiotic Extracted from Cultures of *Streptomyces*. II. Structure of Griselimycin. Bull Soc Chim Fr. 1971; (6):2357–2362. [PubMed: 5568643]

228. Festa C, De Marino S, Sepe V, Monti MC, Luciano P, D'Auria MV, Debitus C, Bucci M, Vellecco V, Zampella A. Perthamides C and D, Two New Potent Anti-Inflammatory Cyclopeptides from a Solomon Lithistid Sponge *Theonella Swinhoei*. Tetrahedron. 2009; 65(50):10424–10429.

229. Bevan K, Davies JS, Hall MJ, Hassall CH, Morton RB, Phillips DA, Ogihara Y, Thomas WA. The Monamycins, a New Family of Cyclodepsipeptide Antibiotics. Experientia. 1970; 26(2):122–123. [PubMed: 4905294]

230. Jiang W, Cacho RA, Chiou G, Garg NK, Tang Y, Walsh CT. EcdGHK Are Three Tailoring Iron Oxygenases for Amino Acid Building Blocks of the Echinocandin Scaffold. J Am Chem Soc. 2013; 135(11):4457–4466. [PubMed: 23451921]

231. Luesch H, Hoffmann D, Hevel JM, Becker JE, Golakoti T, Moore RE. Biosynthesis of 4-Methylproline in Cyanobacteria: Cloning of NosE and NosF Genes and Biochemical Characterization of the Encoded Dehydrogenase and Reductase Activities. J Org Chem. 2003; 68(1):83–91. [PubMed: 12515465]

232. Hoffmann D, Hevel JM, Moore RE, Moore BS. Sequence Analysis and Biochemical Characterization of the Nostopeptolide A Biosynthetic Gene Cluster from *Nostoc* sp. GSV224 Gene. 2003; 311:171–180. [PubMed: 12853152]

233. Hibi M, Kawashima T, Sokolov PM, Smirnov SV, Kodera T, Sugiyama M, Shimizu S, Yokozeki K, Ogawa J. L-Leucine 5-Hydroxylase of *Nostoc punctiforme* Is a Novel Type of Fe(II)/Alpha-Ketoglutarate-Dependent Dioxygenase that Is Useful as a Biocatalyst. Appl Microbiol Biotechnol. 2013; 97(6):2467–2472. [PubMed: 22584432]

234. Hendlin D, Stapley EO, Jackson M, Wallick H, Miller AK, Wolf FJ, Miller TW, Chaiet L, Kahan FM, Foltz EL, et al. Phosphonomycin, a New Antibiotic Produced by Strains of *Streptomyces*. Science. 1969; 166(3901):122–123. [PubMed: 5809587]

235. Christensen BG, Leanza WJ, Beattie TR, Patchett AA, Arison BH, Ormond RE, Kuehl FA Jr, Albers-Schonberg G, Jardetzky O. Phosphonomycin: Structure and Synthesis. Science. 1969; 166(3901):123–125. [PubMed: 5821213]

236. Kim SY, Ju KS, Metcalf WW, Evans BS, Kuzuyama T, van der Donk WA. Different Biosynthetic Pathways to Fosfomycin in *Pseudomonas Syringae* and *Streptomyces* Species. Antimicrob Agents Chemother. 2012; 56(8):4175–4183. [PubMed: 22615277]

237. Kahan FM, Kahan JS, Cassidy PJ, Kropp H. The Mechanism of Action of Fosfomycin (Phosphonomycin). Ann N Y Acad Sci. 1974; 235(0):364–386. [PubMed: 4605290]

238. Hidaka T, Goda M, Kuzuyama T, Takei N, Hidaka M, Seto H. Cloning and Nucleotide Sequence of Fosfomycin Biosynthetic Genes of *Streptomyces Wedmorensis*. Mol Gen Genet. 1995; 249(3):274–280. [PubMed: 7500951]

239. Liu P, Murakami K, Seki T, He X, Yeung S, Kuzuyama T, Seto H, Liu H-W. Protein Purification and Function Assignment of the Epoxidase Catalyzing the Formation of Fosfomycin. J Am Chem Soc. 2001; 123(19):4619–4620. [PubMed: 11457256]

240. Kuzuyama T, Seki T, Kobayashi S, Hidaka T, Seto H. Cloning and Expression in *Escherichia coli* of 2-Hydroxypropylphosphonic Acid Epoxidase from the Fosfomycin Producing Organism, *Pseudomonas Syringae* PB-5123. Biosci Biotechnol Biochem. 1999; 63(12):2222–2224. [PubMed: 10664856]

241. McLuskey K, Cameron S, Hammerschmidt F, Hunter WN. Structure and Reactivity of Hydroxypropylphosphonic Acid Epoxidase in Fosfomycin Biosynthesis by a Cation- and Flavin-Dependent Mechanism. Proc Natl Acad Sci U S A. 2005; 102(40):14221–14226. [PubMed: 16186494]

242. Wang C, Chang W-C, Guo Y, Huang H, Peck SC, Pandelia ME, Lin G-M, Liu H-W, Krebs C, Bollinger JMJ. Evidence that the Fosfomycin-Producing Epoxidase, HppE, Is a Non–Heme-Iron Peroxidase. Science. 2013; 342(6161):991–995. [PubMed: 24114783]

243. Chang W-C, Dey M, Liu P, Mansoorabadi SO, Moon SJ, Zhao Z-K, Drennan CL, Liu H-W. Mechanistic Studies of an Unprecedented Enzyme-Catalysed 1,2-Phosphono-Migration Reaction. Nature. 2013; 496(7443):114–118. [PubMed: 23552950]

244. Zhao Z, Liu P, Murakami K, Kuzuyama T, Seto H, Liu H-W. Mechanistic Studies of HPP Epoxidase: Configuration of the Substrate Governs Its Enzymatic Fate. Angew Chem Int Ed Engl. 2002; 41(23):4529–4532. [PubMed: 12458528]

245. Waxman DJ, Strominger JL. Penicillin-Binding Proteins and the Mechanism of Action of Beta-Lactam Antibiotics. Annu Rev Biochem. 1983; 52:825–869. [PubMed: 6351730]

246. Hamed RB, Gomez-Castellanos JR, Henry L, Ducho C, McDonough MA, Schofield CJ. The Enzymes of Beta-Lactam Biosynthesis. Nat Prod Rep. 2013; 30(1):21–107. [PubMed: 23135477]

247. Ozcengiz G, Demain AL. Recent Advances in the Biosynthesis of Penicillins, Cephalosporins and Clavams and Its Regulation. Biotechnol Adv. 2013; 31(2):287–311. [PubMed: 23228980]

248. Tamanaha E, Zhang B, Guo Y, Chang W-C, Barr EW, Xing G, St Clair J, Ye S, Neese F, Bollinger JMJ, et al. Spectroscopic Evidence for the Two C–H-Cleaving Intermediates of *Aspergillus Nidulans* Isopenicillin N Synthase. J Am Chem Soc. 2016; 138(28):8862–8874. [PubMed: 27193226]

249. Wasserman HH, Rodgers GC, Keith DD. Metacycloprodigiosin, a Tripyrrole Pigment from *Streptomyces Longisporus Ruber*. J Am Chem Soc. 1969; 91(5):1263–1264. [PubMed: 5780510]

250. Gerber NN, Mcinnes AG, Smith DG, Walter JA, Wright JLC, Vining LC. Biosynthesis of Prodiginines. C-13 Resonance Assignments and Enrichment Patterns in Nonyl-, Cyclononyl-, Methylcyclodecyl-, and Butylcycloheptylprodiginine Produced by *Actinomycete* Cultures Supplemented with C-13-Labeled Acetate and N-15-Labeled Nitrate. Can J Chem. 1978; 56(9): 1155–1163.

251. Boonlarppradab C, Kauffman CA, Jensen PR, Fenical W. Marineosins A and B, Cytotoxic Spiroaminals from a Marine-Derived Actinomycete. Org Lett. 2008; 10(24):5505–5508. [PubMed: 19007176]

252. Perez-Tomas R, Vinas M. New Insights on the Antitumoral Properties of Prodiginines. Curr Med Chem. 2010; 17(21):2222–2231. [PubMed: 20459382]

253. Stankovic N, Senerovic L, Ilic-Tomic T, Vasiljevic B, Nikodinovic-Runic J. Properties and Applications of Undecylprodigiosin and Other Bacterial Prodigiosins. Appl Microbiol Biotechnol. 2014; 98(9):3841–3858. [PubMed: 24562326]

254. Sydor PK, Barry SM, Odulate OM, Barona-Gomez F, Haynes SW, Corre C, Song L, Challis GL. Regio- and Stereodivergent Antibiotic Oxidative Carbocyclizations Catalysed by Rieske Oxygenase-Like Enzymes. Nat Chem. 2011; 3(5):388–392. [PubMed: 21505498]

255. Haynes SW, Sydor PK, Stanley AE, Song L, Challis GL. Role and Substrate Specificity of the *Streptomyces Coelicolor* RedH Enzyme in Undecylprodiginine Biosynthesis. Chem Commun (Camb). 2008; (16):1865–1867. [PubMed: 18401500]

256. Withall DM, Haynes SW, Challis GL. Stereochemistry and Mechanism of Undecylprodigiosin Oxidative Carbocyclization to Streptorubin B by the Rieske Oxygenase RedG. J Am Chem Soc. 2015; 137(24):7889–7897. [PubMed: 26023709]

257. Salem SM, Kancharla P, Florova G, Gupta S, Lu W, Reynolds KA. Elucidation of Final Steps of the Marineosins Biosynthetic Pathway Through Identification and Characterization of the Corresponding Gene Cluster. J Am Chem Soc. 2014; 136(12):4565–4574. [PubMed: 24575817]

258. Schramma KR, Bushin LB, Seyedsayamdost MR. Structure and Biosynthesis of a Macrocyclic Peptide Containing an Unprecedented Lysine-to-TryptophanCrosslink. Nat Chem. 2015; 7(5): 431–437. [PubMed: 25901822]

259. Ibrahim M, Guillot A, Wessner F, Algaron F, Besset C, Courtin P, Gardan R, Monnet V. Control of the Transcription of a Short Gene Encoding a Cyclic Peptide in *Streptococcus Thermophilus*: A New Quorum-Sensing System? J Bacteriol. 2007; 189(24):8844–8854. [PubMed: 17921293]

260. Gardan R, Besset C, Guillot A, Gitton C, Monnet V. The Oligopeptide Transport System Is Essential for the Development of Natural Competence in *Streptococcus Thermophilus* Strain LMD-9. J Bacteriol. 2009; 191(14):4647–4655. [PubMed: 19447907]

261. Fleuchot B, Gitton C, Guillot A, Vidic J, Nicolas P, Besset C, Fontaine L, Hols P, Leblond-Bourget N, Monnet V, et al. Rgg Proteins Associated with Internalized Small Hydrophobic Peptides: A New Quorum-Sensing Mechanism in *Streptococci*. Mol Microbiol. 2011; 80(4): 1102–1119. [PubMed: 21435032]

262. Dairi T, Kuzuyama T, Nishiyama M, Fujii I. Convergent Strategies in Biosynthesis. Nat Prod Rep. 2011; 28(6):1054–1086. [PubMed: 21547300]

263. Hiratsuka T, Furihata K, Ishikawa J, Yamashita H, Itoh N, Seto H, Dairi T. An Alternative Menaquinone Biosynthetic Pathway Operating in Microorganisms. Science. 2008; 321(5896): 1670–1673. [PubMed: 18801996]

264. Cooper LE, Fedoseyenko D, Abdelwahed SH, Kim SH, Dairi T, Begley TP. In Vitro Reconstitution of the Radical *S*-Adenosylmethionine Enzyme MqnC Involved in the Biosynthesis of Futalosine-Derived Menaquinone. Biochemistry. 2013; 52(27):4592–4594. [PubMed: 23763543]

265. Yoshida M, Ezaki M, Hashimoto M, Yamashita M, Shigematsu N, Okuhara M, Kohsaka M, Horikoshi K. A Novel Antifungal Antibiotic, Fr-900848. I. Production, Isolation, Physico-Chemical and Biological Properties. J Antibiot (Tokyo). 1990; 43(7):748–754. [PubMed: 2387768]

266. Watanabe H, Tokiwano T, Oikawa H. Biosynthetic Study of FR-900848: Origin of the Aminodeoxynucleoside Part. J Antibiot (Tokyo). 2006; 59(9):607–610. [PubMed: 17136894]

267. Watanabe H, Tokiwano T, Oikawa H. Biosynthetic Study of FR-900848: Unusual Observation on Polyketide Biosynthesis that Did Not Accept Acetate as Origin of Acetyl-CoA. Tetrahedron Lett. 2006; 47(9):1399–1402.

268. Hiratsuka T, Suzuki H, Kariya R, Seo T, Minami A, Oikawa H. Biosynthesis of the Structurally Unique Polycyclopropanated Polyketide-Nucleoside Hybrid Jawsamycin (FR-900848). Angew Chem Int Ed Engl. 2014; 53(21):5423–5426. [PubMed: 24756819]

269. Bauerle MR, Schwalm EL, Booker SJ. Mechanistic Diversity of Radical *S*-Adenosylmethionine (SAM)-Dependent Methylation. J Biol Chem. 2015; 290(7):3995–4002. [PubMed: 25477520]

270. Lotierzo M, Tse Sum Bui B, Florentin D, Escalettes F, Marquet A. Biotin Synthase Mechanism: An Overview. Biochem Soc Trans. 2005; 33(Pt 4):820–823. [PubMed: 16042606]

271. Lotierzo M, Raux E, Tse Sum Bui B, Goasdoue N, Libot F, Florentin D, Warren MJ, Marquet A. Biotin Synthase Mechanism: Mutagenesis of the YNHNLD Conserved Motif. Biochemistry. 2006; 45(40):12274–12281. [PubMed: 17014080]

272. Bui BT, Florentin D, Fournier F, Ploux O, Mejean A, Marquet A. Biotin Synthase Mechanism: on the Origin of Sulphur. FEBS Lett. 1998; 440(1–2):226–230. [PubMed: 9862460]

273. Rana A, Dey S, Agrawal A, Dey A. Density Functional Theory Calculations on the Active Site of Biotin Synthase: Mechanism of S Transfer from the Fe_2S_2 Cluster and the Role of 1st and 2nd Sphere Residues. J Biol Inorg Chem. 2015; 20(7):1147–1162. [PubMed: 26369537]

274. Taylor AM, Stoll S, Britt RD, Jarrett JT. Reduction of the [2Fe-2S] Cluster Accompanies Formation of the Intermediate 9-Mercaptodethiobiotin in *Escherichia coli* Biotin Synthase. Biochemistry. 2011; 50(37):7953–7963. [PubMed: 21859080]

275. Babasaki K, Takao T, Shimonishi Y, Kurahashi K. Subtilosin A, a New Antibiotic Peptide Produced by *Bacillus Subtilis* 168: Isolation, Structural Analysis, and Biogenesis. J Biochem. 1985; 98(3):585–603. [PubMed: 3936839]

276. Flühe L, Knappe TA, Gattner MJ, Schäfer A, Burghaus O, Linne U, Marahiel MA. The Radical SAM Enzyme AlbA Catalyzes Thioether Bond Formation in Subtilosin A. Nat Chem Biol. 2012; 8(4):737–737.

277. Benjdia A, Guillot A, Lefranc B, Vaudry H, Leprince J, Berteau O. Thioether Bond Formation by SPASM Domain Radical SAM Enzymes: Cα H-Atom Abstraction in Subtilosin A Biosynthesis. Chem Commun (Camb). 2016; 52(37):6249–6252. [PubMed: 27087315]

278. Meier JL, Burkart MD. The Chemical Biology of Modular Biosynthetic Enzymes. Chem Soc Rev. 2009; 38(7):2012–2045. [PubMed: 19551180]

279. Akey DL, Kittendorf JD, Giraldes JW, Fecik RA, Sherman DH, Smith JL. Structural Basis for Macrolactonization by the Pikromycin Thioesterase. Nat Chem Biol. 2006; 2(10):537–542. [PubMed: 16969372]

280. Golakoti T, Yoshida WY, Chaganty S, Moore RE. Isolation and Structure Determination of Nostocyclopeptides A1 and A2 from the Terrestrial Cyanobacterium *Nostoc* sp. ATCC53789. J Nat Prod. 2001; 64(1):54–59. [PubMed: 11170666]

281. Becker JE, Moore RE, Moore BS. Cloning, Sequencing, and Biochemical Characterization of the Nostocyclopeptide Biosynthetic Gene Cluster: Molecular Basis for Imine Macrocyclization. Gene. 2004; 325:35–42. [PubMed: 14697508]

282. Kopp F, Mahlert C, Grünewald J, Marahiel MA. Peptide Macrocyclization: The Reductase of the Nostocyclopeptide Synthetase Triggers the Self-Assembly of a Macrocyclic Imine. J Am Chem Soc. 2006; 128(51):16478–16479. [PubMed: 17177378]

283. Arai T, Takahashi K, Kubo A. New Antibiotics Saframycins A, B, C, D and E. J Antibiot (Tokyo). 1977; 30(11):1015–1018. [PubMed: 591455]

284. Cuevas C, Francesch A. Development of Yondelis (Trabectedin, ET-743). A Semisynthetic Process Solves the Supply Problem. Nat Prod Rep. 2009; 26(3):322–337. [PubMed: 19240944]

285. Molinski TF, Dalisay DS, Lievens SL, Saludes JP. Drug Development from Marine Natural Products. Nat Rev Drug Discov. 2009; 8(1):69–85. [PubMed: 19096380]

286. Rath CM, Janto B, Earl J, Ahmed A, Hu FZ, Hiller L, Dahlgren M, Kreft R, Yu F, Wolff JJ, et al. Meta-Omic Characterization of the Marine Invertebrate Microbial Consortium That Produces the Chemotherapeutic Natural Product ET-743. ACS Chem Biol. 2011; 6(11):1244–1256. [PubMed: 21875091]

287. Schofield MM, Jain S, Porat D, Dick GJ, Sherman DH. Identification and Analysis of the Bacterial Endosymbiont Specialized for Production of the Chemotherapeutic Natural Product ET-743. Environ Microbiol. 2015; 17(10):3964–3975. [PubMed: 26013440]

288. Koketsu K, Watanabe K, Suda H, Oguri H, Oikawa H. Reconstruction of the Saframycin Core Scaffold Defines Dual Pictet-Spengler Mechanisms. Nat Chem Biol. 2010; 6(6):408–410. [PubMed: 20453862]

289. Cary JW, Uka V, Han Z, Buyst D, Harris-Coward PY, Ehrlich KC, Wei Q, Bhatnagar D, Dowd PF, Martens SL, et al. An *Aspergillus Flavus* Secondary Metabolic Gene Cluster Containing a Hybrid PKS-NRPS Is Necessary for Synthesis of the 2-Pyridones, Leporins. Fungal Genet Biol. 2015; 81:88–97. [PubMed: 26051490]

290. Wasil Z, Pahirulzaman KAK, Butts C, Simpson TJ, Lazarus CM, Cox RJ. One Pathway, Many Compounds: Heterologous Expression of a Fungal Biosynthetic Pathway Reveals Its Intrinsic Potential for Diversity. Chem Sci. 2013; 4(10):3845–3856.

291. Snider BB, Lu Q. Total Synthesis of (+/−)-Leporin A. J Org Chem. 1996; 61(8):2839–2844. [PubMed: 11667120]

292. Agarwal V, Moore BS. Enzymatic Synthesis of Polybrominated Dioxins from the Marine Environment. ACS Chem Biol. 2014; 9(9):1980–1984. [PubMed: 25061970]

293. Jomon K, Kuroda Y, Ajisaka M, Sakai H. A New Antibiotic, Ikarugamycin. J Antibiot (Tokyo). 1972; 25(5):271–280. [PubMed: 4625358]

294. Cao S, Blodgett JA, Clardy J. Targeted Discovery of Polycyclic Tetramate Macrolactams from an Environmental *Streptomyces* Strain. Org Lett. 2010; 12(20):4652–4654. [PubMed: 20843016]

295. Graupner PR, Thornburgh S, Mathieson JT, Chapin EL, Kemmitt GM, Brown JM, Snipes CE. Dihydromaltophilin; a Novel Fungicidal Tetramic Acid Containing Metabolite from *Streptomyces* sp. J Antibiot (Tokyo). 1997; 50(12):1014–1019. [PubMed: 9510907]
296. Blodgett JA, Oh DC, Cao S, Currie CR, Kolter R, Clardy J. Common Biosynthetic Origins for Polycyclic Tetramate Macrolactams from Phylogenetically Diverse Bacteria. Proc Natl Acad Sci U S A. 2010; 107(26):11692–11697. [PubMed: 20547882]
297. Zhang G, Zhang W, Saha S, Zhang C. Recent Advances in Discovery, Biosynthesis and Genome Mining of Medicinally Relevant Polycyclic Tetramate Macrolactams. Curr Top Med Chem. 2016; 16(15):1727–1739. [PubMed: 26456464]
298. Zhang G, Zhang W, Zhang Q, Shi T, Ma L, Zhu Y, Li S, Zhang H, Zhao YL, Shi R, et al. Mechanistic Insights into Polycycle Formation by Reductive Cyclization in Ikarugamycin Biosynthesis. Angew Chem Int Ed Engl. 2014; 53(19):4840–4844. [PubMed: 24706593]
299. Lou L, Qian G, Xie Y, Hang J, Chen H, Zaleta-Rivera K, Li Y, Shen Y, Dussault PH, Liu F, et al. Biosynthesis of HSAF, a Tetramic Acid-Containing Macrolactam from Lysobacter Enzymogenes. J Am Chem Soc. 2011; 133(4):643–645. [PubMed: 21171605]
300. Antosch J, Schaefers F, Gulder TA. Heterologous Reconstitution of Ikarugamycin Biosynthesis in. E coli Angew Chem Int Ed Engl. 2014; 53(11):3011–3014. [PubMed: 24519911]
301. Liblikas I, Santangelo EM, Sandell J, Baeckstrom P, Svensson M, Jacobsson U, Unelius CR. Simplified Isolation Procedure and Interconversion of the Diastereomers of Nepetalactone and Nepetalactol. J Nat Prod. 2005; 68(6):886–890. [PubMed: 15974613]
302. Sticher O, Meier B. Quantitative Analysis and Isolation of Aucubin and Catalpol from *Folium Plantaginis* by HPLC. Planta Med. 1978; 33(3):295–296.
303. Dinda, B., Debnath, S. Natural Products: Phytochemistry, Botany and Metabolism of Alkaloids, Phenolics and Terpenes. Ramawat, GK., Mérillon, J-M., editors. Springer Berlin Heidelberg; Berlin, Heidelberg: 2013.
304. Kries H, O'Connor SE. Biocatalysts from Alkaloid Producing Plants. Curr Opin Chem Biol. 2016; 31:22–30. [PubMed: 26773811]
305. Geu-Flores F, Sherden NH, Courdavault V, Burlat V, Glenn WS, Wu C, Nims E, Cui Y, O'Connor SE. An Alternative Route to Cyclic Terpenes by Reductive Cyclization in Iridoid Biosynthesis. Nature. 2012; 492(7427):138–142. [PubMed: 23172143]
306. Munkert J, Costa C, Budeanu O, Petersen J, Bertolucci S, Fischer G, Müller-Uri F, Kreis W. Progesterone 5Beta-Reductase Genes of the Brassicaceae Family as Function-Associated Molecular Markers. Plant Biol J. 2015; 17(6):1113–1122.
307. Kries H, Caputi L, Stevenson CE, Kamileen MO, Sherden NH, Geu-Flores F, Lawson DM, O'Connor SE. Structural Determinants of Reductive Terpene Cyclization in Iridoid Biosynthesis. Nat Chem Biol. 2016; 12(1):6–8. [PubMed: 26551396]
308. Dittrich H, Kutchan TM. Molecular Cloning, Expression, and Induction of Berberine Bridge Enzyme, an Enzyme Essential to the Formation of Benzophenanthridine Alkaloids in the Response of Plants to Pathogenic Attack. Proc Natl Acad Sci U S A. 1991; 88:9969–9973. [PubMed: 1946465]
309. Facchini PJ, Penzes C, Johnson AG, Bull D. Molecular Characterization of Berberine Bridge Enzyme Genes from. Opium Poppy Plant Physiol. 1996; 112(4):1669–1677. [PubMed: 8972604]
310. Gaweska HM, Roberts KM, Fitzpatrick PF. Isotope Effects Suggest a Stepwise Mechanism for Berberine Bridge Enzyme. Biochemistry. 2012; 51(37):7342–7347. [PubMed: 22931234]
311. Winkler A, Łyskowski A, Riedl S, Puhl M, Kutchan TM, Macheroux P, Gruber K. A Concerted Mechanism for Berberine Bridge Enzyme. Nat Chem Biol. 2008; 4(12):739–741. [PubMed: 18953357]
312. Kutchan TM, Dirtrich H. Characterization and Mechanism of the Berberine Bridge Enzyme, a Covalently Flavinylated Oxidase of Benzophenanthridine Alkaloid Biosynthesis in Plants. J Biol Chem. 1995; 270(41):24475–24481. [PubMed: 7592663]
313. Wallner S, Winkler A, Riedl S, Dully C, Horvath S, Gruber K, MacHeroux P. Catalytic and Structural Role of a Conserved Active Site Histidine in Berberine Bridge Enzyme. Biochemistry. 2012; 51(31):6139–6147. [PubMed: 22757961]

314. Winkler A, Puhl M, Weber HP, Kutchan TM, Gruber K, Macheroux P. Berberine Bridge Enzyme Catalyzes the Six Electron Oxidation of (*S*)-Reticuline to Dehydroscoulerine. Phytochemistry. 2009; 70(9):1092–1097. [PubMed: 19570558]
315. Winkler A, Kutchan TM, Macheroux P. 6-*S*-Cysteinylation of Bi-Covalently Attached FAD in Berberine Bridge Enzyme Tunes the Redox Potential for Optimal Activity. J Biol Chem. 2007; 282(33):24437–24443. [PubMed: 17573342]
316. Baccile JA, Spraker JE, Le HH, Brandenburger E, Gomez C, Bok JW, Macheleidt J, Brakhage AA, Hoffmeister D, Keller NP, et al. Plant-Like Biosynthesis of Isoquinoline Alkaloids in *Aspergillus Fumigatus*. Nat Chem Biol. 2016; 12(6):419–424. [PubMed: 27065235]
317. Shoyama Y, Tamada T, Kurihara K, Takeuchi A, Taura F, Arai S, Blaber M, Shoyama Y, Morimoto S, Kuroki R. Structure and Function of Δ^1-Tetrahydrocannabinolic Acid (THCA) Synthase, the Enzyme Controlling the Psychoactivity of *Cannabis Sativa*. J Mol Biol. 2012; 423(1):96–105. [PubMed: 22766313]
318. Tsuchiya K, Yamazaki T, Takeuchi Y, Oishi T. Studies on T-2636 Antibiotics. IV. In Vitro and in Vivo Antibacterial Activity of T-2636 Antibiotics. J Antibiot (Tokyo). 1971; 24(1):29–41. [PubMed: 4395750]
319. Harada S. Studies on Lankacidin-Group (T-2636) Antibiotics. VI. Chemical Structures of Lankacidin-Group Antibiotics. II. Chem Pharm Bull (Tokyo). 1975; 23(10):2201–2210. [PubMed: 1212749]
320. Harada S, Kishi T. Studies on Lankacidin-Group (T-2636) Antibiotics. V. Chemical Structures of Lankacidin-Group Antibiotics. 1. Chem Pharm Bull (Tokyo). 1974; 22(1):99–108. [PubMed: 4833376]
321. Uramoto M, Otake N, Ogawa Y, Yonehara H. The Structures of Bundlin A (Lankacidin) and Bundlin B. Tetrahedron Lett. 1969; (27):2249–2254. [PubMed: 5796585]
322. Harada S, Higashide E, Fugono T, Kishi T. Isolation and Structures of T-2636 Antibiotics. Tetrahedron Lett. 1969; (27):2239–2244. [PubMed: 5796583]
323. Hayashi T, Suenaga I, Narukawa N, Yamazaki T. In Vitro and in Vivo Activities of Sedecamycin Against *Treponema Hyodysenteriae*. Antimicrob Agents Chemother. 1988; 32(4):458–461. [PubMed: 3377458]
324. Arakawa K, Sugino F, Kodama K, Ishii T, Kinashi H. Cyclization Mechanism for the Synthesis of Macrocyclic Antibiotic Lankacidin in *Streptomyces Rochei*. Chem Biol. 2005; 12(2):249–256. [PubMed: 15734652]
325. Tokuoka M, Seshime Y, Fujii I, Kitamoto K, Takahashi T, Koyama Y. Identification of a Novel Polyketide Synthase-Nonribosomal Peptide Synthetase (PKS-NRPS) Gene Required for the Biosynthesis of Cyclopiazonic Acid in *Aspergillus Oryzae*. Fungal Genet Biol. 2008; 45(12): 1608–1615. [PubMed: 18854220]
326. Chang PK, Horn BW, Dorner JW. Clustered Genes Involved in Cyclopiazonic Acid Production Are Next to the Aflatoxin Biosynthesis Gene Cluster in *Aspergillus Flavus*. Fungal Genet Biol. 2009; 46(2):176–182. [PubMed: 19038354]
327. Seidler NW, Jona I, Vegh M, Martonosi A. Cyclopiazonic Acid is a Specific Inhibitor of the Ca^{2+}-ATPase of Sarcoplasmic Reticulum. J Biol Chem. 1989; 264(30):17816–17823. [PubMed: 2530215]
328. Liu X, Walsh CT. Cyclopiazonic Acid Biosynthesis in *Aspergillus* sp.: Characterization of a Reductase-Like R* Domain in Cyclopiazonate Synthetase that Forms and Releases Cyclo-Acetoacetyl-L-Tryptophan. Biochemistry. 2009; 48(36):8746–8757. [PubMed: 19663400]
329. Liu X, Walsh CT. Characterization of Cyclo-Acetoacetyl-L-Tryptophan Dimethylallyltransferase in Cyclopiazonic Acid Biosynthesis: Substrate Promiscuity and Site Directed Mutagenesis Studies. Biochemistry. 2009; 48(46):11032–11044. [PubMed: 19877600]
330. Kenney WC, Edmondson DE, Singer TP, Steenkamp DJ, Schabort JC. Identification and Properties of the Covalently Bound Flavin of Beta-Cyclopiazonate Oxidocyclase. Biochemistry. 1976; 15(22):4931–4935. [PubMed: 10963]
331. Schabort JC, Wilkens DC, Holzapfel CW, Potgieter DJJ, Neitz AW. Beta-Cyclopiazonate Oxidocyclase from *Penicillium Cyclopium*. 1. Assay Methods, Isolation and Purification. Biochim Biophys Acta. 1971; 250(2):311–328. [PubMed: 5143339]

332. Steenkamp DJ, Schabort JC, Ferreira NP. Beta-Cyclopiazonate Oxidocyclase from *Penicillium Cyclopium*. 3. Preliminary Studies on the Mechanism of Action. Biochim Biophys Acta. 1973; 309(2):440–456. [PubMed: 4731971]
333. Mantovani SM, Moore BS. Flavin-Linked Oxidase Catalyzes Pyrrolizine Formation of Dichloropyrrole-Containing Polyketide Extender Unit in Chlorizidine A. J Am Chem Soc. 2013; 135(48):18032–18035. [PubMed: 24246014]
334. Alvarez-Mico X, Jensen PR, Fenical W, Hughes CC. Chlorizidine, a Cytotoxic 5H-Pyrrolo[2,1-a]Isoindol-5-One-Containing Alkaloid from a Marine *Streptomyces* sp. Org Lett. 2013; 15(5): 988–991. [PubMed: 23405849]
335. Oman TJ, van der Donk WA. Follow the Leader: the Use of Leader Peptides to Guide Natural Product Biosynthesis. Nat Chem Biol. 2010; 6(1):9–18. [PubMed: 20016494]
336. Donia MS, Ravel J, Schmidt EW. A Global Assembly Line for Cyanobactins. Nat Chem Biol. 2008; 4(6):341–343. [PubMed: 18425112]
337. Melby JO, Nard NJ, Mitchell DA. Thiazole/Oxazole-Modified Microcins: Complex Natural Products from Ribosomal Templates. Curr Opin Chem Biol. 2011; 15(3):369–378. [PubMed: 21429787]
338. Ireland CM, Durso AR, Newman RA, Hacker MP. Antineoplastic Cyclic Peptides from the Marine Tunicate *Lissoclinum Patella*. J Org Chem. 1982; 47(10):1807–1811.
339. Kim MY, Vankayalapati H, Shin-Ya K, Wierzba K, Hurley LH. Telomestatin, a Potent Telomerase Inhibitor that Interacts Quite Specifically with the Human Telomeric Intramolecular *G*-Quadruplex. J Am Chem Soc. 2002; 124(10):2098–2099. [PubMed: 11878947]
340. Bagley MC, Dale JW, Merritt EA, Xiong X. Thiopeptide Antibiotics. Chem Rev. 2005; 105(2): 685–714. [PubMed: 15700961]
341. Dunbar KL, Mitchell DA. Revealing Nature's Synthetic Potential Through the Study of Ribosomal Natural Product Biosynthesis. ACS Chem Biol. 2013; 8(3):473–487. [PubMed: 23286465]
342. Dunbar KL, Chekan JR, Cox CL, Burkhart BJ, Nair SK, Mitchell DA. Discovery of a New ATP-Binding Motif Involved in Peptidic Azoline Biosynthesis. Nat Chem Biol. 2014; 10(10):823–829. [PubMed: 25129028]
343. Dunbar KL, Melby JO, Mitchell DA. YcaO Domains Use ATP to Activate Amide Backbones During Peptide Cyclodehydrations. Nat Chem Biol. 2012; 8(6):569–575. [PubMed: 22522320]
344. Wever WJ, Bogart JW, Baccile JA, Chan AN, Schroeder FC, Bowers AA. Chemoenzymatic Synthesis of Thiazolyl Peptide Natural Products Featuring an Enzyme-Catalyzed Formal [4 + 2] Cycloaddition. J Am Chem Soc. 2015; 137(10):3494–3497. [PubMed: 25742119]
345. Wieland Brown LC, Acker MG, Clardy J, Walsh CT, Fischbach MA. Thirteen Posttranslational Modifications Convert a 14-Residue Peptide into the Antibiotic Thiocillin. Proc Natl Acad Sci U S A. 2009; 106(8):2549–2553. [PubMed: 19196969]
346. Kemp M, Go YM, Jones DP. Nonequilibrium Thermodynamics of Thiol/Disulfide Redox Systems: A Perspective on Redox Systems Biology. Free Radic Biol Med. 2008; 44(6):921–937. [PubMed: 18155672]
347. Rahman I, Kode A, Biswas SK. Assay for Quantitative Determination of Glutathione and Glutathione Disulfide Levels Using Enzymatic Recycling Method. Nat Protoc. 2006; 1(6):3159–3165. [PubMed: 17406579]
348. Grant C, Rahman F, Piekarz R, Peer C, Frye R, Robey RW, Gardner ER, Figg WD, Batest SE. Romidepsin: A New Therapy for Cutaneous T-Cell Lymphoma and a Potential Therapy for Solid Tumors. Expert Rev Anticancer Ther. 2010; 10(7):997–1008. [PubMed: 20645688]
349. Mann BS, Johnson JR, Cohen MH, Justice R, Pazdur R. FDA Approval Summary: Vorinostat for Treatment of Advanced Primary Cutaneous T-cell Lymphoma. Oncologist. 2007; 12(10):1247–1252. [PubMed: 17962618]
350. Kenig M, Reading C. Holomycin and an Antibiotic (MM 19290) Related to Tunicamycin, Metabolites of *Streptomyces Clavuligerus*. J Antibiot (Tokyo). 1979; 32(6):549–554. [PubMed: 468729]

351. Johnson JR, Bruce WF, Dutcher JD. Gliotoxin, the Antibiotic Principle of *Gliocladium Fimbriatum*. I. Production, Physical and Biological Properties. J Am Chem Soc. 1943; 65:2005–2009.
352. Gardiner DM, Waring P, Howlett BJ. The Epipolythiodioxopiperazine (ETP) Class of Fungal Toxins: Distribution, Mode of Action, Functions and Biosynthesis. Microbiology. 2005; 151(Pt 4):1021–1032. [PubMed: 15817772]
353. Scharf DH, Groll M, Habel A, Heinekamp T, Hertweck C, Brakhage AA, Huber EM. Flavoenzyme-Catalyzed Formation of Disulfide Bonds in Natural Products. Angew Chem Int Ed Engl. 2014; 53(8):2221–2224. [PubMed: 24446392]
354. Wang C, Wesener SR, Zhang H, Cheng YQ. An FAD-Dependent Pyridine Nucleotide-Disulfide Oxidoreductase Is Involved in Disulfide Bond Formation in FK228 Anticancer Depsipeptide. Chem Biol. 2009; 16(6):585–593. [PubMed: 19549597]
355. Li B, Walsh CT. *Streptomyces Clavuligerus* HlmI Is an Intramolecular Disulfide-Forming Dithiol Oxidase in Holomycin Biosynthesis. Biochemistry. 2011; 50(21):4615–4622. [PubMed: 21504228]
356. Scharf DH, Remme N, Heinekamp T, Hortschansky P, Brakhage AA, Hertweck C. Transannular Disulfide Formation in Gliotoxin Biosynthesis and Its Role in Self-Resistance of the Human Pathogen *Aspergillus Fumigatus*. J Am Chem Soc. 2010; 132(29):10136–10141. [PubMed: 20593880]
357. Giessen TW, Marahiel MA. Rational and Combinatorial Tailoring of Bioactive Cyclic Dipeptides. Front Microbiol. 2015; 6:785. [PubMed: 26284060]
358. Hara M, Asano K, Kawamoto I, Takiguchi T, Katsumata S, Takahashi K, Nakano H. Leinamycin, a New Antitumor Antibiotic from *Streptomyces*: Producing Organism, Fermentation and Isolation. J Antibiot (Tokyo). 1989; 42(12):1768–1774. [PubMed: 2621160]
359. Tang GL, Cheng YQ, Shen B. Leinamycin Biosynthesis Revealing Unprecedented Architectural Complexity for a Hybrid Polyketide Synthase and Nonribosomal Peptide Synthetase. Chem Biol. 2004; 11(1):33–45. [PubMed: 15112993]
360. Watanabe K, Hotta K, Praseuth AP, Koketsu K, Migita A, Boddy CN, Wang CC, Oguri H, Oikawa H. Total Biosynthesis of Antitumor Nonribosomal Peptides in *Escherichia coli*. Nat Chem Biol. 2006; 2(8):423–428. [PubMed: 16799553]
361. Hotta K, Keegan RM, Ranganathan S, Fang M, Bibby J, Winn MD, Sato M, Lian M, Watanabe K, Rigden DJ, et al. Conversion of a Disulfide Bond into a Thioacetal Group During Echinomycin Biosynthesis. Angew Chem Int Ed Engl. 2014; 53(3):824–828. [PubMed: 24302672]
362. Jiang H, Haltli B, Feng X, Cai P, Summers M, Lotvin J, He M. Investigation of the Biosynthesis of the Pipecolate Moiety of Neuroprotective Polyketide Meridamycin. J Antibiot (Tokyo). 2011; 64(8):533–538. [PubMed: 21610714]
363. Gatto GJ, Boyne MT, Kelleher NL, Walsh CT. Biosynthesis of Pipecolic Acid by RapL, a Lysine Cyclodeaminase Encoded in the Rapamycin Gene Cluster. J Am Chem Soc. 2006; 128(11):3838–3847. [PubMed: 16536560]
364. Sehgal SN, Baker H, Vezina C. Rapamycin (AY-22,989), a New Antifungal Antibiotic. II. Fermentation, Isolation and Characterization. J Antibiot (Tokyo). 1975; 28(10):727–732. [PubMed: 1102509]
365. Tanaka H, Kuroda A, Marusawa H, Hatanaka H, Kino T, Goto T, Hashimoto M, Taga T. Structure of FK506, a Novel Immunosuppressant Isolated from *Streptomyces*. J Am Chem Soc. 1987; 109(16):5031–5033.
366. Salituro GM, Zink DL, Dahl A, Nielsen J, Wu E, Huang LY, Kastner C, Dumont FJ. Meridamycin: A Novel Nonimmunosuppressive FKBP12 Ligand from *Streptomyces Hygroscopicus*. Tetrahedron Lett. 1995; 36(7):997–1000.
367. Fehr T, Sanglier JJ, Schuler W, Gschwind L, Ponelle M, Schilling W, Wioland C. Antascomicins A, B, C, D and E. Novel FKBP12 Binding Compounds from a *Micromonospora* Strain. J Antibiot (Tokyo). 1996; 49(3):230–233. [PubMed: 8626235]
368. Sun Y, Hong H, Samboskyy M, Mironenko T, Leadlay PF, Haydock SF. Organization of the Biosynthetic Gene Cluster in *Streptomyces* sp. DSM 4137 for the Novel Neuroprotectant Polyketide Meridamycin. Microbiology. 2006; 152(Pt12):3507–3515. [PubMed: 17159202]

369. Molnár I, Aparicio JF, Haydock SF, Khaw LE, Schwecke T, König A, Staunton J, Leadlay PF. Organisation of the Biosynthetic Gene Cluster for Rapamycin in *Streptomyces Hygroscopicus*: Analysis of Genes Flanking the Polyketide Synthase. Gene. 1996; 169(1):1–7. [PubMed: 8635730]

370. He M, Haltli B, Summers M, Feng X, Hucul J. Isolation and Characterization of Meridamycin Biosynthetic Gene Cluster from *Streptomyces* sp. NRRL 30748 Gene. 2006; 377:109–118. [PubMed: 16806745]

371. Schwecke T, Aparicio JF, Molnár I, König A, Khaw LE, Haydock SF, Oliynyk M, Caffrey P, Cortés J, Lester JB, et al. The Biosynthetic Gene Cluster for the Polyketide Immunosuppressant Rapamycin. Proc Natl Acad Sci U S A. 1995; 92(17):7839–7843. [PubMed: 7644502]

372. Motamedi H, Shafiee A. The Biosynthetic Gene Cluster for the Macrolactone Ring of the Immunosuppressant FK506. Eur J Biochem. 1998; 256(3):528–534. [PubMed: 9780228]

373. Schardl CL, Panaccione DG, Tudzynski P. Ergot Alkaloids - Biology and Molecular Biology. Alkaloids Chem Biol. 2006; 63:45–86. [PubMed: 17133714]

374. Mead B, Morgan H, Mann-Knowlton A, Tedeschi L, Sloan C, Lang S, Hines C, Gragg M, Stofer J, Riemann K, et al. Reveromycin A-Induced Apoptosis in Osteoclasts Is Not Accompanied by Necrosis. J Cell Biochem. 2015; 116(8):1646–1657. [PubMed: 25754900]

375. Osada H, Koshino H, Isono K, Takahashi H, Kawanishi G. Reveromycin A, a New Antibiotic Which Inhibits the Mitogenic Activity of Epidermal Growth Factor. J Antibiot (Tokyo). 1991; 44(2):259–261. [PubMed: 2010365]

376. Takahashi S, Toyoda A, Sekiyama Y, Takagi H, Nogawa T, Uramoto M, Suzuki R, Koshino H, Kumano T, Panthee S, et al. Reveromycin A Biosynthesis Uses RevG and RevJ for Stereospecific Spiroacetal Formation. Nat Chem Biol. 2011; 7(7):461–468. [PubMed: 21642985]

377. Li W, Ju J, Rajski SR, Osada H, Shen B. Characterization of the Tautomycin Biosynthetic Gene Cluster from *Streptomyces Spiroverticillatus* Unveiling New Insights into Dialkylmaleic Anhydride and Polyketide Biosynthesis. J Biol Chem. 2008; 283(42):28607–28617. [PubMed: 18708355]

378. Sun P, Zhao Q, Yu F, Zhang H, Wu Z, Wang Y, Wang Y, Zhang Q, Liu W. Spiroketal Formation and Modification in Avermectin Biosynthesis Involves a Dual Activity of AveC. J Am Chem Soc. 2013; 135(4):1540–1548. [PubMed: 23294008]

379. Frank B, Knauber J, Steinmetz H, Scharfe M, Blöcker H, Beyer S, Müller R. Spiroketal Polyketide Formation in *Sorangium*: Identification and Analysis of the Biosynthetic Gene Cluster for the Highly Cytotoxic Spirangienes. Chem Biol. 2007; 14(2):221–233. [PubMed: 17317575]

380. Frisvad JC, Rank C, Nielsen KF, Larsen TO. Metabolomics of *Aspergillus Fumigatus*. Med Mycol. 2009; 47:S53–S71. [PubMed: 18763205]

381. Ames BD, Haynes SW, Gao X, Evans BS, Kelleher NL, Tang Y, Walsh CT. Complexity Generation in Fungal Peptidyl Alkaloid Biosynthesis: Oxidation of Fumiquinazoline A to the Heptacyclic Hemiaminal Fumiquinazoline C by the Flavoenzyme Af12070 from *Aspergillus Fumigatus*. Biochemistry. 2011; 50(40):8756–8769. [PubMed: 21899262]

382. Gao X, Chooi YH, Ames BD, Wang P, Walsh CT, Tang Y. Fungal Indole Alkaloid Biosynthesis: Genetic and Biochemical Investigation of the Tryptoquialanine Pathway in *Penicillium Aethiopicum*. J Am Chem Soc. 2011; 133(8):2729–2741. [PubMed: 21299212]

383. Strack D, Vogt T, Schliemann W. Recent Advances in Betalain Research. Phytochemistry. 2003; 62(3):247–269. [PubMed: 12620337]

384. Molitor C, Mauracher SG, Pargan S, Mayer RL, Halbwirth H, Rompel A. Latent and Active Aurone Synthase from Petals of *C. Grandiflora*: A Polyphenol Oxidase with Unique Characteristics. Planta. 2015; 242(3):519–537. [PubMed: 25697287]

385. Molitor C, Mauracher SG, Rompel A. Crystallization and Preliminary Crystallographic Analysis of Latent, Active and Recombinantly Expressed Aurone Synthase, a Polyphenol Oxidase, from *Coreopsis Grandiflora*. Acta Crystallogr F Struct Biol Commun. 2015; 71(Pt6):746–751. [PubMed: 26057806]

386. Kaintz C, Molitor C, Thill J, Kampatsikas I, Michael C, Halbwirth H, Rompel A. Cloning and Functional Expression in *E. coli* of a Polyphenol Oxidase Transcript from *Coreopsis Grandiflora* Involved in Aurone Formation. FEBS lett. 2014; 588(18):3417–3426. [PubMed: 25109778]

387. Elsebai MF, Saleem M, Tejesvi MV, Kajula M, Mattila S, Mehiri M, Turpeinen A, Pirttila AM. Fungal Phenalenones: Chemistry, Biology, Biosynthesis and Phylogeny. Nat Prod Rep. 2014; 31(5):628–645. [PubMed: 24686921]

388. Gao S-S, Duan A, Xu W, Yu P, Hang L, Houk KN, Tang Y. Phenalenone Polyketide Cyclization Catalyzed by Fungal Polyketide Synthase and Flavin-Dependent Monooxygenase. J Am Chem Soc. 2016; 138(12):4249–4259. [PubMed: 26978228]

389. Simpson TJ. C-13 Nuclear Magnetic Resonance Structural and Biosynthetic Studies on Deoxyherqueinone and Herqueichrysin, Phenalenone Metabolites of *Penicillium Herquei*. J Chem Soc, Perkin Trans 1. 1979; (5):1233–1238.

390. Simpson TJ. Biosynthesis of Deoxyherqueinone in *Penicillium Herquei* from [C-13]Acetate and [C-13]Malonate-Assembly Pattern of Acetate into Phenalenone Ring System. J Chem Soc, Chem Commun. 1976; (7):258–260.

391. Piel J, Hertweck C, Shipley PR, Hunt DM, Newman MS, Moore BS. Cloning, Sequencing and Analysis of the Enterocin Biosynthesis Gene Cluster from the Marine Isolate '*Streptomyces Maritimus*': Evidence for the Derailment of an Aromatic Polyketide Synthase. Chem Biol. 2000; 7(12):943–955. [PubMed: 11137817]

392. Cheng Q, Xiang L, Izumikawa M, Meluzzi D, Moore BS. Enzymatic Total Synthesis of Enterocin Polyketides. Nat Chem Biol. 2007; 3(9):557–558. [PubMed: 17704772]

393. Xiang L, Kalaitzis JA, Nilsen G, Chen L, Moore BS. Mutational Analysis of the Enterocin Favorskii Biosynthetic Rearrangement. Org Lett. 2002; 4(6):957–960. [PubMed: 11893195]

394. Xiang L, Kalaitzis JA, Moore BS. EncM, a Versatile Enterocin Biosynthetic Enzyme Involved in Favorskii Oxidative Rearrangement, Aldol Condensation, and Heterocycle Forming Reactions. Proc Natl Acad Sci U S A. 2004; 101(44):15609–15614. [PubMed: 15505225]

395. Teufel R, Miyanaga A, Michaudel Q, Stull F, Louie G, Noel JP, Baran PS, Palfey B, Moore BS. Flavin-Mediated Dual Oxidation Controls an Enzymatic Favorskii-Type Rearrangement. Nature. 2013; 503(7477):552–556. [PubMed: 24162851]

396. Teufel R, Stull F, Meehan MJ, Michaudel Q, Dorrestein PC, Palfey B, Moore BS. Biochemical Establishment and Characterization of EncM's Flavin-N5-Oxide Cofactor. J Am Chem Soc. 2015; 137(25):8078–8085. [PubMed: 26067765]

397. Fehr T, Kallen J, Oberer L, Sanglier JJ, Schilling W. Sanglifehrins A, B, C and D, Novel Cyclophilin-Binding Compounds Isolated from *Streptomyces* sp. A92-308110. II. Structure Elucidation, Stereochemistry and Physico-Chemical Properties. J Antibiot (Tokyo). 1999; 52(5): 474–479. [PubMed: 10480571]

398. Broberg A, Menkis A, Vasiliauskas R. Kutznerides 1–4, Depsipeptides from the Actinomycete *Kutzneria* sp. 744 Inhabiting Mycorrhizal Roots of *Picea Abies* Seedlings. J Nat Prod. 2006; 69(1):97–102. [PubMed: 16441076]

399. Umezawa K, Nakazawa K, Uemura T, Ikeda Y, Kondo S, Naganawa H, Kinoshita N, Hashizume H, Hamada M, Takeuchi T, et al. Polyoxypeptin Isolated from *Streptomyces*: A Bioactive Cyclic Depsipeptide Containing the Novel Amino Acid 3-Hydroxy-3-Methylproline. Tetrahedron Lett. 1998; 39(11):1389–1392.

400. Oh DC, Poulsen M, Currie CR, Clardy J. Dentigerumycin: A Bacterial Mediator of an Ant-Fungus Symbiosis. Nat Chem Biol. 2009; 5(6):391–393. [PubMed: 19330011]

401. Maehr H, Liu CM, Palleroni NJ, Smallheer J, Todaro L, Williams TH, Blount JF. Microbial Products. VIII. Azinothricin, a Novel Hexadepsipeptide Antibiotic. J Antibiot (Tokyo). 1986; 39(1):17–25. [PubMed: 3753967]

402. Neumann CS, Jiang W, Heemstra JR, Gontang EA, Kolter R, Walsh CT. Biosynthesis of Piperazic Acid Via *N*5-Hydroxy-Ornithine in *Kutzneria* spp. 744. ChemBioChem. 2012; 13(7):972–976. [PubMed: 22522643]

403. Kunze B, Reichenbach H, Müller R, Hofle G. Aurafuron A and B, New Bioactive Polyketides from *Stigmatella Aurantiaca* and *Archangium Gephyra* (Myxobacteria). Fermentation, Isolation, Physico-Chemical Properties, Structure and Biological Activity. J Antibiot (Tokyo). 2005; 58(4): 244–251. [PubMed: 15981410]

404. Frank B, Wenzel SC, Bode HB, Scharfe M, Blöcker H, Müller R. From Genetic Diversity to Metabolic Unity: Studies on the Biosynthesis of Aurafurones and Aurafuron-Like Structures in *Myxobacteria* and *Streptomycetes*. J Mol Biol. 2007; 374(1):24–38. [PubMed: 17919655]
405. Minami A, Oikawa H. Recent Advances of Diels-Alderases Involved in Natural Product Biosynthesis. J Antibiot (Tokyo). 2016; 69(7):500–506. [PubMed: 27301662]
406. Klas K, Tsukamoto S, Sherman DH, Williams RM. Natural Diels-Alderases: Elusive and Irresistable. J Org Chem. 2015; 80(23):11672–11685. [PubMed: 26495876]
407. Hauser D, Sigg HP. Isolation and Decomposition of Sordarin. Helv Chim Acta. 1971; 54(4): 1178–1190. [PubMed: 5095217]
408. Dominguez JM, Kelly VA, Kinsman OS, Marriott MS, Gomez de las Heras F, Martin JJ. Sordarins: A New Class of Antifungals with Selective Inhibition of the Protein Synthesis Elongation Cycle in Yeasts. Antimicrob Agents Chemother. 1998; 42(9):2274–2278. [PubMed: 9736548]
409. Soe R, Mosley RT, Justice M, Nielsen-Kahn J, Shastry M, Merrill AR, Andersen GR. Sordarin Derivatives Induce a Novel Conformation of the Yeast Ribosome Translocation Factor eEF2. J Biol Chem. 2007; 282(1):657–666. [PubMed: 17082187]
410. Borschberg, H-J. Juris-Druck und -Verl. 1975. Zur Biogenese des Sordarins.
411. Kudo F, Matsuura Y, Hayashi T, Fukushima M, Eguchi T. Genome Mining of the Sordarin Biosynthetic Gene Cluster from *Sordaria Araneosa* Cain ATCC 36386: Characterization of Cycloaraneosene Synthase and GDP-6-Deoxyaltrose Transferase. J Antibiot (Tokyo). 2016; 69(7):541–548. [PubMed: 27072286]
412. Ichihara A, Tazaki H, Sakamura S. Solanapyrones A, B and C, Phytotoxic Metabolites from the Fungus *Alternaria Solani*. Tetrahedron Lett. 1983; 24(48):5373–5376.
413. Kasahara K, Miyamoto T, Fujimoto T, Oguri H, Tokiwano T, Oikawa H, Ebizuka Y, Fujii I. Solanapyrone Synthase, a Possible Diels-Alderase and Iterative Type I Polyketide Dynthase Encoded in a Biosynthetic Gene Cluster from *Alternaria Solani*. ChemBioChem. 2010; 11(9): 1245–1252. [PubMed: 20486243]
414. Katayama K, Kobayashi T, Oikawa H, Honma M, Ichihara A. Enzymatic Activity and Partial Purification of Solanapyrone Synthase: First Enzyme Catalyzing Diels-Alder Reaction. Biochim Biophys Acta. 1998; 1384(2):387–395. [PubMed: 9659400]
415. Mulder KC, Mulinari F, Franco OL, Soares MS, Magalhaes BS, Parachin NS. Lovastatin Production: From Molecular Basis to Industrial Process Optimization. Biotechnol Adv. 2015; 33(6 Pt 1):648–665. [PubMed: 25868803]
416. Ma SM, Tang Y. Biochemical Characterization of the Minimal Polyketide Synthase Domains in the Lovastatin Nonaketide Synthase LovB. FEBS J. 2007; 274(11):2854–2864. [PubMed: 17466016]
417. Ma SM, Li JW, Choi JW, Zhou H, Lee KK, Moorthie VA, Xie X, Kealey JT, Da Silva NA, Vederas JC, et al. Complete Reconstitution of a Highly Reducing Iterative Polyketide Synthase. Science. 2009; 326(5952):589–592. [PubMed: 19900898]
418. Kennedy J, Auclair K, Kendrew SG, Park C, Vederas JC, Hutchinson CR. Modulation of Polyketide Synthase Activity by Accessory Proteins During Lovastatin Biosynthesis. Science. 1999; 284(5418):1368–1372. [PubMed: 10334994]
419. Cacho RA, Thuss J, Xu W, Sanichar R, Gao Z, Nguyen A, Vederas JC, Tang Y. Understanding Programming of Fungal Iterative Polyketide Synthases: The Biochemical Basis for Regioselectivity by the Methyltransferase Domain in the Lovastatin Megasynthase. J Am Chem Soc. 2015; 137(50):15688–15691. [PubMed: 26630357]
420. Galm U, Sparks TC. Natural Product Derived Insecticides: Discovery and Development of Spinetoram. J Ind Microbiol Biotechnol. 2016; 43(2–3):185–193. [PubMed: 26582335]
421. Kim HJ, Ruszczycky MW, Choi SH, Liu YN, Liu HW. Enzyme-Catalysed [4+2] Cycloaddition Is a Key Step in the Biosynthesis of Spinosyn A. Nature. 2011; 473:109–112. [PubMed: 21544146]
422. Fage CD, Isiorho EA, Liu Y, Wagner DT, Liu H-W, Keatinge-Clay AT. The Structure of SpnF, a Standalone Enzyme that Catalyzes [4 + 2] Cycloaddition. Nat Chem Biol. 2015; 11(4):256–258. [PubMed: 25730549]

423. Patel A, Chen Z, Yang Z, Gutiérrez O, Liu H-W, Houk KN, Singleton DA. Dynamically Complex [6+4] and [4+2] Cycloadditions in the Biosynthesis of Spinosyn A. J Am Chem Soc. 2016; 138(11):3631–3634. [PubMed: 26909570]

424. Aroyan CE, Dermenci A, Miller SJ. The Rauhut-Currier Reaction: A History and Its Synthetic Application. Tetrahedron. 2009; 65(21):4069–4084.

425. Bister B, Bischoff D, Ströbele M, Riedlinger J, Reicke A, Wolter F, Bull AT, Zahner H, Fiedler HP, Süssmuth RD. Abyssomicin C-A Polycyclic Antibiotic from a Marine *Verrucosispora* Strain as an Inhibitor of the *p*-Aminobenzoic Acid/Tetrahydrofolate Biosynthesis Pathway. Angew Chem Int Ed Engl. 2004; 43(19):2574–2576. [PubMed: 15127456]

426. Byrne MJ, Lees NR, Han L-C, van der Kamp MW, Mulholland AJ, Stach JE, Willis CL, Race PR. The Catalytic Mechanism of a Natural Diels–Alderase Revealed in Molecular Detail. J Am Chem Soc. 2016; 138(19):6095–6098. [PubMed: 27140661]

427. Tian Z, Sun P, Yan Y, Wu Z, Zheng Q, Zhou S, Zhang H, Yu F, Jia X, Chen D, et al. An Enzymatic [4+2] Cyclization Cascade Creates the Pentacyclic Core of Pyrroindomycins. Nat Chem Biol. 2015; 11(4):259–265. [PubMed: 25730548]

428. Hashimoto T, Hashimoto J, Teruya K, Hirano T, Shin-ya K, Ikeda H, Liu HW, Nishiyama M, Kuzuyama T. Biosynthesis of Versipelostatin: Identification of an Enzyme-Catalyzed [4+2]-Cycloaddition Required for Macrocyclization of Spirotetronate-Containing Polyketides. J Am Chem Soc. 2015; 137(2):572–575. [PubMed: 25551461]

429. Meninno S, Lattanzi A. Organocatalytic Asymmetric Reactions of Epoxides: Recent Progress. Chemistry. 2016; 22(11):3632–3642. [PubMed: 26785400]

430. He J, Ling J, Chiu P. Vinyl Epoxides in Organic Synthesis. Chem Rev. 2014; 114(16):8037–8128. [PubMed: 24779795]

431. Thibodeaux CJ, Chang WC, Liu HW. Enzymatic Chemistry of Cyclopropane, Epoxide, and Aziridine Biosynthesis. Chem Rev. 2012; 112(3):1681–1709. [PubMed: 22017381]

432. de Vries EJ, Janssen DB. Biocatalytic Conversion of Epoxides. Curr Opin Biotechnol. 2003; 14(4):414–420. [PubMed: 12943851]

433. Taylor SK. Reactions of Epoxides with Ester, Ketone and Amide Enolates. Tetrahedron. 2000; 56(9):1149–1163.

434. Sienel, G., Rieth, R., Rowbottom, KT. Ullmann's Encyclopedia of Industrial Chemistry. Wiley-VCH Verlag GmbH & Co. KGaA; 2000.

435. Jacobsen EN. Asymmetric Catalysis of Epoxide Ring-Opening Reactions. Acc Chem Res. 2000; 33(6):421–431. [PubMed: 10891060]

436. Krake SH, Bergmeier SC. Inter- and Intramolecular Reactions of Epoxides and Aziridines with Pi-Nucleophiles. Tetrahedron. 2010; 66(37):7337–7360.

437. Dominguez de Maria P, van Gemert RW, Straathof AJ, Hanefeld U. Biosynthesis of Ethers: Unusual or Common Natural Events? Nat Prod Rep. 2010; 27(3):370–392. [PubMed: 20179877]

438. Morimoto Y, Iwai T, Kinoshita T. Revised Structure of Squalene-Derived PentaTHF Polyether, Glabrescol, through Its Enantioselective Total Synthesis: Biogenetically Intriguing Cs vs C2 Symmetric Relationships. J Am Chem Soc. 2000; 122(29):7124–7125.

439. Matsuura Y, Shichijo Y, Minami A, Migita A, Oguri H, Watanabe M, Tokiwano T, Watanabe K, Oikawa H. Intriguing Substrate Tolerance of Epoxide Hydrolase Lsd19 Involved in Biosynthesis of the Ionophore Antibiotic Lasalocid A. Org Lett. 2010; 12(10):2226–2229. [PubMed: 20394359]

440. Minami A, Migita A, Inada D, Hotta K, Watanabe K, Oguri H, Oikawa H. Enzymatic Epoxide-Opening Cascades Catalyzed by a Pair of Epoxide Hydrolases in the Ionophore Polyether Biosynthesis. Org Lett. 2011; 13(7):1638–1641. [PubMed: 21375229]

441. Tosin M, Smith L, Leadlay PF. Insights into Lasalocid A Ring Formation by Chemical Chain Termination in Vivo. Angew Chem Int Ed Engl. 2011; 50(50):11930–11933. [PubMed: 22025396]

442. Minami A, Shimaya M, Suzuki G, Migita A, Shinde SS, Sato K, Watanabe K, Tamura T, Oguri H, Oikawa H. Sequential Enzymatic Epoxidation Involved in Polyether Lasalocid Biosynthesis. J Am Chem Soc. 2012; 134(17):7246–7249. [PubMed: 22506807]

443. Hotta K, Chen X, Paton RS, Minami A, Li H, Swaminathan K, Mathews II, Watanabe K, Oikawa H, Houk KN, et al. Enzymatic Catalysis of Anti-Baldwin Ring Closure in Polyether Biosynthesis. Nature. 2012; 483(7389):355–358. [PubMed: 22388816]

444. Wong FT, Hotta K, Chen X, Fang M, Watanabe K, Kim C-Y. Epoxide Hydrolase–Lasalocid A Structure Provides Mechanistic Insight into Polyether Natural Product Biosynthesis. J Am Chem Soc. 2015; 137(1):86–89. [PubMed: 25535803]

445. Gallimore AR, Stark CB, Bhatt A, Harvey BM, Demydchuk Y, Bolanos-Garcia V, Fowler DJ, Staunton J, Leadlay PF, Spencer JB. Evidence for the Role of the MonB Genes in Polyether Ring Formation During Monensin Biosynthesis. Chem Biol. 2006; 13(4):453–460. [PubMed: 16632258]

446. Leadlay PF, Staunton J, Oliynyk M, Bisang C, Cortes J, Frost E, Hughes-Thomas ZA, Jones MA, Kendrew SG, Lester JB, et al. Engineering of Complex Polyketide Biosynthesis--Insights from Sequencing of the Monensin Biosynthetic Gene Cluster. J Ind Microbiol Biotechnol. 2001; 27(6): 360–367. [PubMed: 11774001]

447. Minami A, Ose T, Sato K, Oikawa A, Kuroki K, Maenaka K, Oguri H, Oikawa H. Allosteric Regulation of Epoxide Opening Cascades by a Pair of Epoxide Hydrolases in Monensin Biosynthesis. ACS Chem Biol. 2014; 9(2):562–569. [PubMed: 24320215]

448. Sun Y, Zhou X, Dong H, Tu G, Wang M, Wang B, Deng Z. A Complete Gene Cluster from *Streptomyces Nanchangensis* NS3226 Encoding Biosynthesis of the Polyether Ionophore Nanchangmycin. Chem Biol. 2003; 10(5):431–441. [PubMed: 12770825]

449. Raju R, Piggott AM, Barrientos Diaz LX, Khalil Z, Capon RJ. Heronapyrroles A–C: Farnesylated 2-Nitropyrroles from an Australian Marine-Derived *Streptomyces* sp. Org Lett. 2010; 12(22): 5158–5161. [PubMed: 20949971]

450. Schmidt J, Khalil Z, Capon RJ, Stark CB. Heronapyrrole D: A Case of Co-Inspiration of Natural Product Biosynthesis, Total Synthesis and Biodiscovery. Beilstein J Org Chem. 2014; 10:1228–1232. [PubMed: 24991272]

451. Gleye C, Raynaud S, Hocquemiller R, Laurens A, Fourneau C, Serani L, Laprévote O, Roblot F, Leboeuf M, Fournet A, et al. Muricadienin, Muridienins and Chatenaytrienins, the Early Precursors of Annonaceous Acetogenins. Phytochemistry. 1998; 47(5):749–754.

452. Hu Y, Cecil ARL, Frank X, Gleye C, Figadere B, Brown RCD. Natural *cis*-Solamin Is a Mixture of Two Tetra-Epimeric Diastereoisomers: Biosynthetic Implications for Annonaceous Acetogenins. Org Biomol Chem. 2006; 4(7):1217–1219. [PubMed: 16557308]

453. Johnson KM, Swenson L, Opipari AW, Reuter R, Zarrabi N, Fierke CA, Börsch M, Glick GD. Mechanistic Basis for Differential Inhibition of the F1Fo-ATPase by Aurovertin. Biopolymers. 2009; 91(10):830–840. [PubMed: 19462418]

454. Huang T-C, Chang H-Y, Hsu C-H, Kuo W-H, Chang K-J, Juan H-F. Targeting Therapy for Breast Carcinoma by ATP Synthase Inhibitor Aurovertin B. J Proteome Res. 2008; 7(4):1433–1444. [PubMed: 18275135]

455. Mao XM, Zhan ZJ, Grayson MN, Tang MC, Xu W, Li YQ, Yin WB, Lin HC, Chooi YH, Houk KN, et al. Efficient Biosynthesis of Fungal Polyketides Containing the Dioxabicyclo-Octane Ring System. J Am Chem Soc. 2015; 137(37):11904–11907. [PubMed: 26340065]

456. Thoma R, Schulz-Gasch T, D'Arcy B, Benz J, Aebi J, Dehmlow H, Hennig M, Stihle M, Ruf A. Insight into Steroid Scaffold Formation from the Structure of Human Oxidosqualene Cyclase. Nature. 2004; 432(7013):118–122. [PubMed: 15525992]

457. Chen N, Wang S, Smentek L, Hess BA Jr, Wu R. Biosynthetic Mechanism of Lanosterol: Cyclization. Angew Chem Int Ed Engl. 2015; 54(30):8693–8696. [PubMed: 26069216]

458. Nes WD. Biosynthesis of Cholesterol and Other Sterols. Chem Rev. 2011; 111(10):6423–6451. [PubMed: 21902244]

459. Rees HH, Goad LJ, Goodwin TW. 2,3-Oxidosqualene Cycloartenol Cyclase from *Ochromonas Malhamensis*. Biochim Biophys Acta. 1969; 176(4):892–894. [PubMed: 5797101]

460. Dean PDG, DemontelPr Bloch K, Corey EJ. A Soluble 2,3,Oxidosqualene Sterol Cyclase. J Biol Chem. 1967; 242(12):3014–3015. [PubMed: 6027261]

461. Wendt KU, Poralla K, Schulz GE. Structure and Function of a Squalene Cyclase. Science. 1997; 277(5333):1811–1815. [PubMed: 9295270]

462. Hoshino T, Sato T. Squalene-Hopene Cyclase: Catalytic Mechanism and Substrate Recognition. Chem Commun (camb). 2002; (4):291–301. [PubMed: 12120044]

463. Gas-Pascual E, Berna A, Bach TJ, Schaller H. Plant Oxidosqualene Metabolism: Cycloartenol Synthase-Dependent Sterol Biosynthesis in *Nicotiana Benthamiana*. PloS ONE. 2014; 9(10):e109156. [PubMed: 25343375]

464. Ohyama K, Suzuki M, Kikuchi J, Saito K, Muranaka T. Dual Biosynthetic Pathways to Phytosterol Via Cycloartenol and Lanosterol in *Arabidopsis*. Proc Natl Acad Sci U S A. 2009; 106(3):725–730. [PubMed: 19139393]

465. Shibuya M, Adachi S, Ebizuka Y. Cucurbitadienol Synthase, the First Committed Enzyme for Cucurbitacin Biosynthesis, Is a Distinct Enzyme from Cycloartenol Synthase for Phytosterol Biosynthesis. Tetrahedron. 2004; 60(33):6995–7003.

466. Takase S, Saga Y, Kurihara N, Naraki S, Kuze K, Nakata G, Araki T, Kushiro T. Control of the 1,2-Rearrangement Process by Oxidosqualene Cyclases During Triterpene Biosynthesis. Org Biomol Chem. 2015; 13(26):7331–7336. [PubMed: 26058429]

467. Shan H, Segura MJR, Wilson WK, Lodeiro S, Matsuda SPT. Enzymatic Cyclization of Dioxidosqualene to Heterocyclic Triterpenes. J Am Chem Soc. 2005; 127(51):18008–18009. [PubMed: 16366544]

468. Saleem M. Lupeol, a Novel Anti-Inflammatory and Anti-Cancer Dietary Triterpene. Cancer Lett. 2009; 285(2):109–115. [PubMed: 19464787]

469. Hoshino T, Miyahara Y, Hanaoka M, Takahashi K, Kaneko I. β-Amyrin Biosynthesis: The Methyl-30 Group of (3*S*)-2,3-Oxidosqualene Is More Critical to Its Correct Folding To Generate the Pentacyclic Scaffold than the Methyl-24 Group. Chemistry. 2015; 21(44):15769–15784. [PubMed: 26351084]

470. Hammer SC, Marjanovic A, Dominicus JM, Nestl BM, Hauer B. Squalene Hopene Cyclases Are Protonases for Stereoselective Brønsted Acid Catalysis. Nat Chem Biol. 2015; 11(2):121–126. [PubMed: 25503928]

471. Rudi A, Stein Z, Goldberg I, Yosief T, Kashman Y, Schleyer M. Yardenone and Abudinol Two New Triterpenes from the Marine Sponge *Ptilocaulis Spiculifer*. Tetrahedron Lett. 1998; 39(11): 1445–1448.

472. Domingo V, Arteaga JF, Quilez del Moral JF, Barrero AF. Unusually Cyclized Triterpenes: Occurrence, Biosynthesis and Chemical Synthesis. Nat Prod Rep. 2009; 26(1):115–134. [PubMed: 19374125]

473. Boone MA, Tong R, McDonald FE, Lense S, Cao R, Hardcastle KI. Biomimetic Syntheses from Squalene-Like Precursors: Synthesis of Ent-Abudinol B and Reassessment of the Structure of Muzitone. J Am Chem Soc. 2010; 132(14):5300–5308. [PubMed: 20334383]

474. Tong R, McDonald FE. Mimicking Biosynthesis: Total Synthesis of the Triterpene Natural Product Abudinol B from a Squalene-Like Precursor. Angew Chem Int Ed Engl. 2008; 47(23): 4377–4379. [PubMed: 18459096]

475. Tong R, Valentine JC, McDonald FE, Cao R, Fang X, Hardcastle KI. Total Syntheses of Durgamone, Nakorone, and Abudinol B Via Biomimetic Oxa- and Carbacyclizations. J Am Chem Soc. 2007; 129(5):1050–1051. [PubMed: 17263384]

476. Li H, Sun Y, Zhang Q, Zhu Y, Li SM, Li A, Zhang C. Elucidating the Cyclization Cascades in Xiamycin Biosynthesis by Substrate Synthesis and Enzyme Characterizations. Org Lett. 2015; 17(2):306–309. [PubMed: 25532029]

477. Nozawa K, Nakajima S, Kawai K, Udagawa S. Isolation and Structures of Indoloditerpenes, Possible Biosynthetic Intermediates to the Tremorgenic Mycotoxin, Paxilline, from *Emericella Striata*. J Chem Soc, Perkin Trans 1. 1988; (9):2607–2610.

478. Hosoe T, Itabashi T, Kobayashi N, Udagawa S, Kawai K. Three New Types of Indoloditerpenes, Emindole PA-PC, from *Emericella Purpurea*. Revision of the Structure of Emindole PA. Chem Pharm Bull (Tokyo). 2006; 54(2):185–187. [PubMed: 16462061]

479. Tagami K, Liu C, Minami A, Noike M, Isaka T, Fueki S, Shichijo Y, Toshima H, Gomi K, Dairi T, et al. Reconstitution of Biosynthetic Machinery for Indole-Diterpene Paxilline in *Aspergillus Oryzae*. J Am Chem Soc. 2013; 135(4):1260–1263. [PubMed: 23311903]

480. Tang M-C, Lin H-C, Li D, Zou Y, Li J, Xu W, Cacho RA, Hillenmeyer ME, Garg NK, Tang Y. Discovery of Unclustered Fungal Indole Diterpene Biosynthetic Pathways through Combinatorial Pathway Reassembly in Engineered Yeast. J Am Chem Soc. 2015; 137(43):13724–13727. [PubMed: 26469304]

481. Geris R, Simpson TJ. Meroterpenoids Produced by Fungi. Nat Prod Rep. 2009; 26(8):1063–1094. [PubMed: 19636450]

482. Matsuda Y, Abe I. Biosynthesis of Fungal Meroterpenoids. Nat Prod Rep. 2016; 33(1):26–53. [PubMed: 26497360]

483. Zhang Y, Li C, Swenson DC, Gloer JB, Wicklow DT, Dowd PF. Novel Antiinsectan Oxalicine Alkaloids from Two Undescribed Fungicolous *Penicillium* spp. Org Lett. 2003; 5(5):773–776. [PubMed: 12605512]

484. Hayashi A, Arai M, Fujita M, Kobayashi M. Pyripyropenes, Fungal Sesquiterpenes Conjugated with Alpha-Pyrone and Pyridine Moieties, Exhibits Anti-Angiogenic Activity Against Human Umbilical Vein Endothelial Cells. Biol Pharm Bull. 2009; 32(7):1261–1265. [PubMed: 19571395]

485. Ubillas R, Barnes CL, Gracz H, Rottinghaus GE, Tempesta MS. X-Ray Crystal Structure of Oxalicine A, a Novel Alkaloid from *Penicillium Oxalicum*. J Chem Soc, Chem Commun. 1989; (21):1618–1619.

486. Abe M, Imai T, Ishii N, Usui M, Okuda T, Oki T. Isolation of an Insecticidal Compound Oxalicine B from *Penicillium* sp. TAMA 71 and Confirmation of Its Chemical Structure by X-Ray Crystallographic Analysis. J Pest Sci. 2007; 32(2):124–127.

487. Yaegashi J, Romsdahl J, Chiang Y-M, Wang CC. Genome Mining and Molecular Characterization of the Biosynthetic Gene Cluster of a Diterpenic Meroterpenoid, 15-Deoxyoxalicine B, in *Penicillium Canescens*. Chem Sci. 2015; 6(11):6537–6544.

488. Itoh T, Tokunaga K, Matsuda Y, Fujii I, Abe I, Ebizuka Y, Kushiro T. Reconstitution of a Fungal Meroterpenoid Biosynthesis Reveals the Involvement of a Novel Family of Terpene Cyclases. Nat Chem. 2010; 2(10):858–864. [PubMed: 20861902]

489. Cueto M, MacMillan JB, Jensen PR, Fenical W. Tropolactones A-D, Four Meroterpenoids from a Marine-Derived Fungus of the Genus *Aspergillus*. Phytochemistry. 2006; 67(16):1826–1831. [PubMed: 16500687]

490. Nielsen KF, Dalsgaard PW, Smedsgaard J, Larsen TO. Andrastins A-D, *Penicillium Roqueforti* Metabolites Consistently Produced in Blue-Mold-Ripened Cheese. J Agric Food Chem. 2005; 53(8):2908–2913. [PubMed: 15826038]

491. Simpson TJ, Stenzel DJ, Bartlett AJ, O'Brien E, Holker JSE. Studies on Fungal Metabolites. Part 3. 13C N.M.R. Spectral and Structural Studies on Austin and New Related Meroterpenoids from *Aspergillus Ustus*, *Aspergillus Variecolor*, and *Penicillium Diversum*. J Chem Soc, Perkin Trans 1. 1982; (0):2687–2692.

492. Springer JP, Dorner JW, Cole RJ, Cox RH. Terretonin, a Toxic Compound from *Aspergillus Terreus*. J Org Chem. 1979; 44(26):4852–4854.

493. Rank C, Phipps RK, Harris P, Fristrup P, Larsen TO, Gotfredsen CH. Novofumigatonin, a New Orthoester Meroterpenoid from *Aspergillus Novofumigatus*. Org Lett. 2008; 10(3):401–404. [PubMed: 18179222]

494. Matsuda Y, Awakawa T, Abe I. Reconstituted Biosynthesis of Fungal Meroterpenoid Andrastin A. Tetrahedron. 2013; 69(38):8199–8204.

495. Lo HC, Entwistle R, Guo CJ, Ahuja M, Szewczyk E, Hung JH, Chiang YM, Oakley BR, Wang CC. Two Separate Gene Clusters Encode the Biosynthetic Pathway for the Meroterpenoids Austinol and Dehydroaustinol in *Aspergillus Nidulans*. J Am Chem Soc. 2012; 134(10):4709–4720. [PubMed: 22329759]

496. Guo CJ, Knox BP, Chiang YM, Lo HC, Sanchez JF, Lee KH, Oakley BR, Bruno KS, Wang CC. Molecular Genetic Characterization of a Cluster in *A. Terreus* for Biosynthesis of the Meroterpenoid Terretonin. Org Lett. 2012; 14(22):5684–5687. [PubMed: 23116177]

497. Simpson TJ, Walkinshaw MD. Anditomin, a New C25 Metabolite from *Aspergillus Variecolor*. J Chem Soc, Chem Commun. 1981; (17):914–915.

498. Matsuda Y, Wakimoto T, Mori T, Awakawa T, Abe I. Complete Biosynthetic Pathway of Anditomin: Nature's Sophisticated Synthetic Route to a Complex Fungal Meroterpenoid. J Am Chem Soc. 2014; 136(43):15326–15336. [PubMed: 25216349]

499. Kusano M, Koshino H, Uzawa J, Fujioka S, Kawano T, Kimura Y. Nematicidal Alkaloids and Related Compounds Produced by the Fungus *Penicillium cf. Simplicissimum*. Biosci Biotechnol Biochem. 2000; 64(12):2559–2568. [PubMed: 11210117]

500. Kimura Y, Kusano M, Koshino H, Uzawa J, Fujioka S, Tani K. Penigequinolones A and B, Pollen-Growth Inhibitors Produced by *Penicilium* sp., No. 410. Tetrahedron Lett. 1996; 37(28): 4961–4964.

501. Scherlach K, Hertweck C. Discovery of Aspoquinolones A-D, Prenylated Quinoline-2-One Alkaloids from *Aspergillus Nidulans*, Motivated by Genome Mining. Org Biomol Chem. 2006; 4(18):3517–3520. [PubMed: 17036148]

502. Ishikawa N, Tanaka H, Koyama F, Noguchi H, Wang CC, Hotta K, Watanabe K. Non-heme Dioxygenase Catalyzes Atypical Oxidations of 6,7-Bicyclic Systems to Form the 6,6-Quinolone Core of Viridicatin-Type Fungal Alkaloids. Angew Chem Int Ed Engl. 2014; 53(47):12880–12884. [PubMed: 25251934]

503. Zou Y, Zhan ZJ, Li D, Tang M, Cacho RA, Watanabe K, Tang Y. Tandem Prenyltransferases Catalyze Isoprenoid Elongation and Complexity Generation in Biosynthesis of Quinolone Alkaloids. J Am Chem Soc. 2015; 137(15):4980–4983. [PubMed: 25859931]

504. Uchida R, Imasato R, Yamaguchi Y, Masuma R, Shiomi K, Tomoda H, Omura S. Yaequinolones, New Insecticidal Antibiotics Produced by *Penicillium* sp. FKI-2140. I. Taxonomy, Fermentation, Isolation and Biological Activity. J Antibiot (Tokyo). 2006; 59(10):646–651. [PubMed: 17191680]

505. Uchida R, Imasato R, Tomoda H, Omura S. Yaequinolones, New Insecticidal Antibiotics Produced by *Penicillium* sp. FKI-2140. II. Structural Elucidation. J Antibiot (Tokyo). 2006; 59(10):652–658. [PubMed: 17191681]

506. Zou Y, Garcia-Borràs M, Tang M-C, Hirayama Y, Li D-H, Li L, Watanabe K, Houk KN, Tang Y. Enzyme-Catalyzed Cationic Epoxide Rearrangements in Quinolone Alkaloid Biosynthesis. Nat Chem Biol. 2016 In press.

507. Kunze B, Hofle G, Reichenbach H. The Aurachins, New Quinoline Antibiotics from Myxobacteria: Production, Physico-Chemical and Biological Properties. J Antibiot (Tokyo). 1987; 40(3):258–265. [PubMed: 3106289]

508. Pistorius D, Li Y, Sandmann A, Müller R. Completing the Puzzle of Aurachin Biosynthesis in *Stigmatella Aurantiaca* Sg a15. Mol Biosyst. 2011; 7(12):3308–3315. [PubMed: 21979787]

509. Willenbring D, Tantillo DJ. Mechanistic Possibilities for Oxetane Formation in the Biosynthesis of Taxol's D Ring. Russ J Gen Chem. 2008; 78(4):723–731.

510. Guo CJ, Yeh HH, Chiang YM, Sanchez JF, Chang SL, Bruno KS, Wang CC. Biosynthetic Pathway for the Epipolythiodioxopiperazine Acetylaranotin in *Aspergillus Terreus* Revealed by Genome-Based Deletion Analysis. J Am Chem Soc. 2013; 135(19):7205–7213. [PubMed: 23586797]

511. Gardiner DM, Howlett BJ. Bioinformatic and Expression Analysis of the Putative Gliotoxin Biosynthetic Gene Cluster of *Aspergillus Fumigatus*. FEMS Microbiol Lett. 2005; 248(2):241–248. [PubMed: 15979823]

512. Scharf DH, Heinekamp T, Remme N, Hortschansky P, Brakhage AA, Hertweck C. Biosynthesis and Function of Gliotoxin in *Aspergillus Fumigatus*. Appl Microbiol Biotechnol. 2012; 93(2): 467–472. [PubMed: 22094977]

513. Walsh CT, Haynes SW, Ames BD, Gao X, Tang Y. Short Pathways to Complexity Generation: Fungal Peptidyl Alkaloid Multicyclic Scaffolds from Anthranilate Building Blocks. ACS Chem Biol. 2013; 8(7):1366–1382. [PubMed: 23659680]

514. Gao X, Haynes SW, Ames BD, Wang P, Vien LP, Walsh CT, Tang Y. Cyclization of Fungal Nonribosomal Peptides by a Terminal Condensation-Like Domain. Nat Chem Biol. 2012; 8(10): 823–830. [PubMed: 22902615]

515. Ames BD, Liu X, Walsh CT. Enzymatic Processing of Fumiquinazoline F: A Tandem Oxidative-Acylation Strategy for the Generation of Multicyclic Scaffolds in Fungal Indole Alkaloid Biosynthesis. Biochemistry. 2010; 49(39):8564–8576. [PubMed: 20804163]

516. Larsen TO, Petersen BO, Duus JØ. Lumpidin, a Novel Biomarker of Some Ochratoxin A Producing *Penicillia*. J Agric Food Chem. 2001; 49(10):5081–5084. [PubMed: 11600070]

517. Wong SM, Musza LL, Kydd GC, Kullnig R, Gillum AM, Cooper R. Fiscalins: New Substance P Inhibitors Produced by the Fungus *Neosartorya Fischeri*. Taxonomy, Fermentation, Structures, and Biological Properties. J Antibiot (Tokyo). 1993; 46(4):545–553. [PubMed: 7684734]

518. Fremlin LJ, Piggott AM, Lacey E, Capon RJ. Cottoquinazoline A and Cotteslosins A and B, Metabolites from an Australian Marine-Derived Strain of *Aspergillus Versicolor*. J Nat Prod. 2009; 72(4):666–670. [PubMed: 19245260]

519. Jiao RH, Xu S, Liu JY, Ge HM, Ding H, Xu C, Zhu HL, Tan RX. Chaetominine, a Cytotoxic Alkaloid Produced by Endophytic *Chaetomium* sp. IFB-E015. Org Lett. 2006; 8(25):5709–5712. [PubMed: 17134253]

520. Goetz MA, Lopez M, Monaghan RL, Chang RS, Lotti VJ, Chen TB. Asperlicin, a Novel Non-Peptidal Cholecystokinin Antagonist from *Aspergillus Alliaceus*. Fermentation, Isolation and Biological Properties. J Antibiot (Tokyo). 1985; 38(12):1633–1637. [PubMed: 3005212]

521. Li S, Finefield JM, Sunderhaus JD, McAfoos TJ, Williams RM, Sherman DH. Biochemical Characterization of NotB as an FAD-Dependent Oxidase in the Biosynthesis of Notoamide Indole Alkaloids. J Am Chem Soc. 2012; 134(2):788–791. [PubMed: 22188465]

522. Cui CB, Kakeya H, Osada H. Spirotryprostatin B, a Novel Mammalian Cell Cycle Inhibitor Produced by *Aspergillus Fumigatus*. J Antibiot (Tokyo). 1996; 49(8):832–835. [PubMed: 8823522]

523. Tsunematsu Y, Ishikawa N, Wakana D, Goda Y, Noguchi H, Moriya H, Hotta K, Watanabe K. Distinct Mechanisms for Spiro-Carbon Formation Reveal Biosynthetic Pathway Crosstalk. Nat Chem Biol. 2013; 9(12):818–825. [PubMed: 24121553]

524. Li H, Zhang Q, Li S, Zhu Y, Zhang G, Zhang H, Tian X, Zhang S, Ju J, Zhang C. Identification and Characterization of Xiamycin A and Oxiamycin Gene Cluster Reveals an Oxidative Cyclization Strategy Tailoring Indolosesquiterpene Biosynthesis. J Am Chem Soc. 2012; 134(21):8996–9005. [PubMed: 22591327]

525. Raju R, Piggott AM, Conte MM, Capon RJ. Heronamides A-C, New Polyketide Macrolactams from an Australian Marine-Derived *Streptomyces* sp. A Biosynthetic Case for Synchronized Tandem Electrocyclization. Org Biomol Chem. 2010; 8(20):4682–4689. [PubMed: 20733977]

526. Booth TJ, Alt S, Capon RJ, Wilkinson B. Synchronous Intramolecular Cycloadditions of the Polyene Macrolactam Polyketide Heronamide C. Chem Commun (Camb). 2016; 52(38):6383–6386. [PubMed: 27091090]

527. Yu P, Patel A, Houk KN. Transannular [6 + 4] and Ambimodal Cycloaddition in the Biosynthesis of Heronamide A. J Am Chem Soc. 2015; 137(42):13518–13523. [PubMed: 26435377]

528. Bloch P, Tamm C, Bollinger P, Petcher TJ, Weber HP. Pseurotin, a New Metabolite of *Pseudeurotium Ovalis* STOLk Having an Unusual Hetero-Spirocyclic System. Helv Chim Acta. 1976; 59(1):133–137. [PubMed: 1248942]

529. Maiya S, Grundmann A, Li X, Li S-M, Turner G. Identification of a Hybrid PKS/NRPS Required for Pseurotin A Biosynthesis in the Human Pathogen *Aspergillus Fumigatus*. ChemBioChem. 2007; 8(14):1736–1743. [PubMed: 17722120]

530. Tsunematsu Y, Fukutomi M, Saruwatari T, Noguchi H, Hotta K, Tang Y, Watanabe K. Elucidation of Pseurotin Biosynthetic Pathway Points to *trans*-Acting C-Methyltransferase: Generation of Chemical Diversity. Angew Chem Int Ed Engl. 2014; 53(32):8475–8479. [PubMed: 24939566]

531. Zou Y, Xu W, Tsunematsu Y, Tang M, Watanabe K, Tang Y. Methylation-Dependent Acyl Transfer between Polyketide Synthase and Nonribosomal Peptide Synthetase Modules in Fungal Natural Product Biosynthesis. Org Lett. 2014; 16(24):6390–6393. [PubMed: 25494235]

532. Yamamoto T, Tsunematsu Y, Hara K, Suzuki T, Kishimoto S, Kawagishi H, Noguchi H, Hashimoto H, Tang Y, Hotta K, et al. Oxidative *trans* to *cis* Isomerization of Olefins in Polyketide Biosynthesis. Angew Chem Int Ed Engl. 2016; 55(21):6207–6210. [PubMed: 27072782]

533. Brash AR, Boeglin WE, Stec DF, Voehler M, Schneider C, Cha JK. Isolation and Characterization of Two Geometric Allene Oxide Isomers Synthesized from 9S-Hydroperoxylinoleic Acid by Cytochrome P450 CYP74C3: STEREOCHEMICAL ASSIGNMENT OF NATURAL FATTY ACID ALLENE OXIDES. J Biol Chem. 2013; 288(29):20797–20806. [PubMed: 23709224]

534. Oldham ML, Brash AR, Newcomer ME. The Structure of Coral Allene Oxide Synthase Reveals a Catalase Adapted for Metabolism of a Fatty Acid Hydroperoxide. Proc Natl Acad Sci U S A. 2005; 102(2):297–302. [PubMed: 15625113]

535. Fujii I, Mori Y, Watanabe A, Kubo Y, Tsuji G, Ebizuka Y. Enzymatic Synthesis of 1,3,6,8-Tetrahydroxynaphthalene Solely from Malonyl Coenzyme A by a Fungal Iterative Type I Polyketide Synthase PKS1. Biochemistry. 2000; 39(30):8853–8858. [PubMed: 10913297]

536. Funa N, Ohnishi Y, Fujii I, Shibuya M, Ebizuka Y, Horinouchi S. A New Pathway for Polyketide Synthesis in Microorganisms. Nature. 1999; 400(6747):897–899. [PubMed: 10476972]

537. Kaysser L, Bernhardt P, Nam SJ, Loesgen S, Ruby JG, Skewes-Cox P, Jensen PR, Fenical W, Moore BS. Merochlorins A-D, Cyclic Meroterpenoid Antibiotics Biosynthesized in Divergent Pathways with Vanadium-Dependent Chloroperoxidases. J Am Chem Soc. 2012; 134(29):11988–11991. [PubMed: 22784372]

538. Teufel R, Kaysser L, Villaume MT, Diethelm S, Carbullido MK, Baran PS, Moore BS. One-Pot Enzymatic Synthesis of Merochlorin A and B. Angew Chem Int Ed Engl. 2014; 53(41):11019–11022. [PubMed: 25115835]

539. Diethelm S, Teufel R, Kaysser L, Moore BS. A Multitasking Vanadium-Dependent Chloroperoxidase as an Inspiration for the Chemical Synthesis of the Merochlorins. Angew Chem Int Ed Engl. 2014; 53(41):11023–11026. [PubMed: 25147132]

540. Bernhardt P, Okino T, Winter JM, Miyanaga A, Moore BS. A Stereoselective Vanadium-Dependent Chloroperoxidase in Bacterial Antibiotic Biosynthesis. J Am Chem Soc. 2011; 133(12):4268–4270. [PubMed: 21384874]

541. Winter JM, Moffitt MC, Zazopoulos E, McAlpine JB, Dorrestein PC, Moore BS. Molecular Basis for Chloronium-Mediated Meroterpene Cyclization: Cloning, Sequencing, and Heterologous Expression of the Napyradiomycin Biosynthetic Gene Cluster. J Biol Chem. 2007; 282(22):16362–16368. [PubMed: 17392281]

542. Ishihara J, Kanoh N, Murai A. Enzymatic Reaction of (3E,6S,7S)-Laurediol and the Molecular Modeling Studies on the Cyclization of Laurediols. Tetrahedron Lett. 1995; 36(5):737–740.

543. Carter-Franklin JN, Butler A. Vanadium Bromoperoxidase-Catalyzed Biosynthesis of Halogenated Marine Natural Products. J Am Chem Soc. 2004; 126(46):15060–15066. [PubMed: 15548002]

544. Chang ZX, Sitachitta N, Rossi JV, Roberts MA, Flatt PM, Jia JY, Sherman DH, Gerwick WH. Biosynthetic Pathway and Gene Cluster Analysis of Curacin A, an Antitubulin Natural Product from the Tropical Marine Cyanobacterium *Lyngbya Majuscula*. J Nat Prod. 2004; 67(8):1356–1367. [PubMed: 15332855]

545. Gu L, Jia J, Liu H, Hakansson K, Gerwick WH, Sherman DH. Metabolic Coupling of Dehydration and Decarboxylation in the Curacin A Pathway: Functional Identification of a Mechanistically Diverse Enzyme Pair. J Am Chem Soc. 2006; 128(28):9014–9015. [PubMed: 16834357]

546. Gu L, Wang B, Kulkarni A, Geders TW, Grindberg RV, Gerwick L, Hakansson K, Wipf P, Smith JL, Gerwick WH, et al. Metamorphic Enzyme Assembly in Polyketide Diversification. Nature. 2009; 459(7247):731–735. [PubMed: 19494914]

547. Geng XQ, Cheng JY, Gangadharan A, Mackey D. The Coronatine Toxin of *Pseudomonas Syringae* Is a Multifunctional Suppressor of *Arabidopsis* Defense. Plant Cell. 2012; 24(11):4763–4774. [PubMed: 23204405]

548. Geng XQ, Jin L, Shimada M, Kim MG, Mackey D. The Phytotoxin Coronatine Is a Multifunctional Component of the Virulence Armament of *Pseudomonas Syringae*. Planta. 2014; 240(6):1149–1165. [PubMed: 25156488]

549. Vaillancourt FH, Yeh E, Vosburg DA, O'Connor SE, Walsh CT. Cryptic Chlorination by a Non-Haem Iron Enzyme During Cyclopropyl Amino Acid Biosynthesis. Nature. 2005; 436(7054):1191–1194. [PubMed: 16121186]

550. Fujimori DG, Hrvatin S, Neumann CS, Strieker M, Marahiel MA, Walsh CT. Cloning and Characterization of the Biosynthetic Gene Cluster for Kutznerides. Proc Natl Acad Sci U S A. 2007; 104(42):16498–16503. [PubMed: 17940045]

551. Neumann CS, Walsh CT. Biosynthesis of (–)-(1S,2*R*)-Allocoronamic Acyl Thioester by an FeII-Dependent Halogenase and a Cyclopropane-Forming Flavoprotein. J Am Chem Soc. 2008; 130(43):14022–14023. [PubMed: 18828590]

552. Cox R. Oxidative Rearrangements During Fungal Biosynthesis. Nat Prod Rep. 2014; 31(10): 1405–1424. [PubMed: 25060008]

553. Bräuer A, Beck P, Hintermann L, Groll M. Structure of the Dioxygenase AsqJ: Mechanistic Insights into a One-Pot Multistep Quinolone Antibiotic Biosynthesis. Angew Chem Int Ed Engl. 2016; 55(1):422–426. [PubMed: 26553478]

554. Chang WC, Li J, Lee JL, Cronican AA, Guo Y. Mechanistic Investigation of a Non-Heme Iron Enzyme Catalyzed Epoxidation in (-)-4′-Methoxycyclopenin Biosynthesis. J Am Chem Soc. 2016; 138(33):10390–10393. [PubMed: 27442345]

555. Brian PW. Effects of Gibberellins on Plant Growth and Development. Biol Rev. 1959; 34(1):37–77.

556. Helliwell CA, Poole A, Peacock WJ, Dennis ES. Arabidopsis Ent-Kaurene Oxidase Catalyzes Three Steps of Gibberellin Biosynthesis. Plant Physiol. 1999; 119(2):507–510. [PubMed: 9952446]

557. Helliwell CA, Chandler PM, Poole A, Dennis ES, Peacock WJ. The CYP88A Cytochrome P450, Ent-Kaurenoic Acid Oxidase, Catalyzes Three Steps of the Gibberellin Biosynthesis Pathway. Proc Natl Acad Sci U S A. 2001; 98(4):2065–2070. [PubMed: 11172076]

558. Williams PG, Asolkar RN, Kondratyuk T, Pezzuto JM, Jensen PR, Fenical W. Saliniketals A and B, Bicyclic Polyketides from the Marine Actinomycete *Salinispora Arenicola*. J Nat Prod. 2007; 70(1):83–88. [PubMed: 17253854]

559. Wilson MC, Gulder TAM, Mahmud T, Moore BS. Shared Biosynthesis of the Saliniketals and Rifamycins in *Salinispora Arenicola* is Controlled by the Sare1259-Encoded Cytochrome P450. J Am Chem Soc. 2010; 132(36):12757–12765. [PubMed: 20726561]

560. Stroshane RM, Chan JA, Rubalcaba EA, Garretson AL, Aszalos AA, Roller PP. Isolation and Structure Elucidation of a Novel Griseorhodin. J Antibiot (Tokyo). 1979; 32(3):197–204. [PubMed: 110759]

561. Li A, Piel J. A Gene Cluster from a Marine *Streptomyces* Encoding the Biosynthesis of the Aromatic Spiroketal Polyketide Griseorhodin A. Chem Biol. 2002; 9(9):1017–1026. [PubMed: 12323376]

562. Yunt Z, Reinhardt K, Li A, Engeser M, Dahse HM, Gutschow M, Bruhn T, Bringmann G, Piel J. Cleavage of Four Carbon-Carbon Bonds During Biosynthesis of the Griseorhodin a Spiroketal Pharmacophore. J Am Chem Soc. 2009; 131(6):2297–2305. [PubMed: 19175308]

563. Ainsworth AM, Chicarelli-Robinson MI, Copp BR, Fauth U, Hylands PJ, Holloway JA, Latif M, O'Beirne GB, Porter N, Renno DV, et al. Xenovulene A, a Novel GABA-Benzodiazepine Receptor Binding Compound Produced by *Acremonium Strictum*. J Antibiot (Tokyo). 1995; 48(7):568–573. [PubMed: 7649852]

564. Raggatt ME, Simpson TJ, Raggatt ME, Chicarelli-Robinson MI. Biosynthesis of Xenovulene A®: Formation of a Cyclopentenone Via a Unique Ring Expansion-Ring Contraction Mechanism. Chem Commun (camb). 1997; (22):2245–2247.

565. Kamerbeek NM, Janssen DB, van Berkel WJH, Fraaije MW. Baeyer-Villiger Monooxygenases, an Emerging Family of Flavin-Dependent Biocatalysts. Adv Syn Catal. 2003; 345(6–7):667–678.

566. Leisch H, Morley K, Lau PCK. Baeyer-Villiger Monooxygenases: More Than Just Green Chemistry. Chem Rev. 2011; 111(7):4165–4222. [PubMed: 21542563]

567. Pazmino DET, Dudek HM, Fraaije MW. Baeyer-Villiger Monooxygenases: Recent Advances and Future Challenges. Curr Opin Chem Biol. 2010; 14(2):138–144. [PubMed: 20015679]

568. Mascotti ML, Lapadula WJ, Ayub MJ. The Origin and Evolution of Baeyer-Villiger Monooxygenases (BVMOs): An Ancestral Family of Flavin Monooxygenases. PloS ONE. 2015; 10(7):e0132689. [PubMed: 26161776]

569. Cane DE, Rossi T. The Isolation and Structural Elucidation of Pentalenolactone E. Tetrahedron Lett. 1979; 20(32):2973–2974.

570. Tillman AM, Cane DE. Pentalenolactone F, a New Metabolite Isolated from *Streptomyces*. Isolation and Structure Elucidation. J Antibiot (Tokyo). 1983; 36(2):170–172. [PubMed: 6833133]

571. Cane DE, Oliver JS, Harrison PHM, Abell C, Hubbard BR, Kane CT, Lattman R. Biosynthesis of Pentalenene and Pentalenolactone. J Am Chem Soc. 1990; 112(11):4513–4524.

572. Tetzlaff CN, You Z, Cane DE, Takamatsu S, Omura S, Ikeda H. A Gene Cluster for Biosynthesis of the Sesquiterpenoid Antibiotic Pentalenolactone in *Streptomyces Avermitilis*. Biochemistry. 2006; 45(19):6179–6186. [PubMed: 16681390]

573. Seo M-J, Zhu D, Endo S, Ikeda H, Cane DE. Genome Mining in *Streptomyces*. Elucidation of the Role of Baeyer–Villiger Monooxygenases and Non-Heme Iron-Dependent Dehydrogenase/Oxygenases in the Final Steps of the Biosynthesis of Pentalenolactone and Neopentalenolactone. Biochemistry. 2011; 50(10):1739–1754. [PubMed: 21250661]

574. Matsuda Y, Awakawa T, Wakimoto T, Abe I. Spiro-Ring Formation is Catalyzed by a Multifunctional Dioxygenase in Austinol Biosynthesis. J Am Chem Soc. 2013; 135(30):10962–10965. [PubMed: 23865690]

575. Scherlach K, Boettger D, Remme N, Hertweck C. The Chemistry and Biology of Cytochalasans. Nat Prod Rep. 2010; 27(6):869–886. [PubMed: 20411198]

576. Qiao KJ, Chooi YH, Tang Y. Identification and Engineering of the Cytochalasin Gene Cluster from *Aspergillus Clavatus* NRRL 1. Metab Eng. 2011; 13(6):723–732. [PubMed: 21983160]

577. Hu YC, Dietrich D, Xu W, Patel A, Thuss JAJ, Wang JJ, Yin WB, Qiao KJ, Houk KN, Vederas JC, et al. A Carbonate-Forming Baeyer-Villiger Monooxygenase. Nat Chem Biol. 2014; 10(7):552–554. [PubMed: 24838010]

578. Jager CE, Symons GM, Nomura T, Yamada Y, Smith JJ, Yamaguchi S, Kamiya Y, Weller JL, Yokota T, Reid JB. Characterization of Two Brassinosteroid C-6 Oxidase Genes in Pea. Plant Physiol. 2007; 143(4):1894–1904. [PubMed: 17322341]

579. Nomura T, Kushiro T, Yokota T, Kamiya Y, Bishop GJ, Yamaguchi S. The Last Reaction Producing Brassinolide Is Catalyzed by Cytochrome P-450s, CYP85A3 in Tomato and CYP85A2 in *Arabidopsis*. J Biol Chem. 2005; 280(18):17873–17879. [PubMed: 15710611]

580. Valegard K, van Scheltinga AC, Lloyd MD, Hara T, Ramaswamy S, Perrakis A, Thompson A, Lee HJ, Baldwin JE, Schofield CJ, et al. Structure of a Cephalosporin Synthase. Nature. 1998; 394(6695):805–809. [PubMed: 9723623]

581. Dotzlaf JE, Yeh WK. Purification and Properties of Deacetoxycephalosporin C Synthase from Recombinant *Escherichia coli* and its Comparison with the Native Enzyme Purified from *Streptomyces Clavuligerus*. J Biol Chem. 1989; 264(17):10219–10227. [PubMed: 2656705]

582. Lee HJ, Lloyd MD, Harlos K, Clifton IJ, Baldwin JE, Schofield CJ. Kinetic and Crystallographic Studies on Deacetoxycephalosporin C Synthase (DAOCS). J Mol Biol. 2001; 308(5):937–948. [PubMed: 11352583]

583. Bentley R. Aromatic Synthesis in Molds: Formation of the Tropolone, Stipitatic Acid. Biochim Biophys Acta. 1958; 29(3):666–667. [PubMed: 13584386]

584. Davison J, al Fahad A, Cai M, Song Z, Yehia SY, Lazarus CM, Bailey AM, Simpson TJ, Cox RJ. Genetic, Molecular, and Biochemical Basis of Fungal Tropolone Biosynthesis. Proc Natl Acad Sci U S A. 2012; 109(20):7642–7647. [PubMed: 22508998]

585. Cox RJ, Al-Fahad A. Chemical Mechanisms Involved During the Biosynthesis of Tropolones. Curr Opin Chem Biol. 2013; 17(4):532–536. [PubMed: 23870699]

586. Teufel R, Friedrich T, Fuchs G. An Oxygenase that Forms and Deoxygenates Toxic Epoxide. Nature. 2012; 483(7389):359–362. [PubMed: 22398448]

587. Moore BS, Walker K, Tornus I, Handa S, Poralla K, Floss HG. Biosynthetic Studies of ω-Cycloheptyl Fatty Acids in *Alicyclobacillus Cycloheptanicus*. Formation of Cycloheptanecarboxylic Acid from Phenylacetic Acid. J Org Chem. 1997; 62(7):2173–2185. [PubMed: 11671526]

588. Bergmann S, Schumann J, Scherlach K, Lange C, Brakhage AA, Hertweck C. Genomics-Driven Discovery of PKS-NRPS Hybrid Metabolites from *Aspergillus Nidulans*. Nat Chem Biol. 2007; 3(4):213–217. [PubMed: 17369821]

589. Xu W, Cai X, Jung ME, Tang Y. Analysis of Intact and Dissected Fungal Polyketide Synthase-Nonribosomal Peptide Synthetase in Vitro and in *Saccharomyces Cerevisiae*. J Am Chem Soc. 2010; 132(39):13604–13607. [PubMed: 20828130]

590. Liu C, Tagami K, Minami A, Matsumoto T, Frisvad JC, Suzuki H, Ishikawa J, Gomi K, Oikawa H. Reconstitution of biosynthetic machinery for the synthesis of the highly elaborated indole diterpene penitrem. Angew Chem Int Ed Engl. 2015; 54(19):5748–5752. [PubMed: 25831977]

591. Minami A, Liu C, Oikawa H. Total Biosynthesis of Fungal Indole Diterpenes Using Cell Factories. Heterocycles. 2016; 92(3):397–421.

592. Lin H-C, Chooi YH, Dhingra S, Xu W, Calvo AM, Tang Y. The Fumagillin Biosynthetic Gene Cluster in *Aspergillus Fumigatus* Encodes a Cryptic Terpene Cyclase Involved in the Formation of β-*trans*-Bergamotene. J Am Chem Soc. 2013; 135(12):4616–4619. [PubMed: 23488861]

593. Ingber D, Fujita T, Kishimoto S, Sudo K, Kanamaru T, Brem H, Folkman J. Synthetic Analogs of Fumagillin That Inhibit Angiogenesis and Suppress Tumor Growth. Nature. 1990; 348(6301): 555–557. [PubMed: 1701033]

594. Sin N, Meng L, Wang MQ, Wen JJ, Bornmann WG, Crews CM. The Anti-Angiogenic Agent Fumagillin Covalently Binds and Inhibits the Methionine Aminopeptidase, MetAP-2. Proc Natl Acad Sci U S A. 1997; 94(12):6099–6103. [PubMed: 9177176]

595. Griffith EC, Su Z, Niwayama S, Ramsay CA, Chang YH, Liu JO. Molecular Recognition of Angiogenesis Inhibitors Fumagillin and Ovalicin by Methionine Aminopeptidase 2. Proc Natl Acad Sci U S A. 1998; 95(26):15183–15188. [PubMed: 9860943]

596. Liu SP, Widom J, Kemp CW, Crews CM, Clardy J. Structure of Human Methionine Aminopeptidase-2 Complexed with Fumagillin. Science. 1998; 282(5392):1324–1327. [PubMed: 9812898]

597. Ortiz de Montellano, PRE. Cytochrome P450-Structure, Mechanism, and Biochemistry. Springer; New York: 2015.

598. Ohmomo S, Oguma K, Ohashi T, Abe M. Isolation of a New Indole Alkaloid, Roquefortine D, from the Cultures of *Penicillium Roqueforti*. Agric Biol Chem. 1978; 42(12):2387–2389.

599. Sumarah MW, Miller JD, Blackwell BA. Isolation and Metabolite Production by *Penicillium Roqueforti*, *P. Paneum* and *P. Crustosum* Isolated in Canada. Mycopathologia. 2005; 159(4):571–577. [PubMed: 15983744]

600. Bhat B, Harrison DM, Lamont HM. The Biosynthesis of the Mould Metabolites Roquefortine and Aszonalenin from L-[2,4,5,6,7-2H5]Tryptophan. Tetrahedron. 1993; 49(46):10663–10668.

601. Garcia-Estrada C, Ullan RV, Albillos SM, Fernandez-Bodega MA, Durek P, von Dohren H, Martin JF. A Single Cluster of Coregulated Genes Encodes the Biosynthesis of the Mycotoxins Roquefortine C and Meleagrin in *Penicillium Chrysogenum*. Chem Biol. 2011; 18(11):1499–1512. [PubMed: 22118684]

602. Ali H, Ries MI, Nijland JG, Lankhorst PP, Hankemeier T, Bovenberg RAL, Vreeken RJ, Driessen AJM. A Branched Biosynthetic Pathway Is Involved in Production of Roquefortine and Related Compounds in *Penicillium Chrysogenum*. PloS ONE. 2013; 8(6):e65328. [PubMed: 23776469]

603. Terui Y, Chu YW, Li JY, Ando T, Yamamoto H, Kawamura Y, Tomishima Y, Uchida S, Okazaki T, Munetomo E, et al. Xantholipin, a Novel Inhibitor of HSP47 Gene Expression Produced by *Streptomyces* sp. Tetrahedron Lett. 2003; 44(29):5427–5430.

604. Kong L, Zhang W, Chooi YH, Wang L, Cao B, Deng Z, Chu Y, You D. A Multifunctional Monooxygenase XanO4 Catalyzes Xanthone Formation in Xantholipin Biosynthesis via a Cryptic Demethoxylation. Cell Chem Biol. 2016; 23(4):508–516. [PubMed: 27105283]

605. Leach BE, Calhoun KM, Johnson LE, Teeters CM, Jackson WG. Chartreusin, a New Antibiotic Produced by *Streptomyces Chartreusis*, a New Species. J Am Chem Soc. 1953; 75(16):4011–4012.

606. Xu Z, Jakobi K, Welzel K, Hertweck C. Biosynthesis of the Antitumor Agent Chartreusin Involves the Oxidative Rearrangement of an Anthracyclic Polyketide. Chem Biol. 2005; 12(5): 579–588. [PubMed: 15911378]

607. Ayer SW, Mcinnes AG, Thibault P, Walter JA, Doull JL, Parnell T, Vining LC. Jadomycin, a Novel 8H-Benz[b]Oxazolo[3,2-f]Phenanthridine Antibiotic from *Streptomyces Venezuelae* ISP5230. Tetrahedron Lett. 1991; 32(44):6301–6304.

608. Doull JL, Ayer SW, Singh AK, Thibault P. Production of a Novel Polyketide Antibiotic, Jadomycin B, by *Streptomyces Venezuelae* Following Heat Shock. J Antibiot (Tokyo). 1993; 46(5):869–871. [PubMed: 8514643]

609. Tibrewal N, Pahari P, Wang GJ, Kharel MK, Morris C, Downey T, Hou YP, Bugni TS, Rohr J. Baeyer-Villiger C-C Bond Cleavage Reaction in Gilvocarcin and Jadomycin Biosynthesis. J Am Chem Soc. 2012; 134(44):18181–18184. [PubMed: 23102024]

610. Fan KQ, Pan GH, Peng XJ, Zheng JT, Gao WB, Wang J, Wang WS, Li Y, Yang KQ. Identification of JadG as the B Ring Opening Oxygenase Catalyzing the Oxidative C-C Bond Cleavage Reaction in Jadomycin Biosynthesis. Chem Biol. 2012; 19(11):1381–1390. [PubMed: 23177193]

611. Han L, Yang KQ, Ramalingam E, Mosher RH, Vining LC. Cloning and Characterization of Polyketide Synthase Genes for Jadomycin B Biosynthesis in *Streptomyces Venezuelae* ISP5230. Microbiology. 1994; 140:3379–3389. [PubMed: 7881555]

612. Gould SJ, Cheng X-C. Biosynthesis of the Benz[α]Anthraquinone Antibiotic PD 116198. Tetrahedron. 1993; 49(48):11135–11144.

613. Gould SJ, Halley KA. Biosynthesis of the Benz[a]Anthraquinone Antibiotic PD 116198: Evidence for a Rearranged Skeleton. J Am Chem Soc. 1991; 113(13):5092–5093.

614. Sasaki E, Ogasawara Y, Liu HW. A Biosynthetic Pathway for BE-7585A, a 2-Thiosugar-Containing Angucycline-Type Natural Product. J Am Chem Soc. 2010; 132(21):7405–7417. [PubMed: 20443562]

615. Yu J, Chang PK, Ehrlich KC, Cary JW, Bhatnagar D, Cleveland TE, Payne GA, Linz JE, Woloshuk CP, Bennett JW. Clustered Pathway Genes in Aflatoxin Biosynthesis. Appl Environ Microbiol. 2004; 70(3):1253–1262. [PubMed: 15006741]

616. Townsend CA. Aflatoxin and Deconstruction of Type I, Iterative Polyketide Synthase Function. Nat Prod Rep. 2014; 31(10):1260–1265. [PubMed: 25079257]

617. Yabe K, Nakajima H. Enzyme Reactions and Genes in Aflatoxin Biosynthesis. Appl Microbiol Biotechnol. 2004; 64(6):745–755. [PubMed: 15022028]

618. McKeown DSJ, McNicholas C, Simpson TJ, Willett NJ. Biosynthesis of Norsolorinic Acid and Averufin: Substrate Specificity of Norsolorinic Acid Synthase. Chem Commun (camb). 1996; (3):301–302.

619. Crawford JM, Korman TP, Labonte JW, Vagstad AL, Hill EA, Kamari-Bidkorpeh O, Tsai SC, Townsend CA. Structural Basis for Biosynthetic Programming of Fungal Aromatic Polyketide Cyclization. Nature. 2009; 461(7267):1139–1143. [PubMed: 19847268]

620. Ehrlich KC, Scharfenstein LL, Chang PK, Li P, Bhatnagar D. Characterization of the Anthrone Oxidase in Aflatoxin Biosynthesis. FASEB J. 2009; 23(1 Supplement):535.532.

621. Yu JJ, Chang PK, Cary JW, Bhatnagar D, Cleveland TE. AvnA, a Gene Encoding a Cytochrome P-450 Monooxygenase, Is Involved in the Conversion of Averantin to Averufin in Aflatoxin Biosynthesis in *Aspergillus Parasiticus*. Appl Environ Microbiol. 1997; 63(4):1349–1356. [PubMed: 9097431]

622. Sakuno E, Wen Y, Hatabayashi H, Arai H, Aoki C, Yabe K, Nakajima H. *Aspergillus Parasiticus* Cyclase Catalyzes Two Dehydration Steps in Aflatoxin Biosynthesis. Appl Environ Microbiol. 2005; 71(6):2999–3006. [PubMed: 15932995]

623. Keller NP, Watanabe CMH, Kelkar HS, Adams TH, Townsend CA. Requirement of Monooxygenase-Mediated Steps for Sterigmatocystin Biosynthesis by *Aspergillus Nidulans*. Appl Environ Microbiol. 2000; 66(1):359–362. [PubMed: 10618248]

624. Townsend CA, Christensen SB. Concerning the Role of Nidurufin in Aflatoxin Biosynthesis. J Am Chem Soc. 1985; 107(1):270–271.

625. Townsend CA, Davis SG, Koreeda M, Hulin B. A Cationic Model of the Chain-Branching Step in Aflatoxin Biosynthesis. J Org Chem. 1985; 50(25):5428–5430.

626. Townsend CA, Isomura Y, Davis SG, Hodge JA. Reaction Models of the Oxidative Rearrangement of Averufin to 1′-Hydroxyversicolorone: The First Step in Dihydrobisfuran Formation in Aflatoxin Biosynthesis. Tetrahedron. 1989; 45(8):2263–2276.

627. Yabe K, Chihaya N, Hamamatsu S, Sakuno E, Hamasaki T, Nakajima H, Bennett JW. Enzymatic Conversion of Averufin to Hydroxyversicolorone and Elucidation of a Novel Metabolic Grid Involved in Aflatoxin Biosynthesis. Appl Environ Microbiol. 2003; 69(1):66–73. [PubMed: 12513978]

628. Yu J, Chang PK, Bhatnagar D, Cleveland TE. Genes Encoding Cytochrome P450 and Monooxygenase Enzymes Define One End of the Aflatoxin Pathway Gene Cluster in *Aspergillus Parasiticus*. Appl Microbiol Biotechnol. 2000; 53(5):583–590. [PubMed: 10855719]

629. Lin BK, Anderson JA. Purification and Properties of Versiconal Cyclase from *Aspergillus Parasiticus*. Arch Biochem Biophys. 1992; 293(1):67–70. [PubMed: 1731640]

630. Yabe K, Hamasaki T. Stereochemistry During Aflatoxin Biosynthesis: Cyclase Reaction in the Conversion of Versiconal to Versicolorin B and Racemization of Versiconal Hemiacetal Acetate. Appl Environ Microbiol. 1993; 59(8):2493–2500. [PubMed: 8368837]

631. Henry KM, Townsend CA. Ordering the Reductive and Cytochrome P450 Oxidative Steps in Demethylsterigmatocystin Formation Yields General Insights into the Biosynthesis of Aflatoxin and Related Fungal Metabolites. J Am Chem Soc. 2005; 127(11):3724–3733. [PubMed: 15771506]

632. Yu J, Cary JW, Bhatnagar D, Cleveland TE, Keller NP, Chu FS. Cloning and Characterization of a cDNA from *Aspergillus Parasiticus* Encoding an *O*-Methyltransferase Involved in Aflatoxin Biosynthesis. Appl Environ Microbiol. 1993; 59(11):3564–3571. [PubMed: 8285664]

633. Lee LW, Chiou CH, Linz JE. Function of Native OmtA in Vivo and Expression and Distribution of this Protein in Colonies of *Aspergillus Parasiticus*. Appl Environ Microbiol. 2002; 68(11): 5718–5727. [PubMed: 12406770]

634. Yabe K, Nakamura M, Hamasaki T. Enzymatic Formation of G-Group Aflatoxins and Biosynthetic Relationship Between G- and B-Group Aflatoxins. Appl Environ Microbiol. 1999; 65(9):3867–3872. [PubMed: 10473388]

635. Yu J, Chang PK, Ehrlich KC, Cary JW, Montalbano B, Dyer JM, Bhatnagar D, Cleveland TE. Characterization of the Critical Amino Acids of an *Aspergillus Parasiticus* Cytochrome P-450 Monooxygenase Encoded by OrdA that Is Involved in the Biosynthesis of Aflatoxins B1, G1, B2, and G2. Appl Environ Microbiol. 1998; 64(12):4834–4841. [PubMed: 9835571]

636. Prieto R, Woloshuk CP. Ord1, an Oxidoreductase Gene Responsible for Conversion of *O*-Methylsterigmatocystin to Aflatoxin in *Aspergillus Flavus*. Appl Environ Microbiol. 1997; 63(5): 1661–1666. [PubMed: 9143099]

637. Kimler L, Larson RA, Messenger L, Moore JB, Mabry TJ. Betalamic Acid, a New Naturally Occurring Pigment. J Chem Soc D. 1971; (21):1329–1330.

638. Gandia-Herrero F, Escribano J, Garcia-Carmona F. Purification and Antiradical Properties of the Structural Unit of Betalains. J Nat Prod. 2012; 75(6):1030–1036. [PubMed: 22642551]

639. Gandia-Herrero F, Garcia-Carmona F. Characterization of Recombinant Beta Vulgaris 4,5-DOPA-Extradiol-Dioxygenase Active in the Biosynthesis of Betalains. Planta. 2012; 236(1):91–100. [PubMed: 22270561]

640. Lipscomb JD. Mechanism of Extradiol Aromatic Ring-Cleaving Dioxygenases. Curr Opin Struct Biol. 2008; 18(6):644–649. [PubMed: 19007887]

641. Demain AL, Fang A. The Natural Functions of Secondary Metabolites. Adv Biochem Eng Biotechnol. 2000; 69:1–39. [PubMed: 11036689]

642. Crawford JM, Townsend CA. New Insights into the Formation of Fungal Aromatic Polyketides. Nat Rev Microbiol. 2010; 8(12):879–889. [PubMed: 21079635]

643. Hertweck C, Luzhetskyy A, Rebets Y, Bechthold A. Type II Polyketide Synthases: Gaining a Deeper Insight into Enzymatic Teamwork. Nat Prod Rep. 2007; 24(1):162–190. [PubMed: 17268612]

644. Dickschat JS. Bacterial Terpene Cyclases. Nat Prod Rep. 2016; 33(1):87–110. [PubMed: 26563452]

645. Ashour M, Wink M, Gershenzon J. Biochemistry of Terpenoids: Monoterpenes Sesquiterpenes and Diterpenes. Annu Plant Rev. 2010; 40:258–303.

646. Tholl D. Biosynthesis and Biological Functions of Terpenoids in Plants. Adv Biochem Eng Biotechnol. 2015; 148:63–106. [PubMed: 25583224]

647. Abe I. Enzymatic Synthesis of Cyclic Triterpenes. Nat Prod Rep. 2007; 24(6):1311–1331. [PubMed: 18033581]

648. Baunach M, Franke J, Hertweck C. Terpenoid Biosynthesis Off the Beaten Track: Unconventional Cyclases and Their Impact on Biomimetic Synthesis. Angew Chem Int Ed Engl. 2015; 54(9): 2604–2626. [PubMed: 25488271]

649. Hammer SC, Syren PO, Seitz M, Nestl BM, Hauer B. Squalene Hopene Cyclases: Highly Promiscuous and Evolvable Catalysts for Stereoselective C-C and C-X Bond Formation. Curr Opin Chem Biol. 2013; 17(2):293–300. [PubMed: 23485581]

650. Siedenburg G, Jendrossek D. Squalene-Hopene Cyclases. Appl Environ Microbiol. 2011; 77(12): 3905–3915. [PubMed: 21531832]

651. Syren PO, Henche S, Eichler A, Nestl BM, Hauer B. Squalene-Hopene Cyclases-Evolution, Dynamics and Catalytic Scope. Curr Opin Struct Biol. 2016; 41:73–82. [PubMed: 27336183]

652. Crotti, P., Pineschi, M. Aziridines and Epoxides in Organic Synthesis. Yudin, AK., editor. Vol. chap. 8. Wiley-VCH; Weinheim: 2006. p. 271-313.

653. Olofsson, B., Somfai, P. Aziridines and Epoxides in Organic Synthesis. Yudi, AK., editor. Vol. chap. 9. Wiley-VCH; Weinheim: 2006. p. 315-347.

654. Hagel JM, Facchini PJ. Benzylisoquinoline Alkaloid Metabolism: A Century of Discovery and a Brave New World. Plant Cell Physiol. 2013; 54(5):647–672. [PubMed: 23385146]

655. Winter JM, Jansma AL, Handel TM, Moore BS. Formation of the Pyridazine Natural Product Azamerone by Biosynthetic Rearrangement of an Aryl Diazoketone. Angew Chem Int Ed Engl. 2009; 48(4):767–770. [PubMed: 19072974]

Biographies

Man-Cheng Tang was born in 1982 in Hunan, China. He received his B. Sc. in Chemistry from Wuhan University in 2003 and his Ph. D. in Organic Chemistry from Shanghai Institute of Organic Chemistry (SIOC), CAS, in 2010 under the supervision of Prof. Gong-Li Tang. He then worked as a research associate in Prof. Gong-Li Tang's group at SIOC and was appointed as an Associate Professor at SIOC in 2013. In 2014, he joined Prof. Yi Tang's lab at University of California, Los Angeles as a postdoctoral scholar. His is interested in understanding the enzymology of natural products biosynthesis.

Yi Zou was born in 1983 in Guizhou, China. He received his B. Sc. degree in 2006 and MS degree in 2009 in Pharmaceutical Engineering from Southwest University, China. He received his Ph.D. in Microbiology in 2013 from Shanghai JiaoTong Univeristy, China, under the guidance of Prof. Shuangjun Lin. During his doctoral work, he worked on identifying the gene clusters and novel enzymes involved in polyketides and alkaloids biosynthesis from *Streptomyces*. In 2014, He joined Prof. Yi Tang's lab at University of California, Los Angeles as a postdoctoral scholar. His current research interests focus on the biosynthesis of fungal natural products.

Kenji Watanabe, born in 1969, received his Ph.D. in 2000 in bioorganic chemistry from Hokkaido University, Japan. His postdoctoral fellowships included a year at University of Wisconsin-Madison and a two-year appointment at Stanford University. In 2003, he returned to Hokkaido University as an assistant professor. In 2004, he joined the department of pharmaceutical sciences at University of Southern California as a research assistant

professor. In 2008, he received a tenure-track position at Okayama University. He was promoted to associate professor in 2009 and professor in 2016 at University of Shizuoka. His research interest has been focused on developing a heterologous production system for natural products from PKS, NRPS and other important molecules of interest. Also, he has placed much effort into the mechanistic and structural characterization of enzymes involved in natural product biosynthesis.

Christopher T. Walsh, born in 1944, studied biology at Harvard and completed his PhD in biochemistry under Fritz Lipmann at The Rockefeller University. From 1972 to 1987 he held a faculty position at MIT and later moved on to continue his work at Harvard Medical School. He served as Chair of the Department of Chemistry at MIT from 1978 to 1982 and of the Department of Biological Chemistry & Molecular Pharmacology at Harvard Medical School from 1987 to 1995. In 2014, he was appointed a Consulting Professor of Chemistry at Stanford University and a member of the Stanford Institute for Chemistry, Engineering, and Medicine for Human Health (ChEM-H). His research interests focus on the molecular logic and enzymatic machinery of peptide-based natural product biosynthesis.

Yi Tang, born in 1976, received his undergraduate degree in Chemical Engineering and Material Science from Penn State University in 1997. He received his Ph.D. in Chemical Engineering from California Institute of Technology under the guidance of Prof. David A. Tirrell in 2002. After NIH postdoctoral training in Chemical Biology from Prof. Chaitan Khosla at Stanford University, he started his independent career at University of California Los Angeles in 2004. He is currently Professor in the Department of Chemical and Biomolecular Engineering at UCLA, and holds joint appointments in the Department of Chemistry and Biochemistry; and Department of Bioengineering. His lab is interested in identifying new enzymes from the biosynthetic pathways of polyketides, nonribosomal peptides, terpenoids, alkaloids and hybrid compounds.

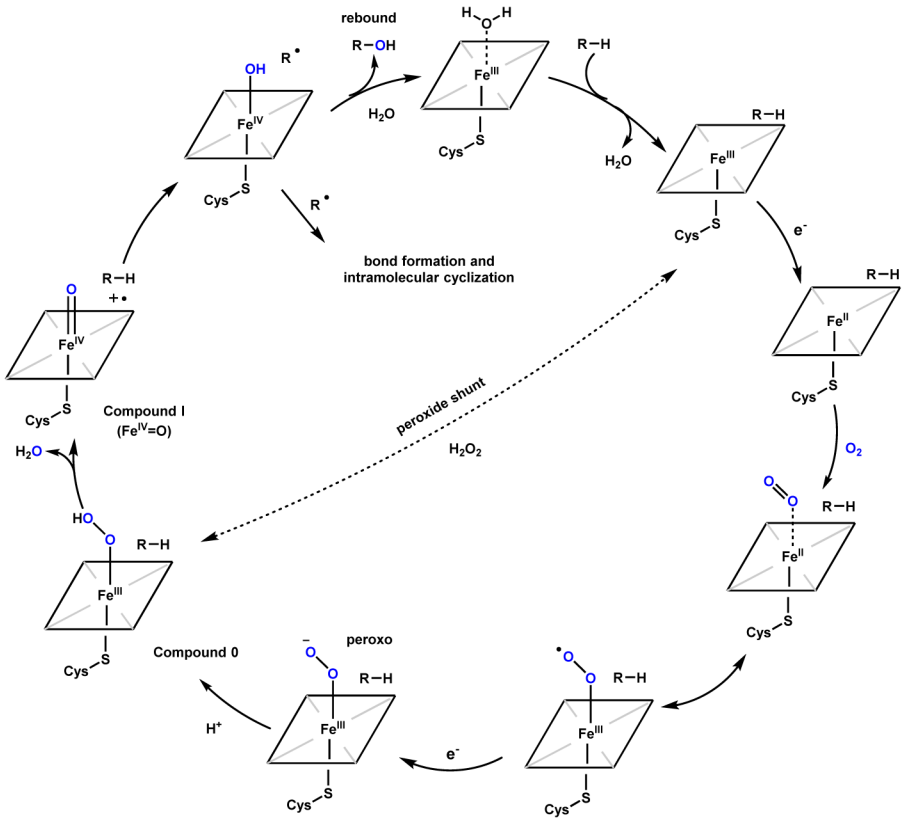

Scheme 1.
Catalytic Cycle of Cytochrome P450

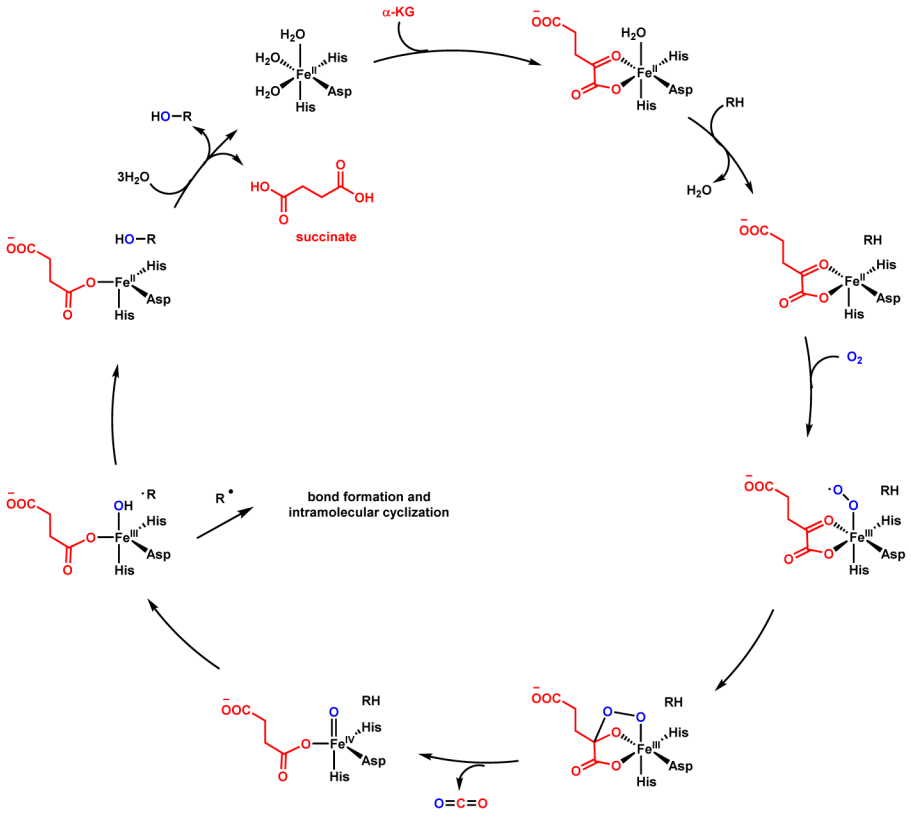

Scheme 2.
Catalytic Cycle of Nonheme Iron α-KG-Dependent Oxygenase

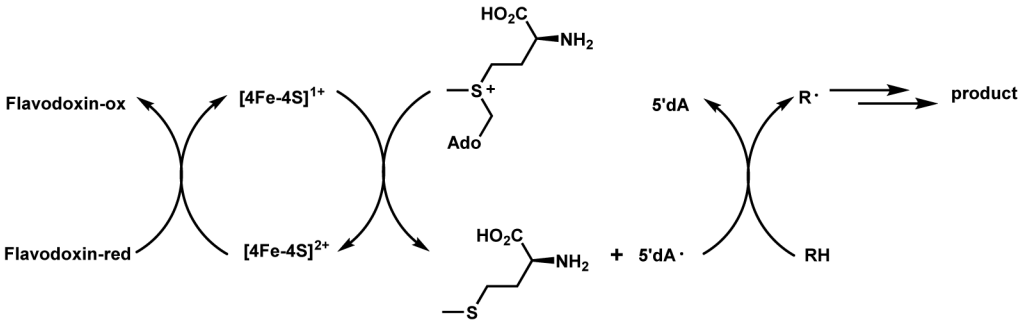

Scheme 3.
Catalytic Cycle of Radical SAM Enzyme

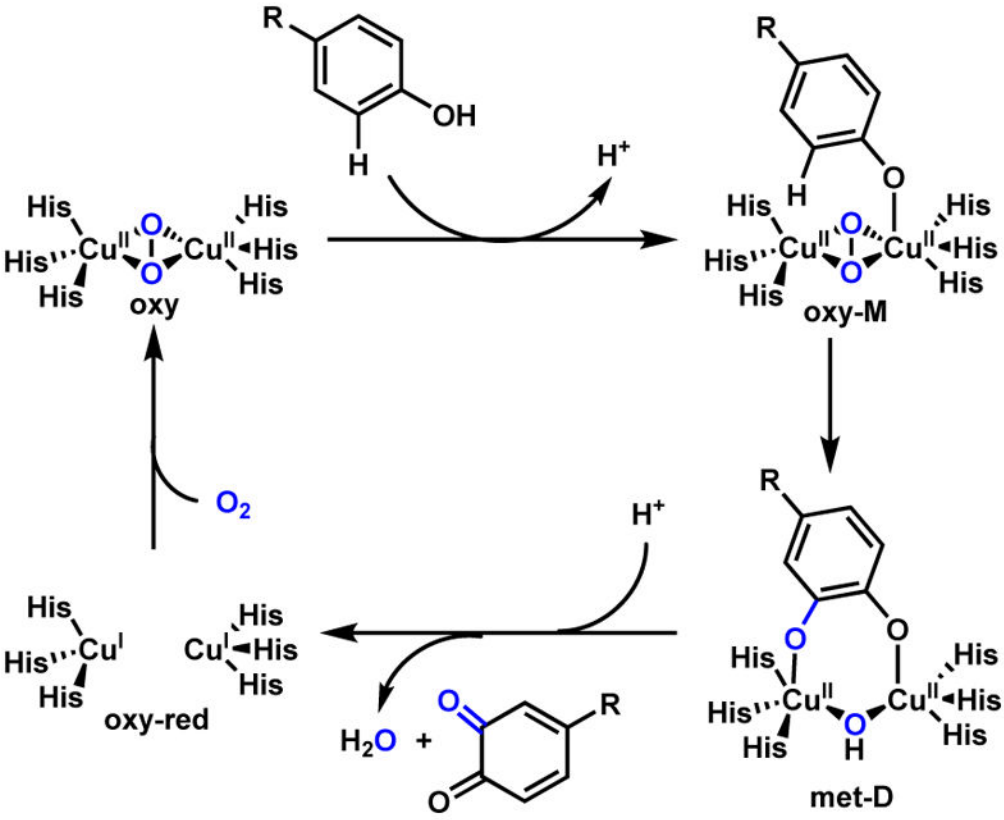

Scheme 4.
Catalytic Cycle of Copper-Dependent Tyrosinase

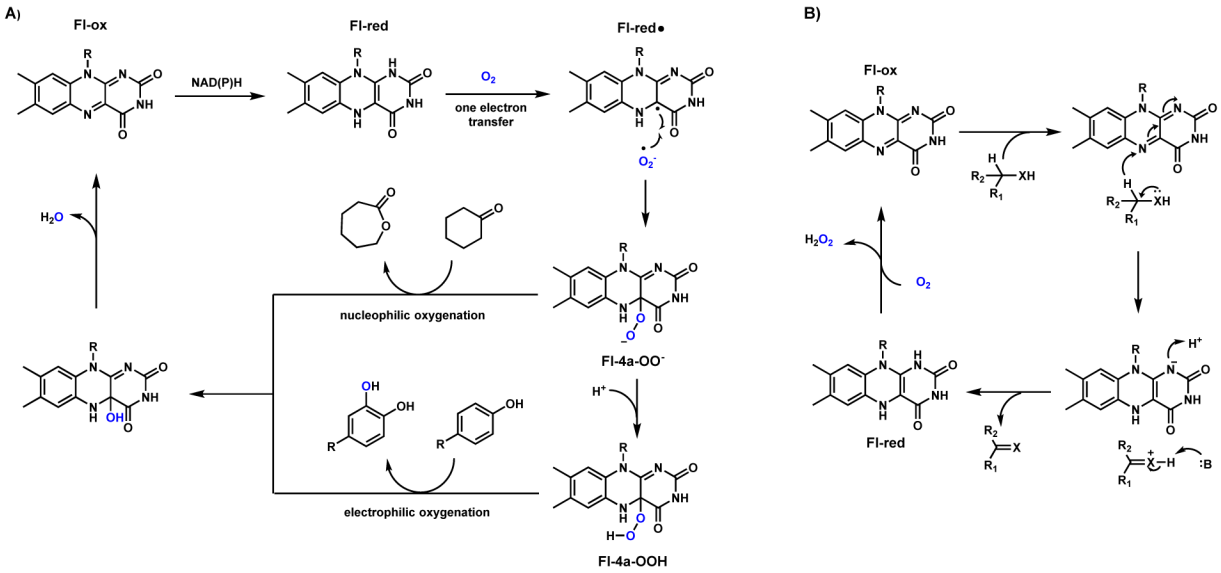

Scheme 5.
Catalytic Cycle of Flavin-Dependent Monooxygenase

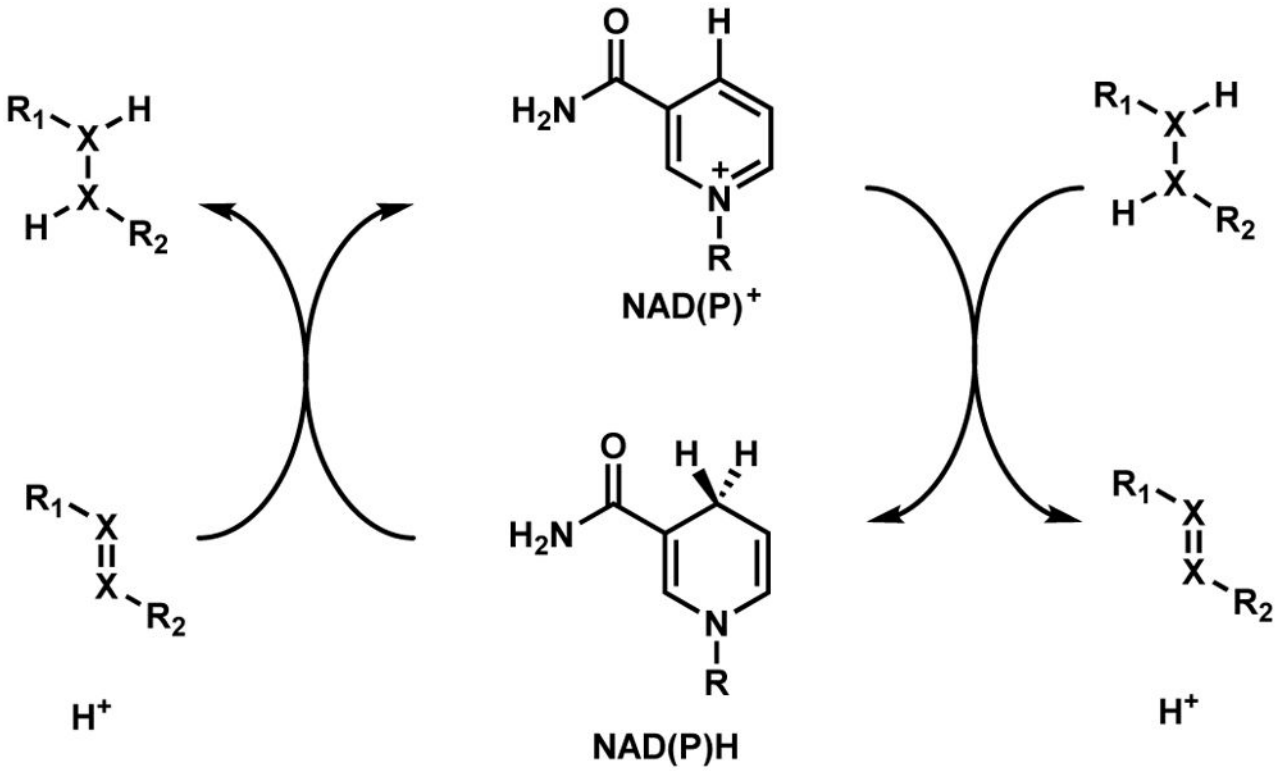

Scheme 6.
NAD(P)H-Dependent Reductases and Dehydrogenases

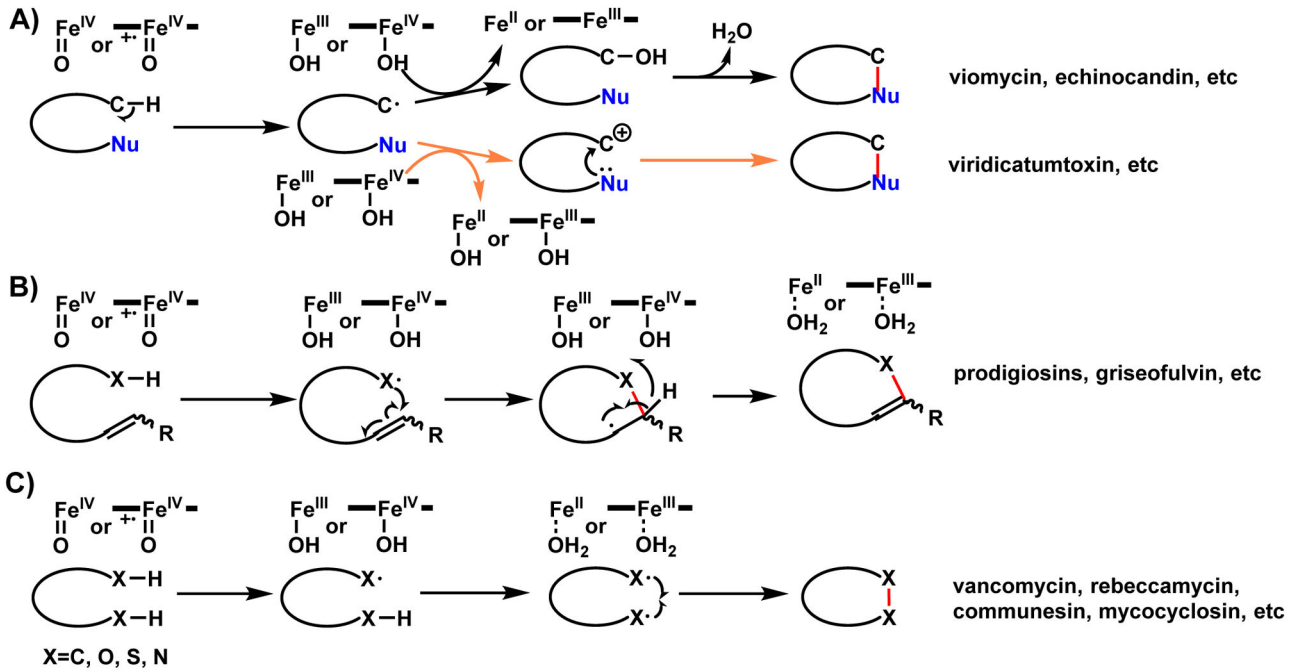

Scheme 7.
Models of Radical Cyclization in Natural Product Biosynthesis

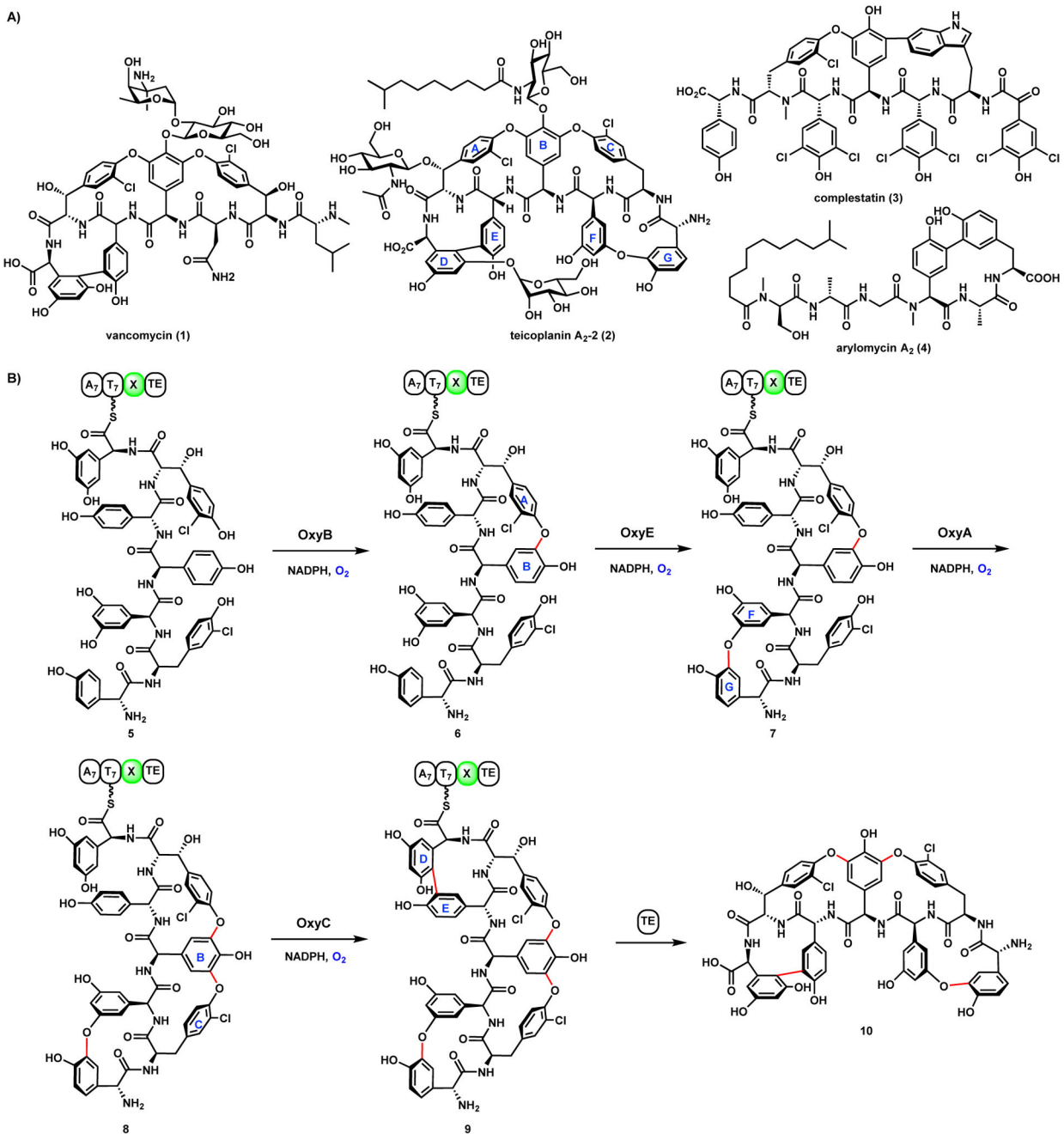

Scheme 8.
P450-Catalyzed Phenol Coupling Reactions in Glycopeptide Biosynthesis

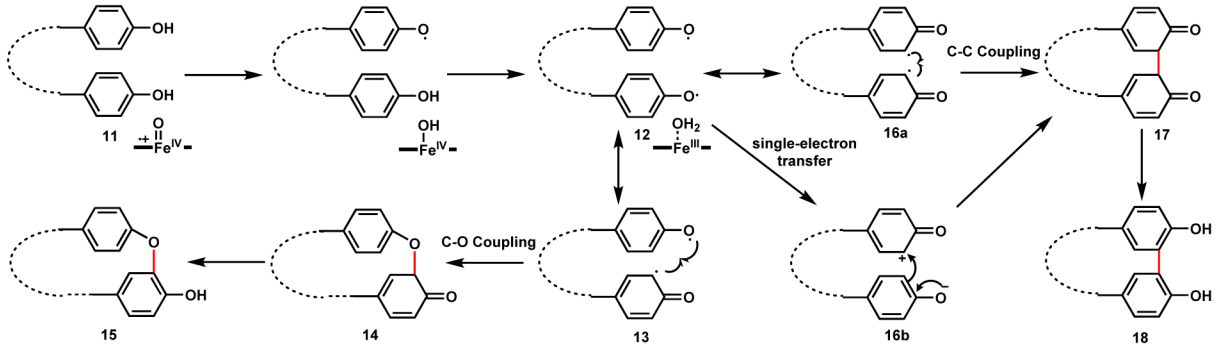

Scheme 9.

Mechanistic Proposal of C-C and C-O Phenol Coupling Catalyzed by P450

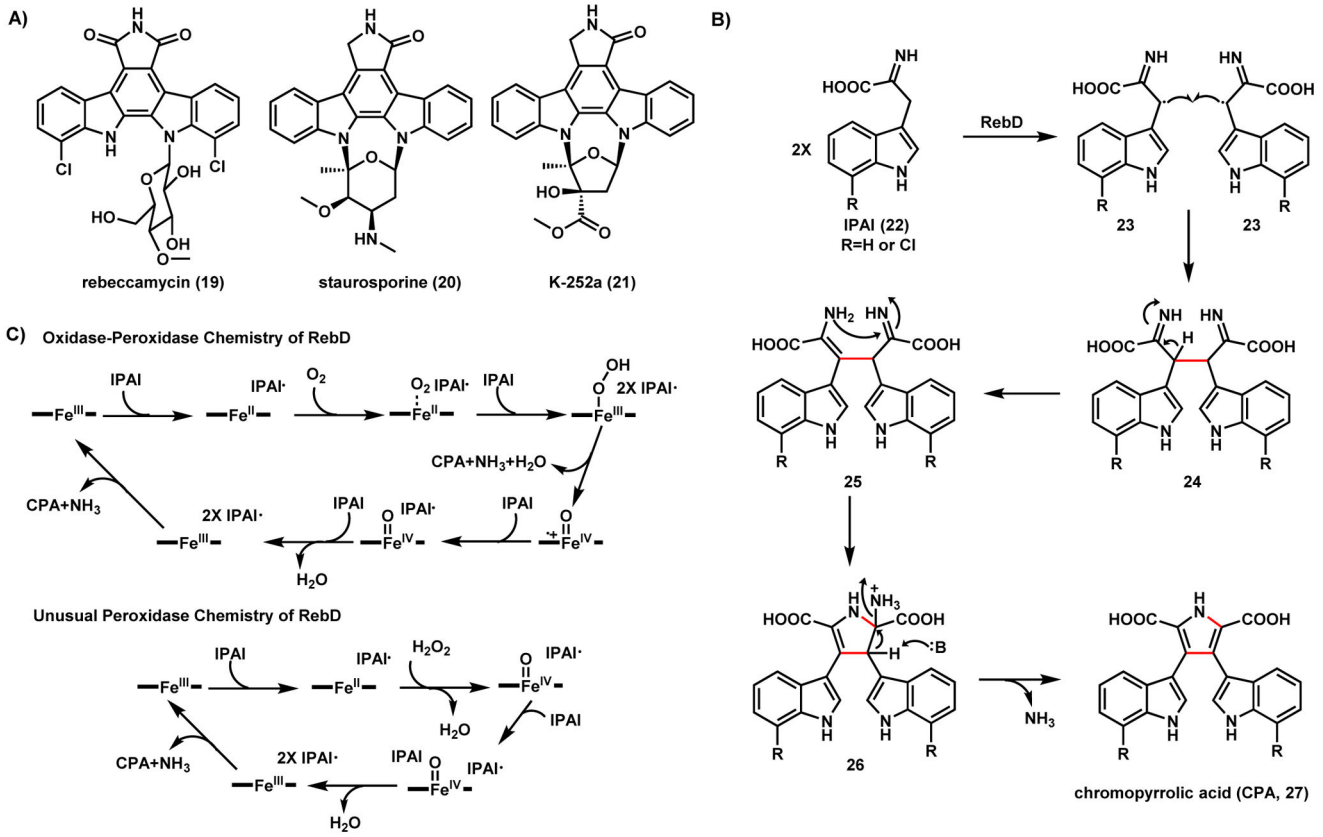

Scheme 10.
Oxidative Coupling in Indolocarbazole Biosynthesis

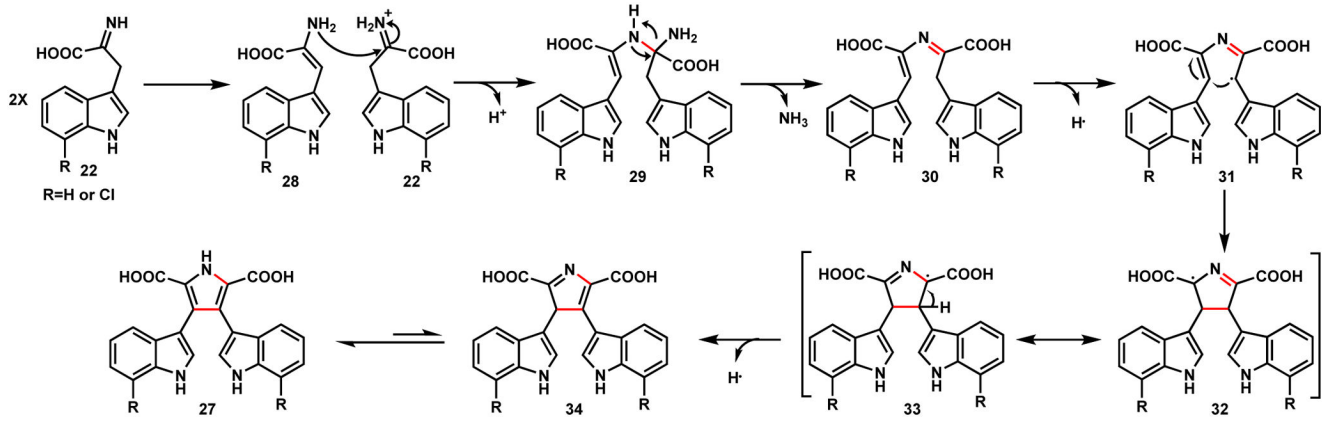

Scheme 11.
Mechanistic Proposal for Chromopyrrolic Acid Formation

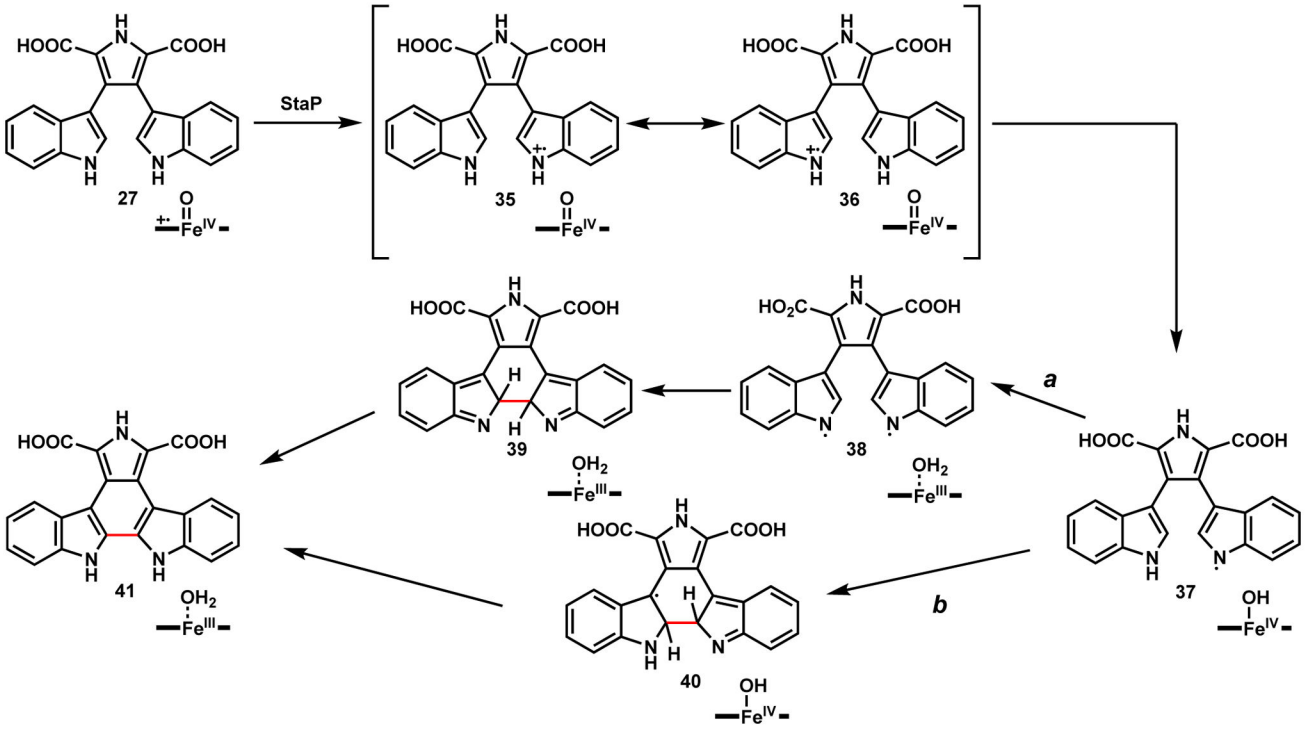

Scheme 12.
Proposed Catalytic Mechanism of Indole Coupling in Indolocarbazole Biosynthesis

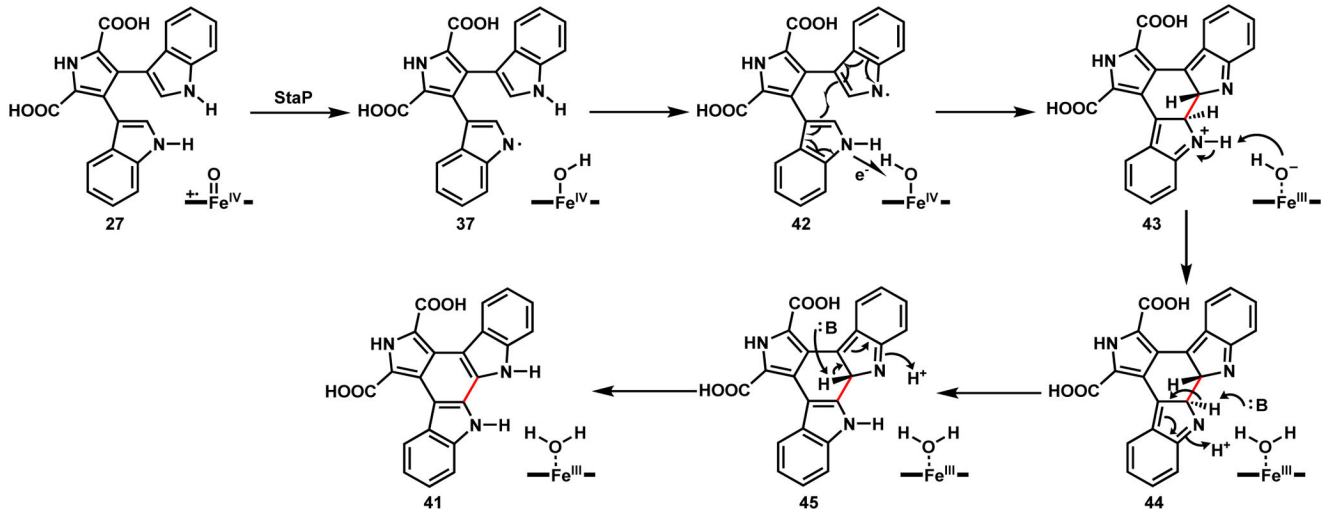

Scheme 13.
Alternative Proposal for the Mechanism of StaP

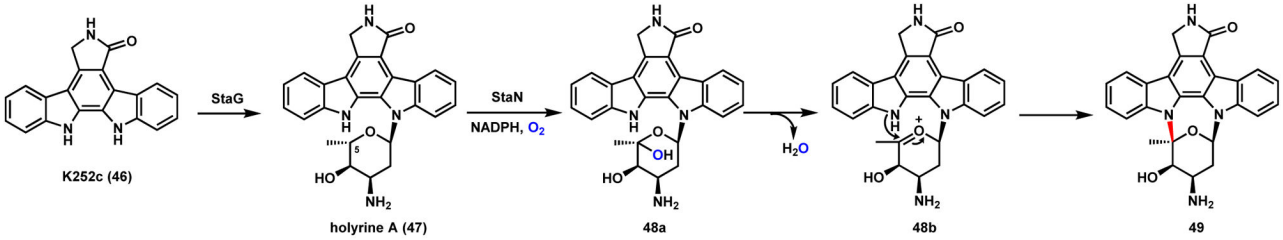

Scheme 14.

Proposed Catalytic Mechanism for the Last C-N Coupling Step in Staurosporine Biosynthesis

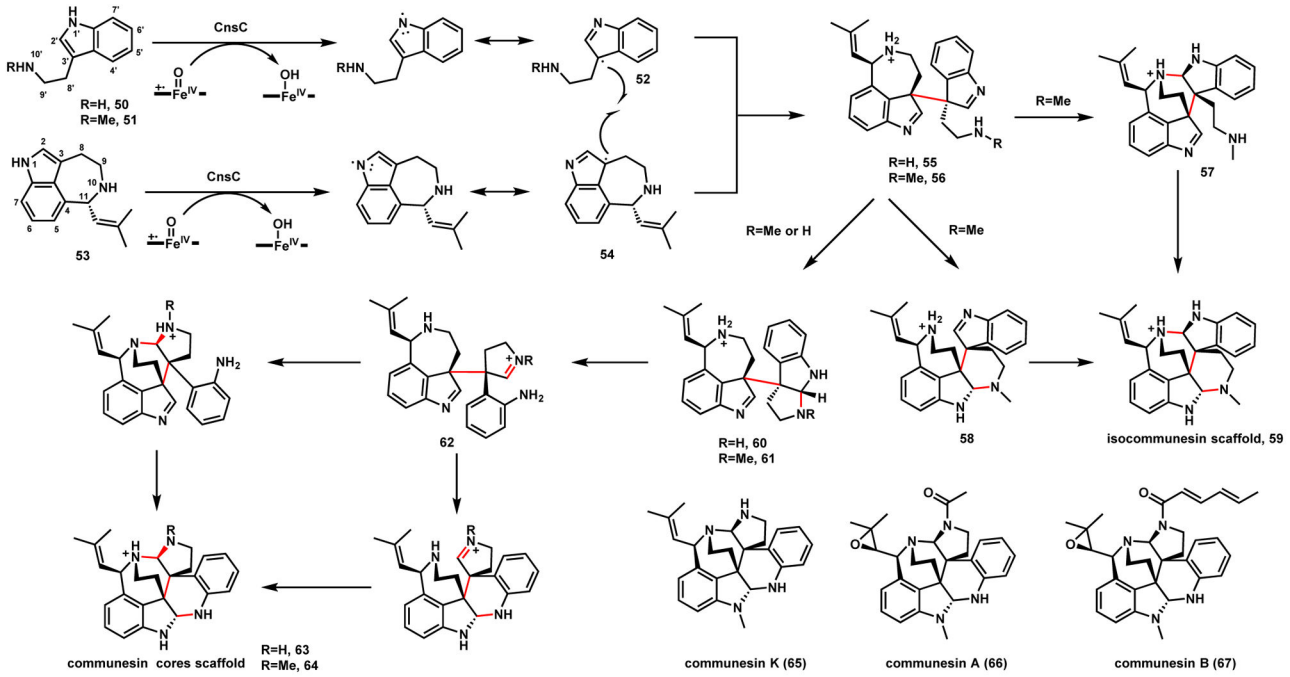

Scheme 15.
Formation of the Communesin Core by the P450 CnsC

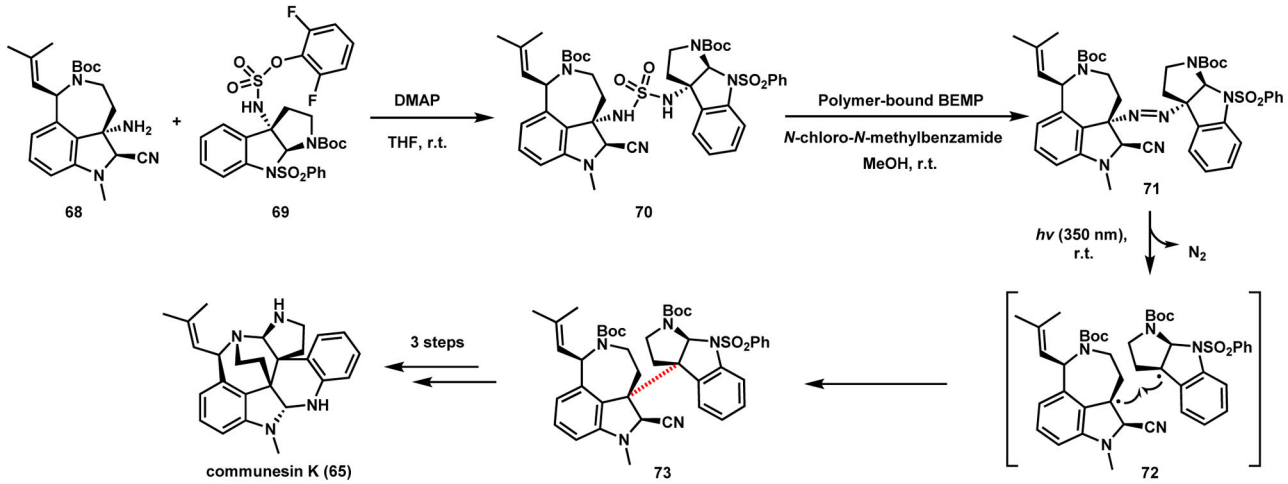

Scheme 16.
Biomimetic Synthesis of Communesin K by Movassaghi

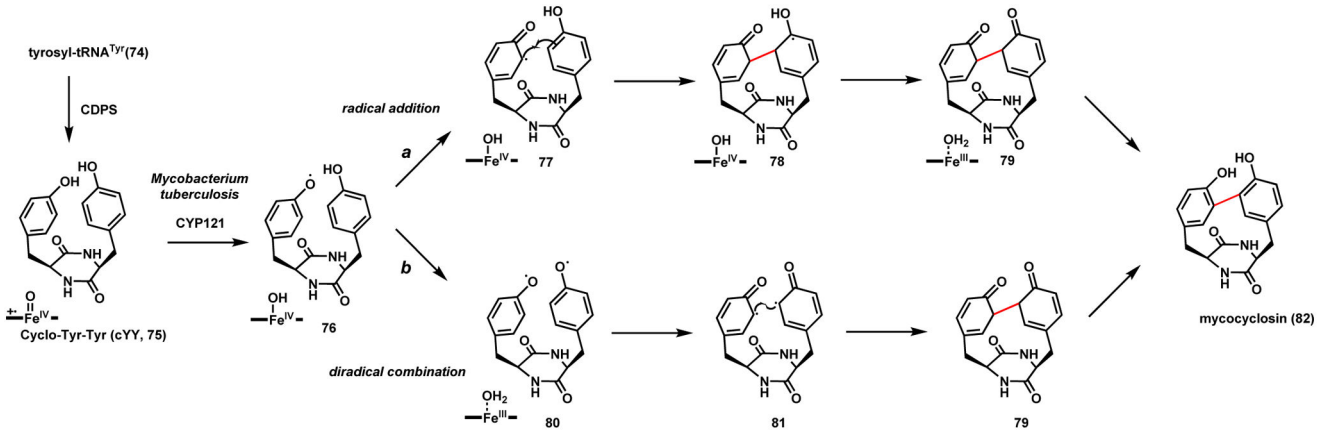

Scheme 17.
Possible Mechanisms of CYP121 catalyzed C-C coupling in Mycocyclosin Pathway

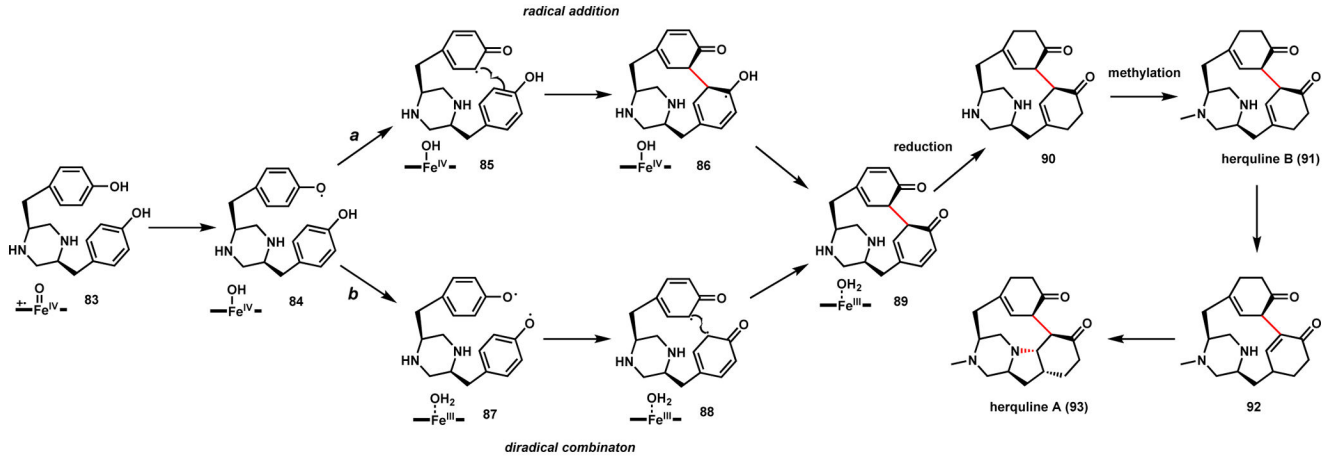

Scheme 18.
Possible Mechanisms of P450-catalyzed C-C Coupling in Herquline Pathway

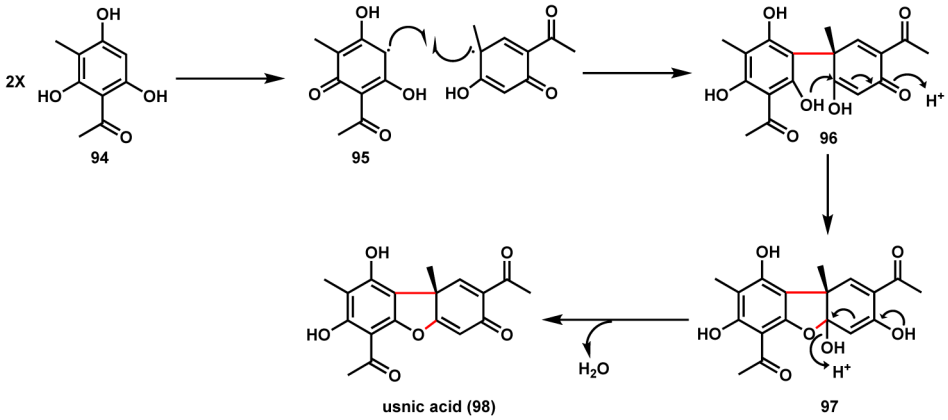

Scheme 19.
Proposed Pathway for C-C Coupling in Usnic Acid

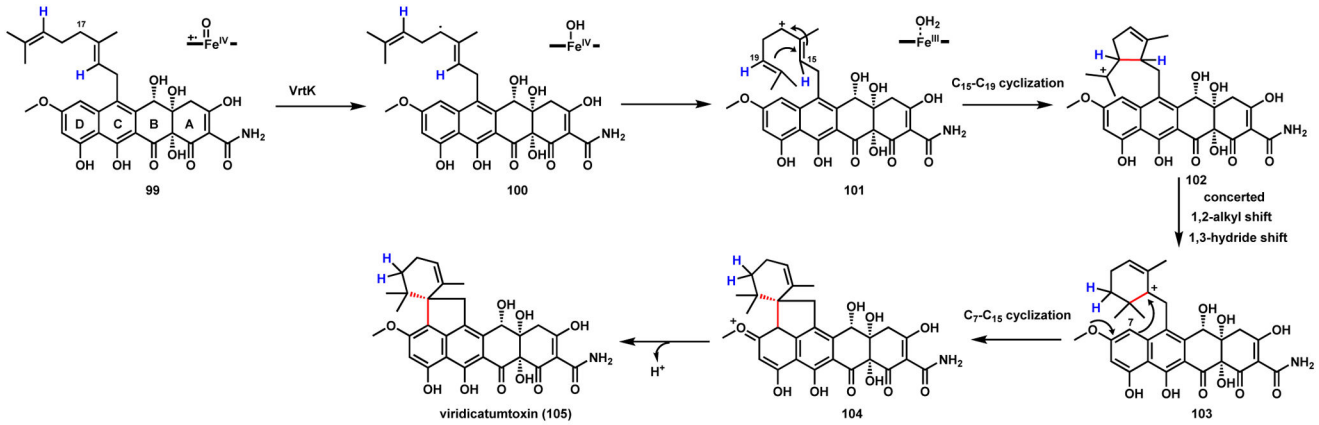

Scheme 20.
Computationally Predicted Oxidative Cyclization Mechanism of VrtK

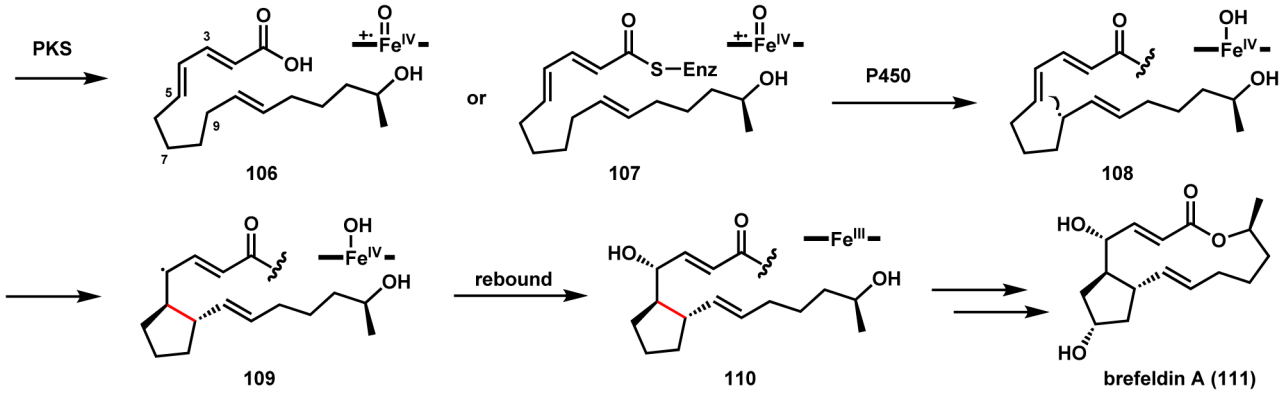

Scheme 21.
Proposed Radical Mediated Cyclization in Brefeldin A Biosynthesis

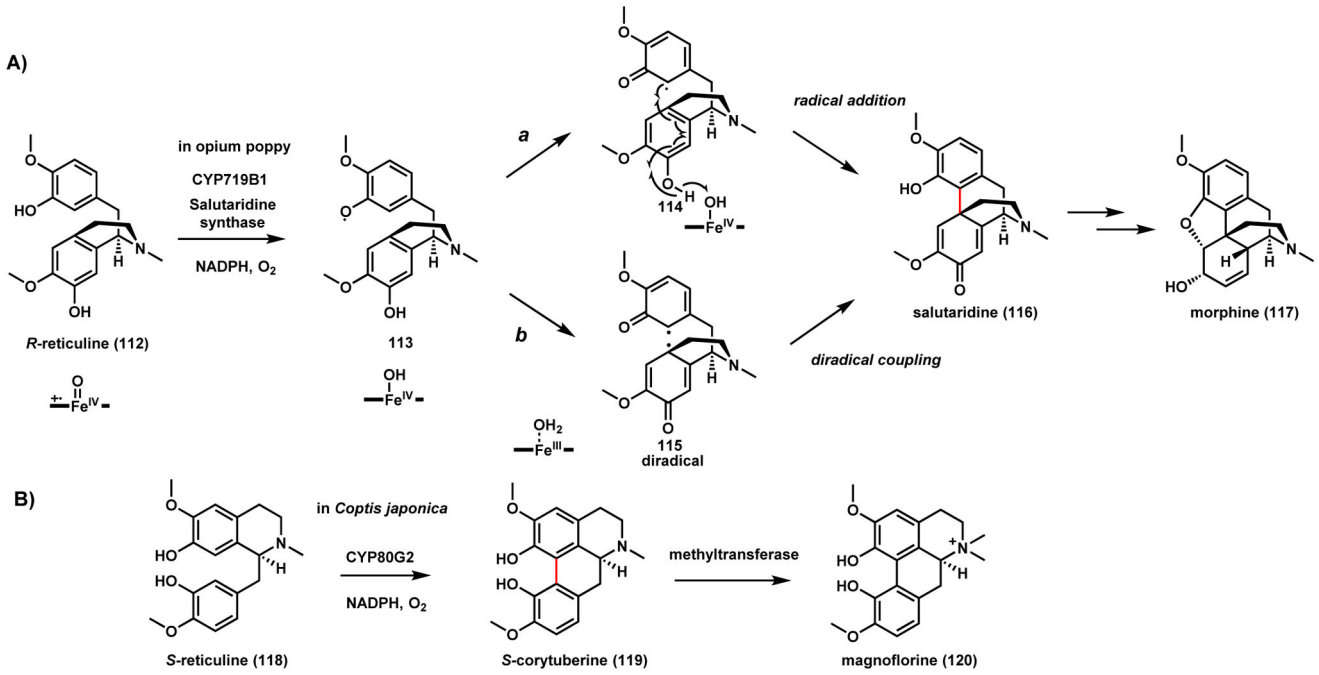

Scheme 22.
P450 Catalyzed C-C Coupling in Salutaridine and Magnoflorine Biosynthesis

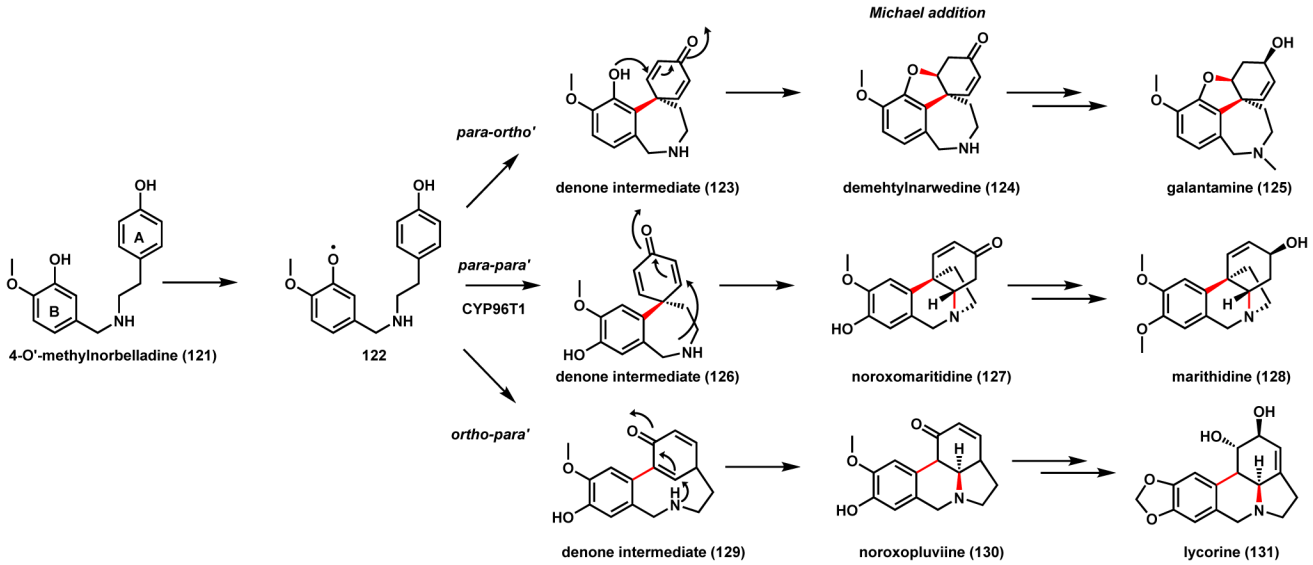

Scheme 23.
P450 Catalyzed Phenol Coupling in Amaryllidaceae Alkaloid Biosynthesis

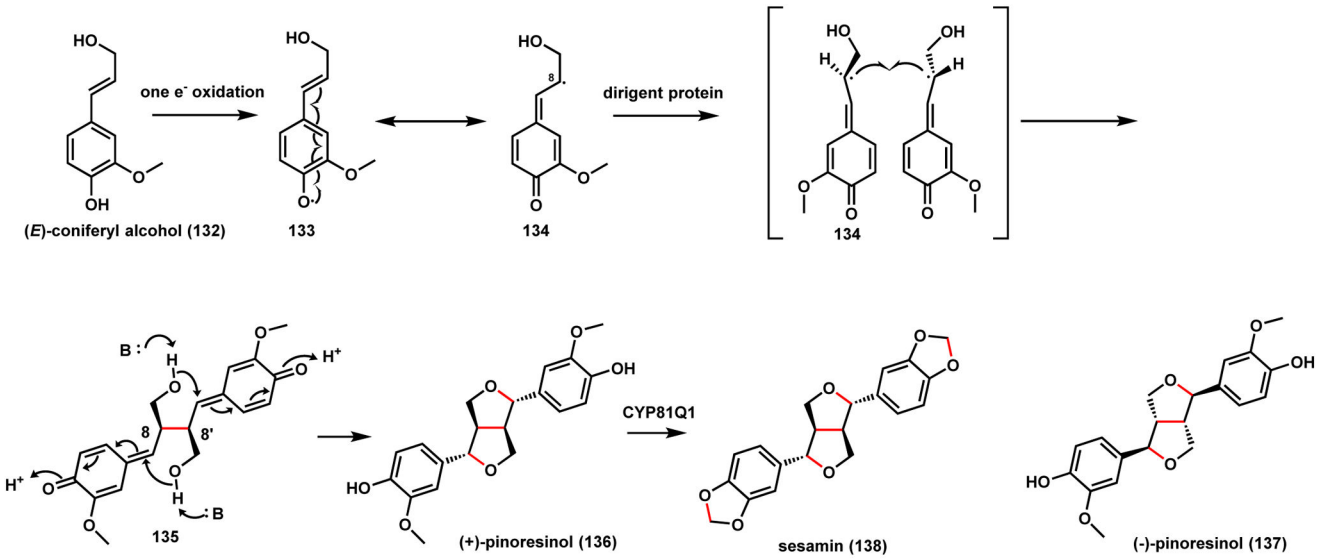

Scheme 24.
Diradical Combination in (+)-Pinoresinol Biosynthesis

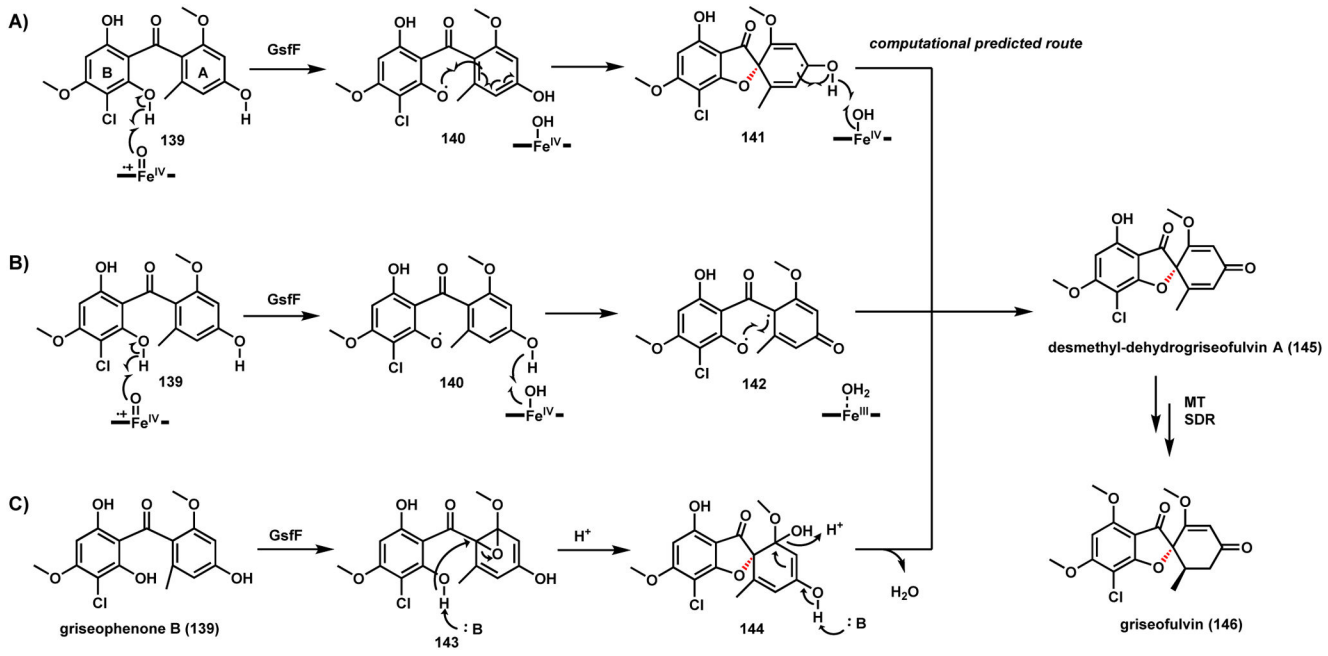

Scheme 25.
Possible Mechanisms of GsfF catalyzed C-O Coupling in Griseofulvin Biosynthesis

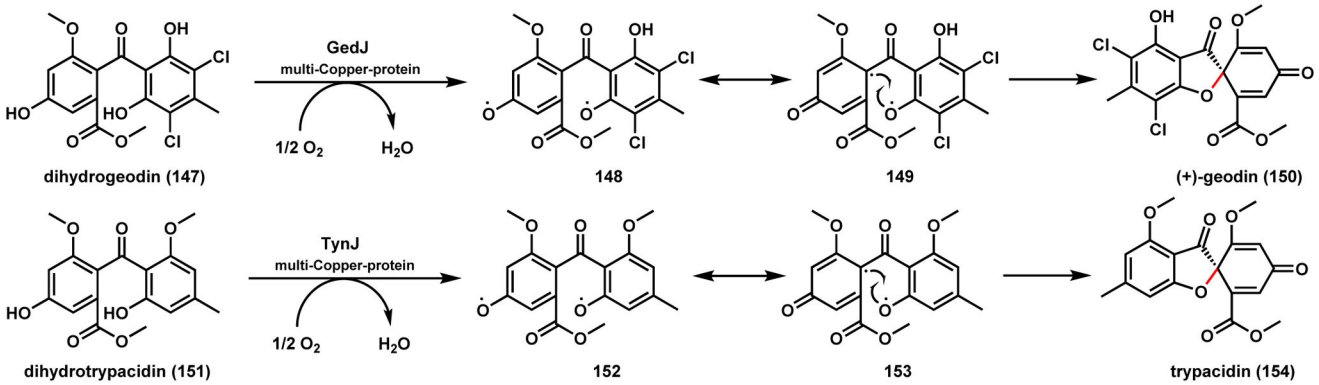

Scheme 26.

Multi-copper Protein Catalyzed C-O Coupling to from Grisan-Containing Compounds

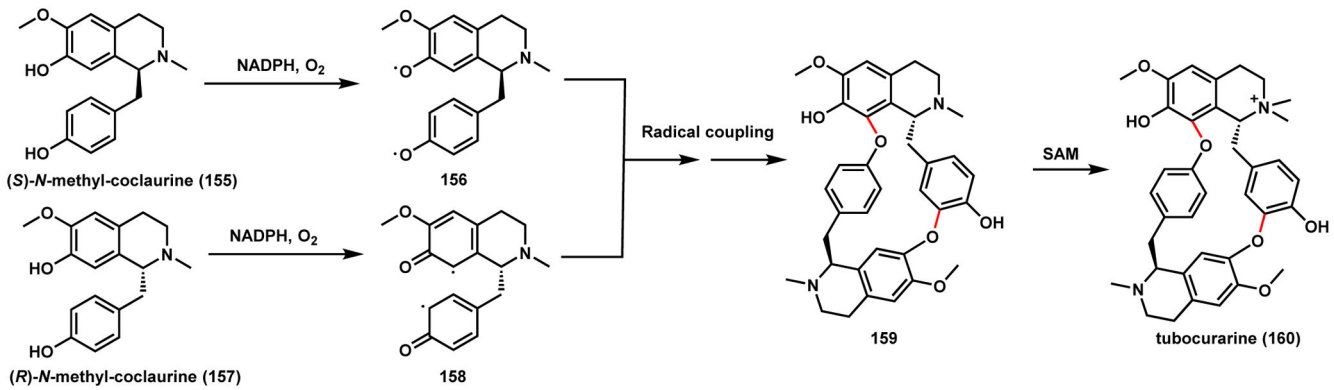

Scheme 27.
Heterodimeric Radical Coupling in Tubocurarine Biosynthesis

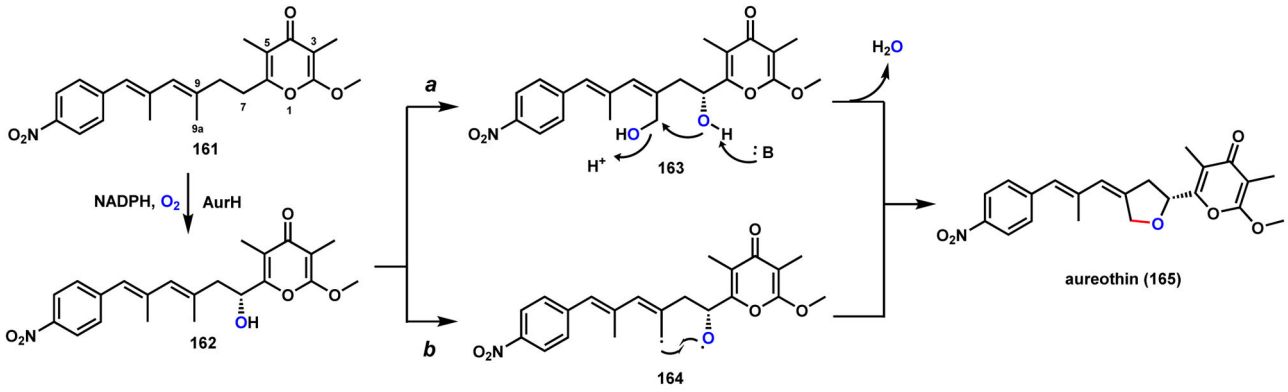

Scheme 28.

Proposed Mechanisms of P450-catalyzed Formation of Tetrahydrofuran in Aureothin

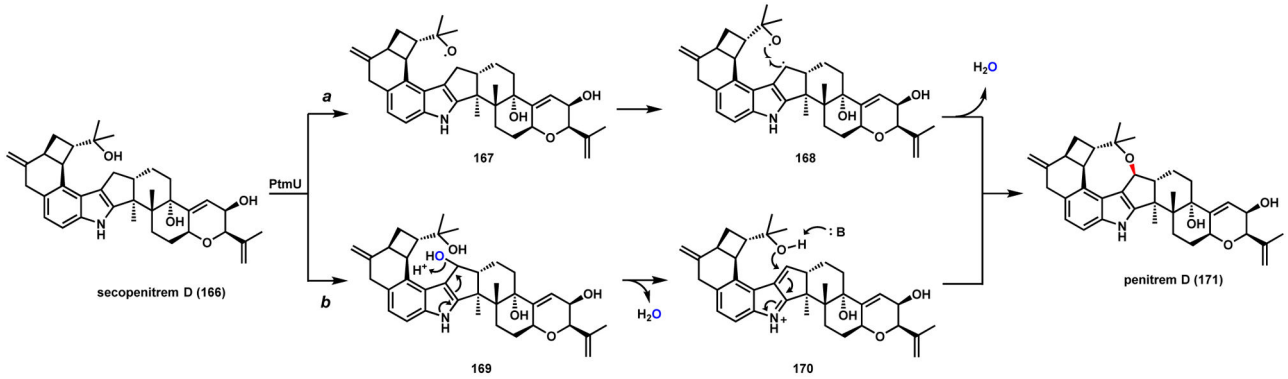

Scheme 29.

Proposed mechanisms of P450 Catalyzed Oxidative Cyclization in Penitrem D Pathway

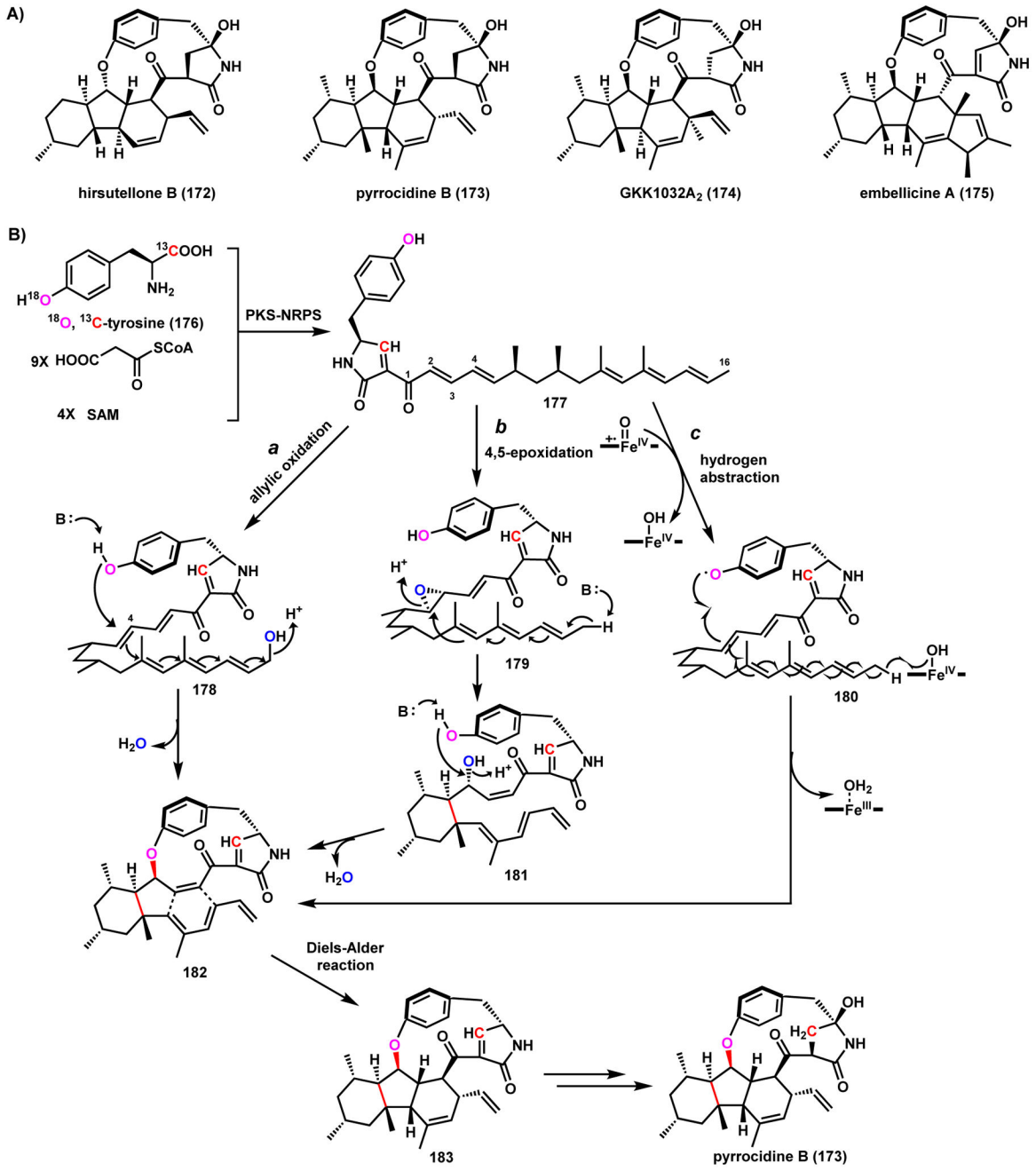

Scheme 30.

Proposed Oxidative Cyclization Mechanisms in Pyrrocidine Biosynthesis

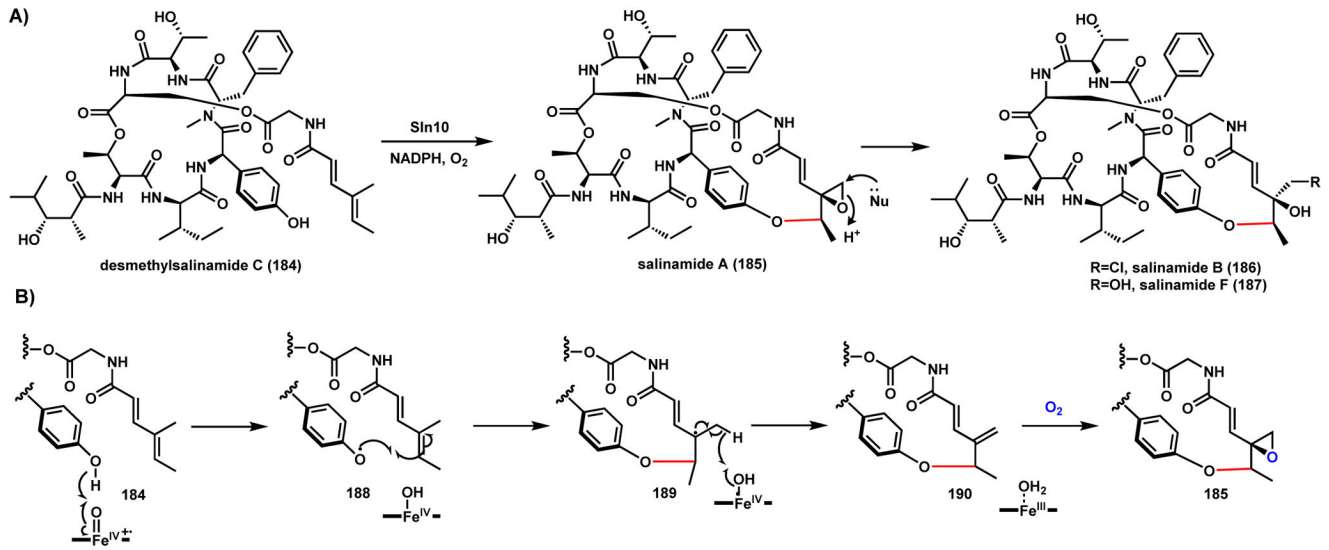

Scheme 31.
Proposed Mechanism of P450 Catalyzed Phenoxy Radical Addition in Salinamide Pathway

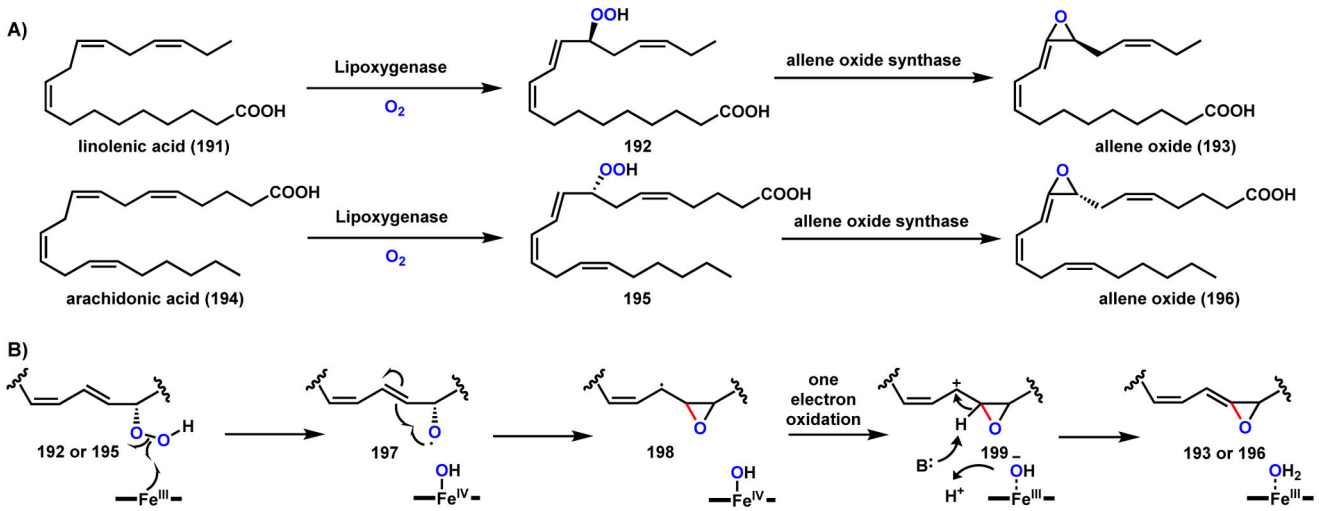

Scheme 32.

Mechanism of Reactions Catalyzed by Allene Oxide Synthase (CYP74A)

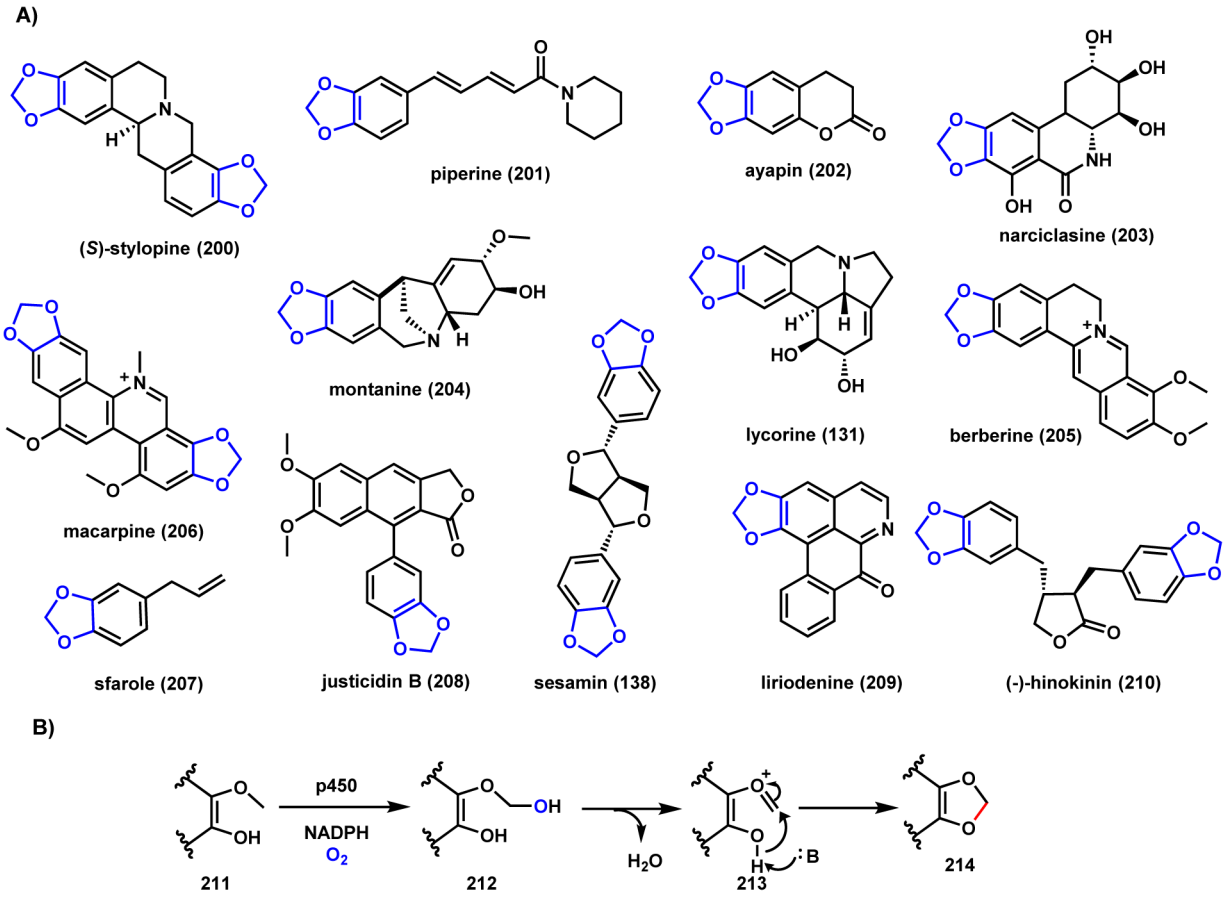

Scheme 33.
P450 Catalyzed Formation of Methylenedioxy Bridge in Natural Products

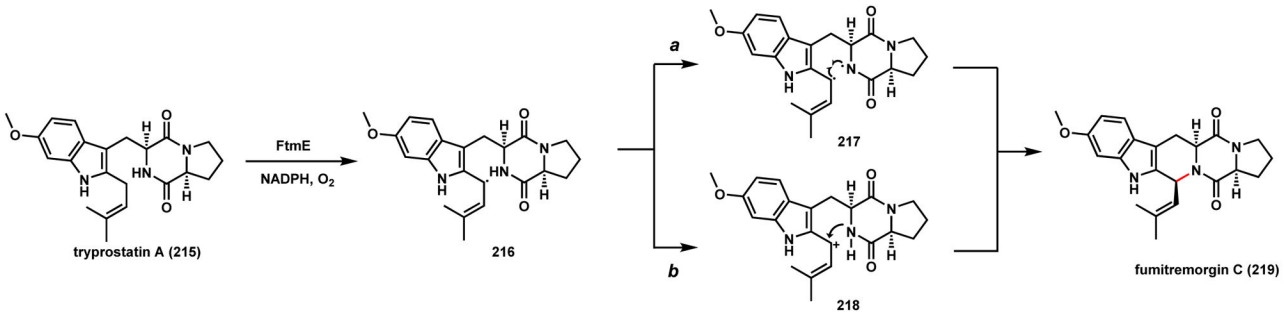

Scheme 34.
Possible Mechanisms of P450 Catalyzed C-N Coupling in Fumitremorgin C Pathway

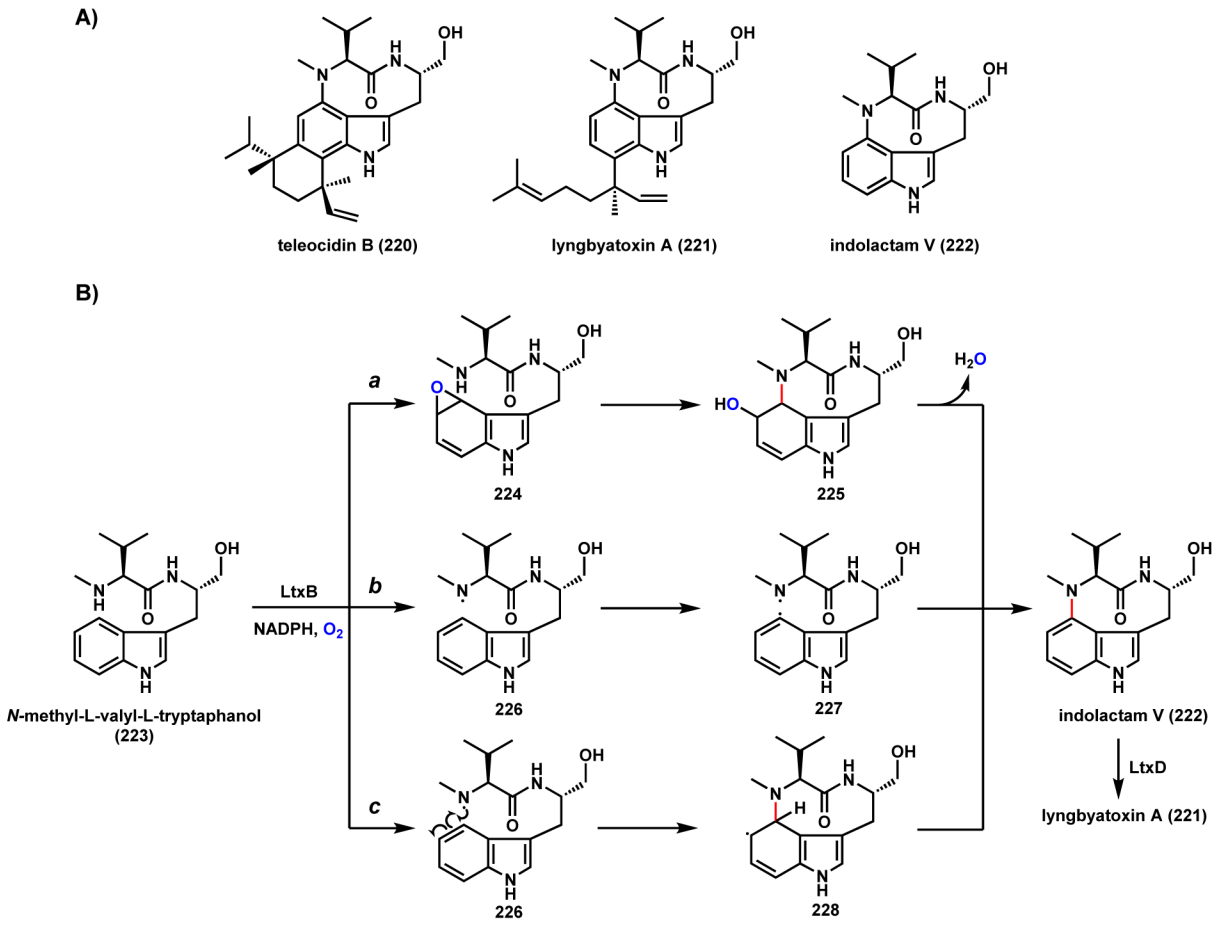

Scheme 35.
Possible Mechanisms of P450-Catalyzed C-N Coupling in Indolactam Pathway

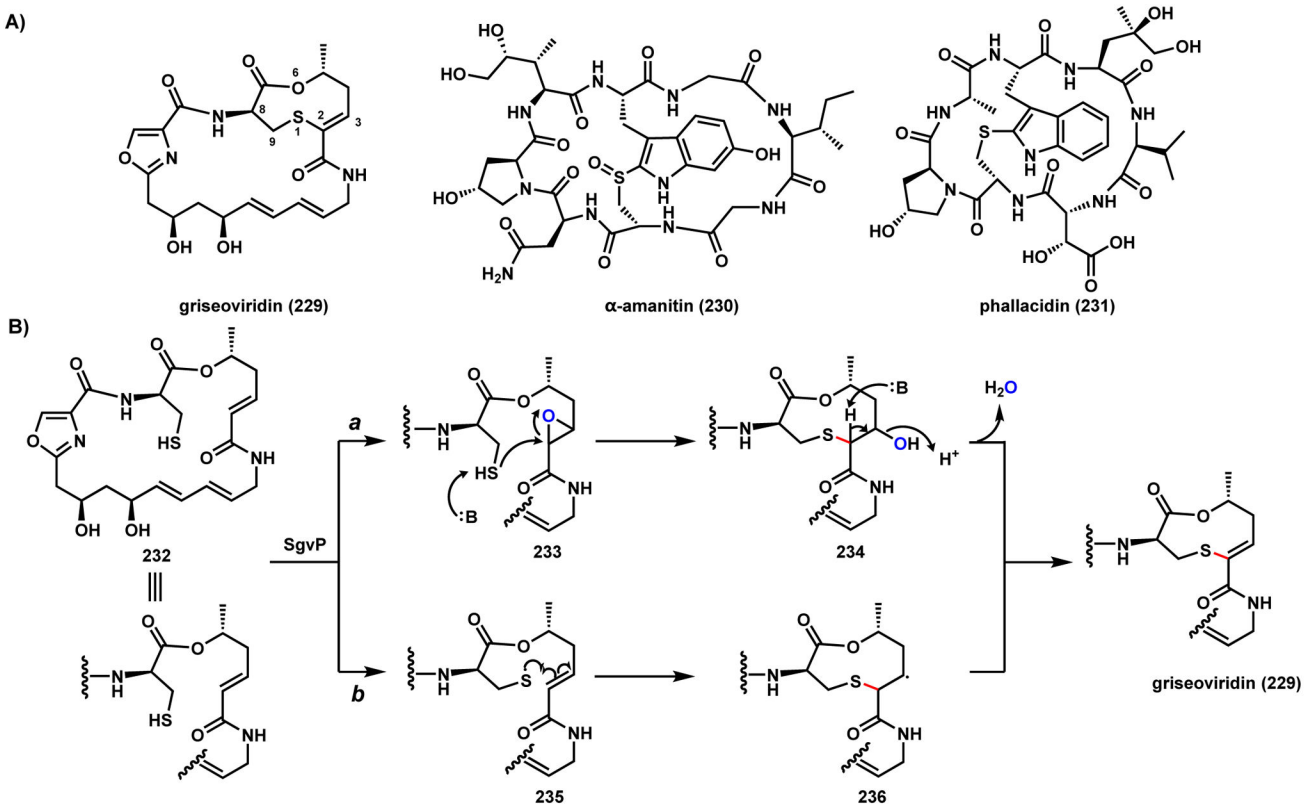

Scheme 36.
Possible Mechanisms of P450 Catalyzed C-S Coupling in Griseoviridin Pathway

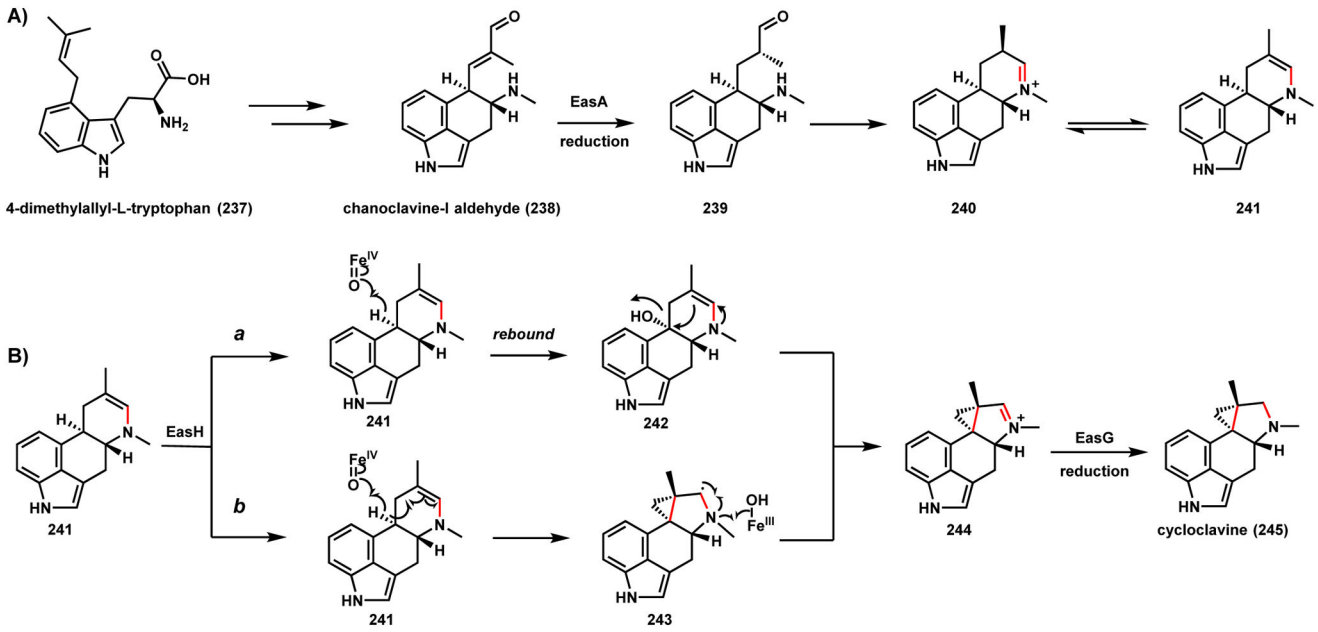

Scheme 37.
Possible Mechansims of the EasH Catalyzed Cyclopropane Formation in Cycloclavine

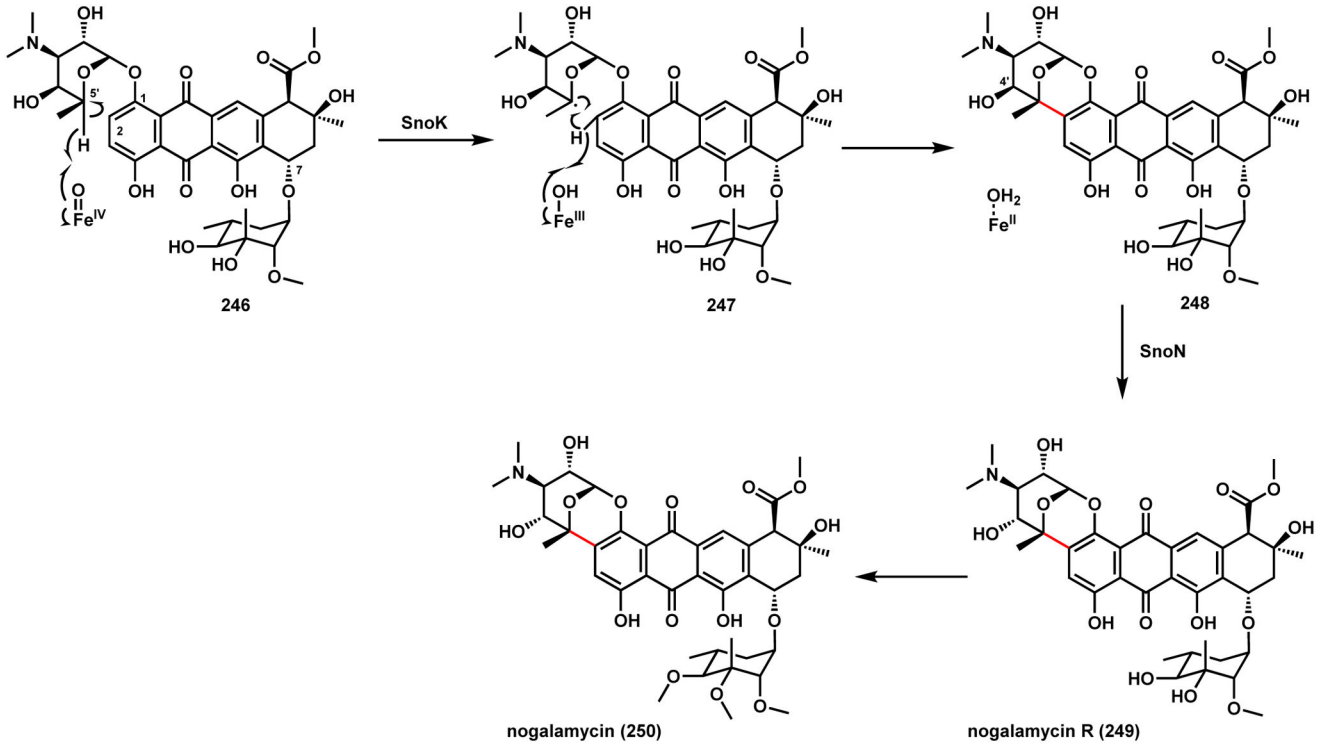

Scheme 38.
Mechanism of SnoK Catalyzed C-C Coupling in Nogalamycin Biosynthesis

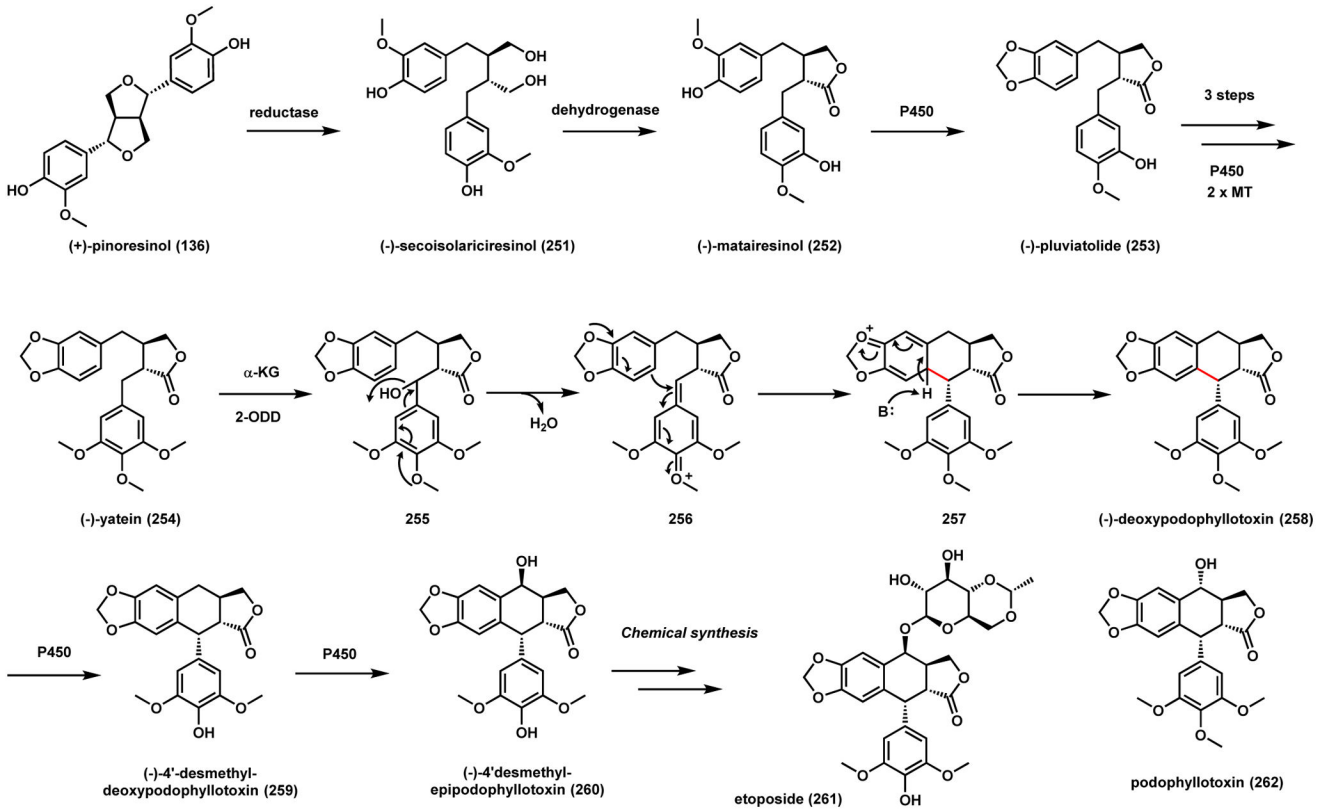

Scheme 39.

Biosynthetic Pathway of (−)-4-Desmethylepipodophyllotoxin in Mayapple

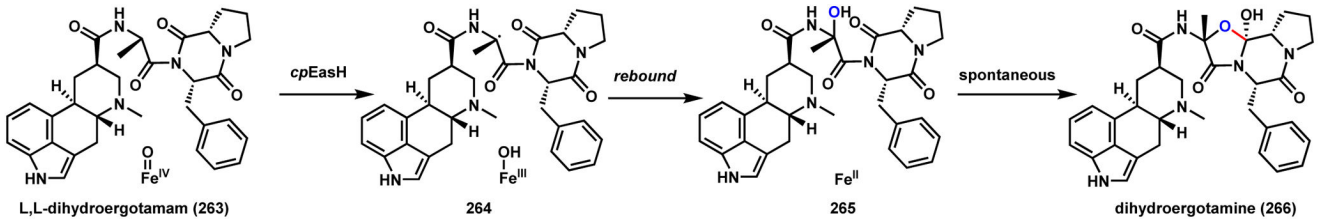

Scheme 40.

*cp*EasH Catalyzed C-O coupling in Dihydroergotamine Biosynthesis

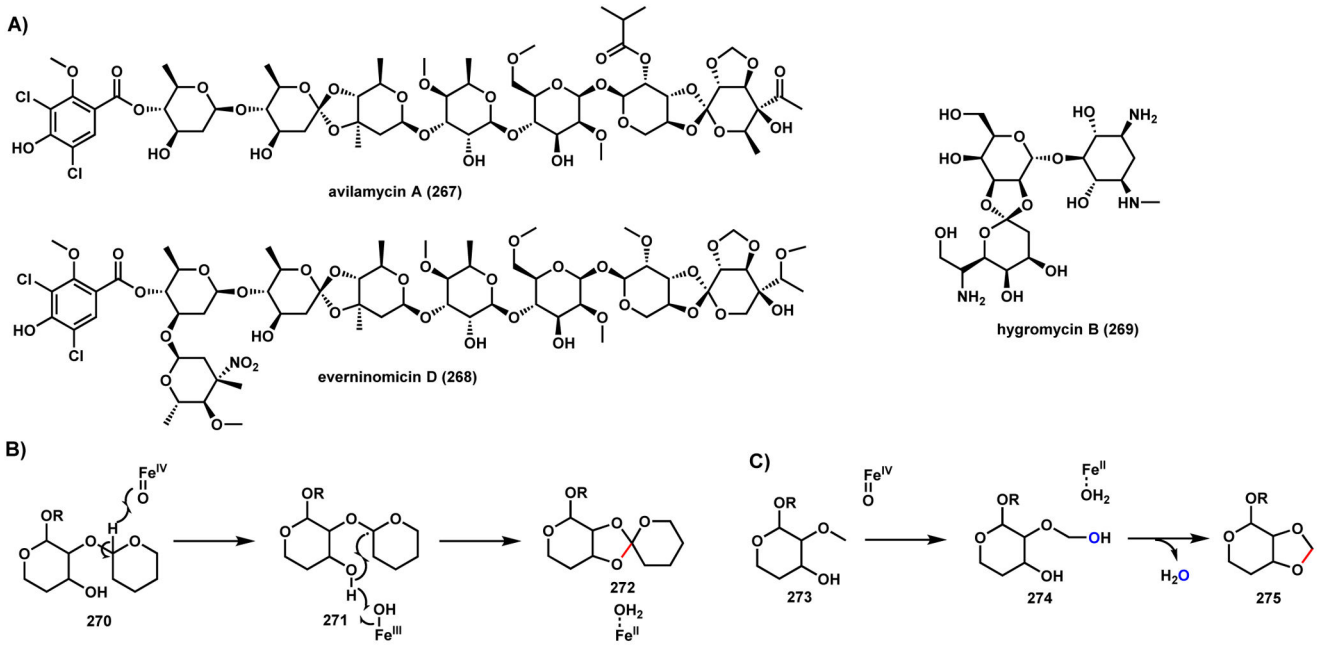

Scheme 41.
Oxidative Cyclization in Orthosomycin Biosynthesis

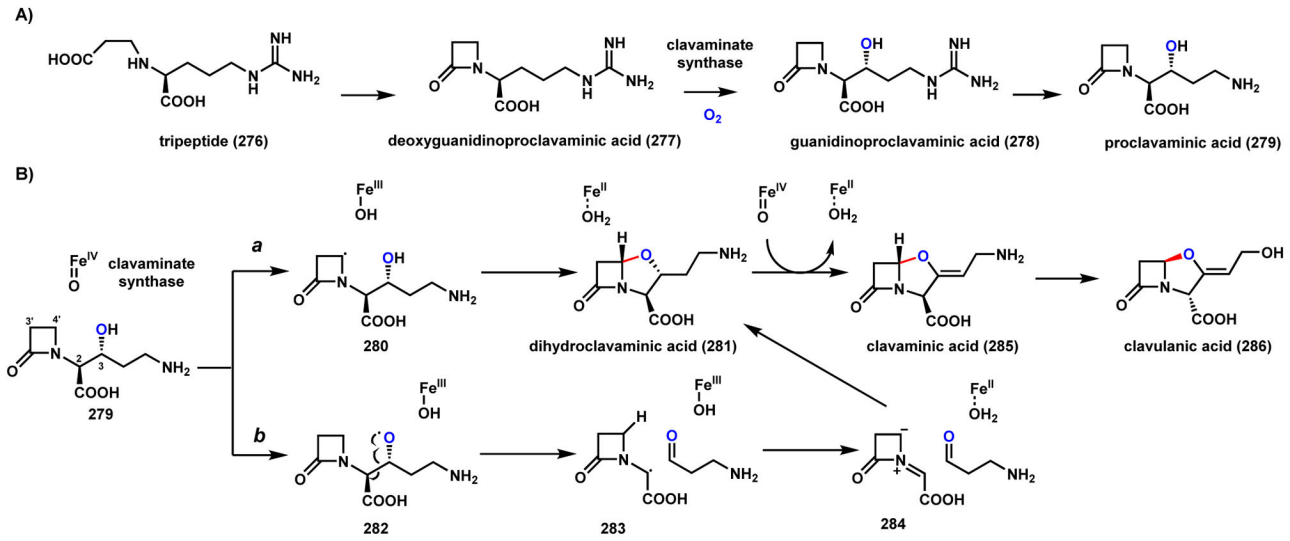

Scheme 42.
Mechanism of Oxidative Cyclization During Clavaminic Acid Formation

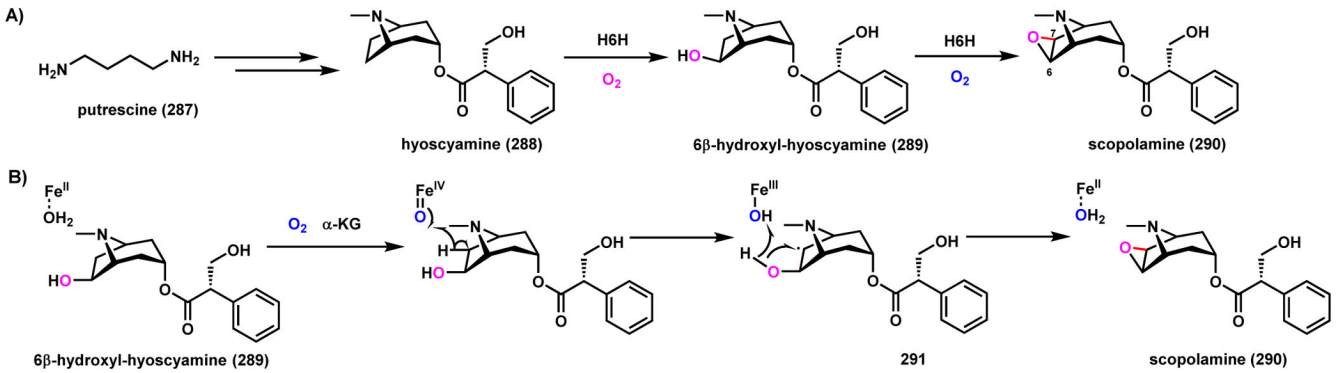

Scheme 43.

Proposed Mechanism of Epoxide Formation in Scopolamine by Hyoscyamine 6β-Hydroxylase

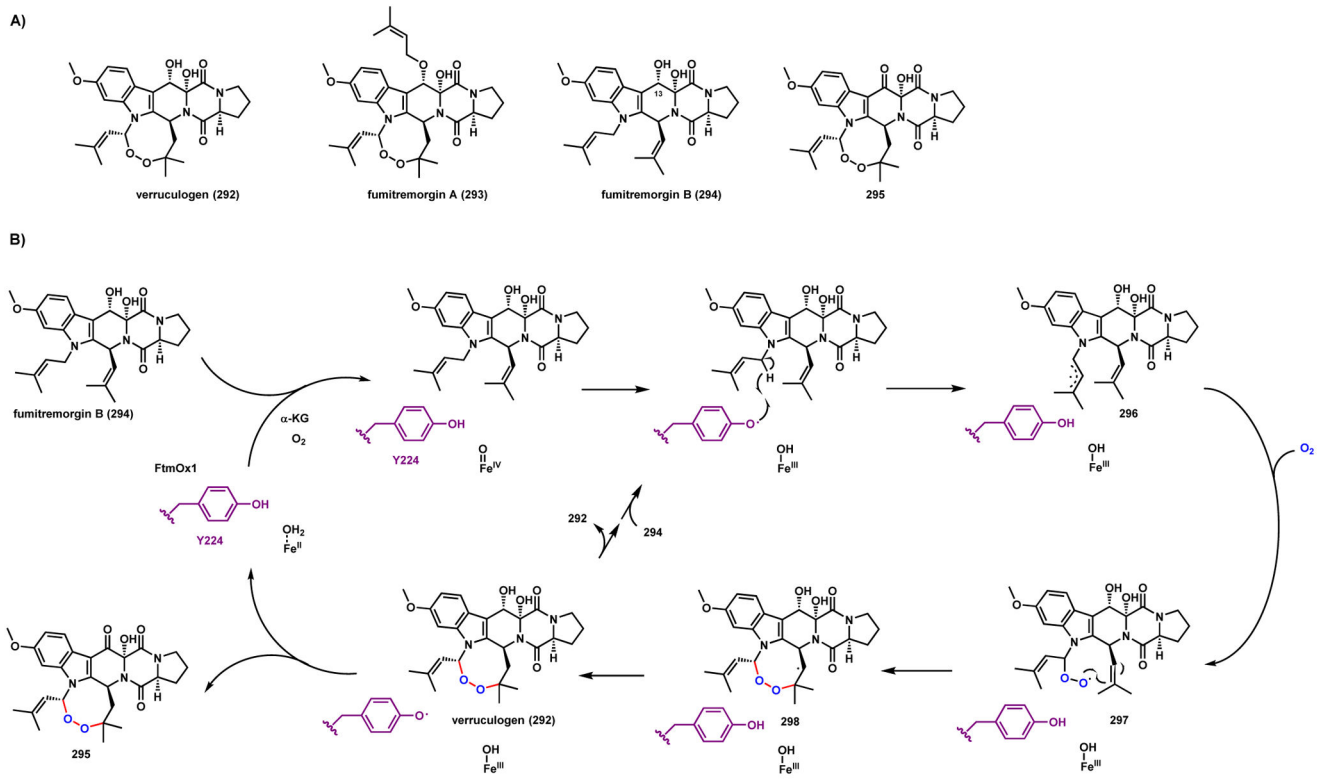

Scheme 44.
Proposed Mechanism of FtmOx1 Catalyzed Endoperoxide Formation

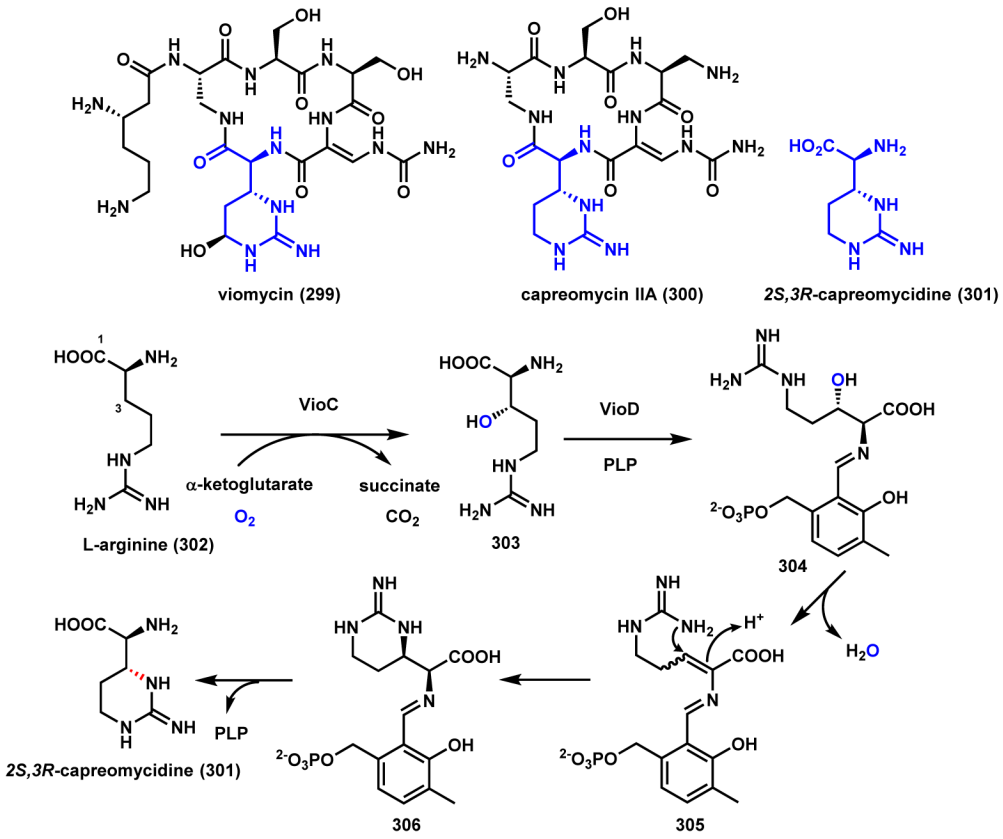

Scheme 45.
Mechanism of C-N Coupling in Capreomycidine Formation

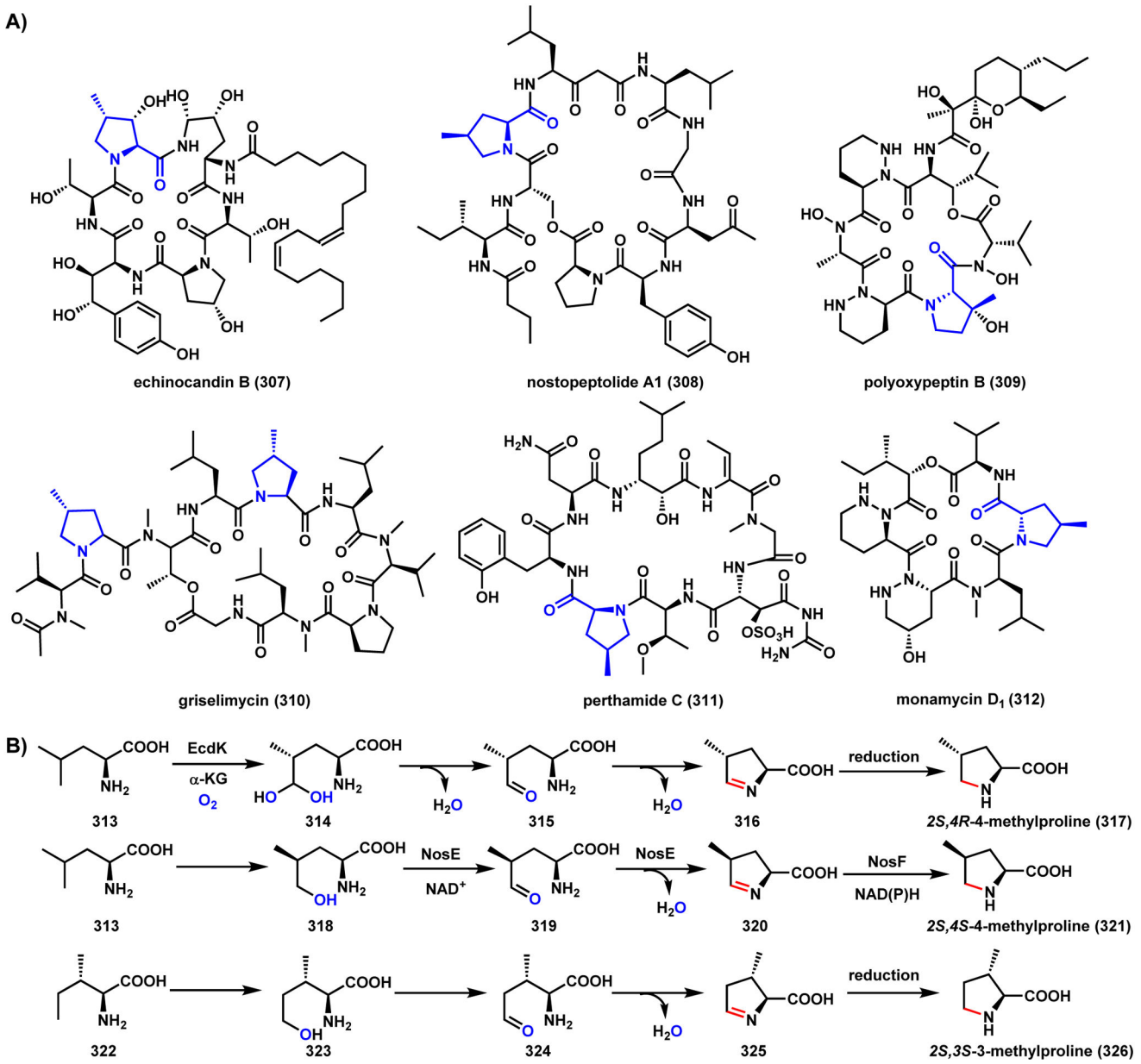

Scheme 46.
Mechanisms of Methylproline Formation in NRP Natural Products

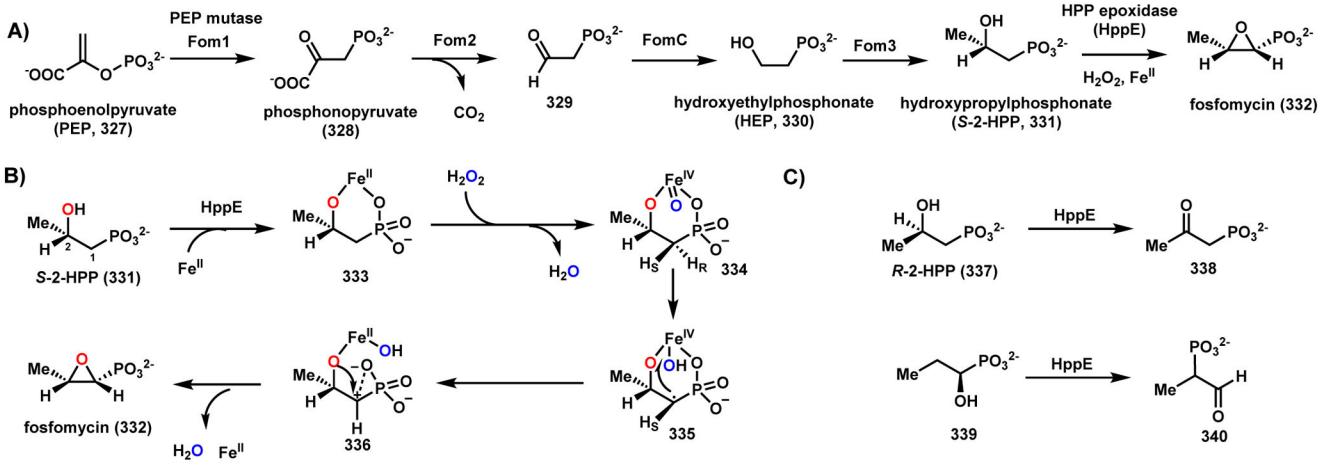

Scheme 47.

Biosynthesis of Fosfomycin and Proposed Mechanism of HppE

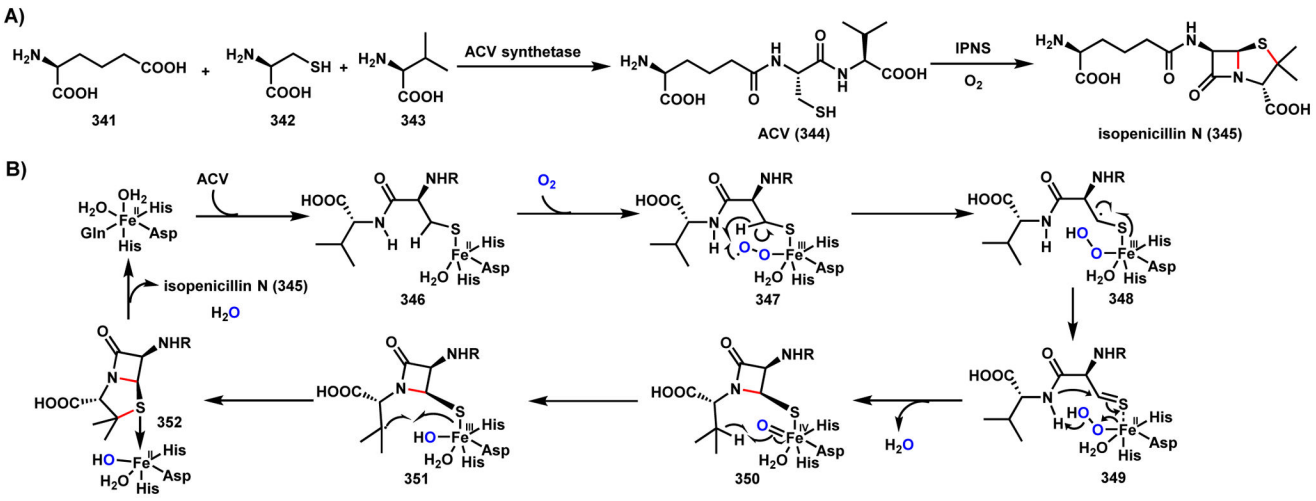

Scheme 48.
Mechanism of Isopenicillin N Synthase

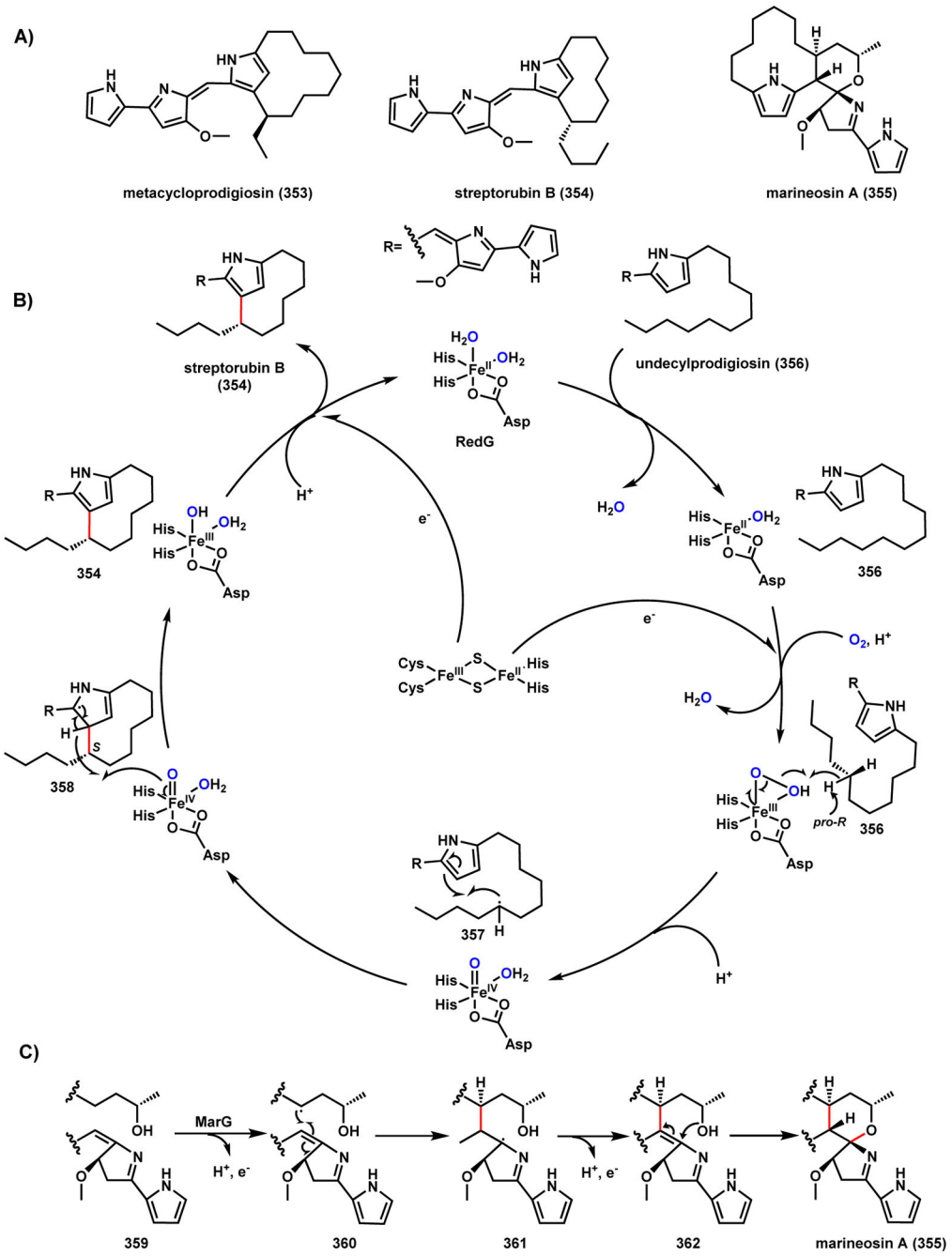

Scheme 49.
Proposed Catalytic Cycle of Rieske Oxygenases in Prodiginine Biosynthesis

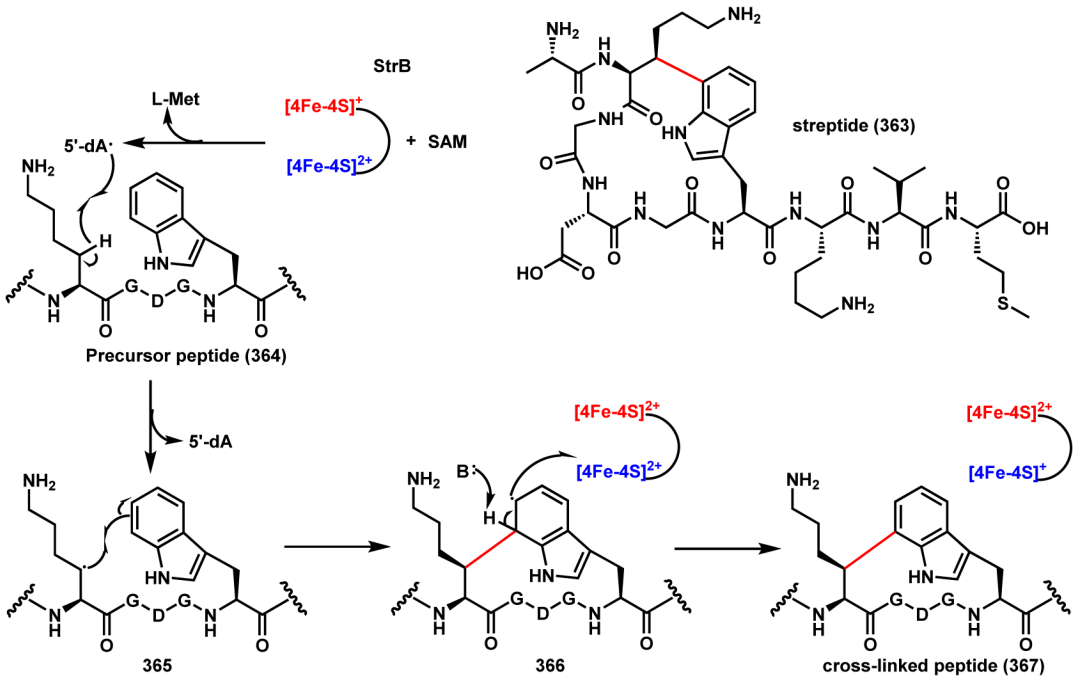

Scheme 50.

Proposed Mechanism of C-C coupling in Streptide Biosynthesis

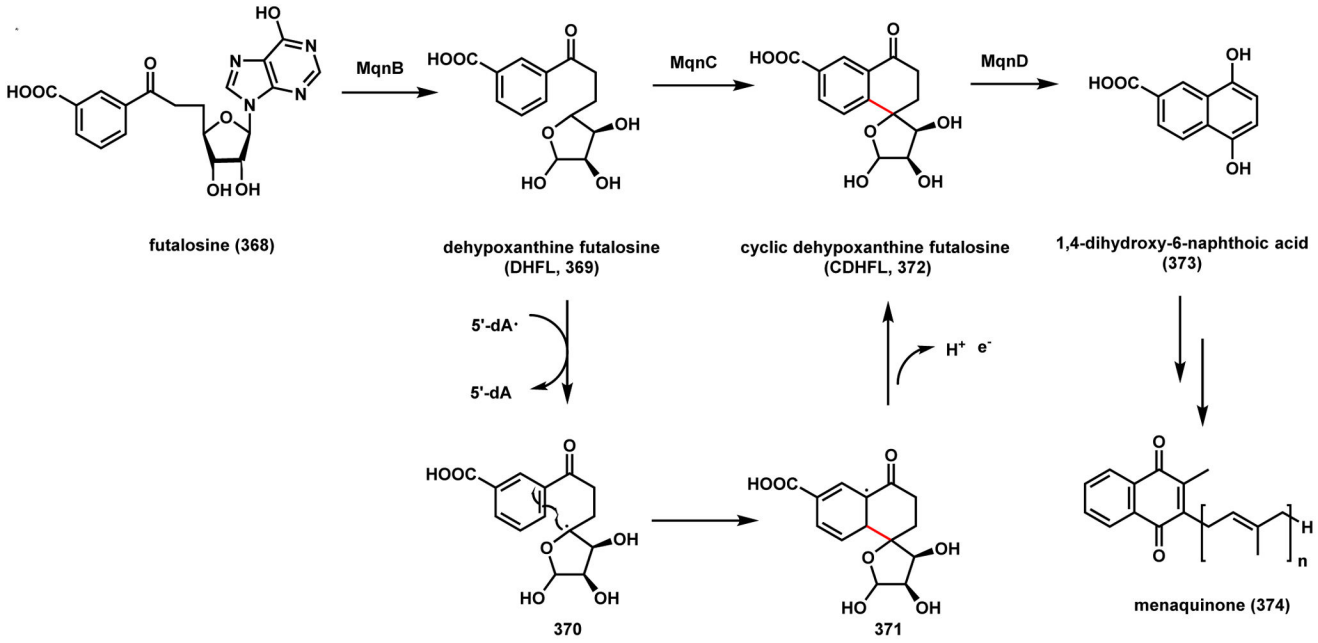

Scheme 51.
Proposed mechanism of C-C Coupling in Menaquinone Biosynthesis

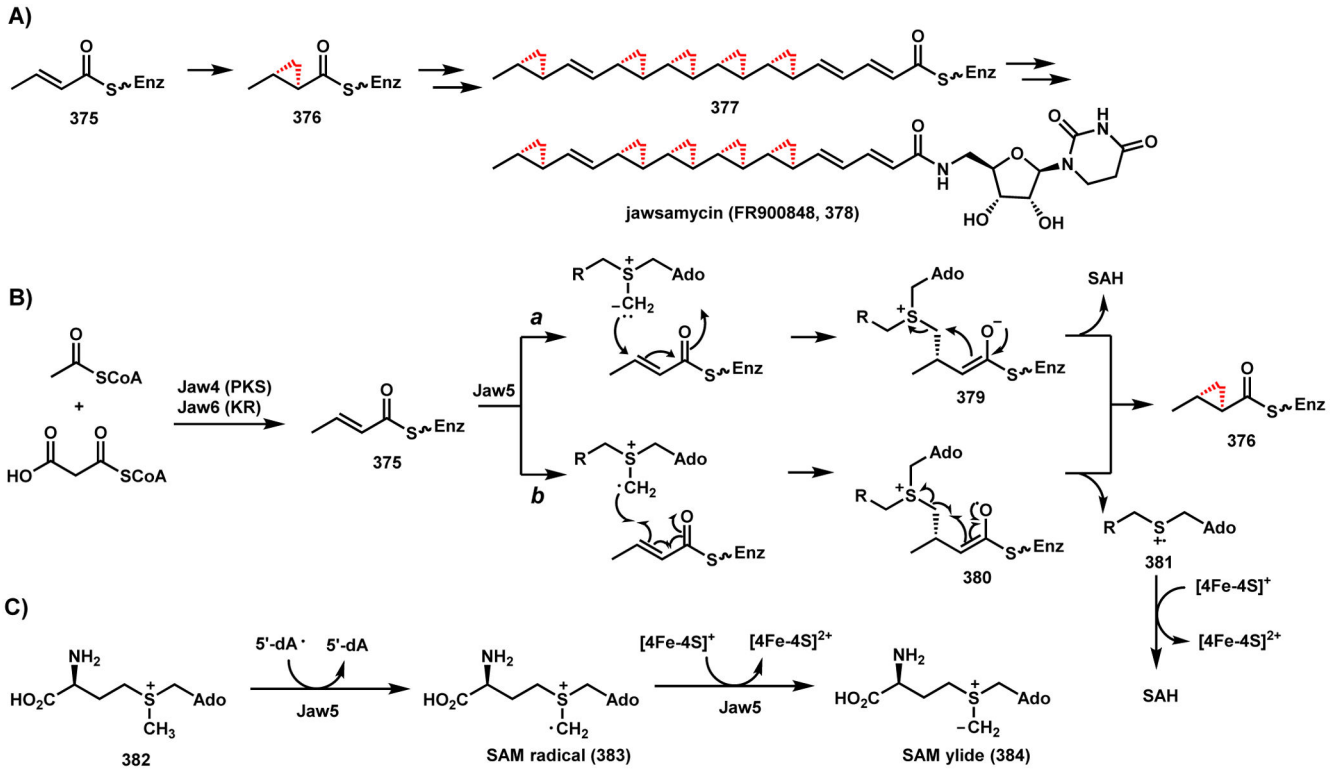

Scheme 52.

Proposed Mechanism of Radical-SAM Enzyme Catalyzed Cyclopropanation in Jawsamycin

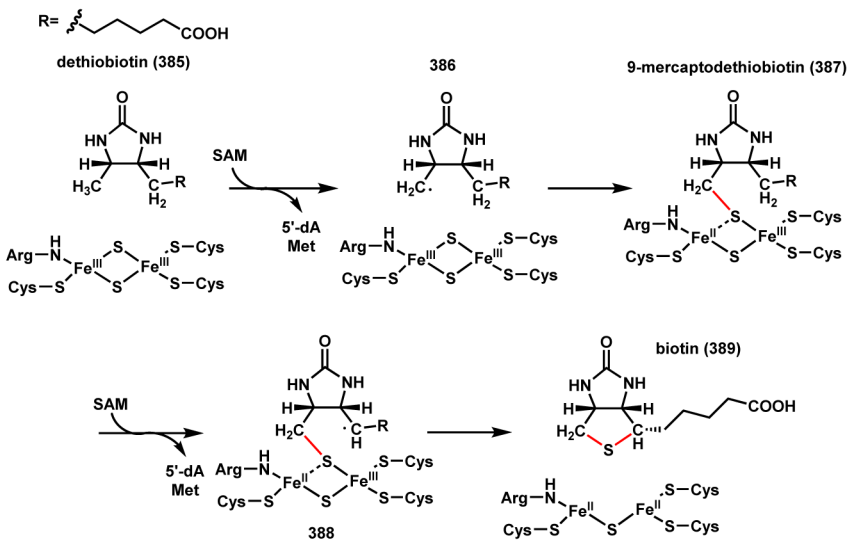

Scheme 53.
Mechanism of C-S Coupling Steps in Biotin Biosynthesis

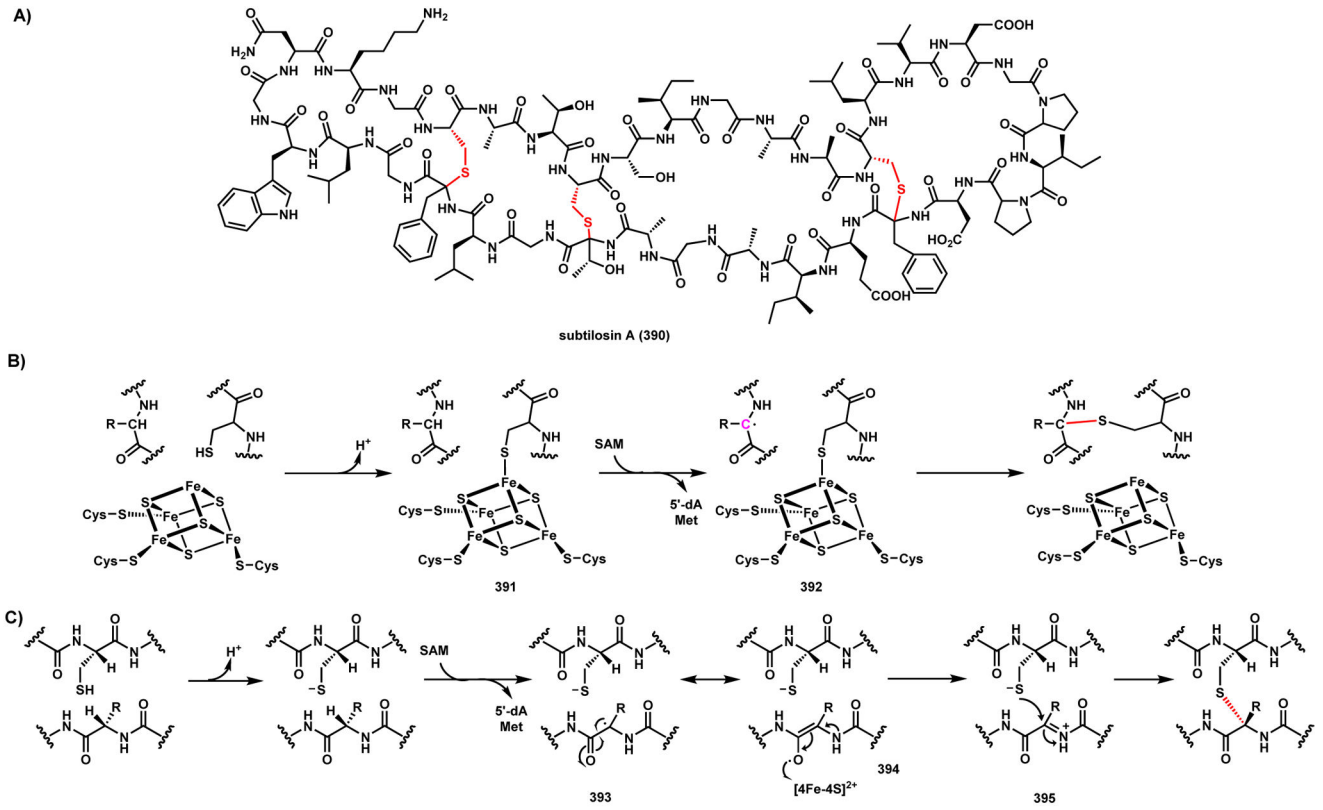

Scheme 54.
Proposed Mechanisms of C-S Coupling Steps in Subtilosin Biosynthesis

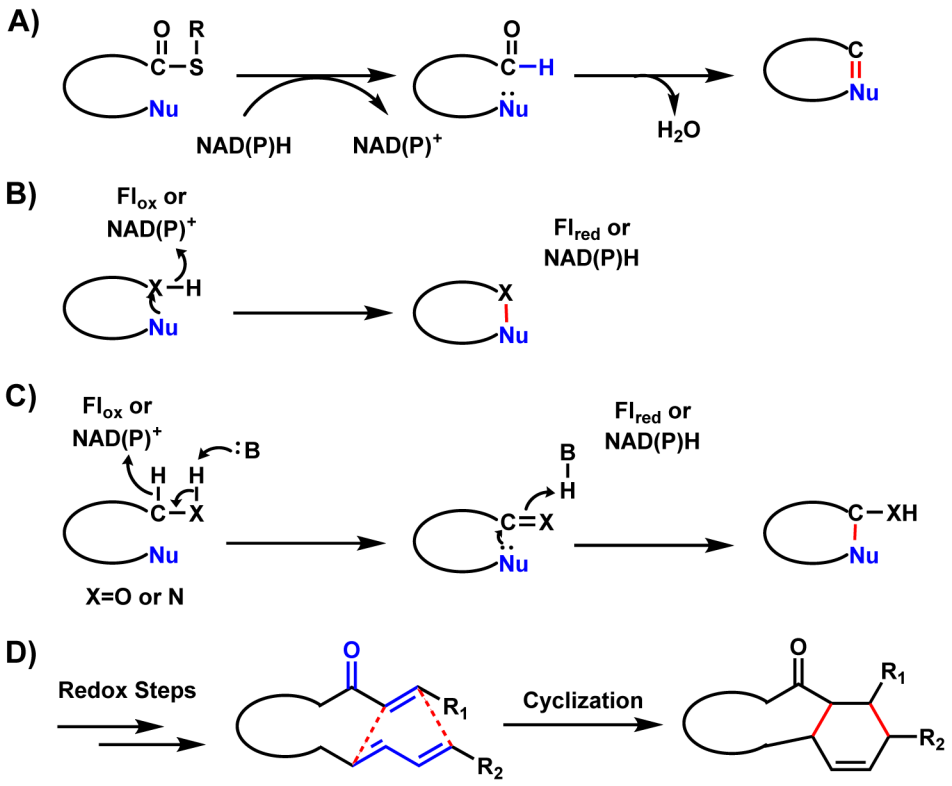

Scheme 55.
Models of Nonradical Cyclization in Natural Product Biosynthesis

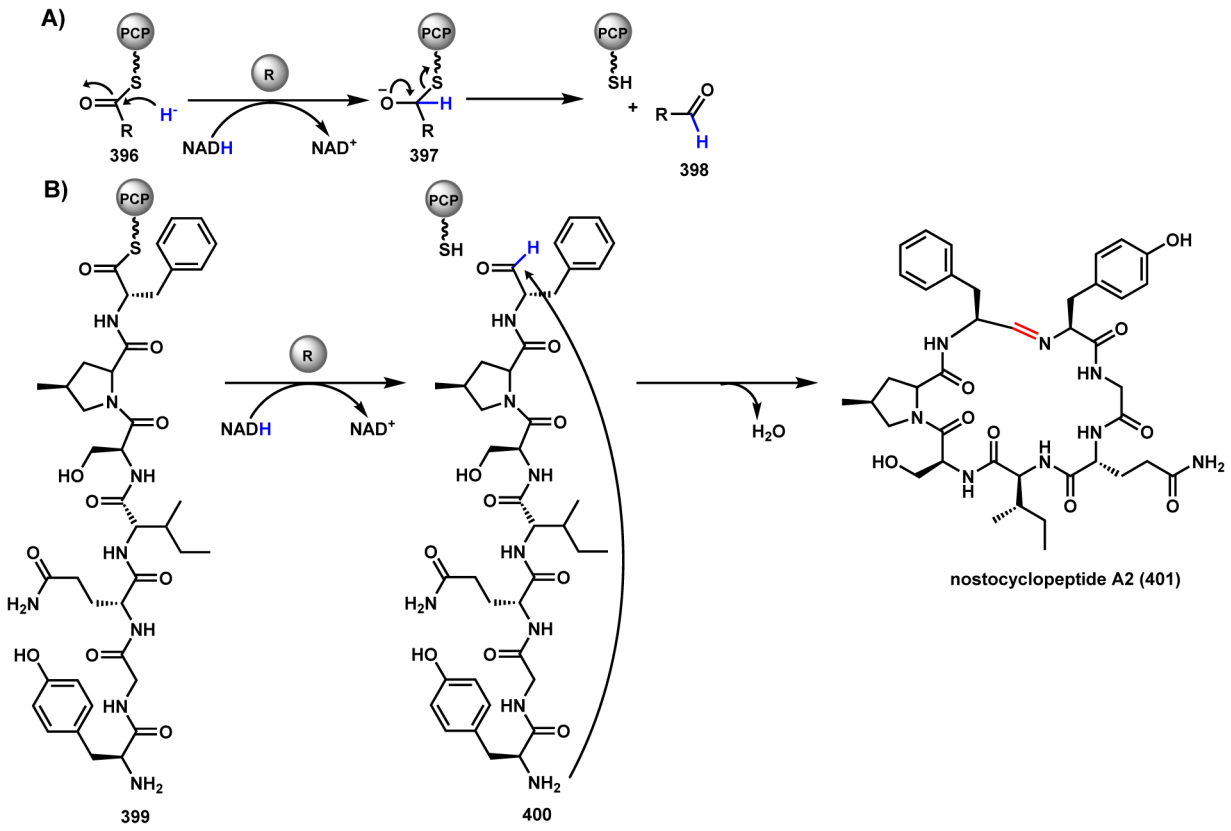

Scheme 56.
Reduction-Enabled Cyclization in Nostocyclopeptide A2 Biosynthesis

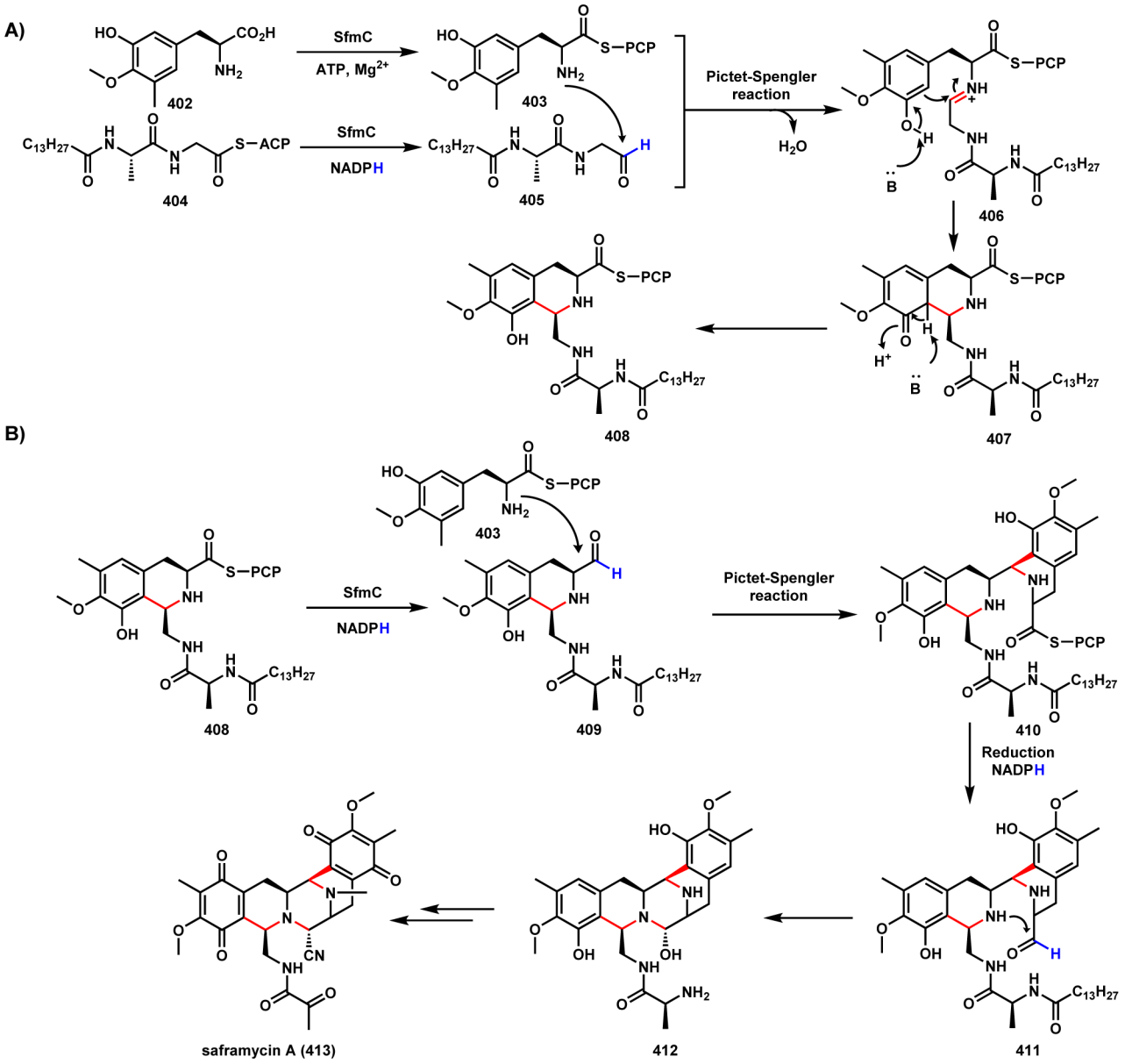

Scheme 57.
Pictet-Spengler Reactions in Saframycin A Biosynthesis

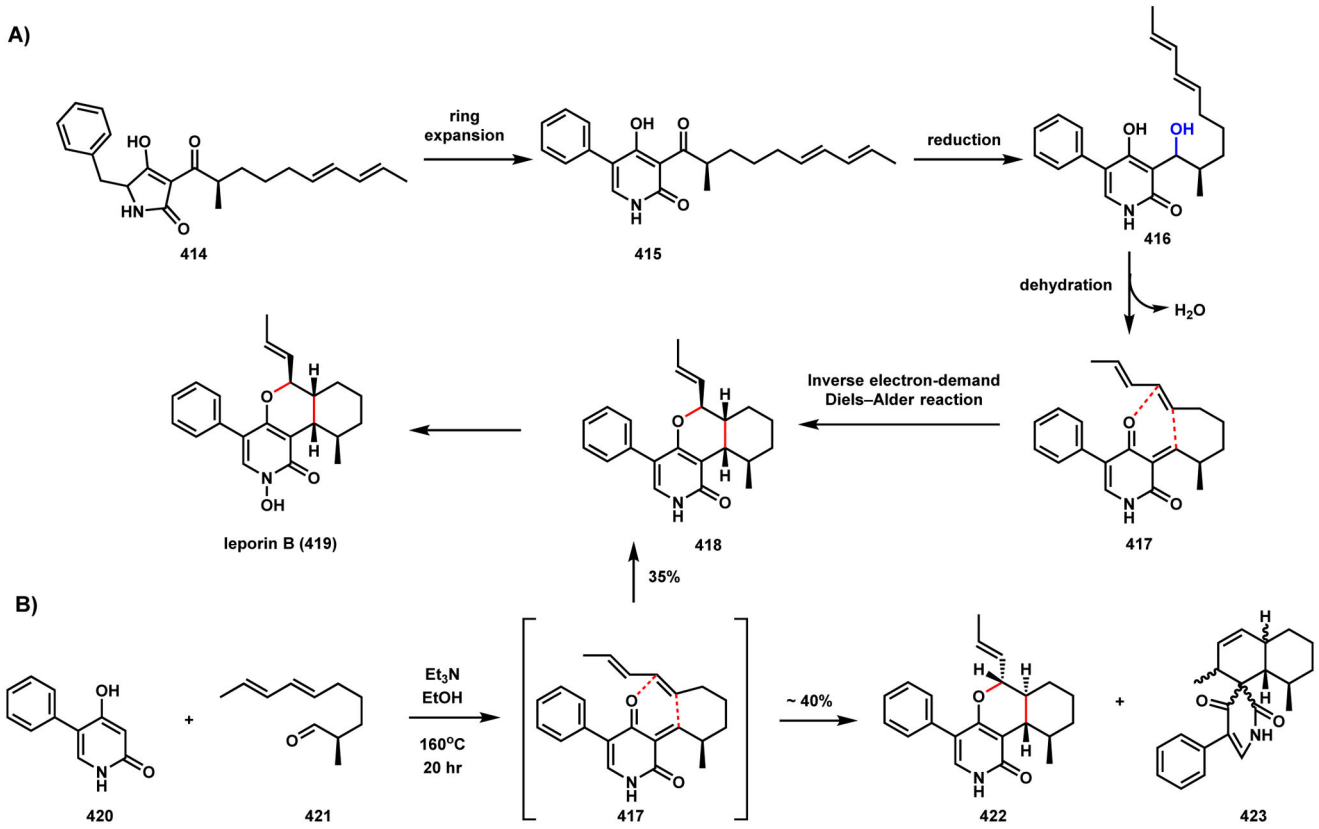

Scheme 58.
Reduction-Enabled Hetero Diel-Alder Cyclization in Leporin Biosynthesis

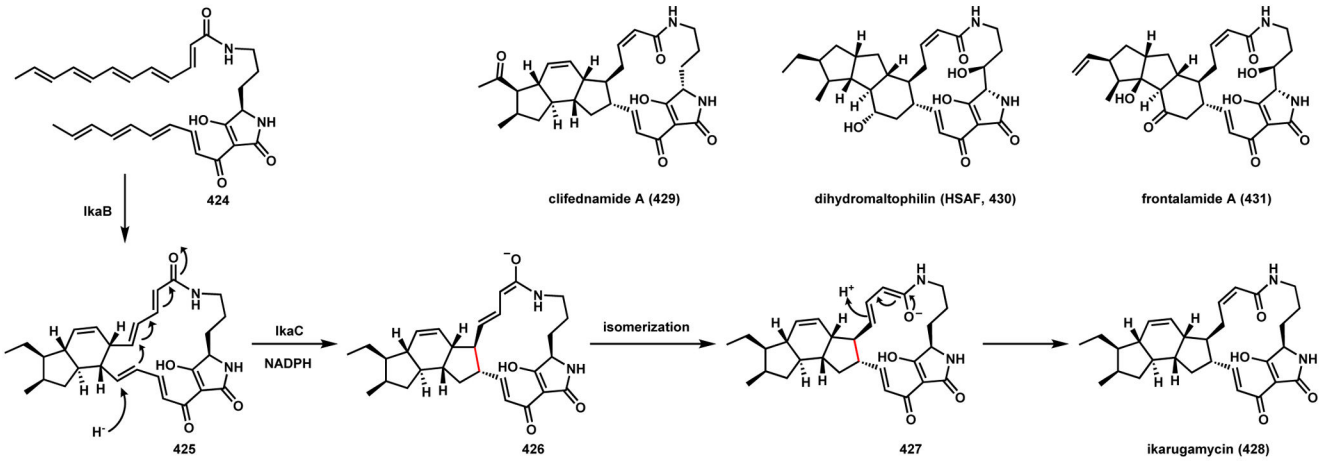

Scheme 59.
Hydride-Mediated Cyclization in Ikarugamycin Biosynthesis

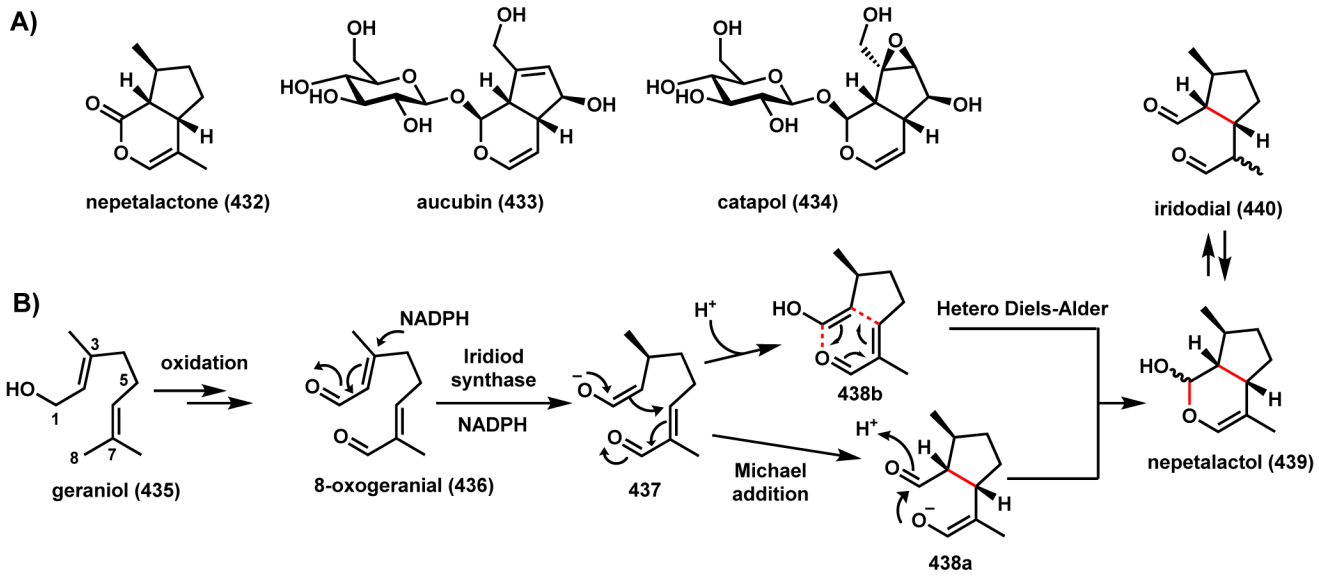

Scheme 60.
Reductive Cyclization of Iridoid by Iridoid Synthase in Plants

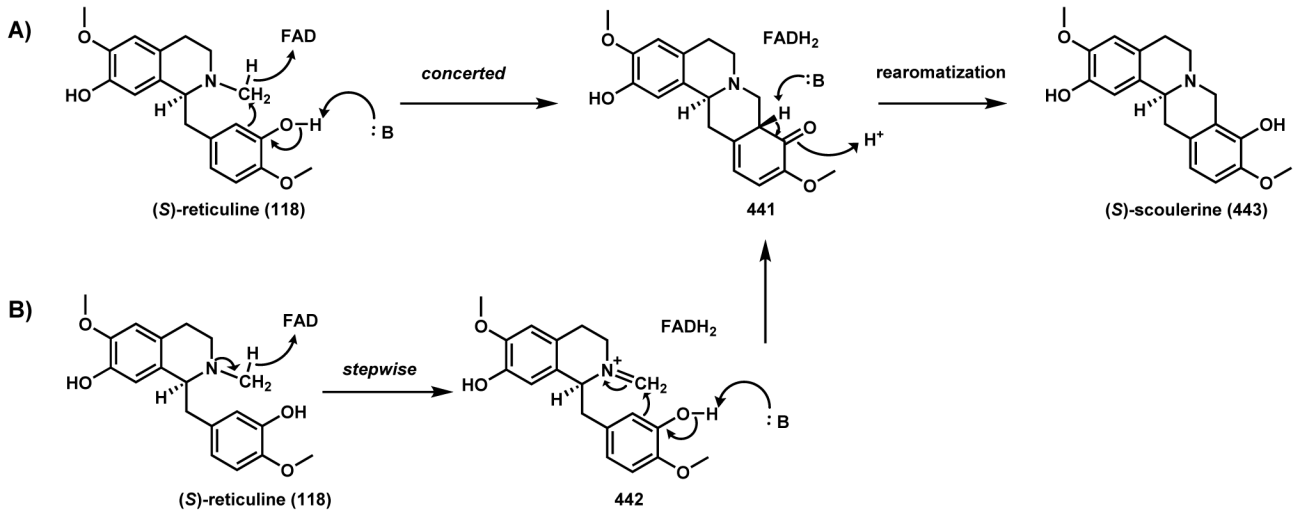

Scheme 61.

The Reaction Catalyzed by Berberine Bridge Enzyme in *S*-Scoulerine Biosynthesis

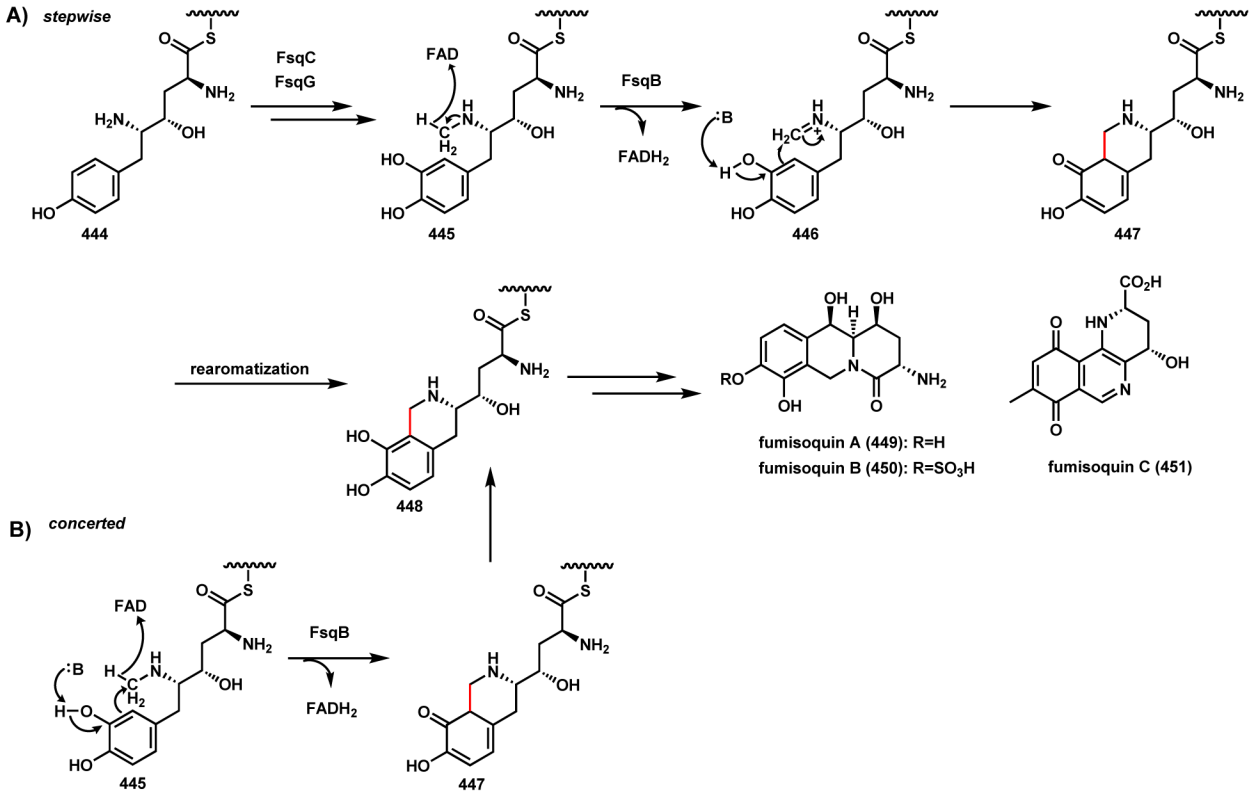

Scheme 62.
Proposed Role of BBE in Fumoisoquins Biosynthesis

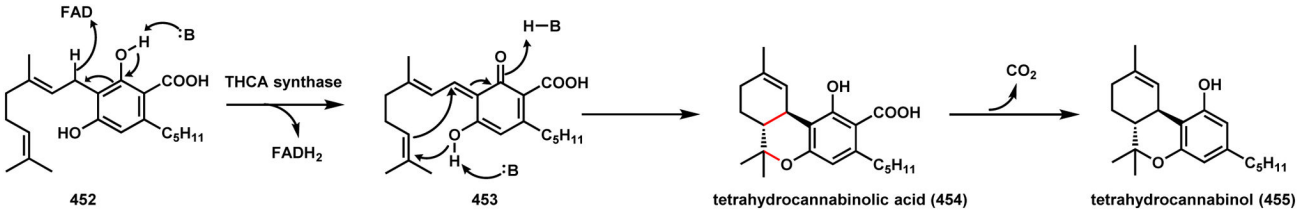

452 453 tetrahydrocannabinolic acid (454) tetrahydrocannabinol (455)

Scheme 63.
Proposed Mechanism of Tetrahydrocannabinol Biosynthesis

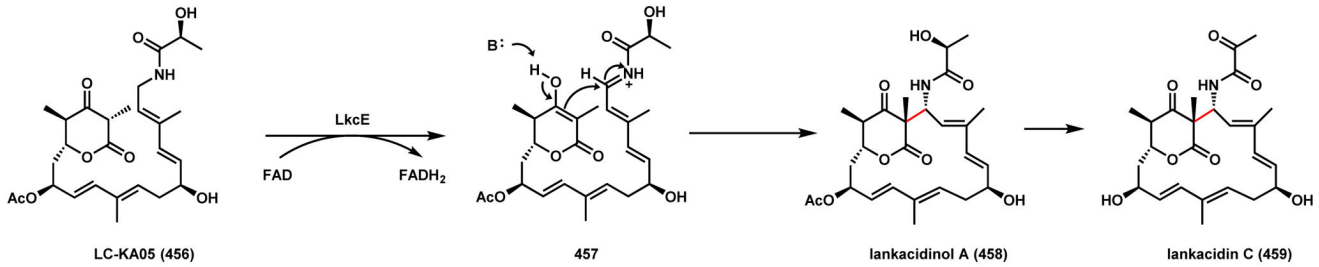

Scheme 64.
Desaturative Macrocyclization in Lankacidin Biosynthesis

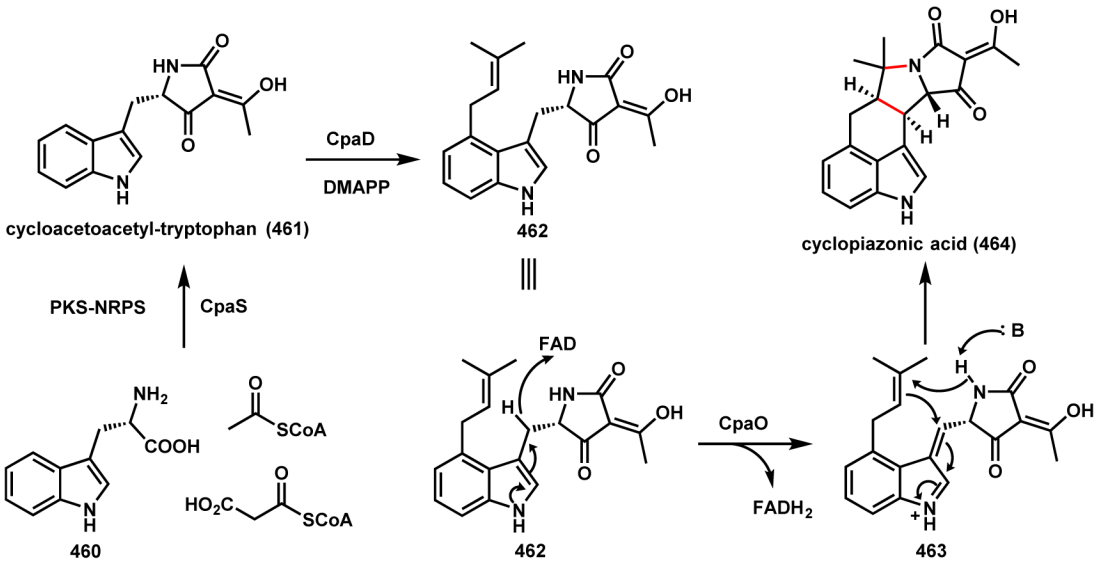

Scheme 65.
Desaturative Cyclization in Cyclopiazonic acid Biosynthesis

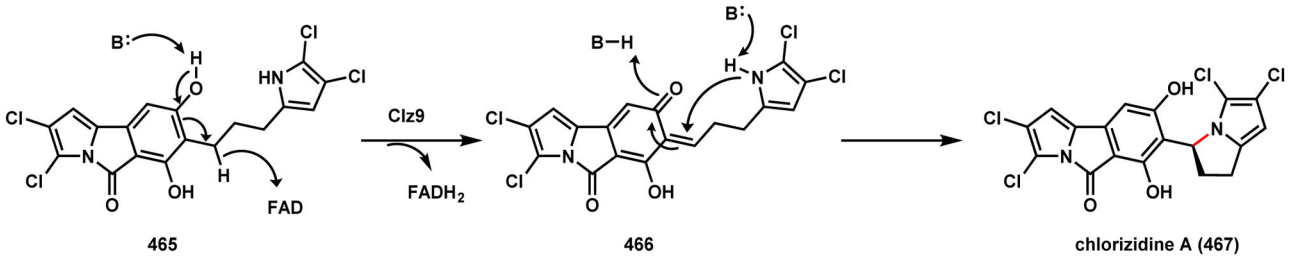

465 466 chlorizidine A (467)

Scheme 66.
Mechanism of Chlorizidine A Cyclization

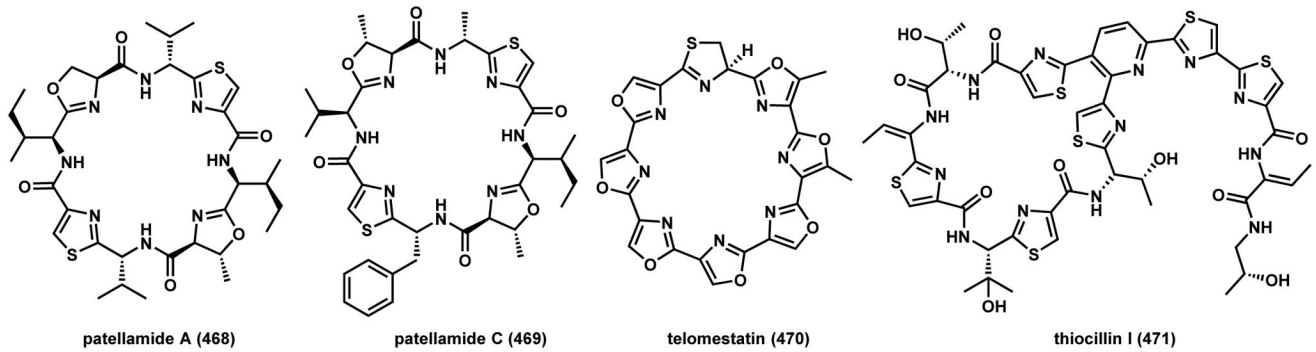

Scheme 67.
Selected Natural Products that Contain Oxazole and Thiazole Rings

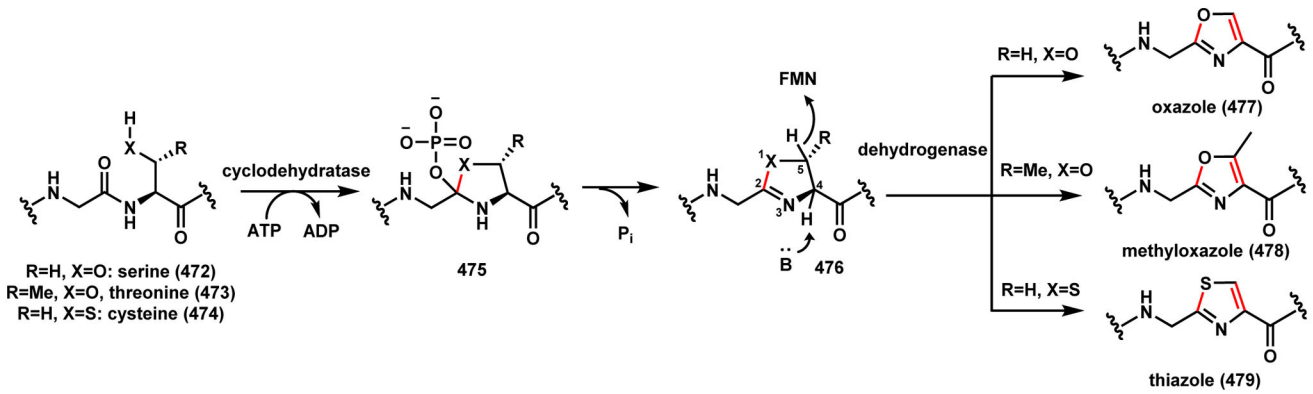

Scheme 68.
Mechanisms of Oxazole and Thiozole Formation

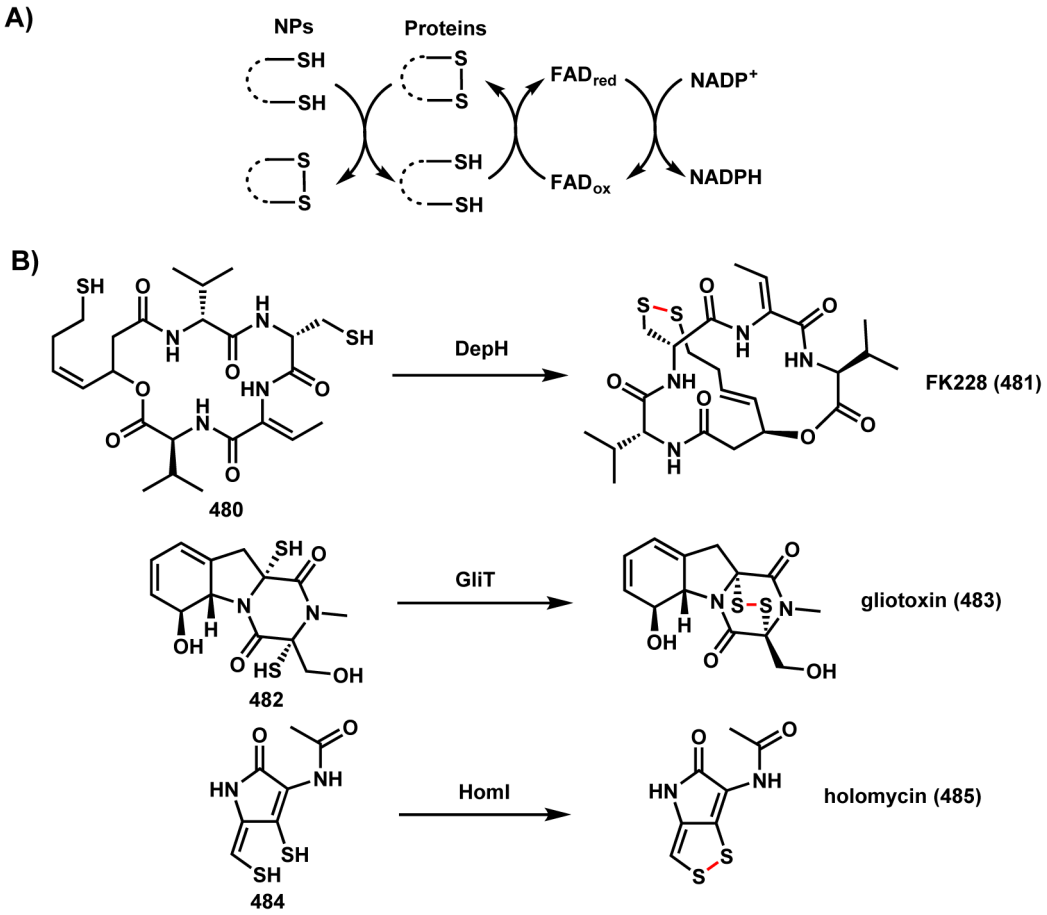

Scheme 69.
Disulfide Bond Formation from Dithiols in Natural Products Biosynthesis

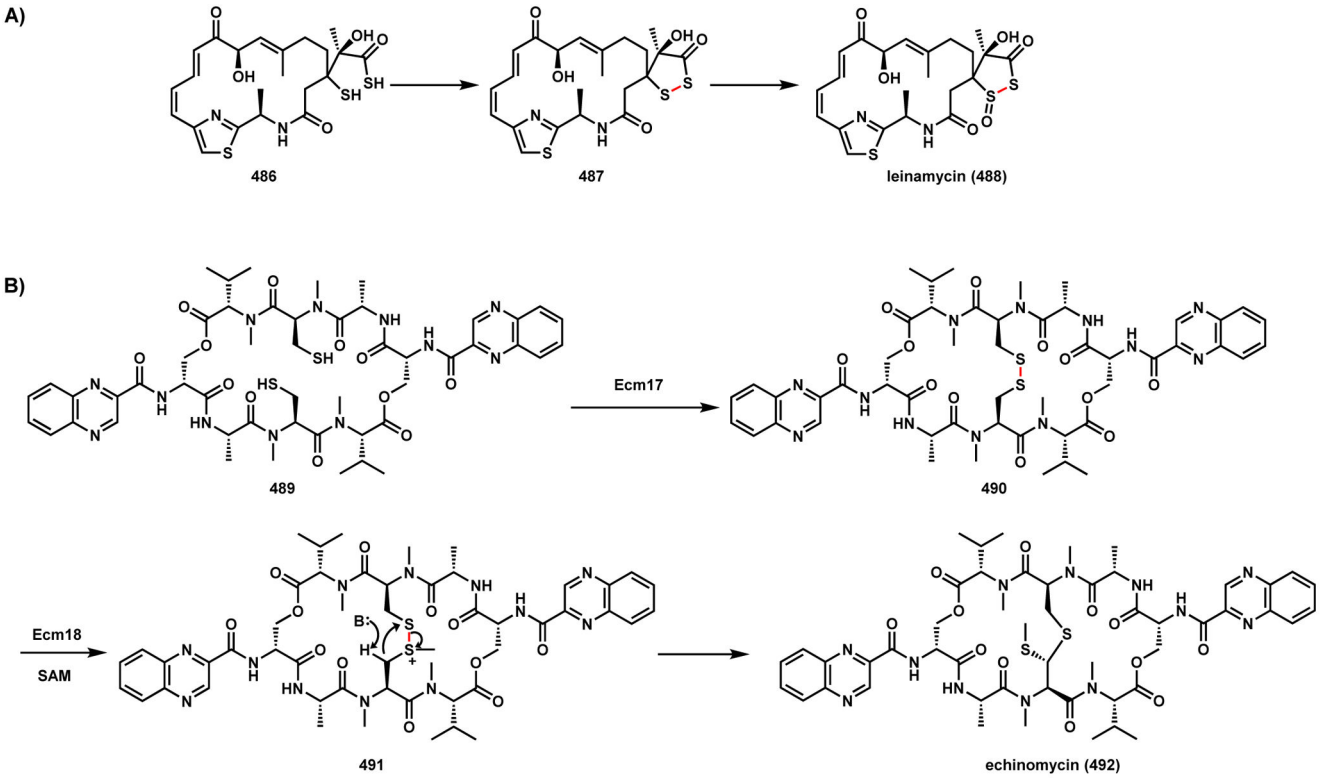

Scheme 70.
Examples of Disulfide Variants in Leinamycin and Echinomycin

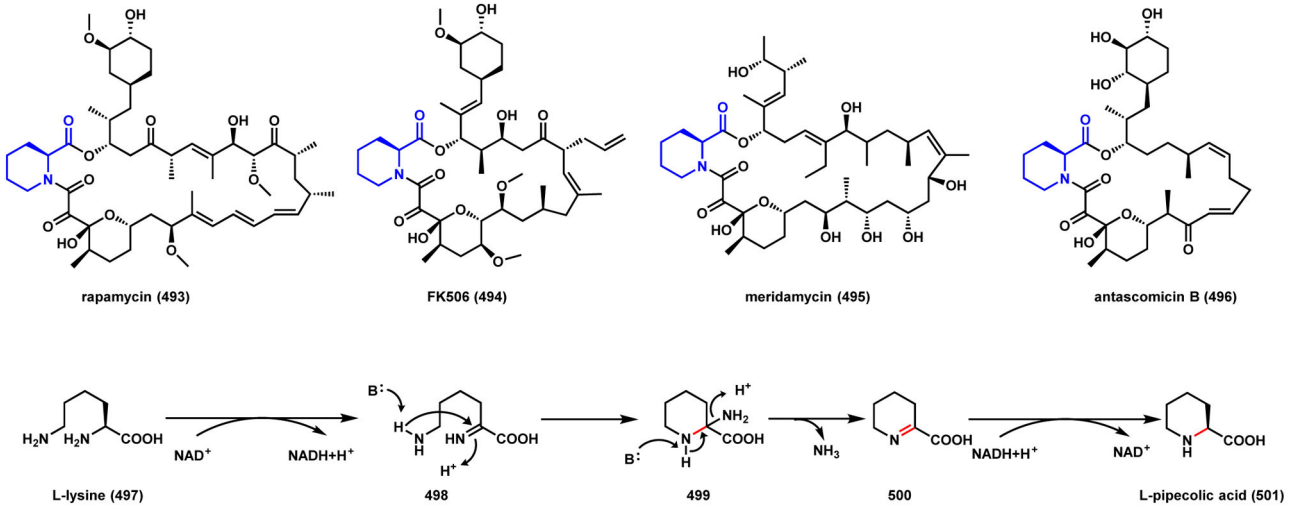

Scheme 71.
Formation of L-Pipecolic Acid in Natural Products

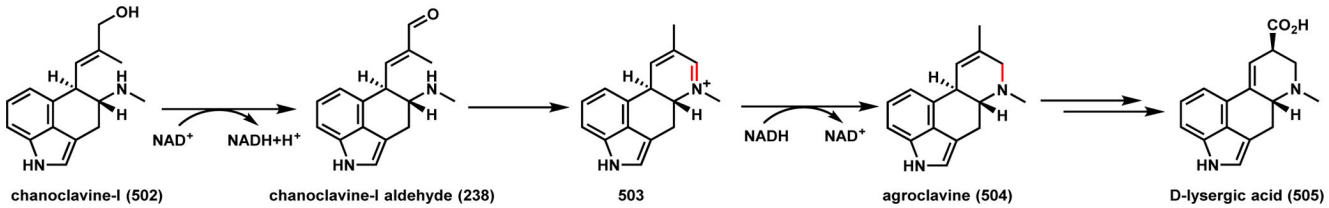

Scheme 72.
Cyclization of Chanoclavine-I to D-Lysergic Acid

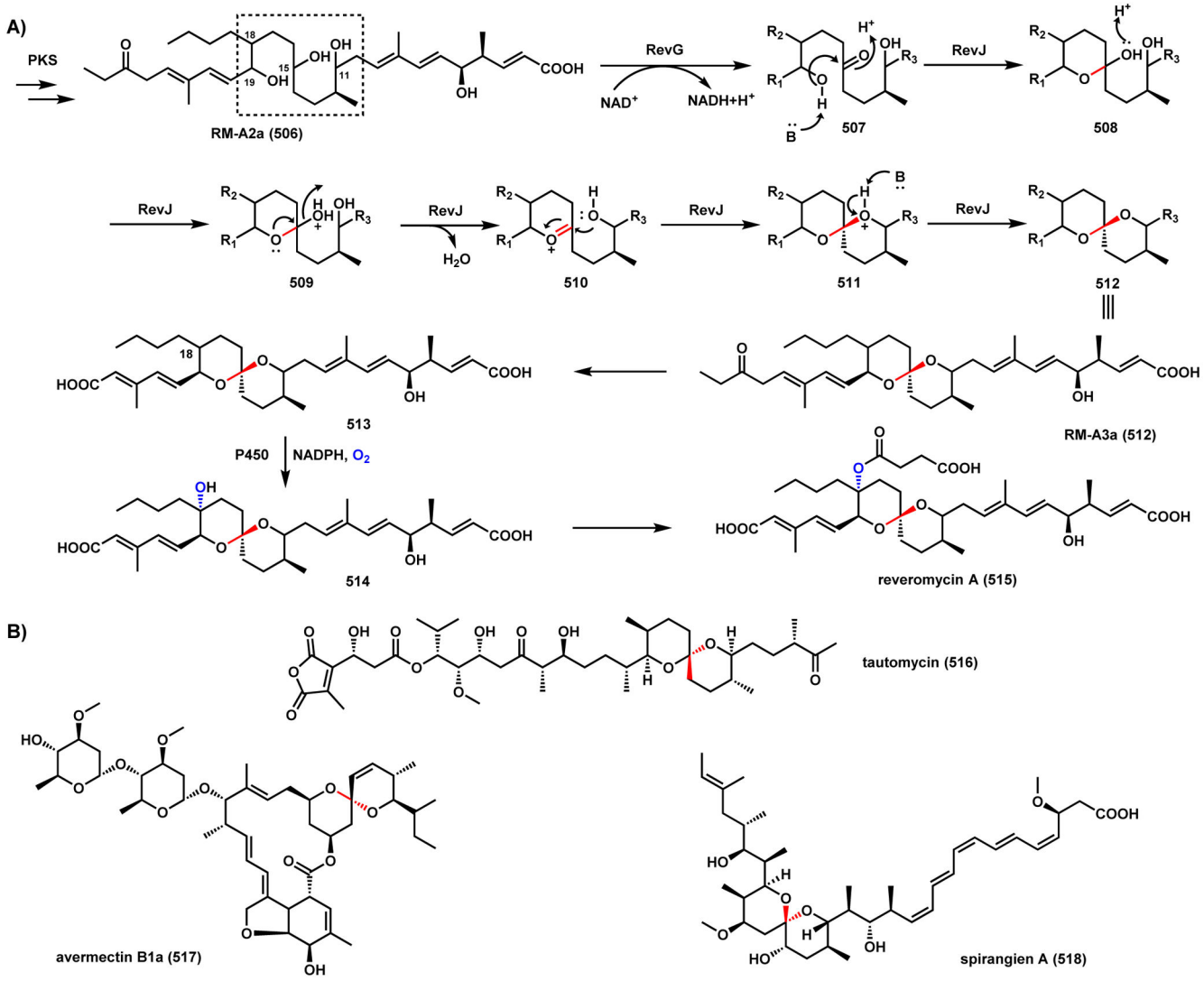

Scheme 73.

Oxidative Formation of 6,6-Spiroacetal as Shown in Reveromycin

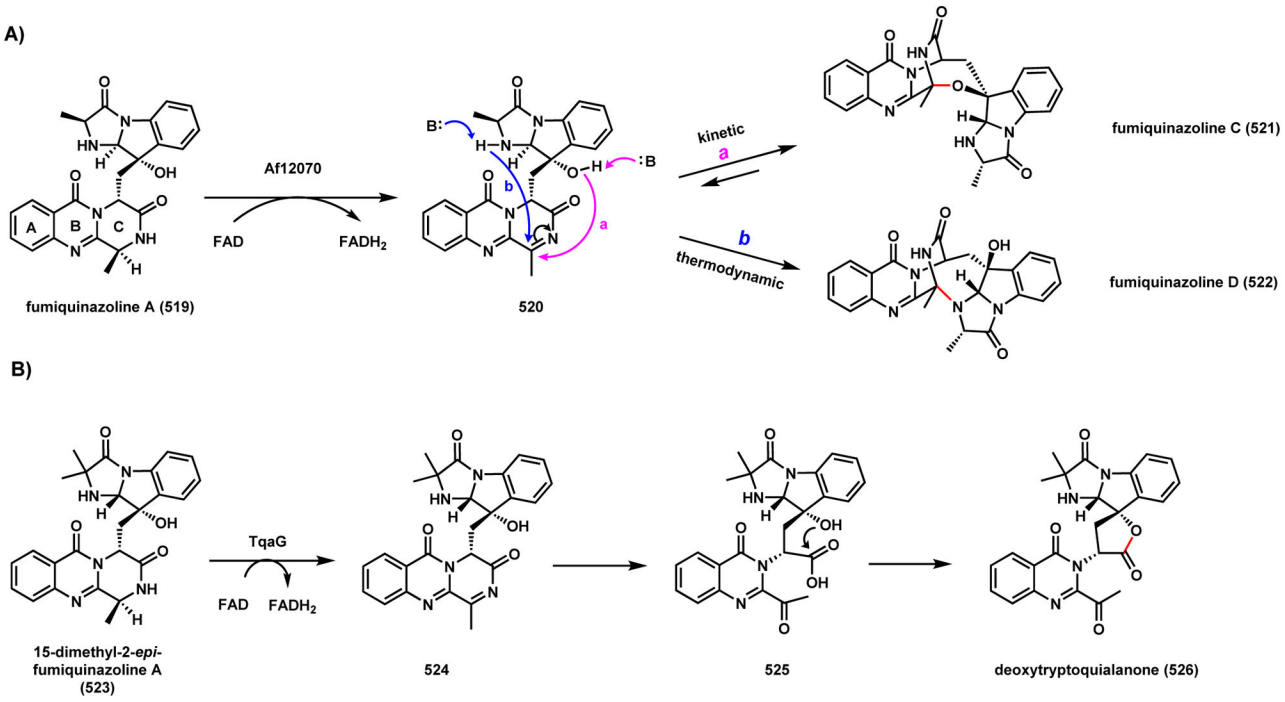

Scheme 74.
Oxidative Scaffold Maturation in Fungal Indole Alkaloid Biosynthesis

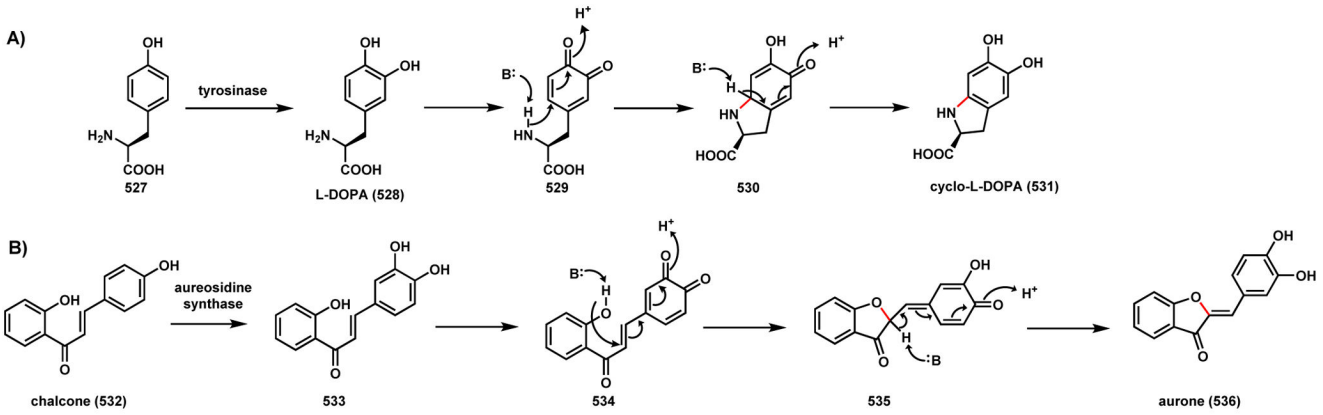

Scheme 75.
Transient Oxidation of Catechols to Set up Cyclization

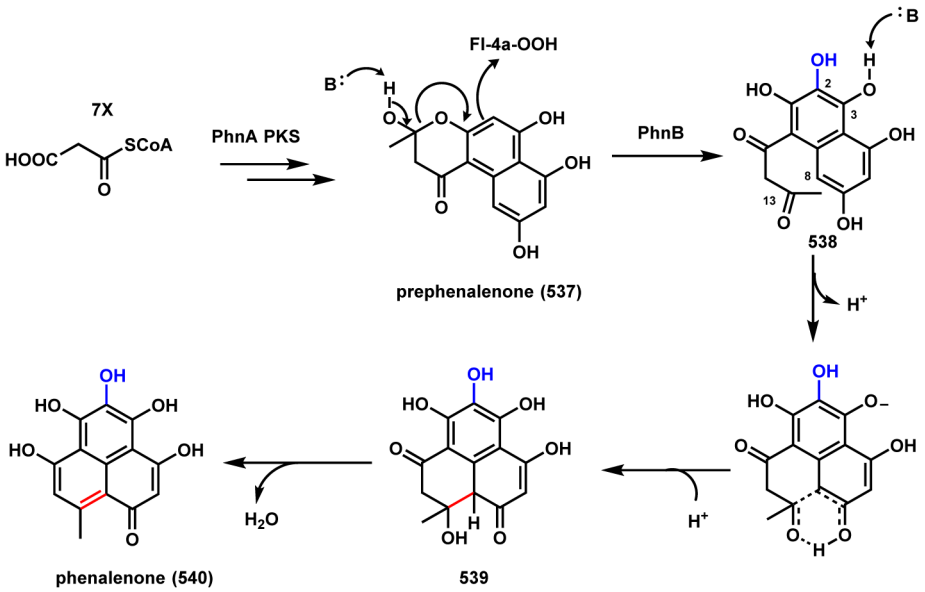

Scheme 76.
Oxidative Formation of Phenalenone

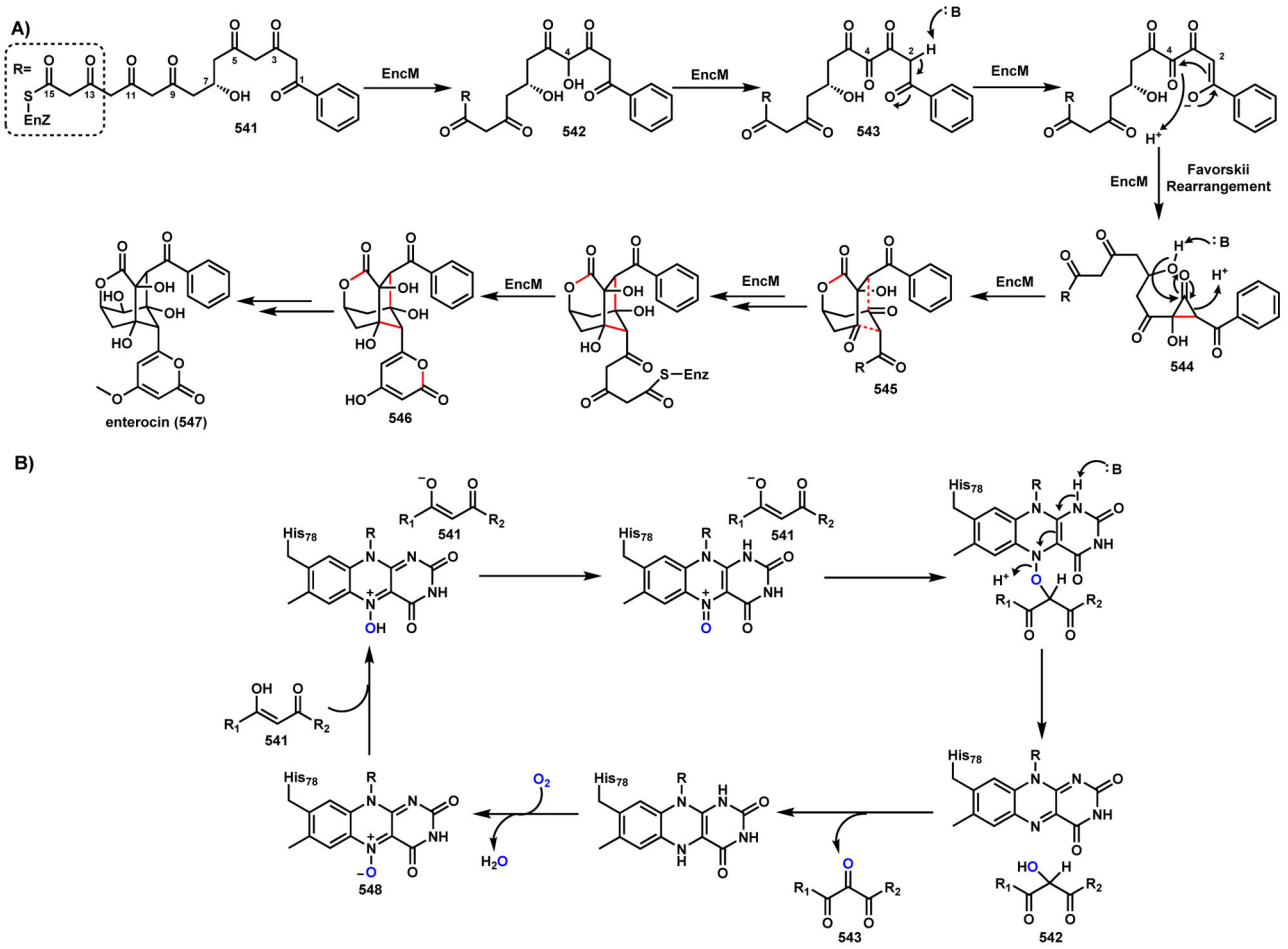

Scheme 77.
Flavoenzyme Catalyzed Favorskii Rearrangement in Enterocin Biosynthesis

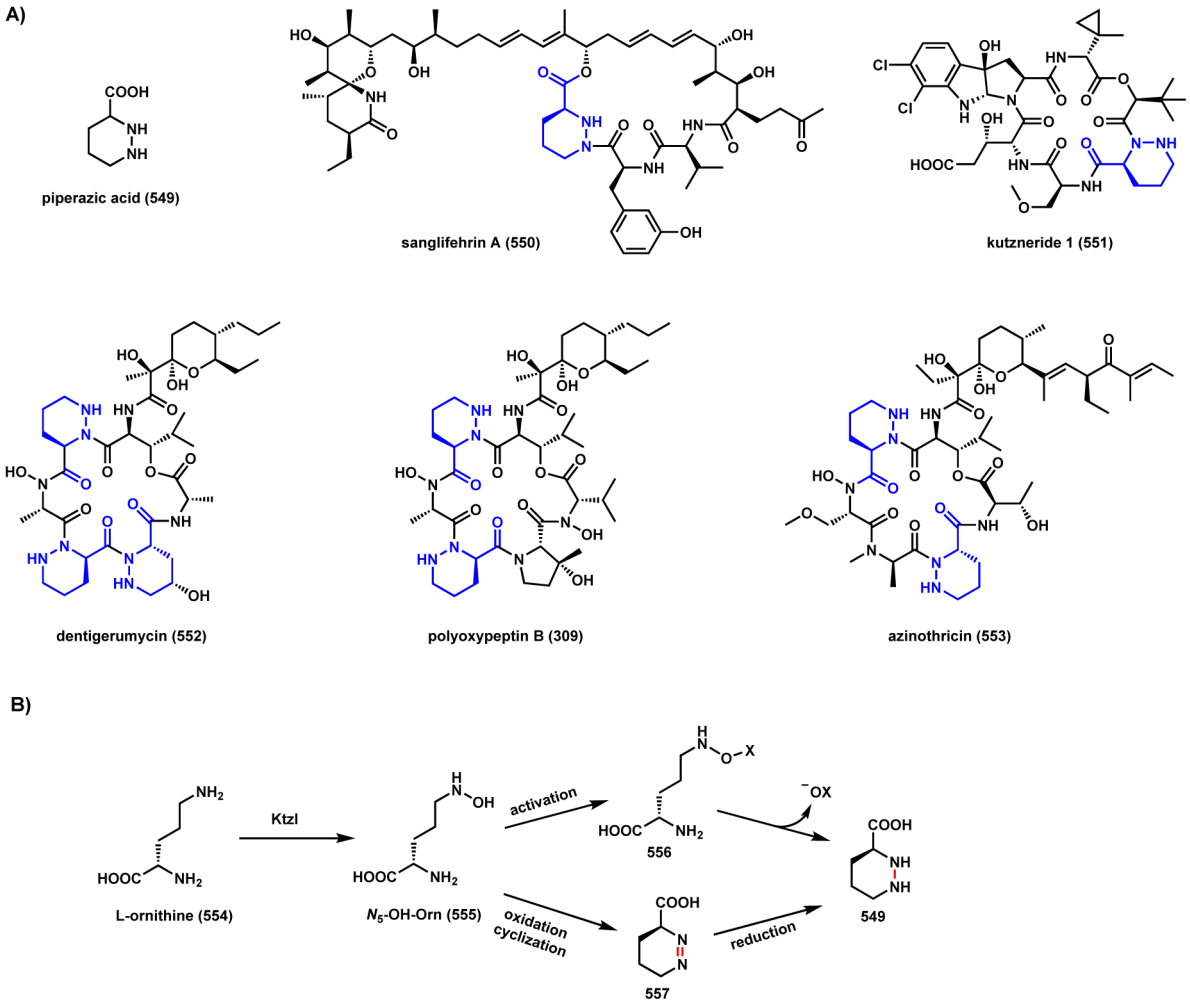

Scheme 78.
Cyclization of L-Ornithine to Piperazic Acid in NRP Natural Products

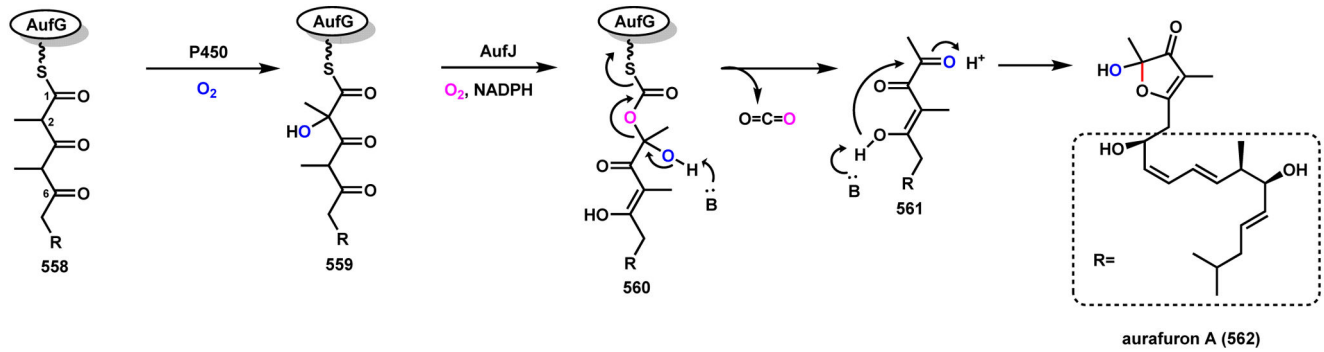

Scheme 79.
Proposed Formation of Furanone Scaffold in Aurafuron A Biosynthesis

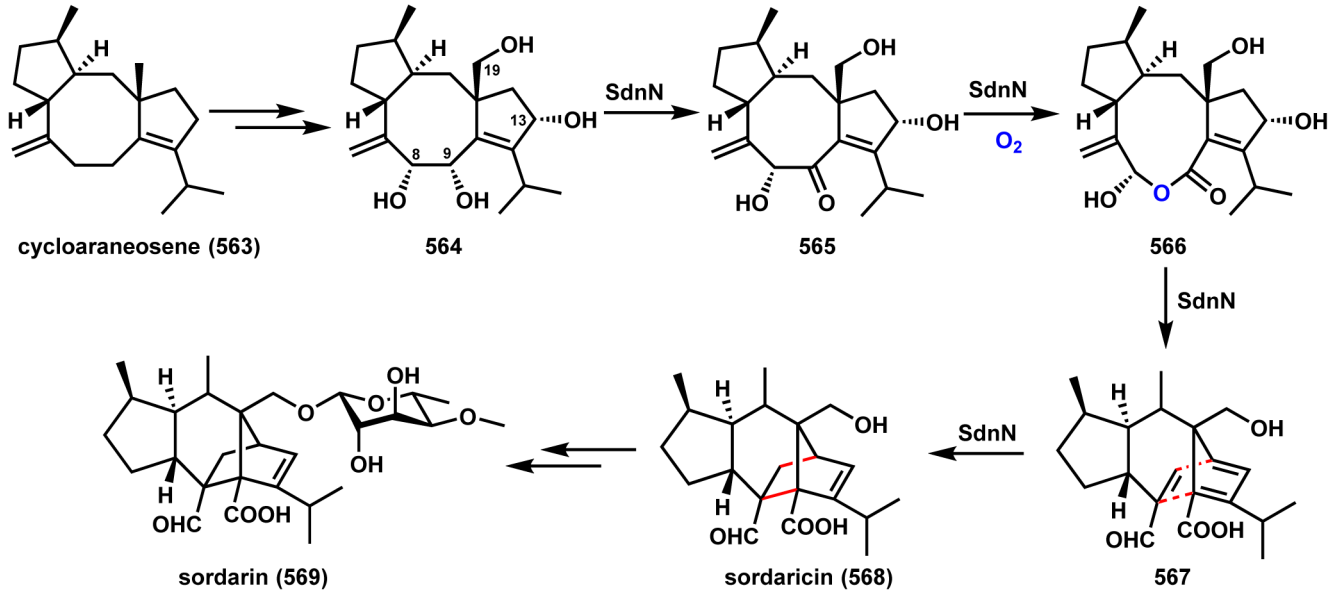

Scheme 80.
Proposed Diels-Alder Reaction in Sordarin Biosynthesis

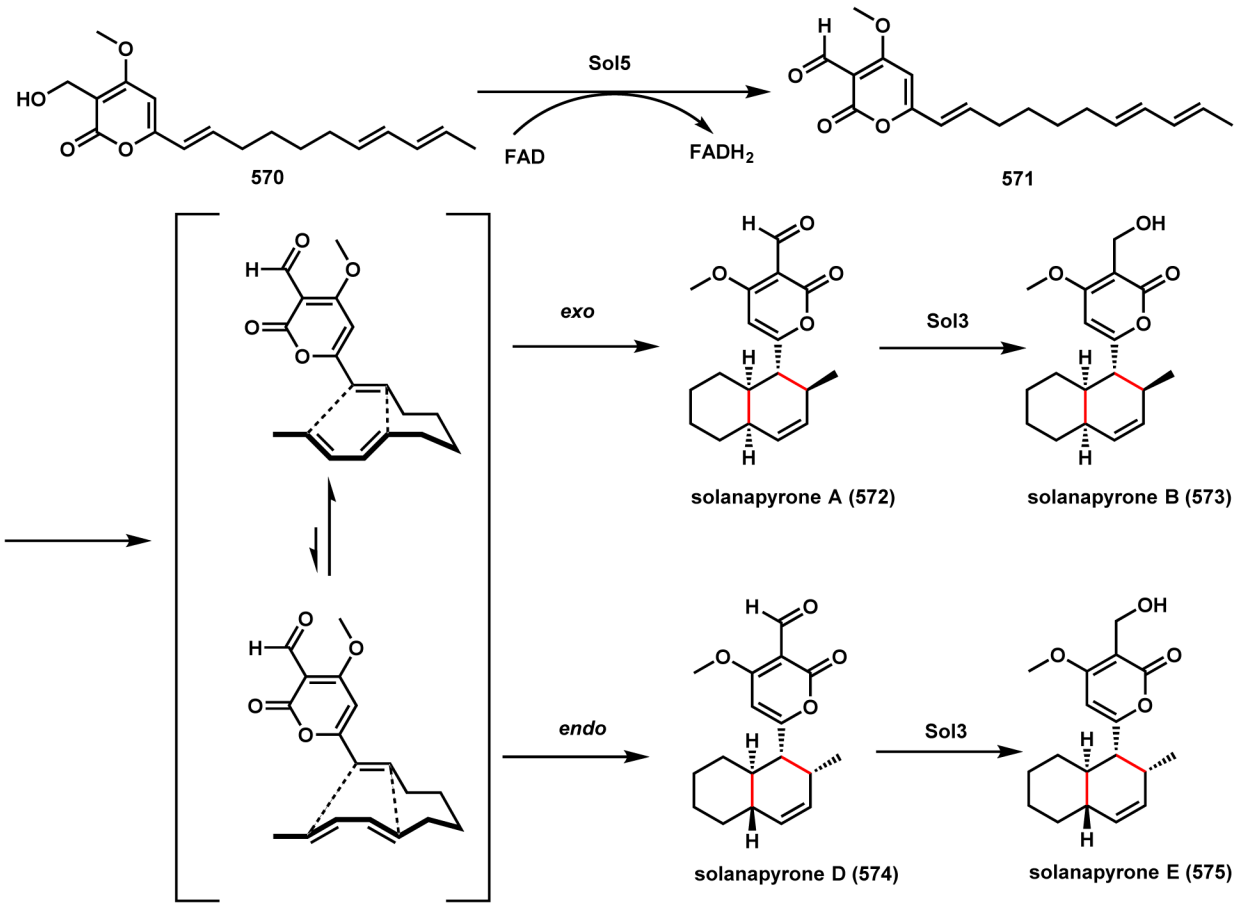

Scheme 81.
Oxidation Mediated [4+2] Cyclizations in Solanapyrone Biosynthesis

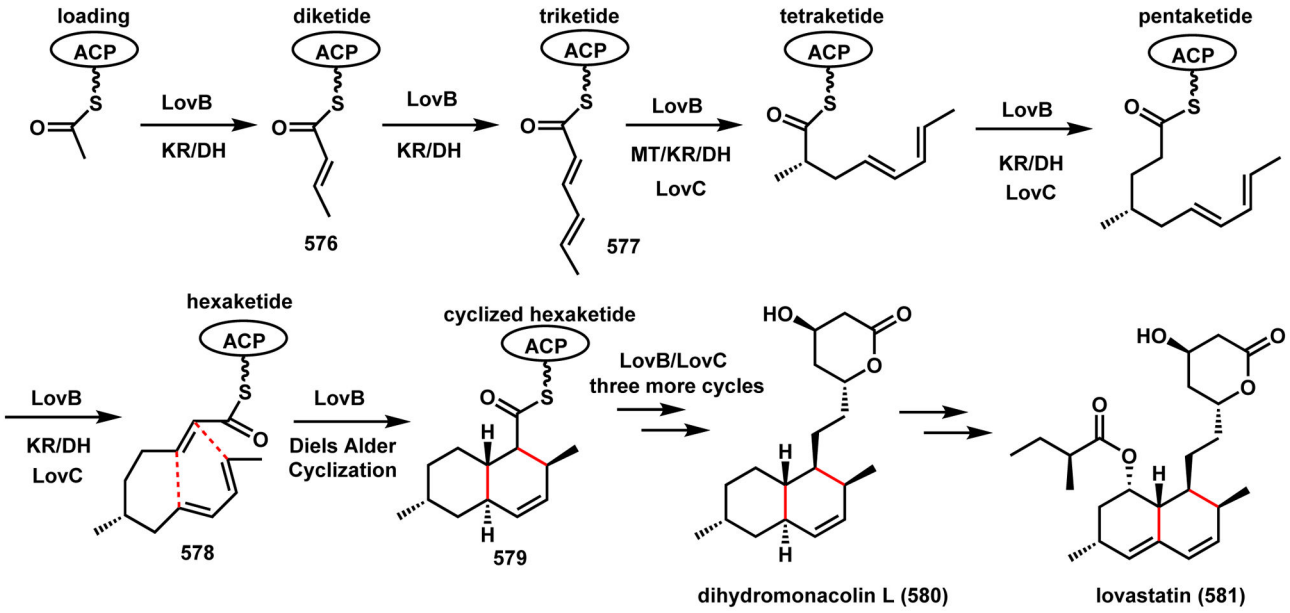

Scheme 82.

On-Assembly Line Diels-Alder Reaction During Lovastatin Biosynthesis

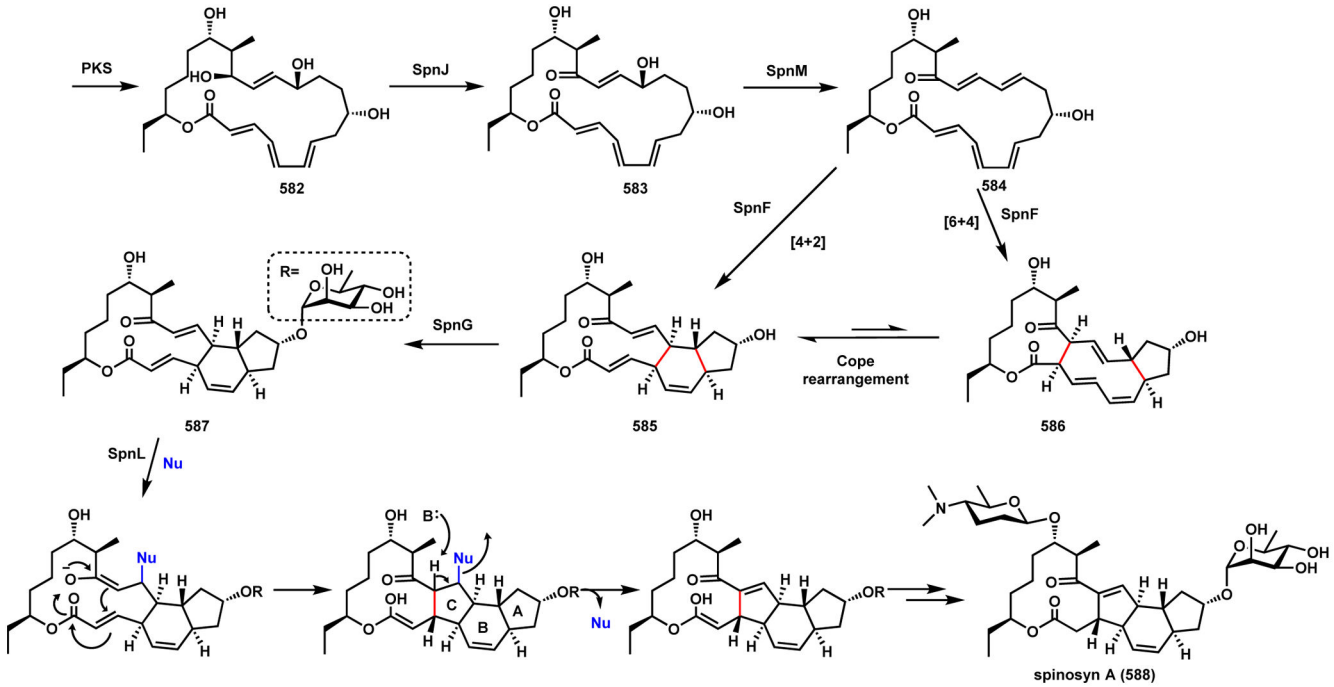

Scheme 83.
Cyclization Steps in Spinosyn A Biosynthesis

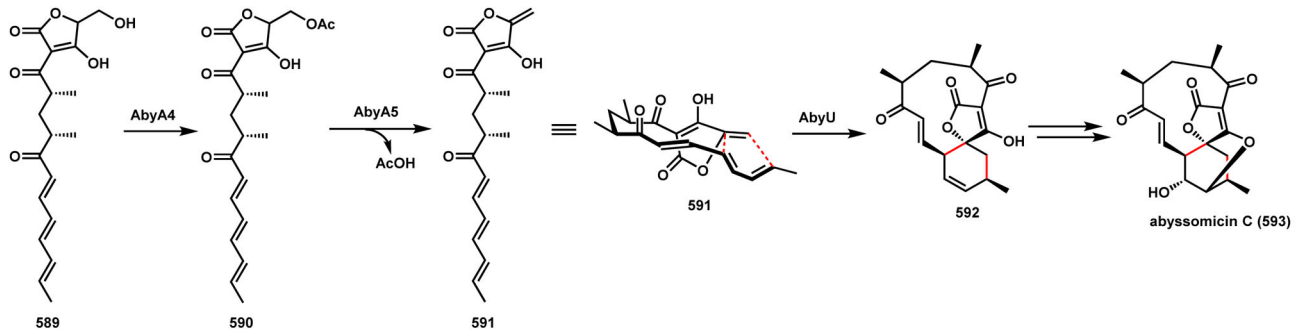

Scheme 84.
[4+2] Cyclization in Formation of 5,6-Spirocycle in Abyssomicin C

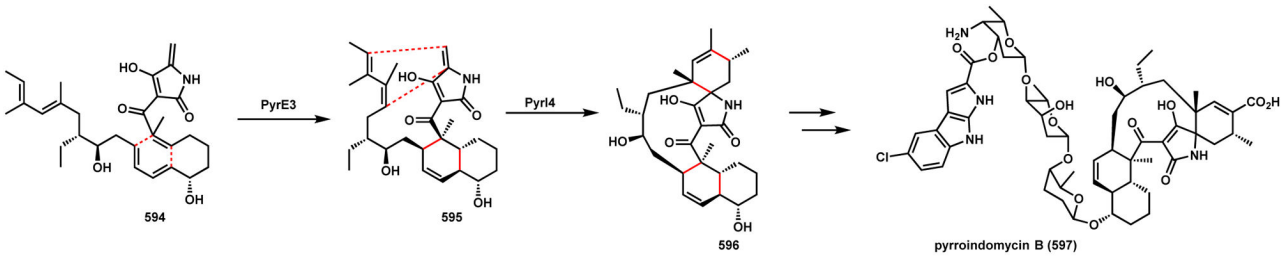

Scheme 85.

[4+2] Cyclizations in Formation of *cis*-Decalin and 5,6-Spirocycle in Pyrroindomycin B

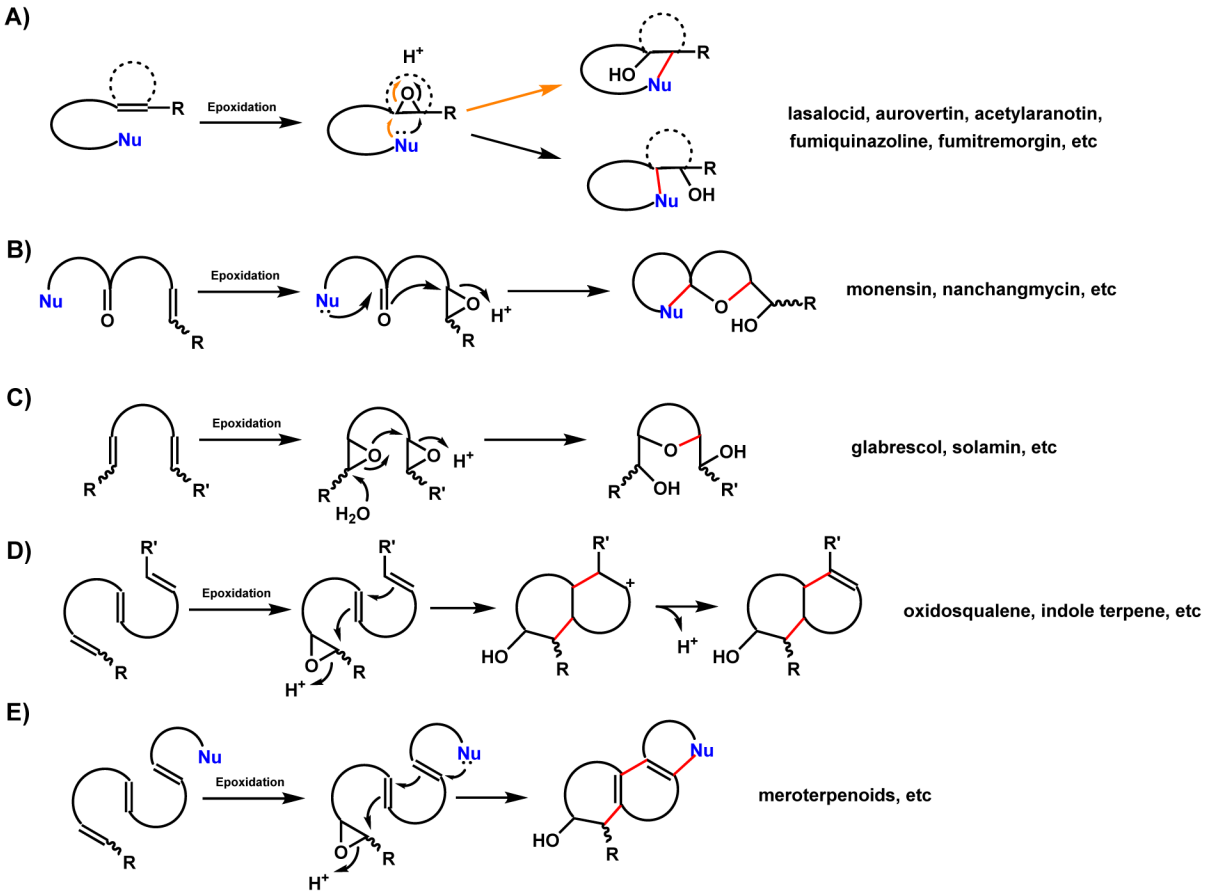

Scheme 86.
Models of Cyclization via Epoxidation in Natural Product Biosynthesis

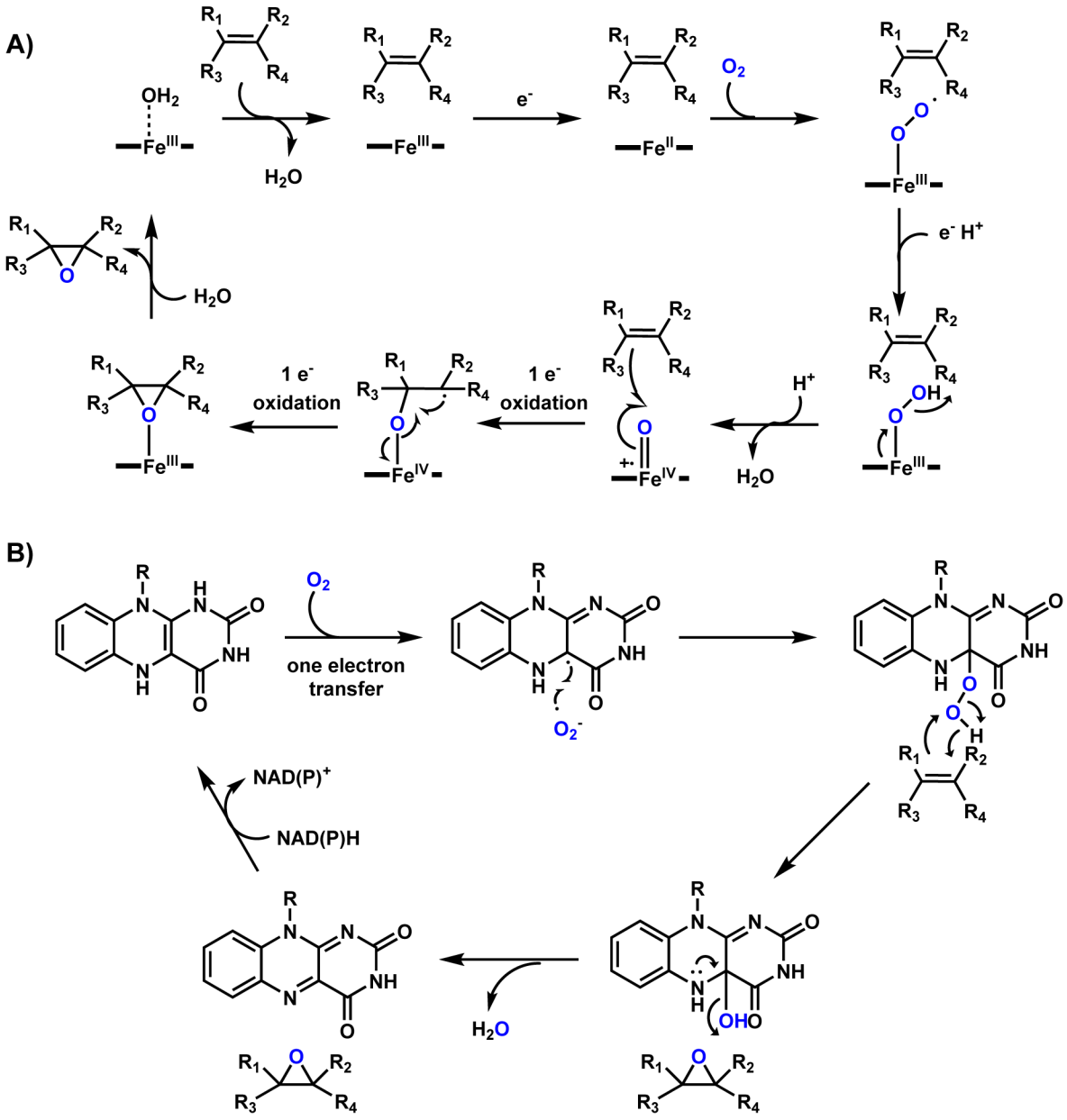

Scheme 87.
P450 and Flavoenzyme Catalyzed Formation of Epoxides

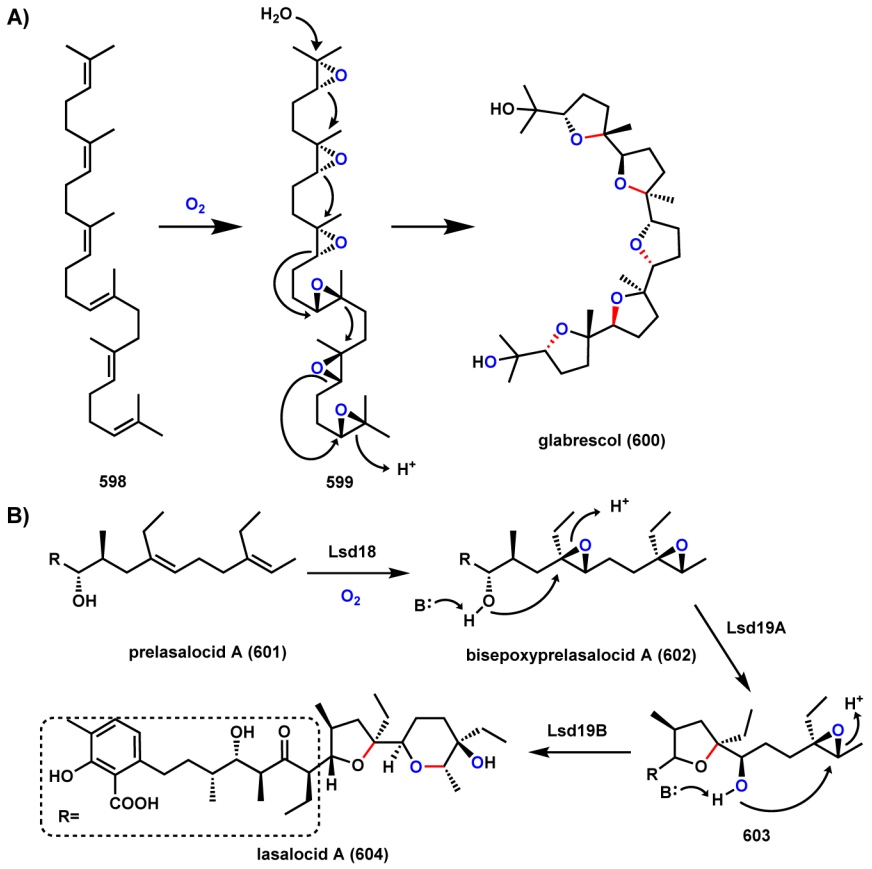

Scheme 88.
Cyclic Polyethers formation via Epoxide Intermediates

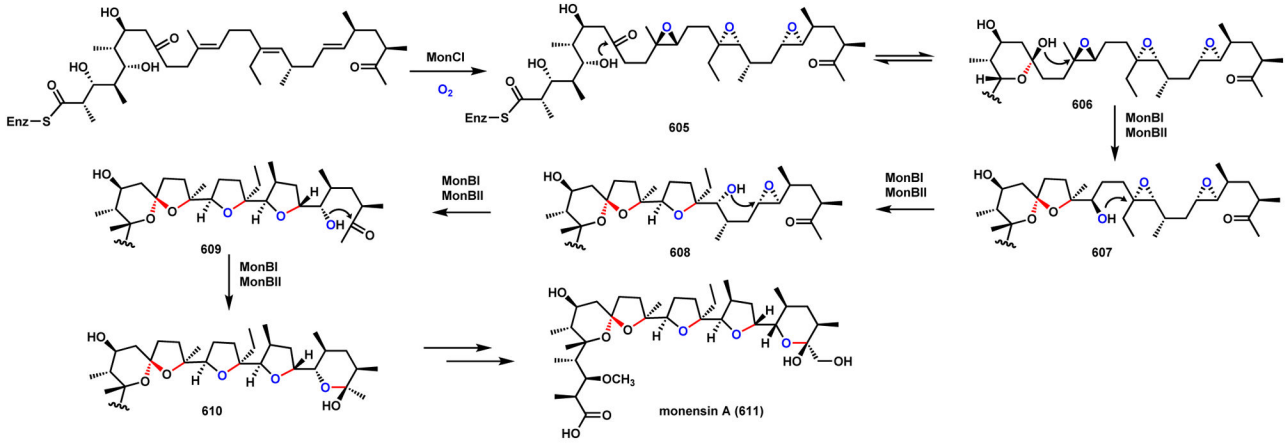

Scheme 89.
Mechanism of Polyether Formation in Monensin Biosynthesis

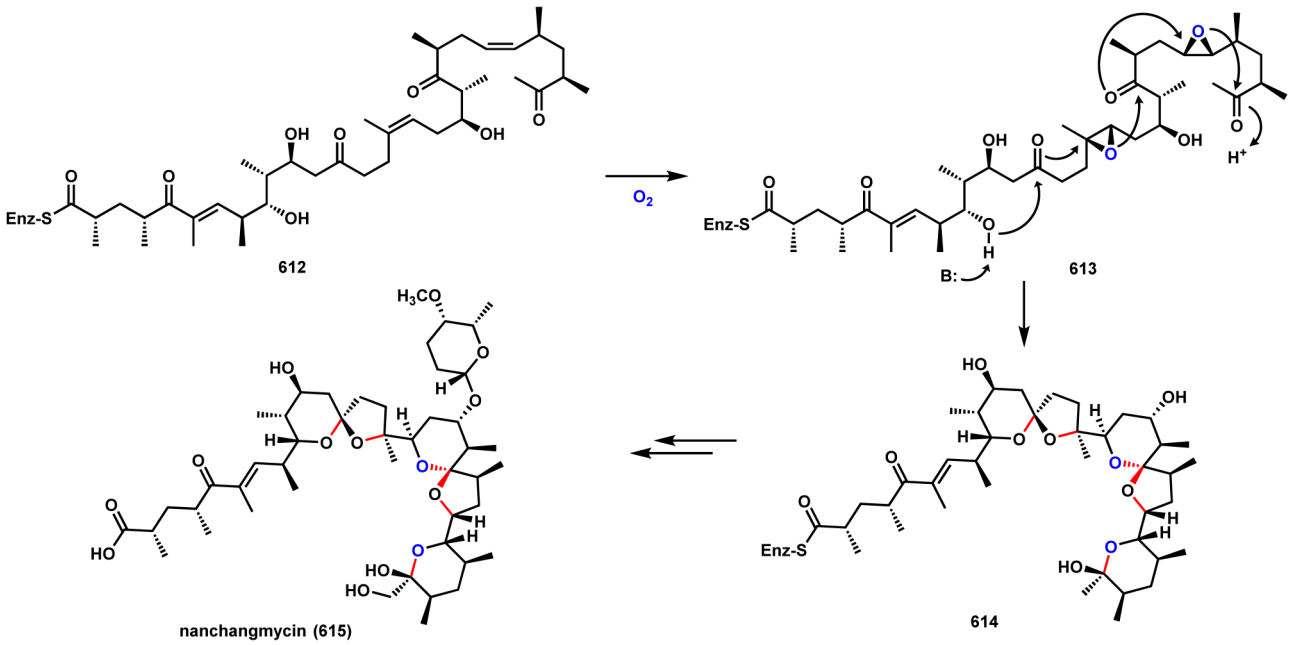

Scheme 90.
Mechanism of Polyether Formation in Nanchangmycin Biosynthesis

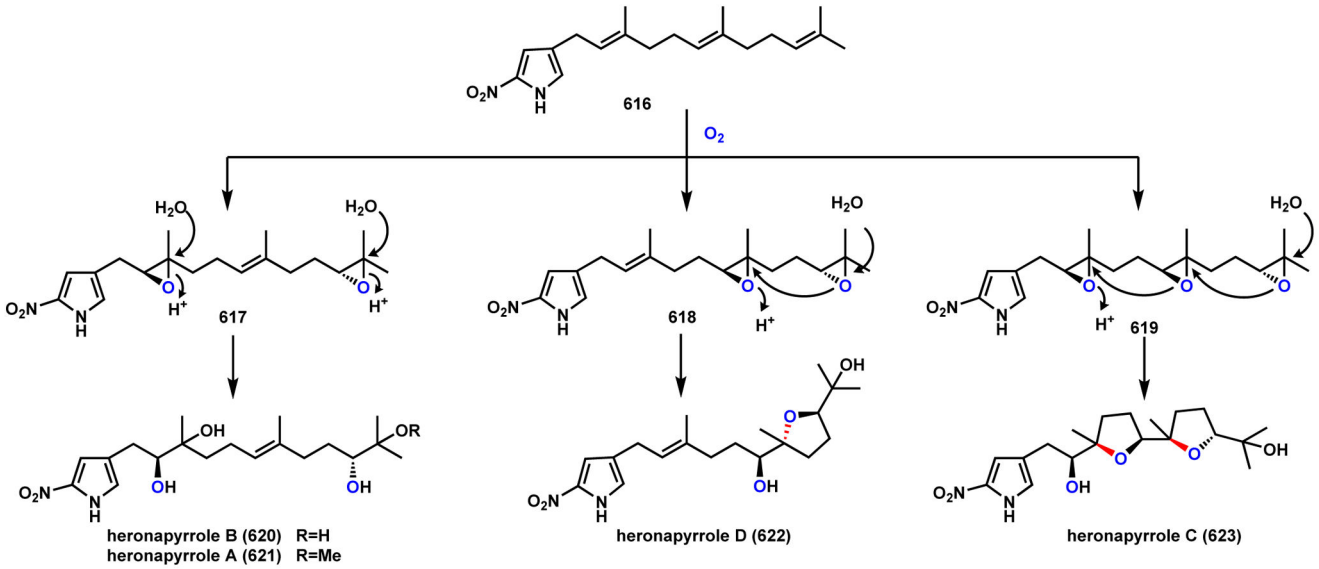

Scheme 91.

Proposed mechanism of Polyether Formation in Heronapyrrole Biosynthesis

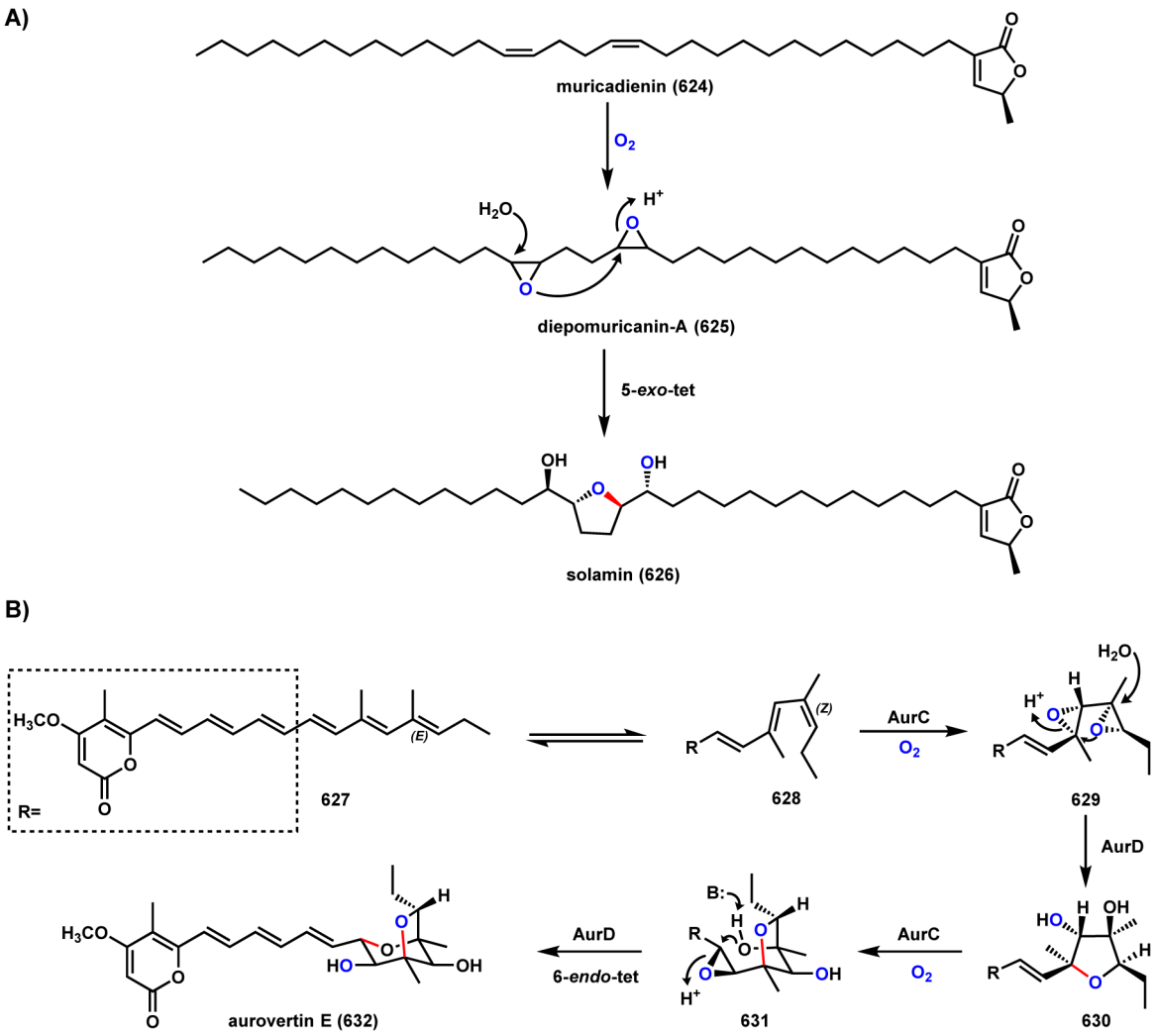

Scheme 92.

Cyclic Ethers formation via Epoxide Intermediates in Solamin and Aurovertin

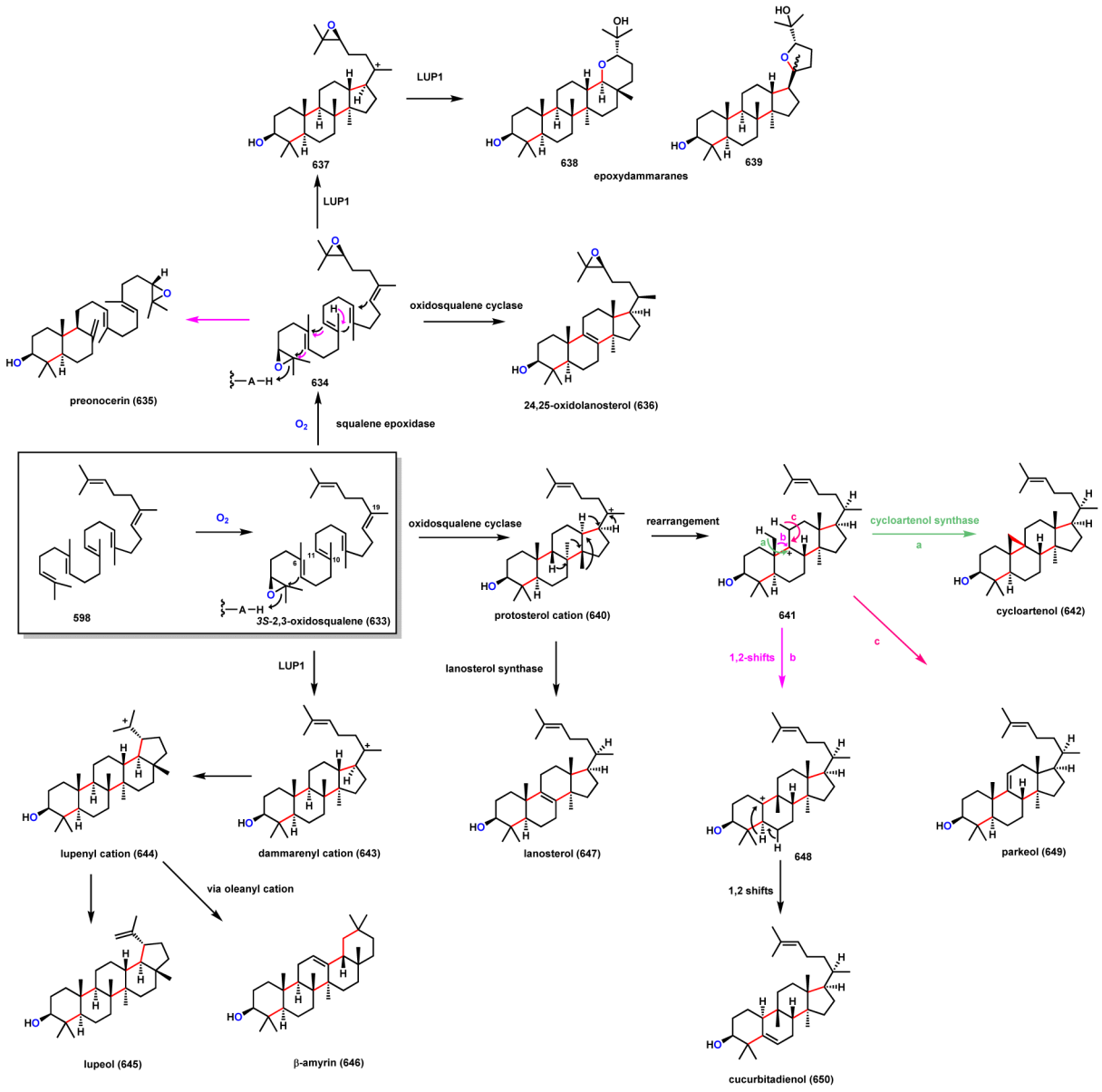

Scheme 93.
Triterpene Cyclization via Epoxide and Cation Intermediates

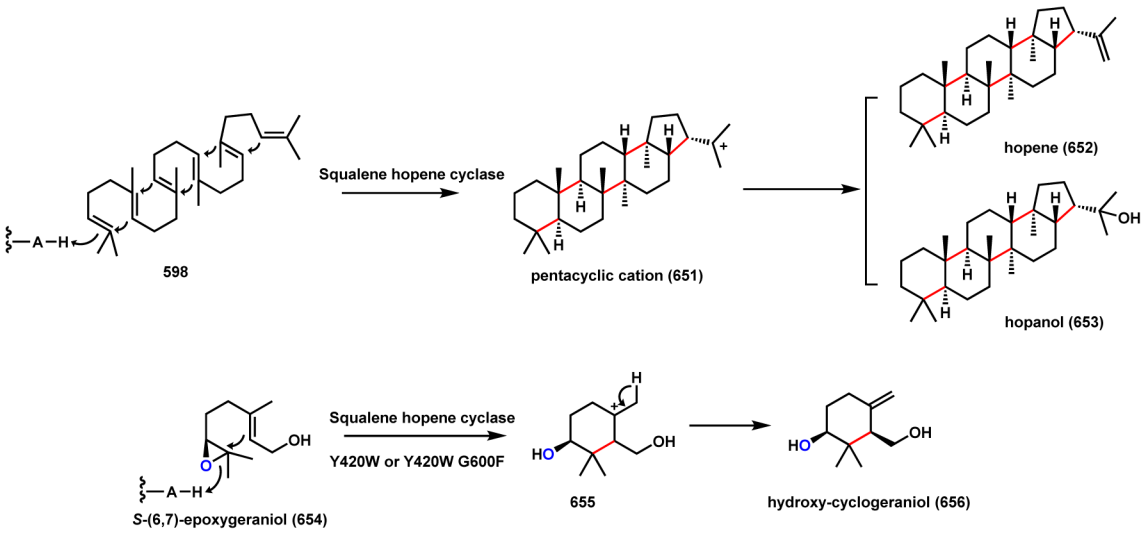

Scheme 94.
Engineering of Squalene-Hopene Cyclase as a Protonase

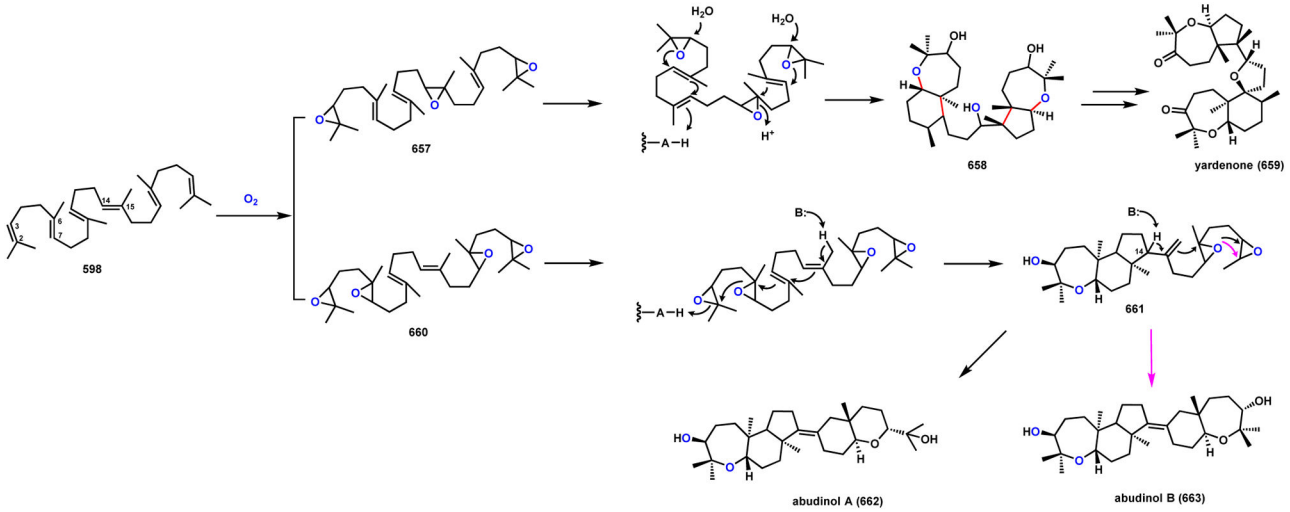

Scheme 95.
Alternative Triterpene Cyclization in Yardenone and Abudinol Biosynthesis

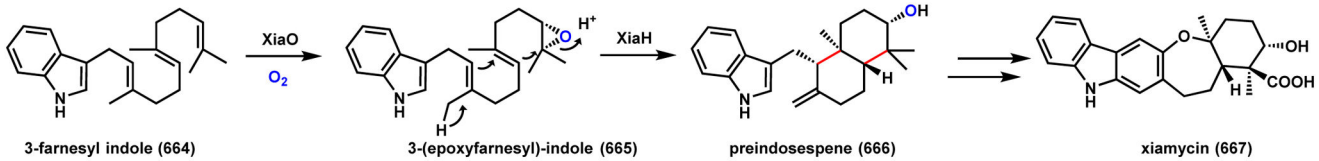

Scheme 96.
Epoxide Mediated Cyclization in Xiamycin Biosynthesis

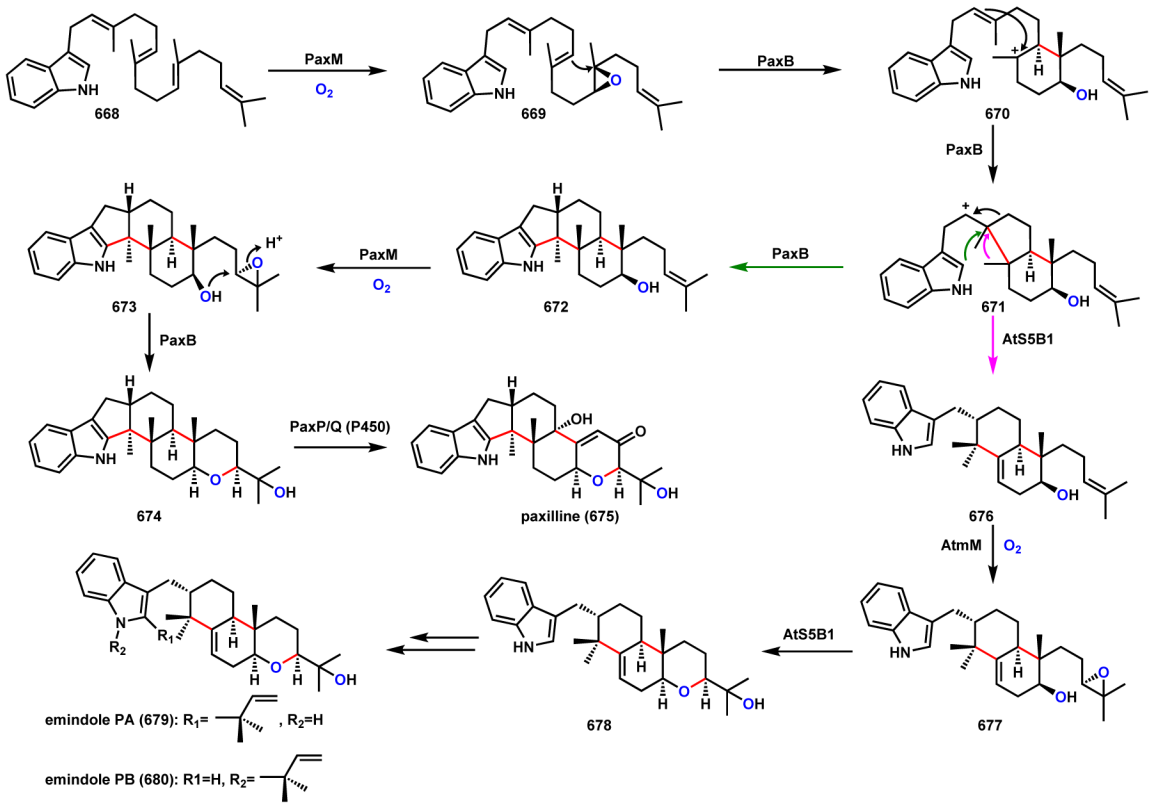

Scheme 97.
Epoxide Mediated Cyclization in Paxilline and Emindoles Biosynthesis

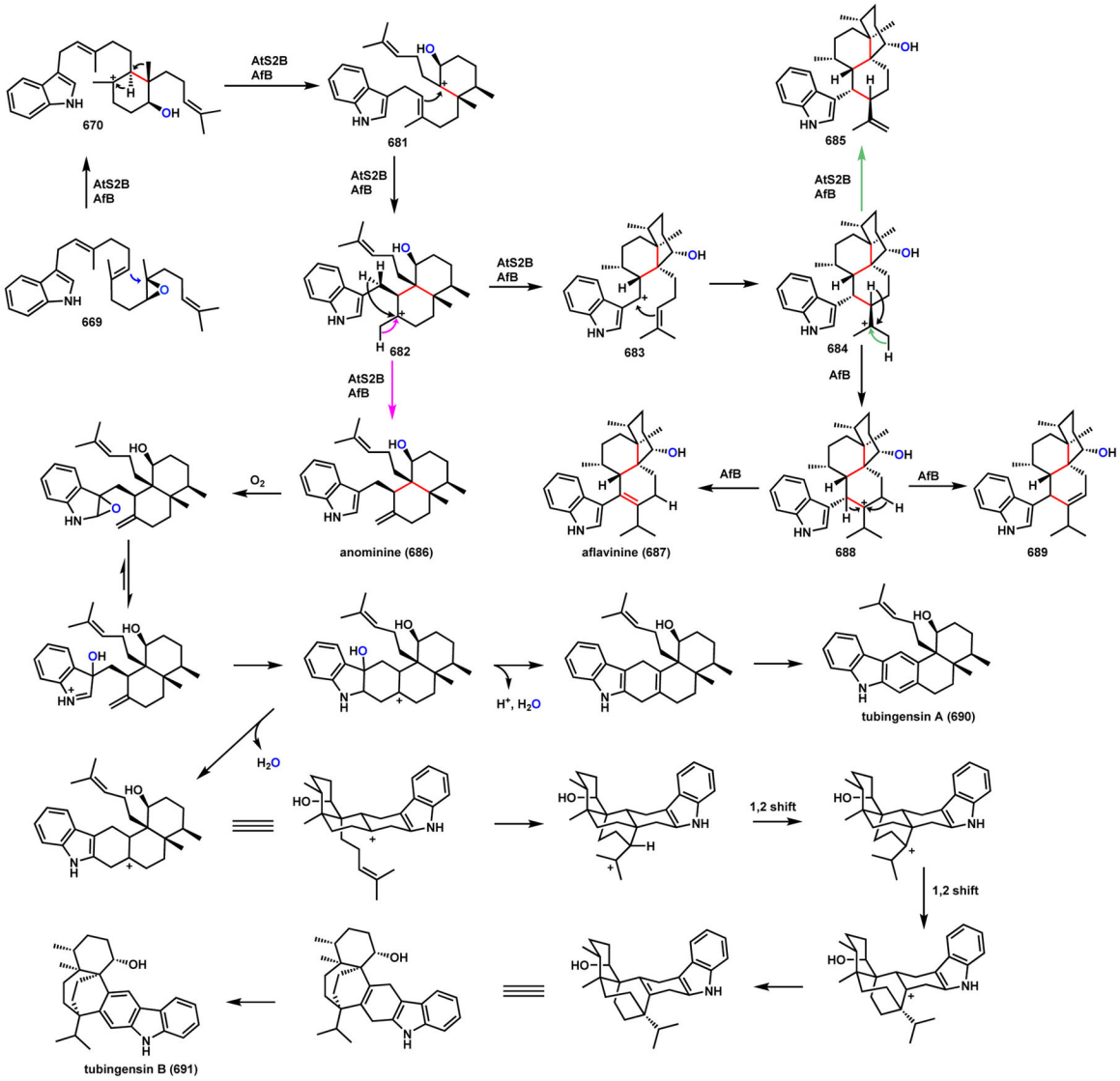

Scheme 98.

Epoxide Mediated Cyclization in Anominine, Aflavinine and Tubingensin Biosynthesis

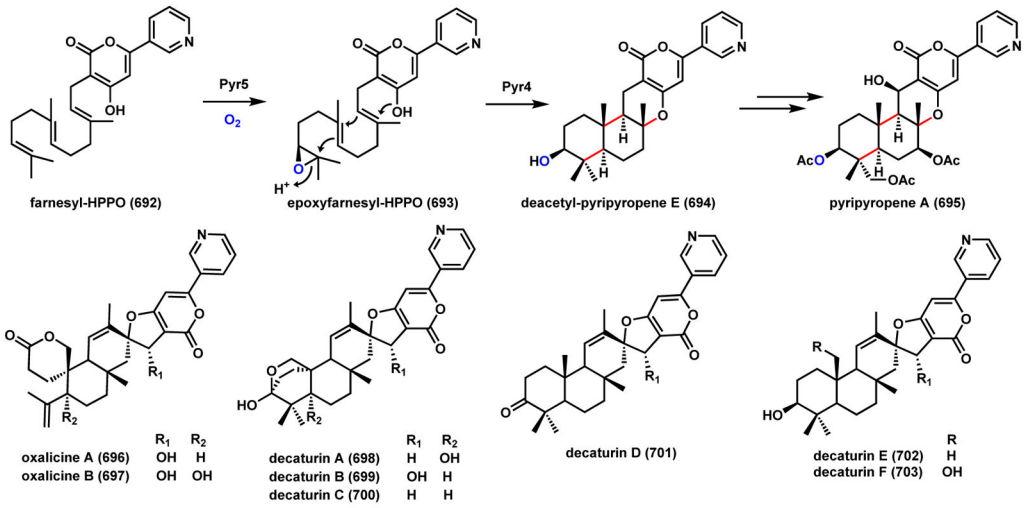

Scheme 99.
Epoxide Mediated Cyclization in Pyripyopene Biosynthesis

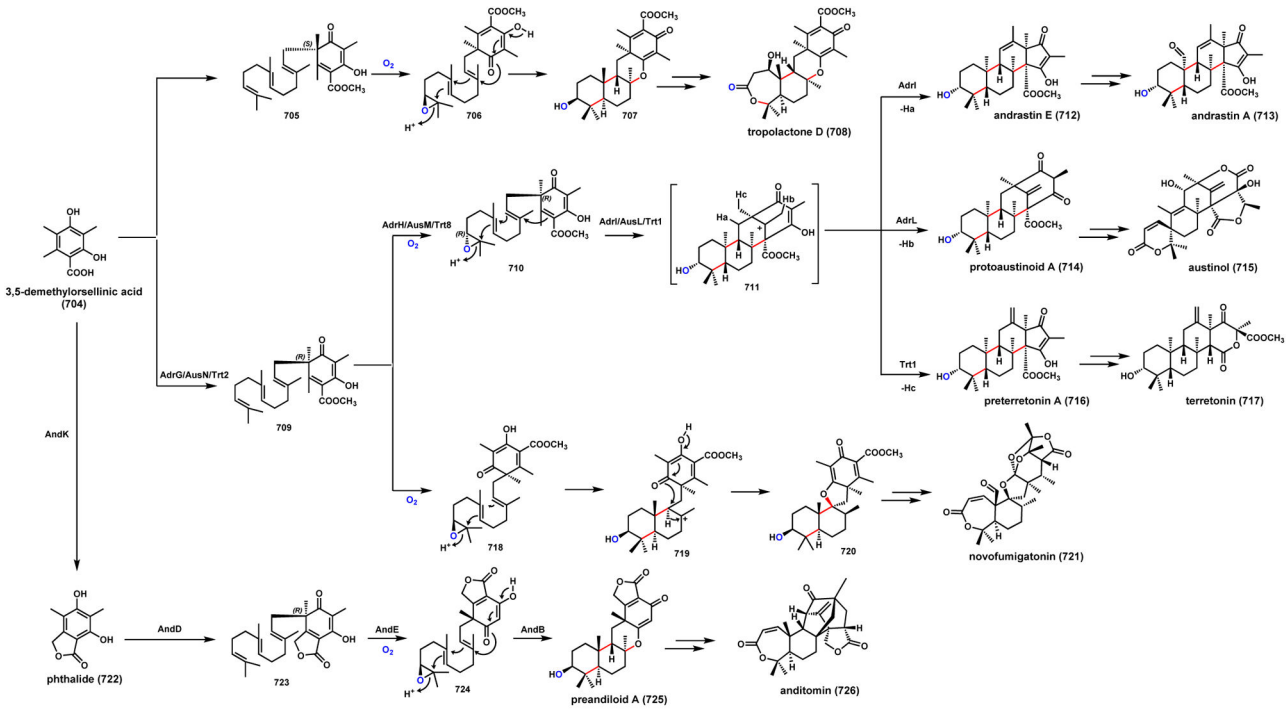

Scheme 100.
Biosynthetic Pathway of Fungal Meroterpenoids

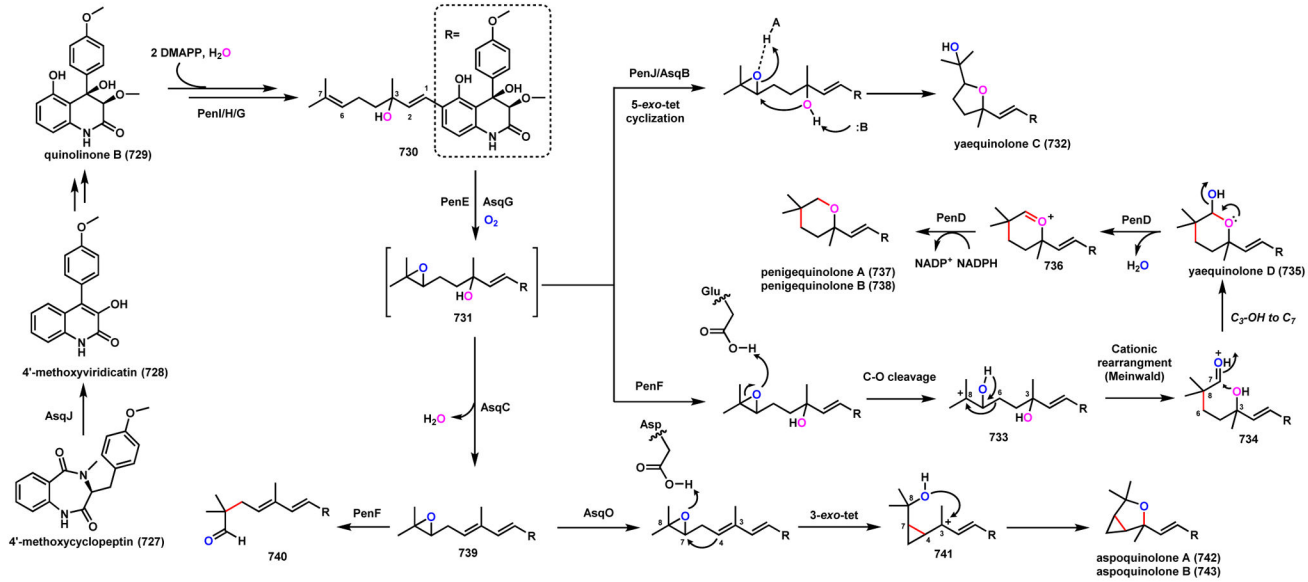

Scheme 101.

Enzyme-Catalyzed Cationic Epoxide Rearrangements in Quinolone Alkaloid Biosynthesis

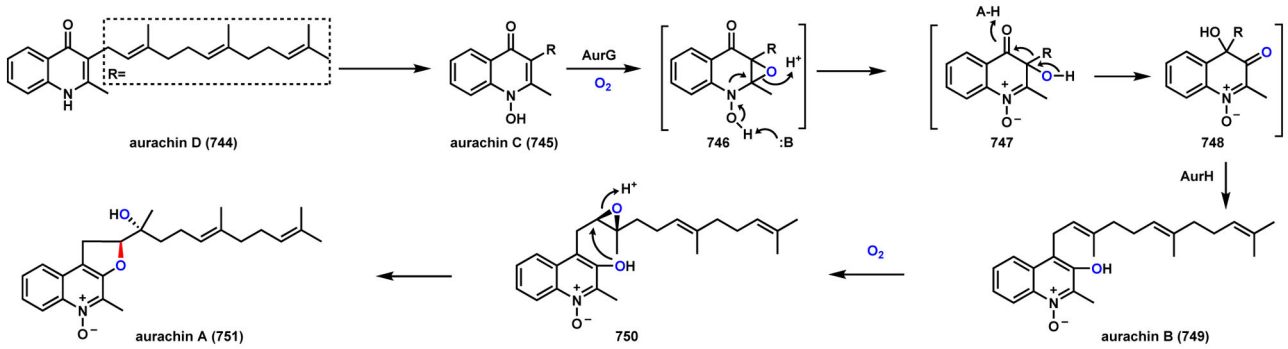

Scheme 102.
Proposed Cyclization Mechanism during Aurachin A Biosynthesis

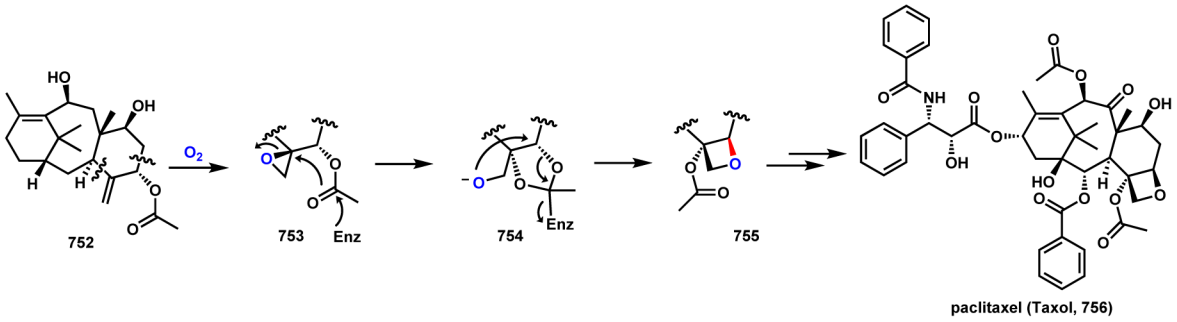

Scheme 103.

Oxetane Formation via an Epoxide Intermediate During Paclitaxel Maturation

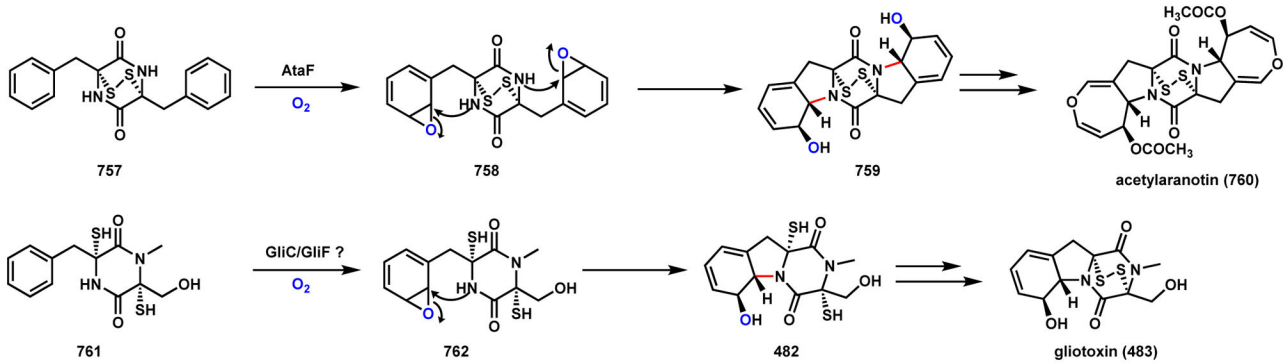

Scheme 104.

Proposed Epoxide Intermediates in Acetylaranotin and Gliotoxin Biosynthesis

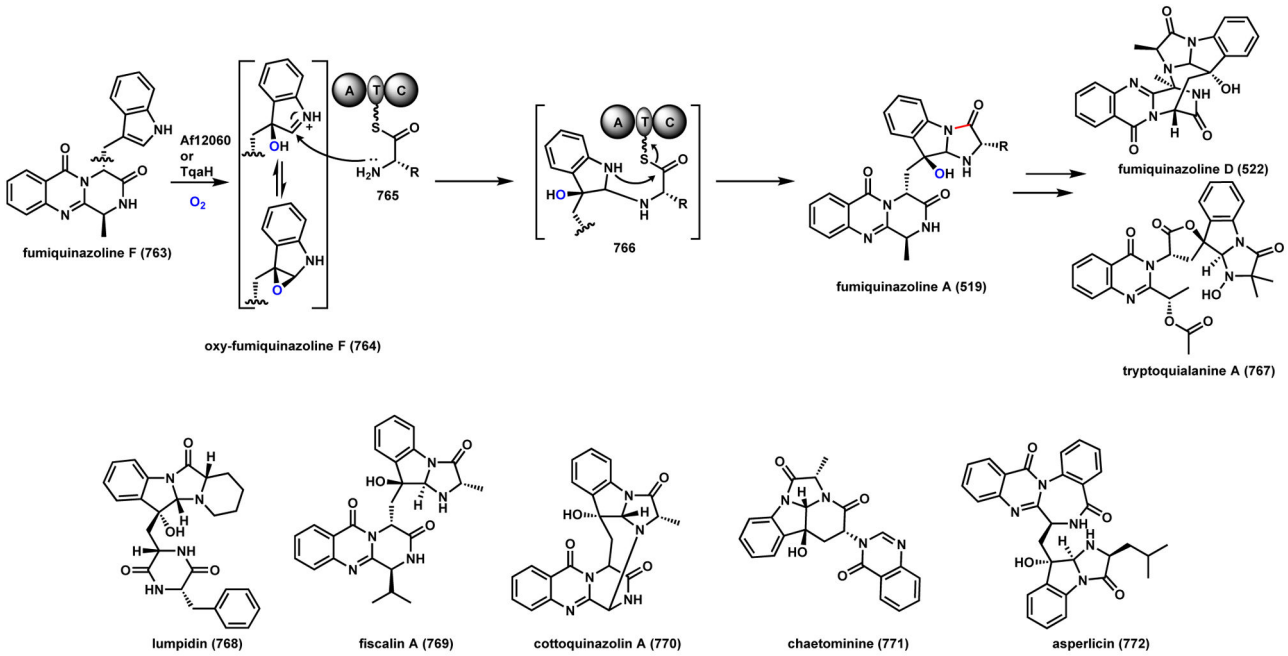

Scheme 105.

Indole Epoxidation as a Key Step in Fungal Indole Alkaloid Biosynthesis

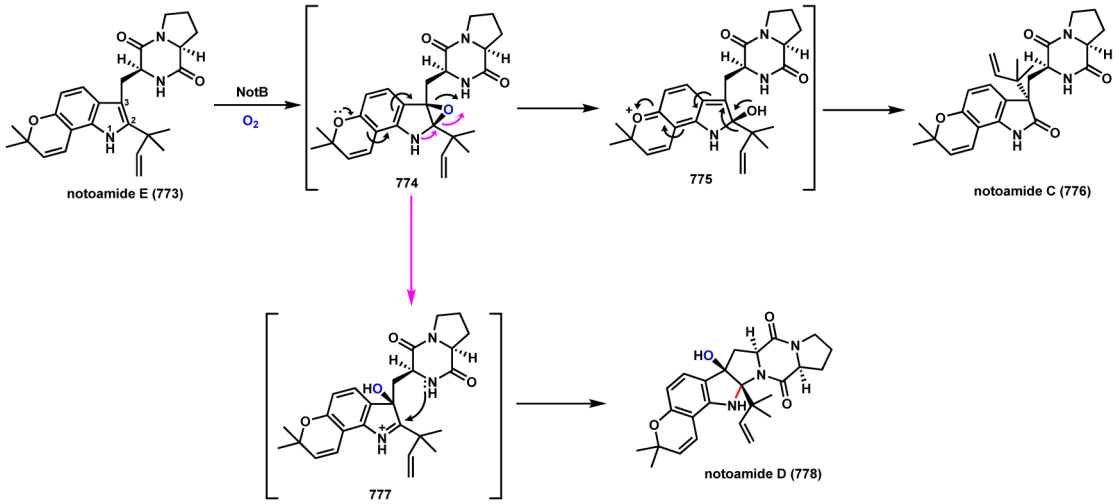

Scheme 106.
Indole Epoxidation in Notoamide Biosynthesis

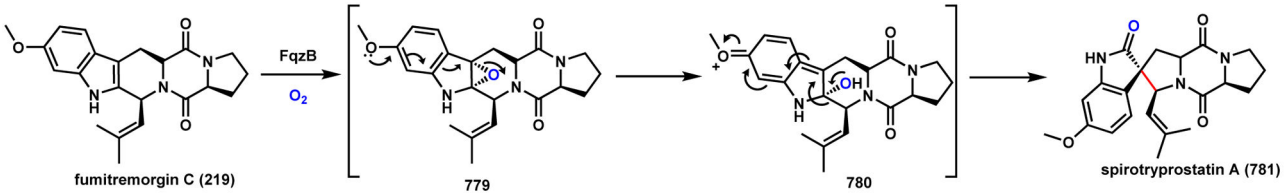

Scheme 107.

Indole Epoxidation Sets Up Spirocycle Formation in Spirotryprostatin

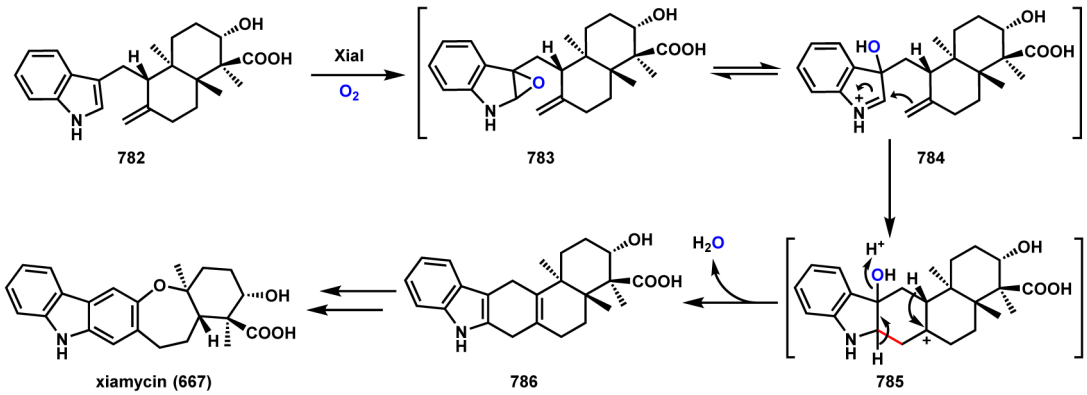

Scheme 108.
Indole Epoxidation Mediated Carbazole Formation in Xiamycin Biosynthesis

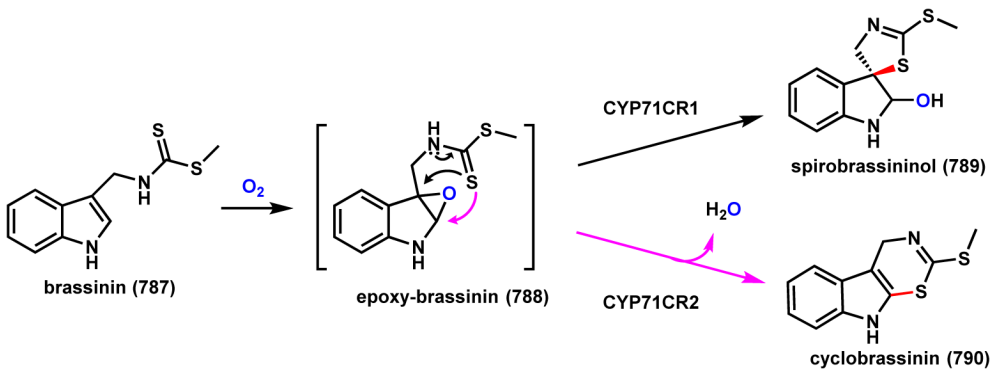

Scheme 109.
Indole Epoxidation Mediated Cyclization in Plant Metabolite Biosynthesis

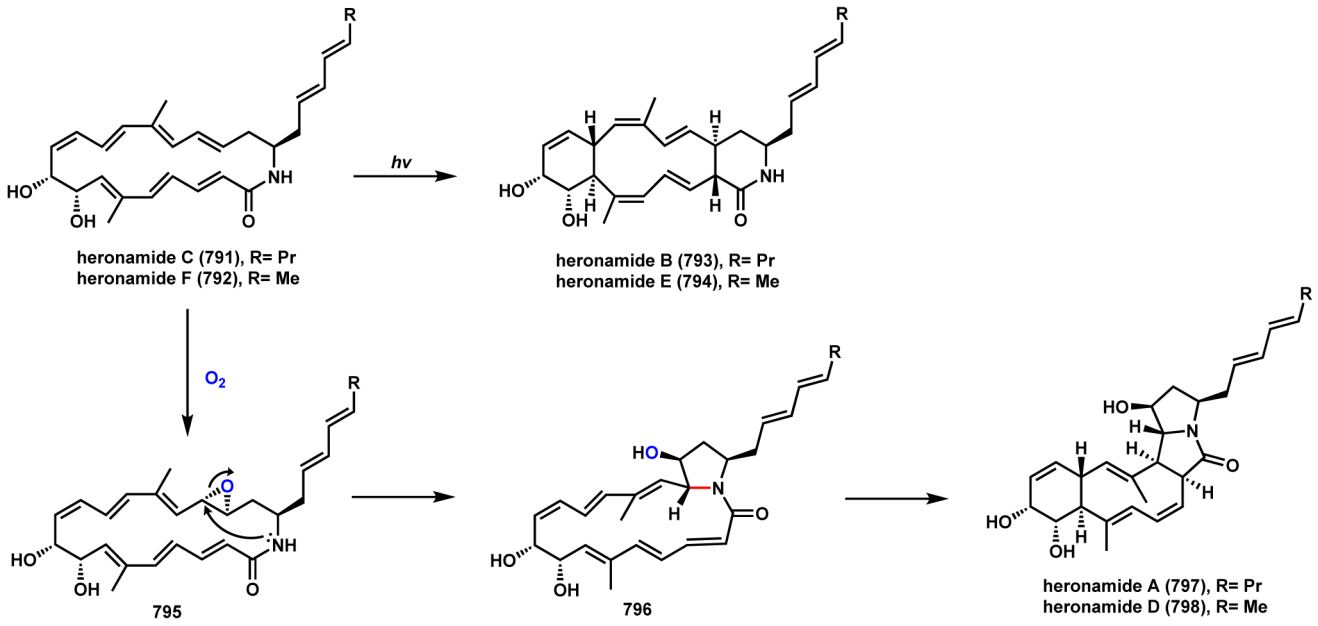

Scheme 110.

Epoxidation Mediated Cyclization in Heronamides Biosynthesis

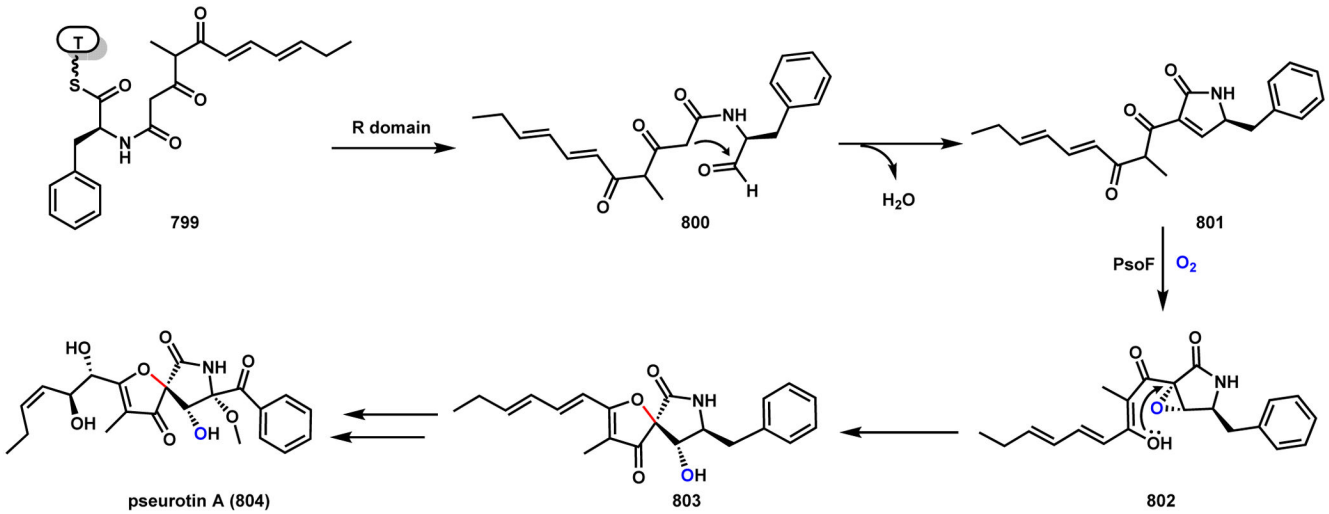

Scheme 111.
Epoxidation Mediated Oxo-Spiro Ring Formation in Pseurotin A Biosynthesis

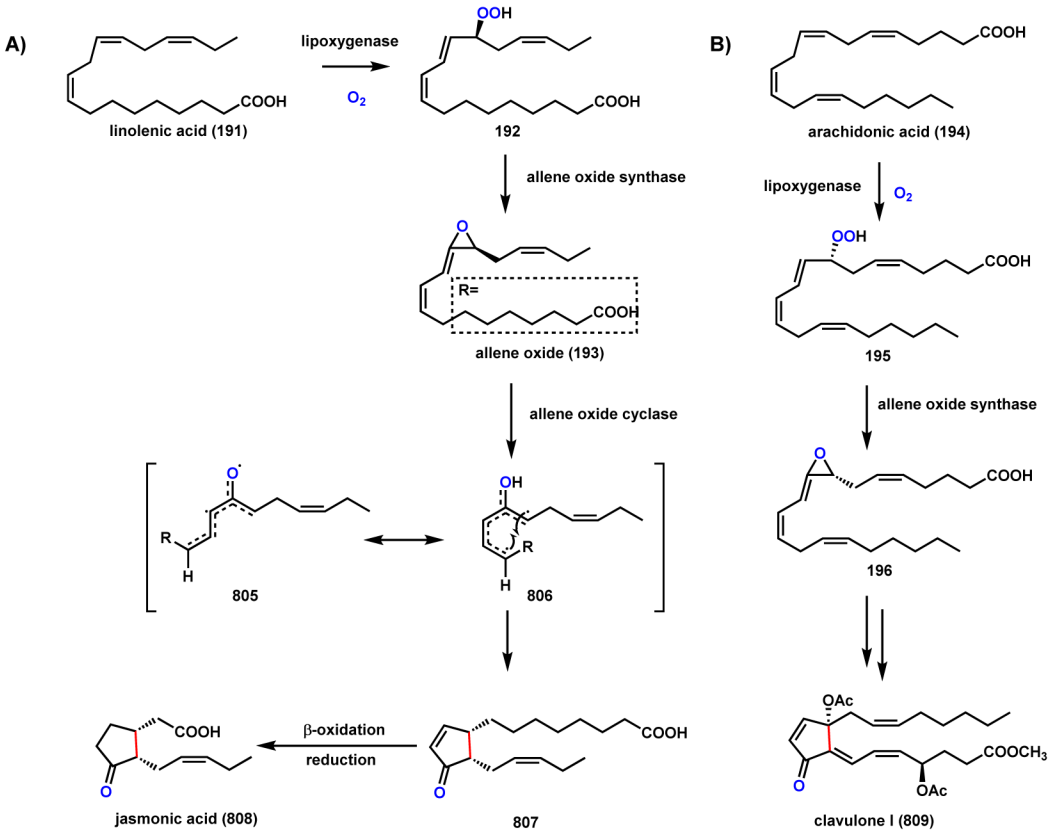

Scheme 112.
Cyclopentenone Formation in Jasmonic acid and Clavulone I Biosynthesis

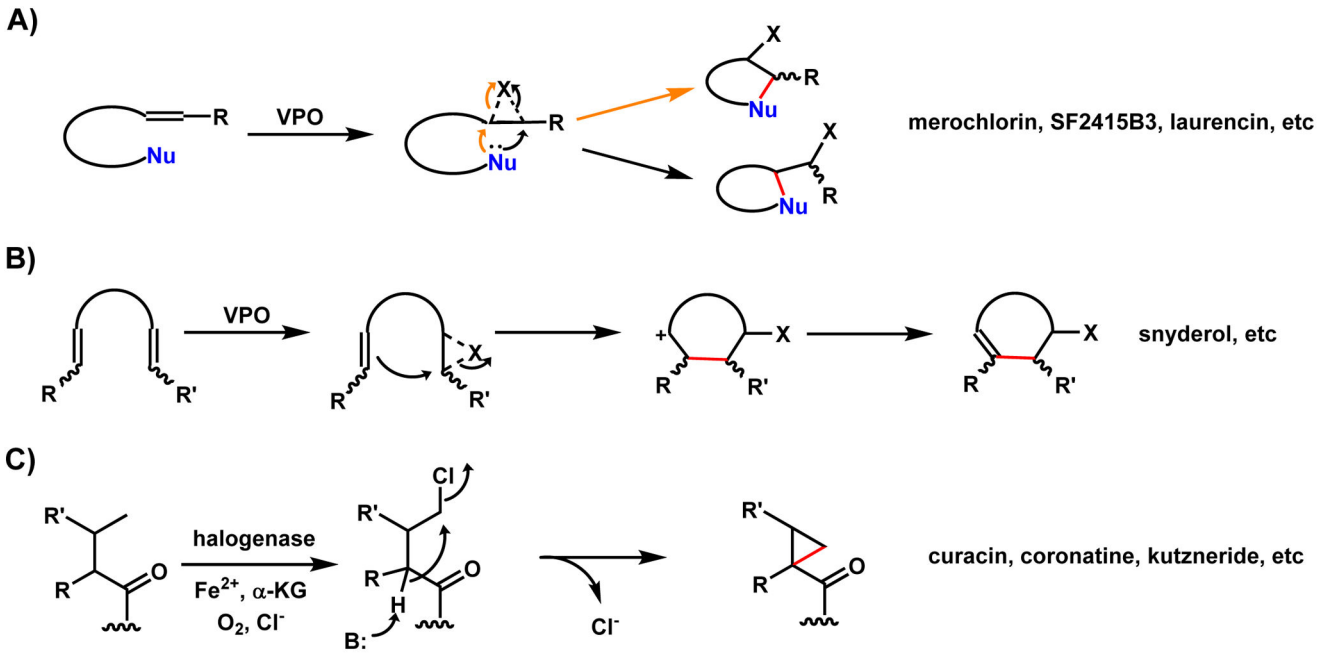

Scheme 113.
Models of Cyclization via Halogenation in Natural Product Biosynthesis

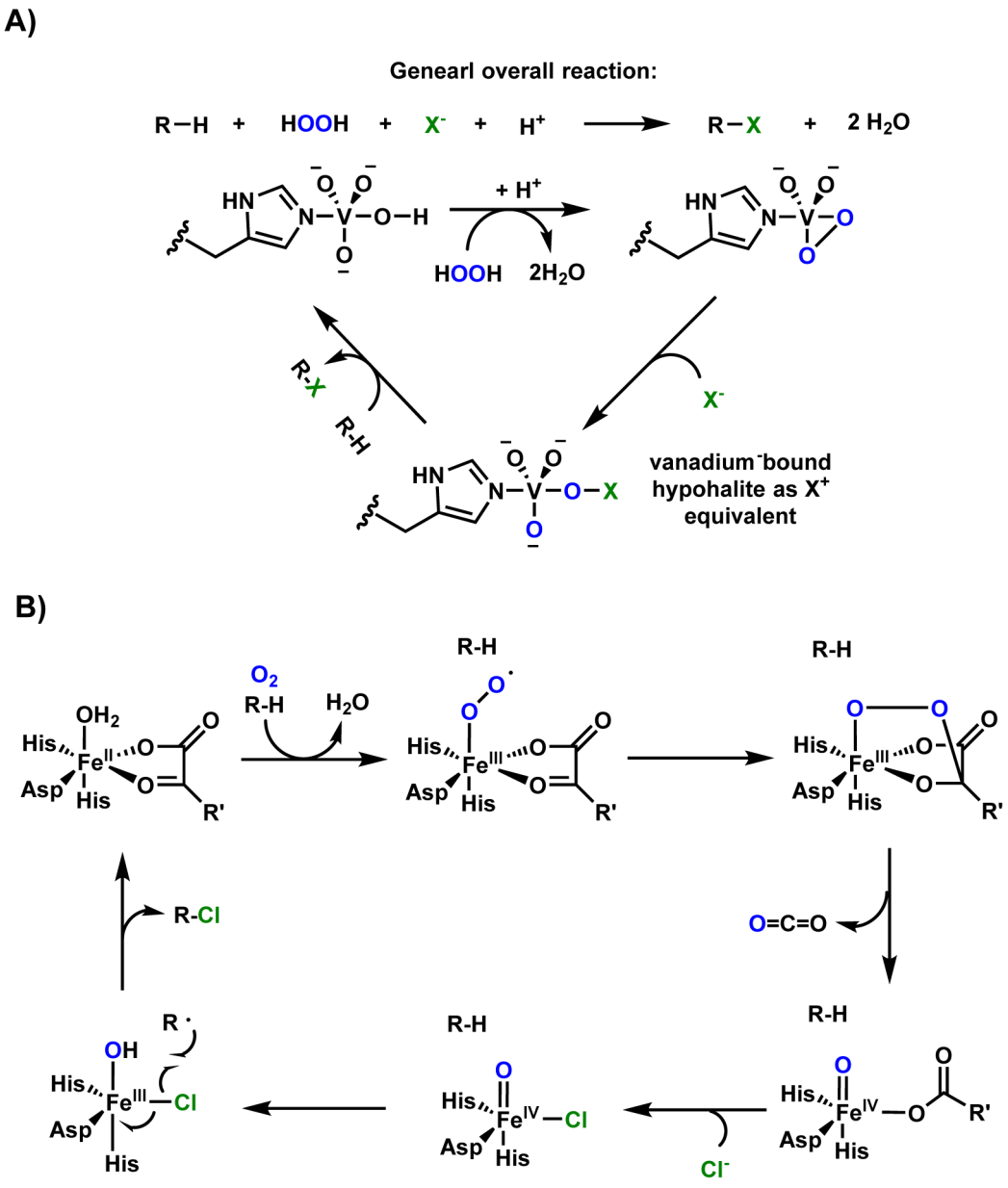

Scheme 114.

Catalytic Cycles of Vanadium Haloperoxidases and α-KG Dependent Halogenase

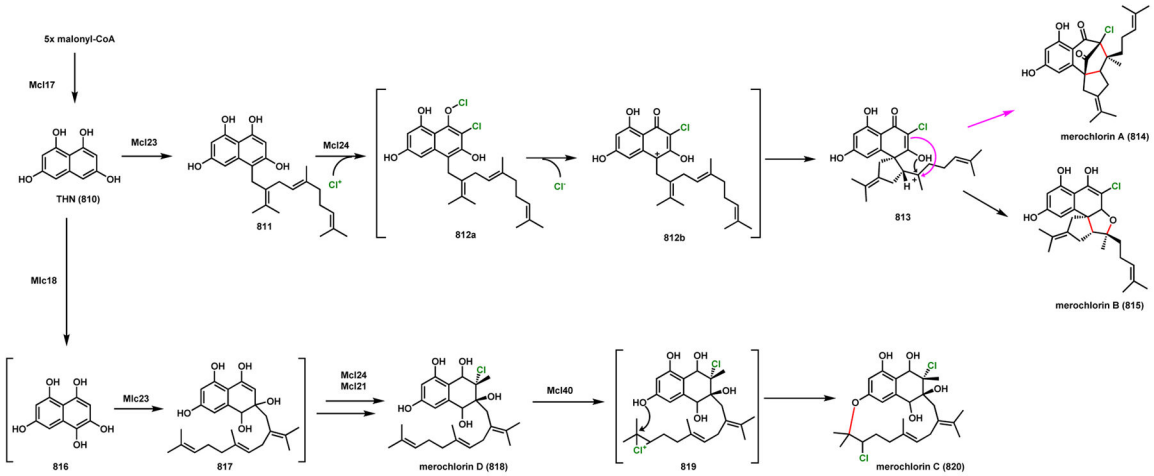

Scheme 115.
VHPO Catalyzed Formation of Merochlorins

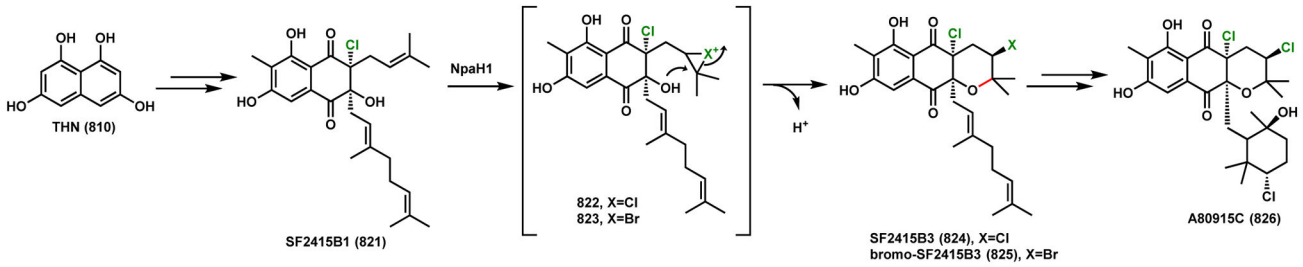

Scheme 116.
Halogenation as a Key Step in SF2415B3 Biosynthesis

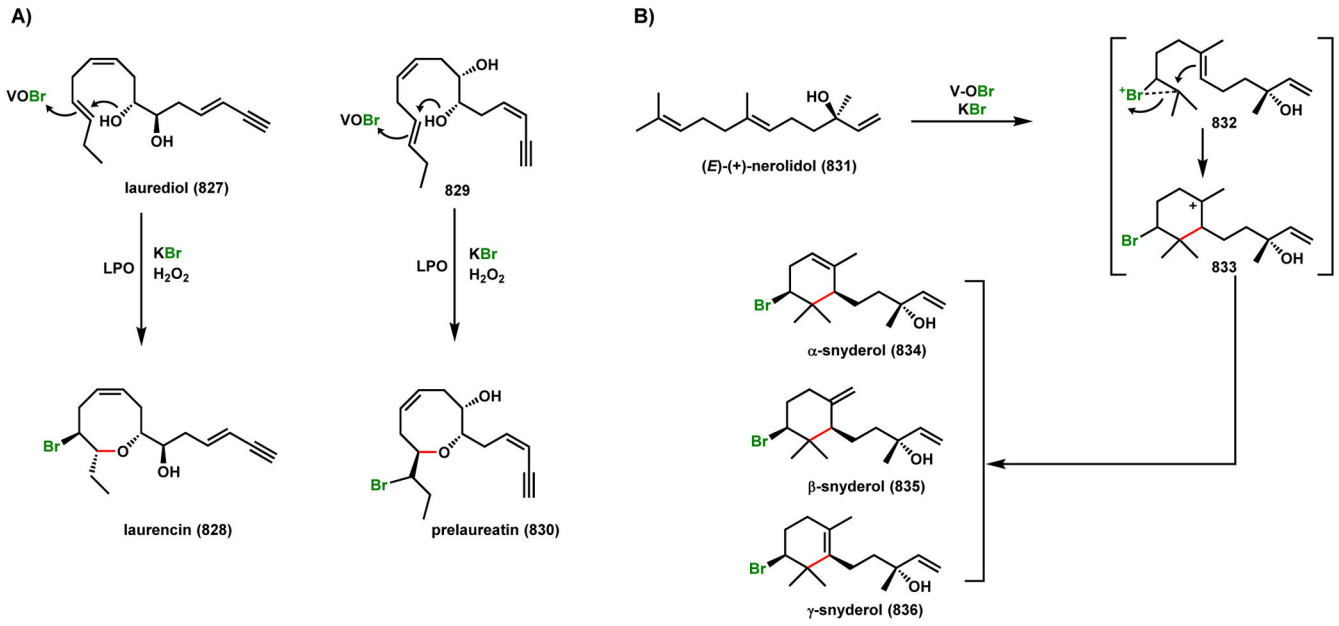

Scheme 117.
Bromination Triggered Cyclization in Laurencin, Laureatin and Snyderol Biosynthesis

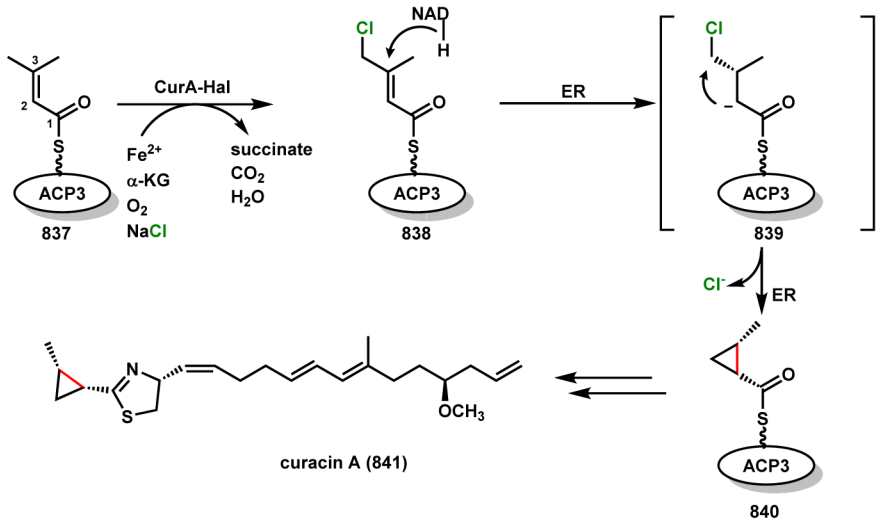

Scheme 118.
Chlorination Mediated Cyclopropane Formation During Curacin A Biosynthesis

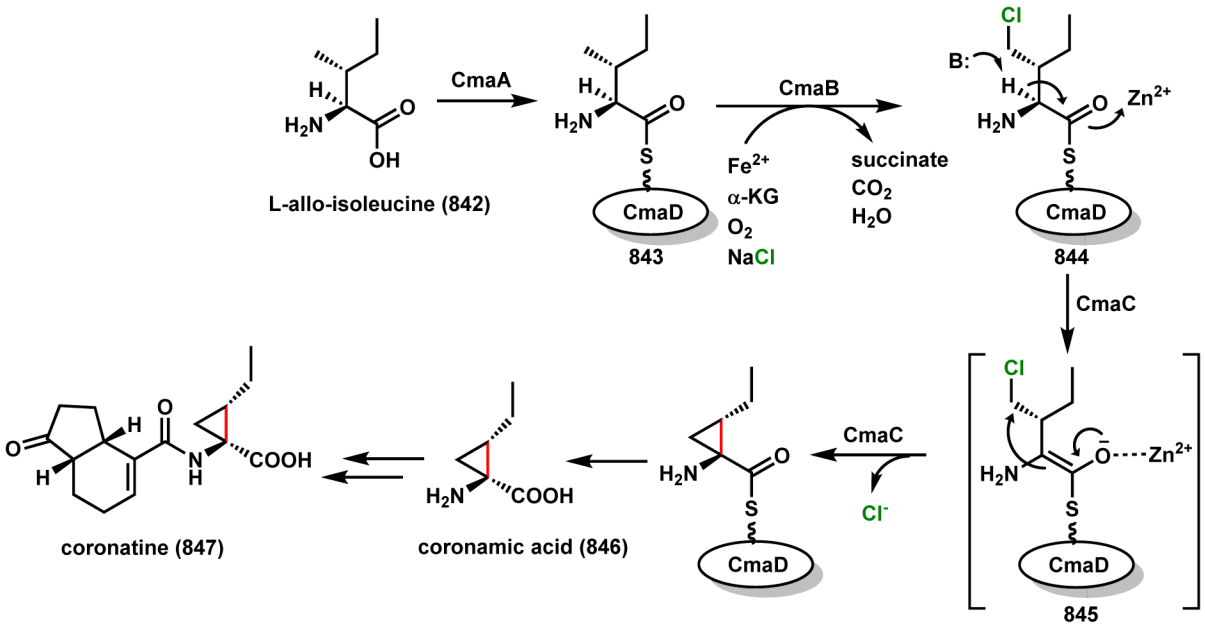

Scheme 119.
Chlorination Mediated Cyclopropane Formation During Coronatine Biosynthesis

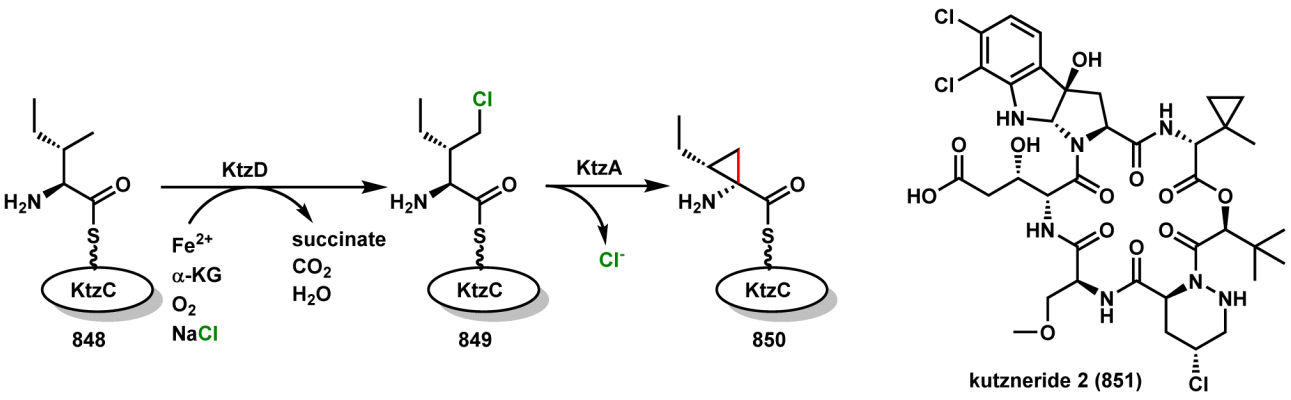

Scheme 120.

Chlorination Mediated Cyclopropane Formation During Kutzneride Biosynthesis

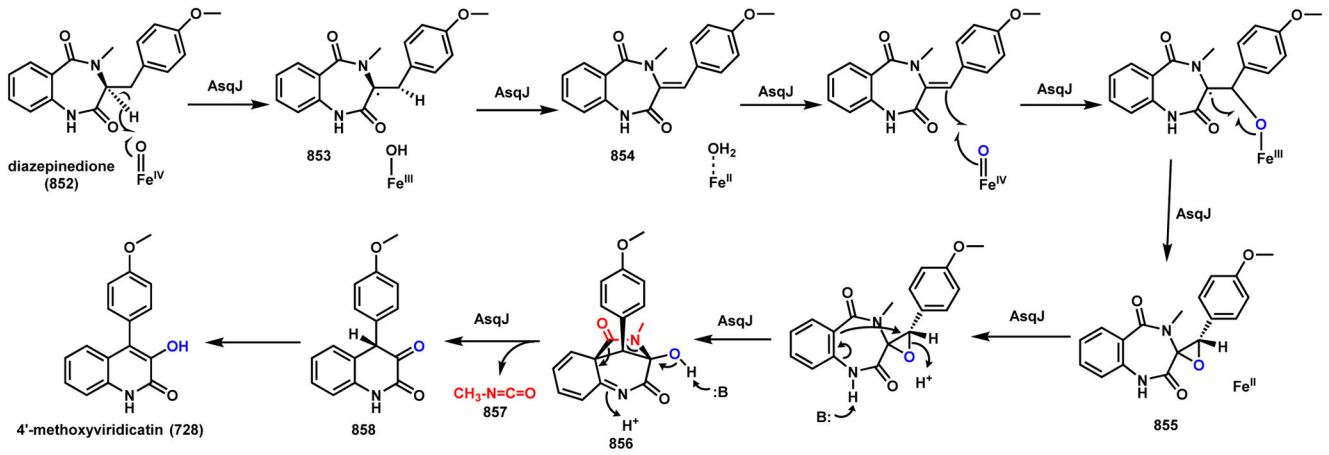

Scheme 121.
Oxidative Ring Contraction to Form Viridicatin

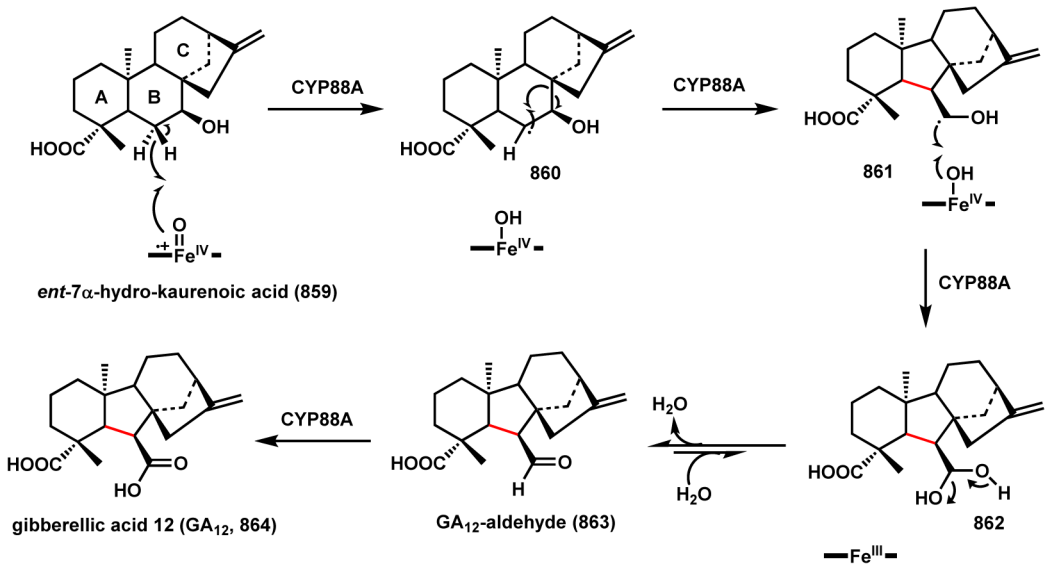

Scheme 122.

P450 Catalyzed Ring Contraction in Gibberellic Acid 12 Biosynthesis

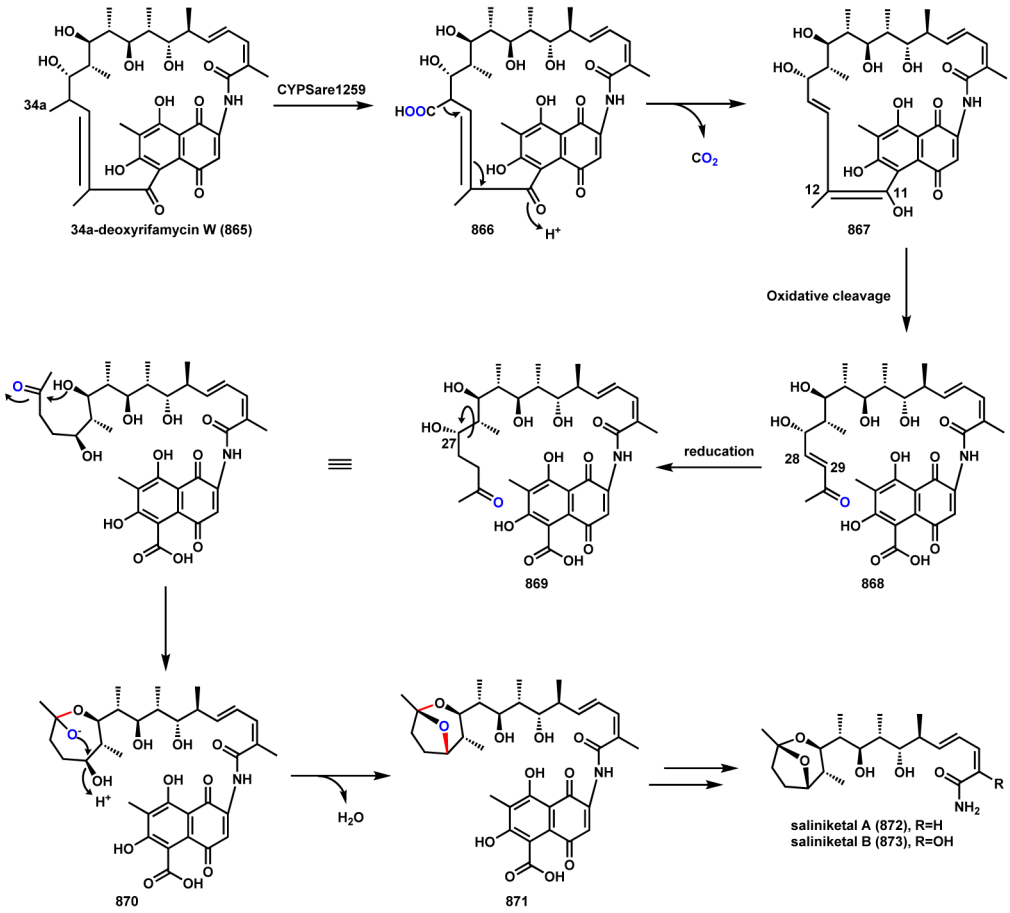

Scheme 123.
Dioxabicyclo[3.2.1]octane Formation in Saliniketals Biosynthesis

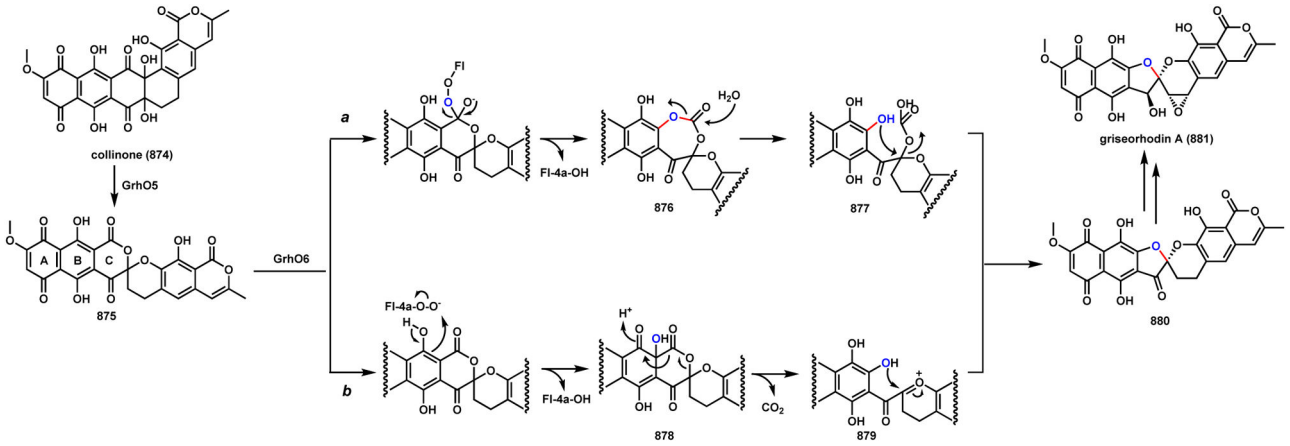

Scheme 124.
Oxidative Ring Contraction in Griseorhodin A Biosynthesis

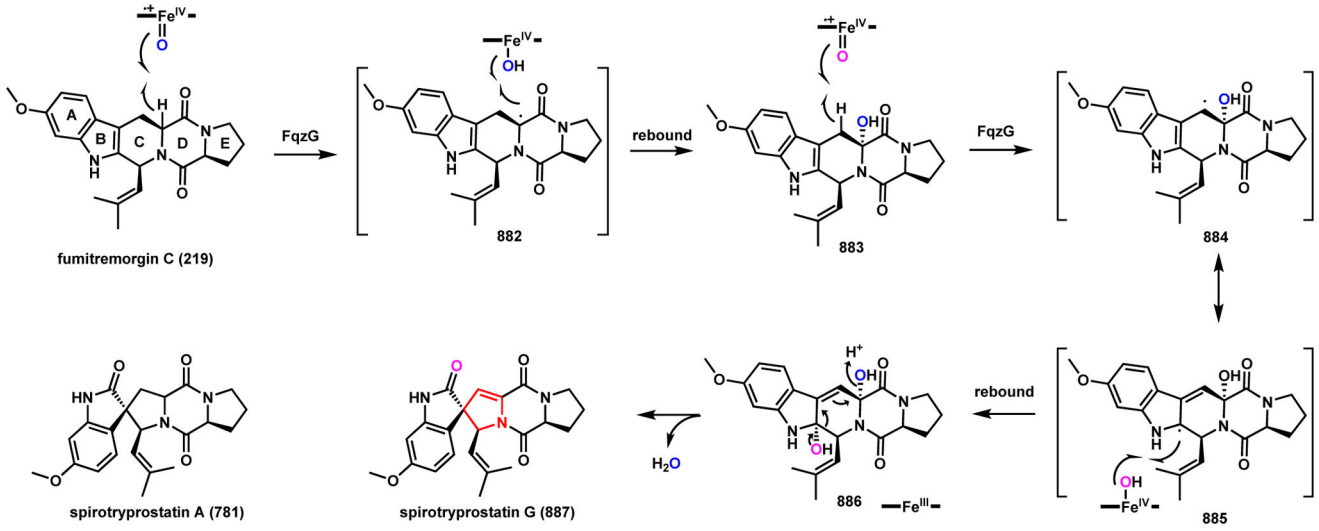

Scheme 125.
Oxidative Ring Contraction in Spirotryprostatin G Biosynthesis

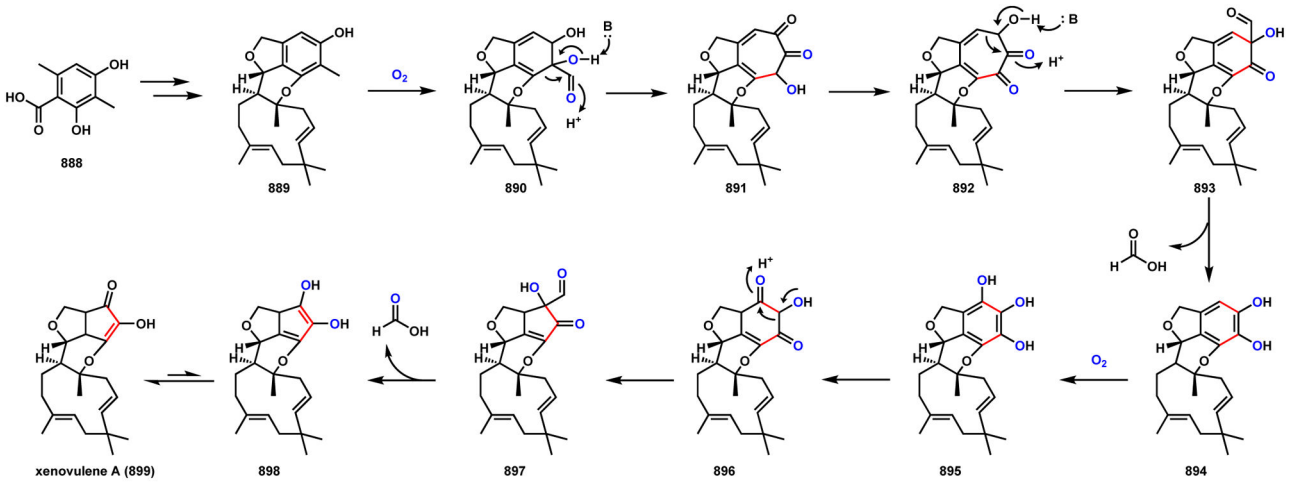

Scheme 126.
Cyclopentenone Ring Formation in Xenovulene A Biosynthesis

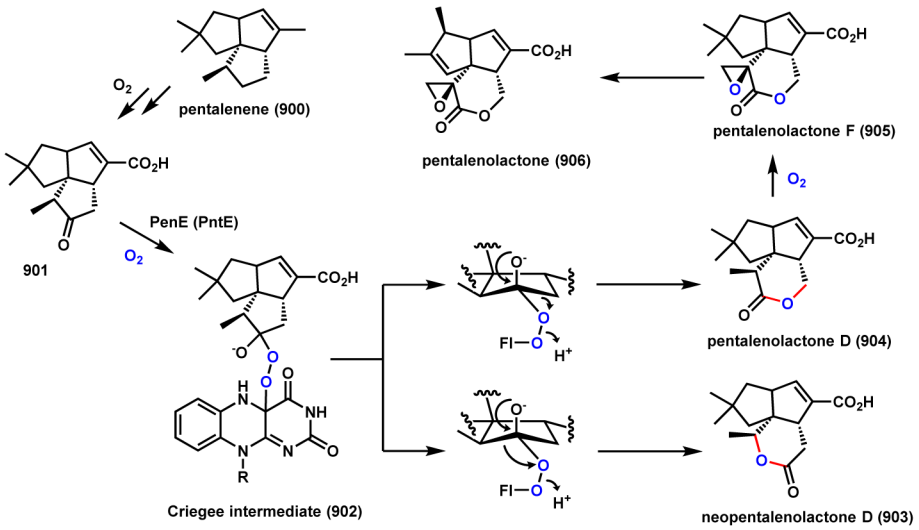

Scheme 127.
Baeyer-Villiger Oxidation in Pentalenolactone Biosynthesis

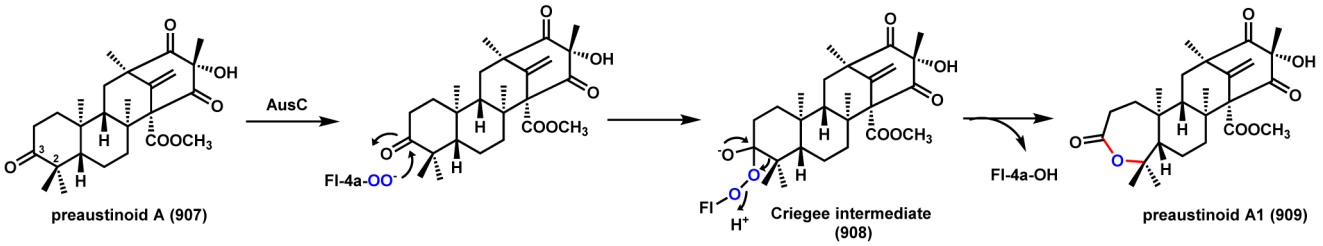

Scheme 128.
Baeyer-Villiger Oxidation in Preaustinoid A1 Biosynthesis

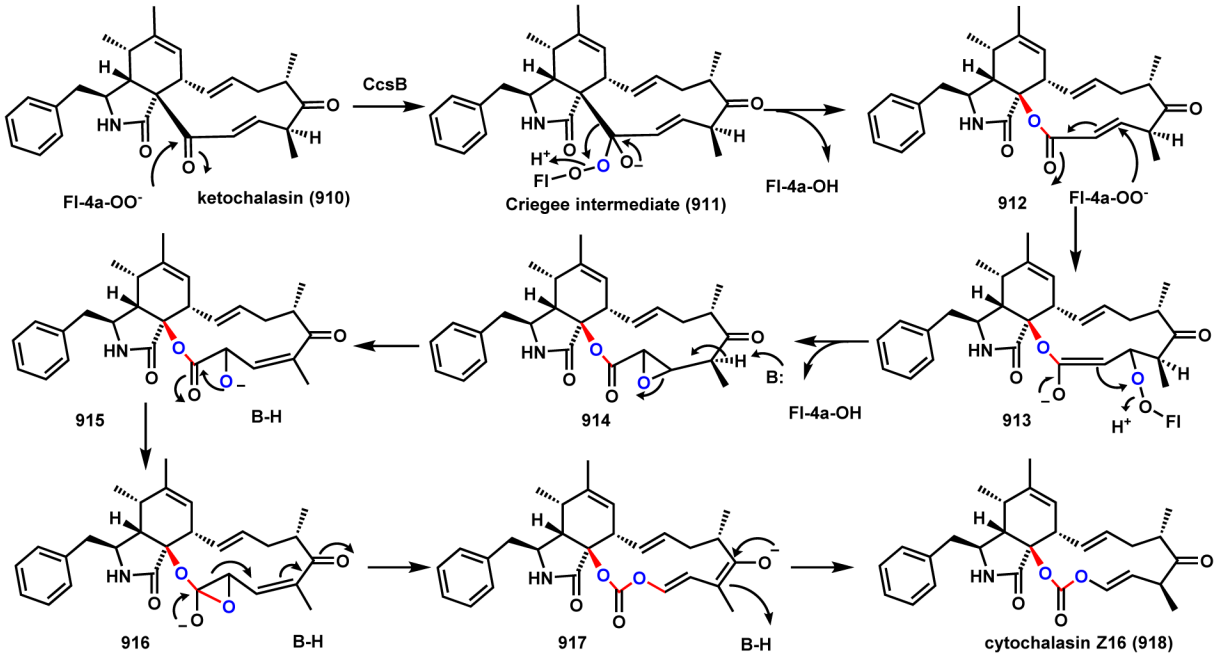

Scheme 129.
Baeyer-Villiger Oxidation in Cytochalasin Biosynthesis

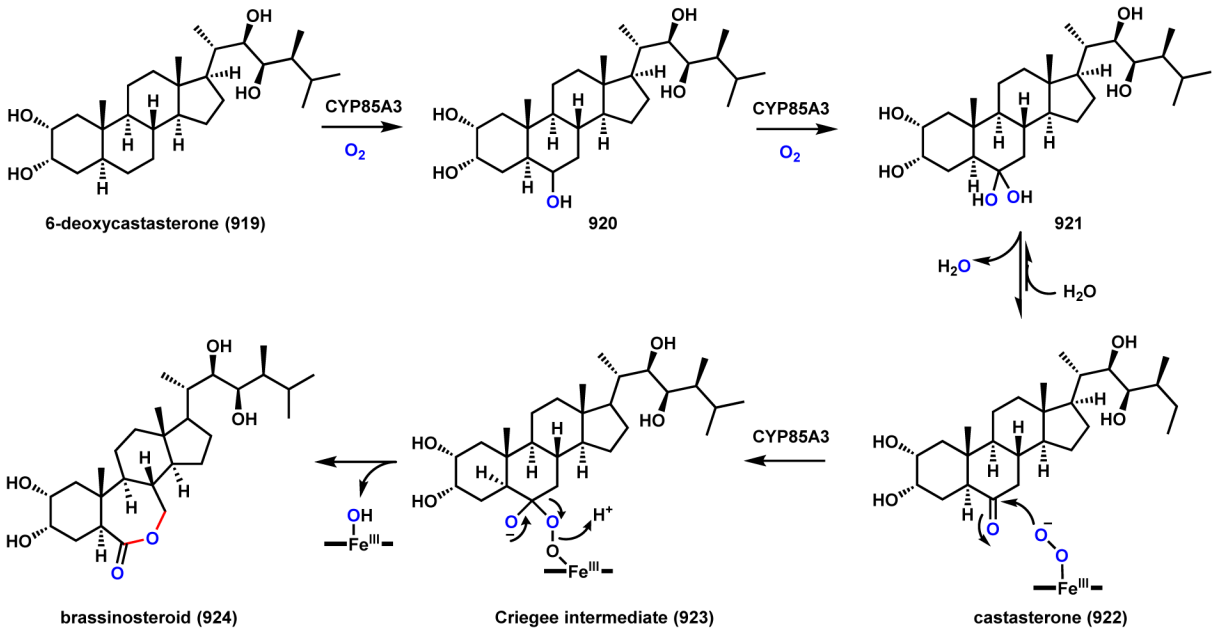

Scheme 130.

P450 Catalyzed Baeyer-Villiger Ring Expansion in Brassinosteroid Biosynthesis

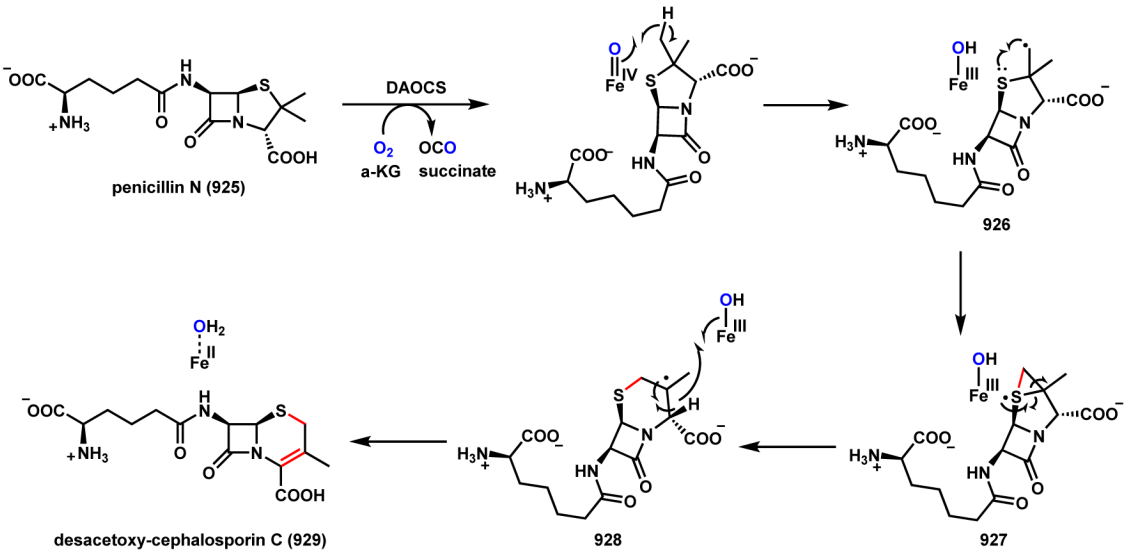

Scheme 131.

Oxidative Ring Expansion in Desacetoxycephalosporin C Biosynthesis

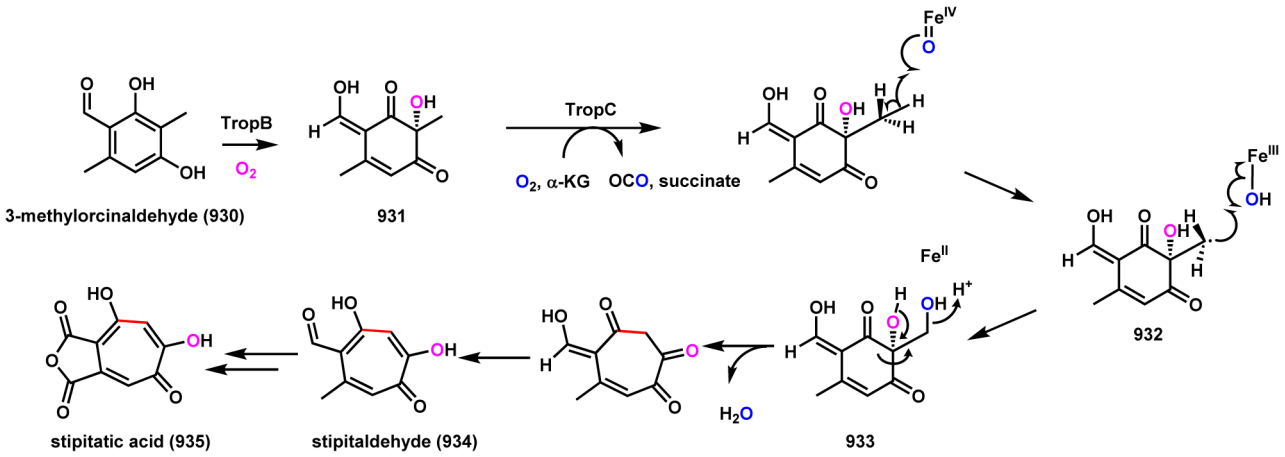

Scheme 132.
Tropolone Ring Formation in Stipitatic Acid Biosynthesis

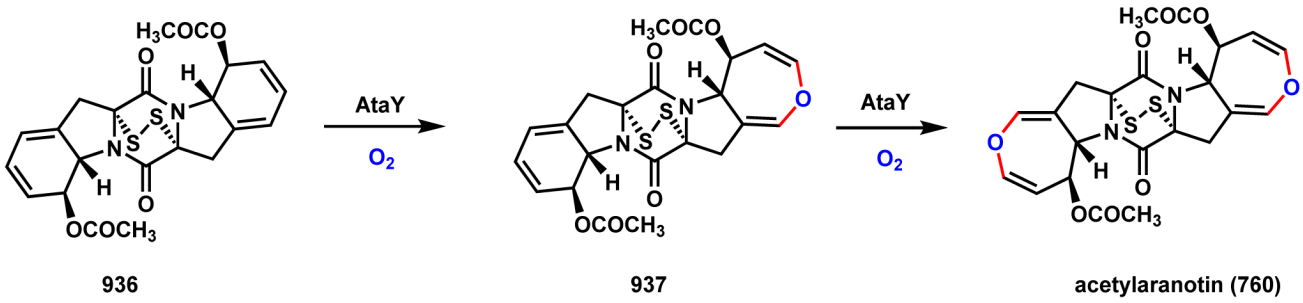

936 937 acetylaranotin (760)

Scheme 133.

Oxidative Ring Expansion in Acetylaranotin Biosynthesis

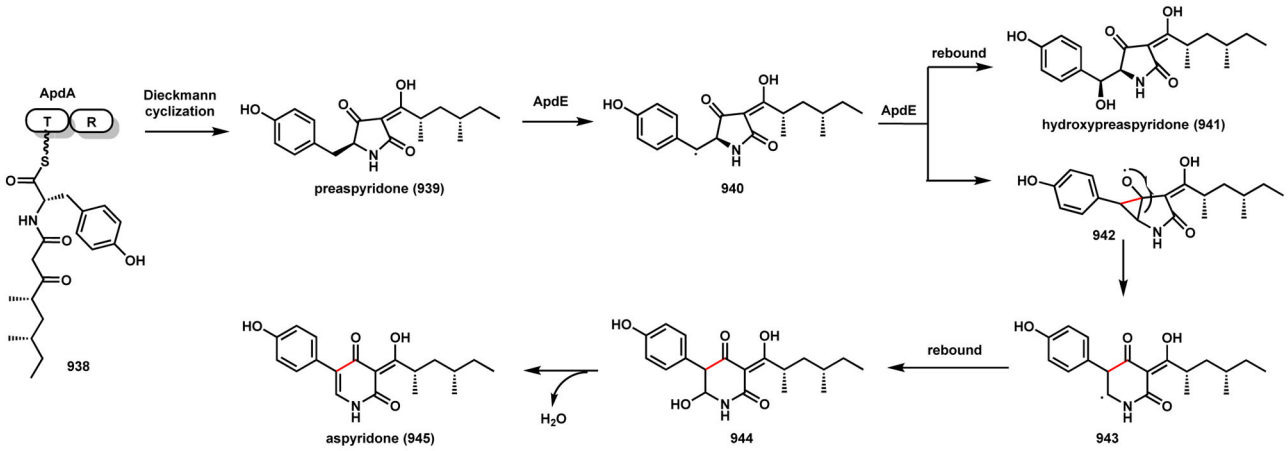

Scheme 134.

P450 Catalyzed Tetramic Acid to Pyridone in Aspyridone Biosynthesis

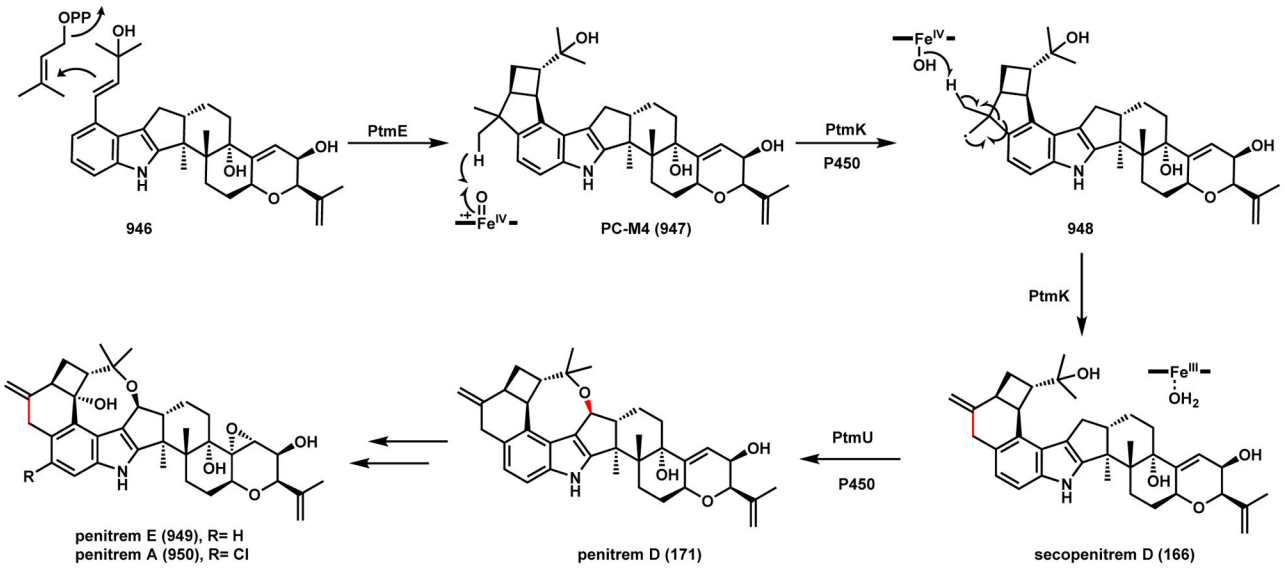

Scheme 135.
P450 Catalyzed Ring Expansion in Penitrem A Biosynthesis

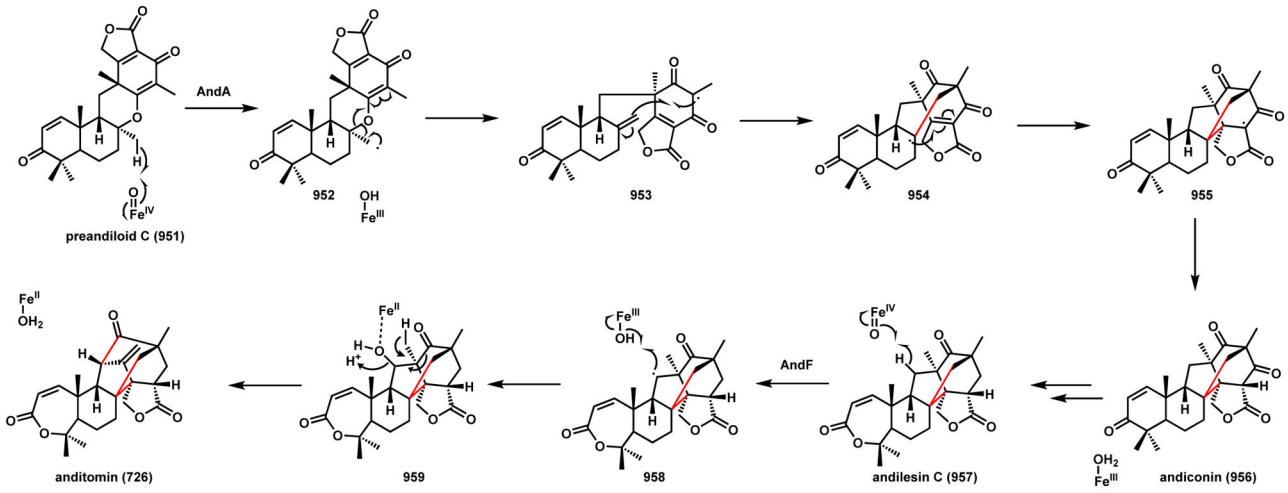

Scheme 136.
Ring Modifications in Anditomin Biosynthesis

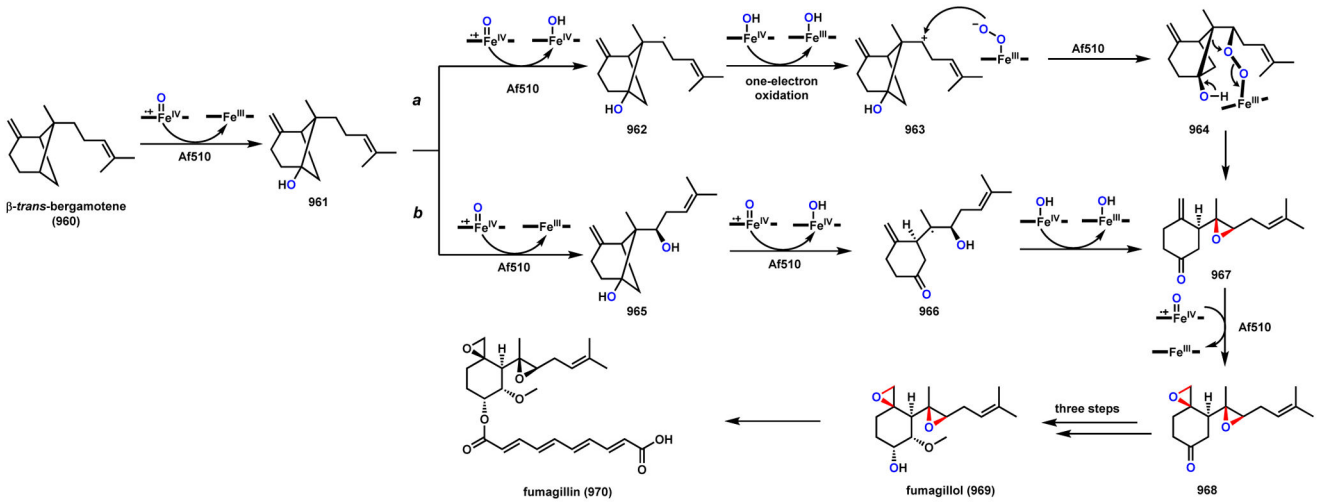

Scheme 137.
Proposed Mechanisms of Carbon Scaffold Rearrangement during Fumagillin Biosynthesis

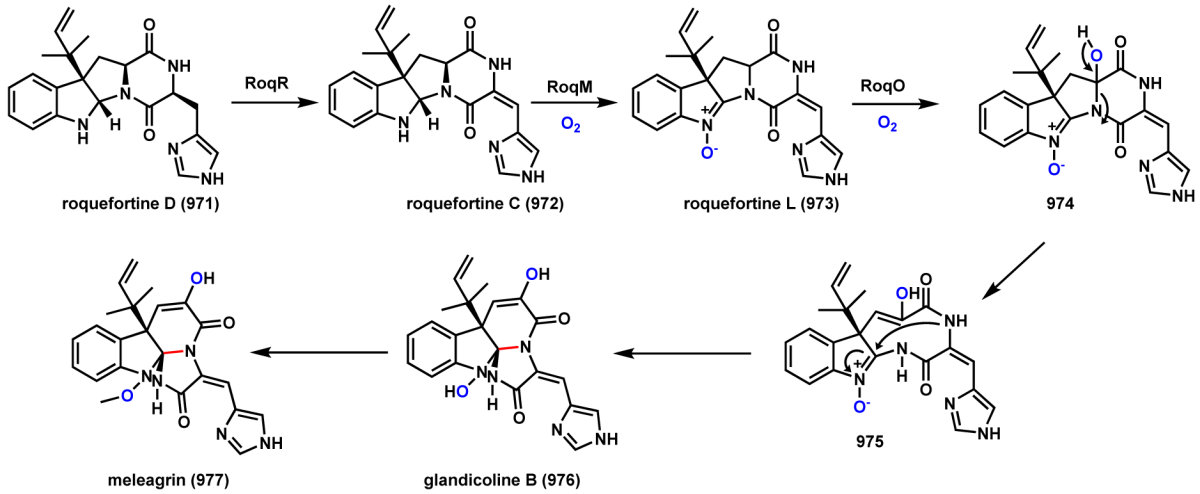

Scheme 138.
Tri-aminal Formation during Meleagrin Biosynthesis

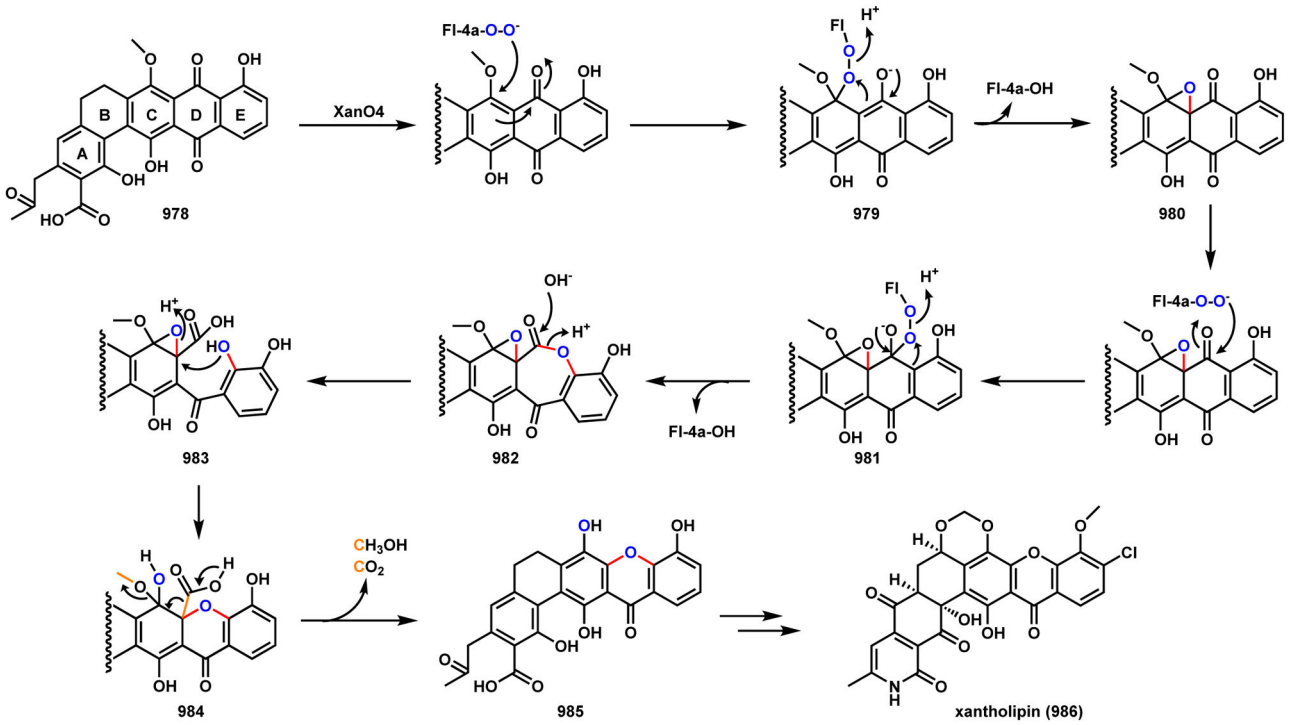

Scheme 139.
Xanthone Formation via a Cryptic Demethoxylation in Xantholipin Biosynthesis

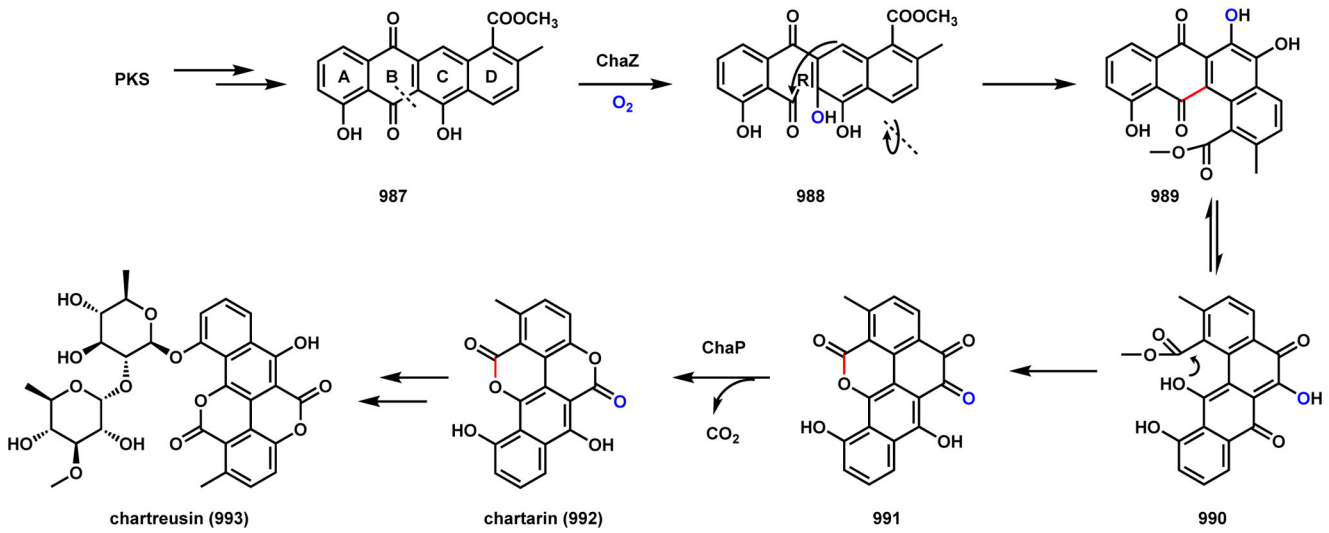

Scheme 140.
Angular Polyaromatic Framework Formation in Chartreusin Biosynthesis

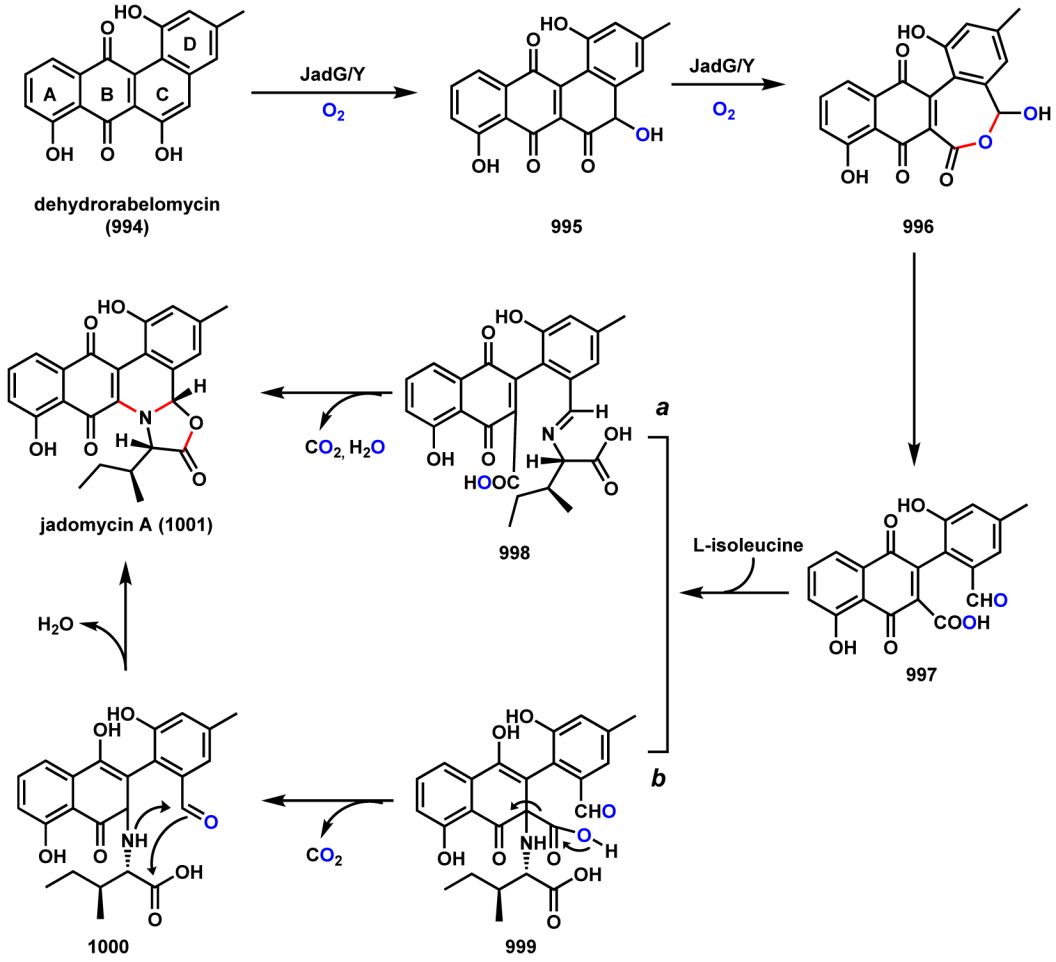

Scheme 141.
Proposed pathways of Oxazolidinone Formation in Jadomycin Biosynthesis

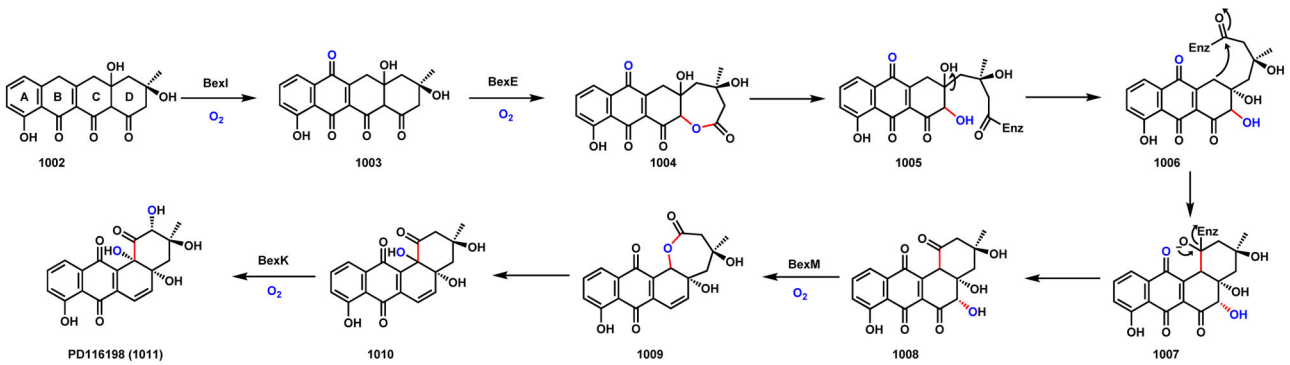

Scheme 142.
Anthracycline to Angucycline Rearrangement in PD116198 Biosynthesis

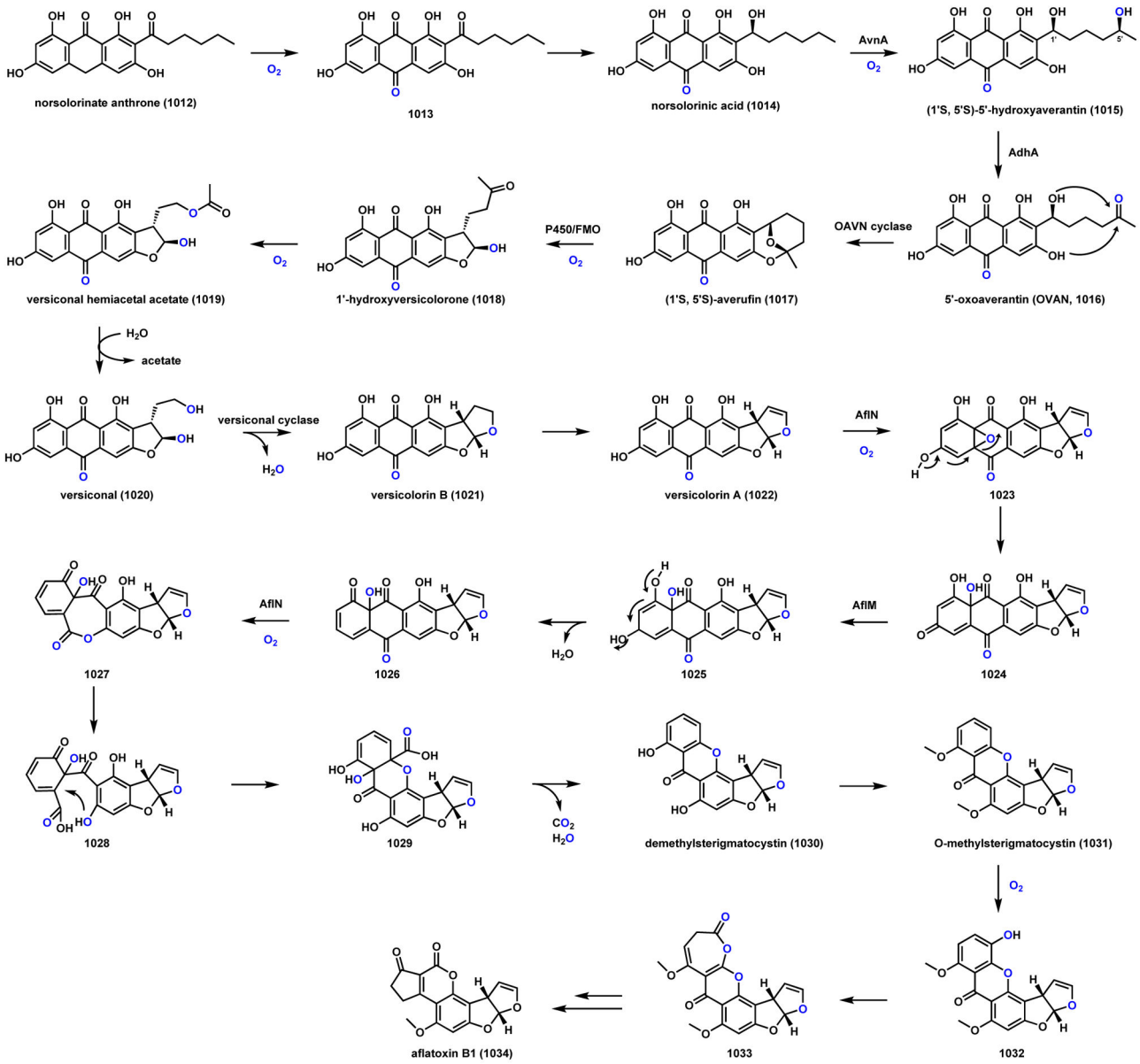

Scheme 143.
Oxidative Ring Arrangements During Aflatoxin Maturation

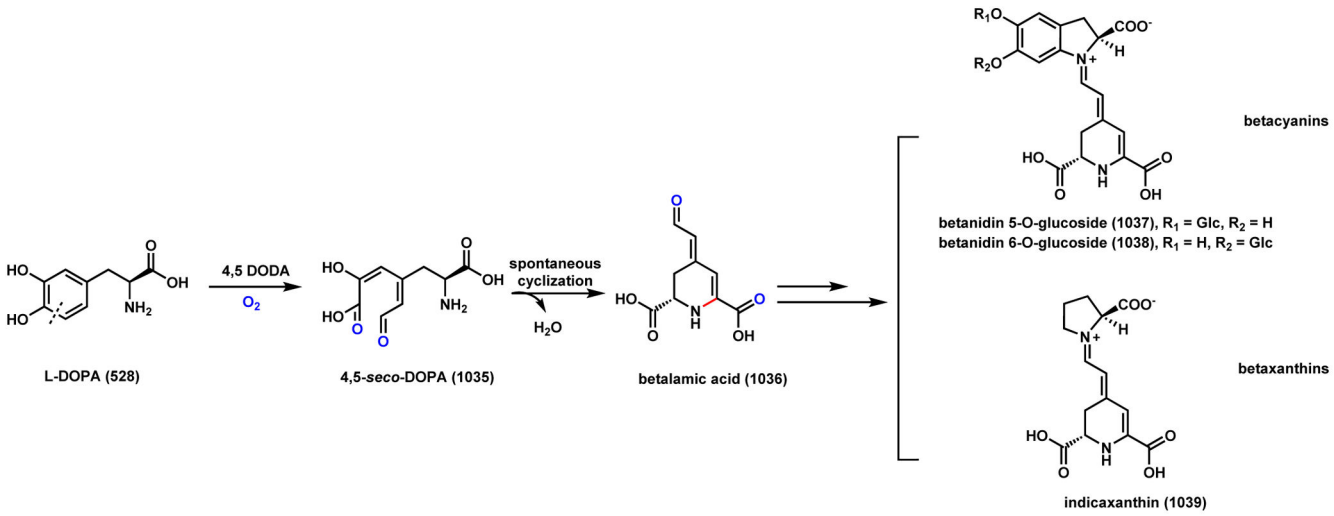

Scheme 144.
Oxidative Rearrangements in Betalamic Acid Biosynthesis